

**Studies on Functionalization of Carbon–Fluorine  
Bonds Catalyzed by Aluminum–Rhodium Complexes**

**Ikuya Fujii**

**2023**



## Contents

### Chapter 1

Introduction and General Summary – 1

### Chapter 2

Magnesiumation of Aryl Fluorides Catalyzed by a Rhodium–Aluminum Complex – 30

### Chapter 3

The Kumada–Tamao–Corriu Coupling Reaction Catalyzed by Rhodium–Aluminum Bimetallic Complexes – 84

### Chapter 4

Site-Selective Magnesiumation of Multi-Fluorinated Arenes Catalyzed by Rhodium–Aluminum Bimetallic Complexes – 117

### Chapter 5

Magnesiumation of Alkyl Fluorides Catalyzed by Rhodium–Aluminum Bimetallic Complexes – 176

**List of Publications** – 202

**Acknowledgments** – 204

## Abbreviations

Ac	acetyl		1,3-bis(diphenylphosphino)propane
acac	acetylacetonato		
Anal.	elemental analysis	ECP	effective core potential
Å	ångström	EI	electron ionization
APCI	atmospheric pressure chemical ionization	El	electrophile
aq.	aqueous solution	eq.	equivalent(s)
Ar	aryl	Eq.	equation
atm	atmospheric pressure	ESI	electrospray ionization
BDE	bond dissociation energy	ESP	electrostatic potential
Bn	benzyl	Et	ethyl
br s	broad singlet (spectra)	Et <sub>2</sub> O	diethyl ether
Calcd.	calculated	eV	electron volt
cat.	catalyst	EXP.	experimental
CCSD	coupled-cluster singles-and-doubles	FIA	fluoride ion affinity
cod	1,5-cyclooctadiene	FID	flame ionization detector
conv.	conversion	g	gram
Cp*	pentamethylcyclopentadienyl	$G^\circ$	standard Gibbs free energy
Cy	cyclohexyl	$G^{\circ\dagger}$	standard Gibbs free energy of transition state
$\delta$	chemical shift in parts per million (spectra)	GC	gas chromatography
$\Delta$	delta, difference	h	hour(s)
°	degree	Halo	halogen
°C	degrees Celsius	HMDS	hexamethyldisilazide
d	doublet (spectra)	HOMO	highest occupied molecular orbital
dba	dibenzylideneacetone	HRMS	high resolution mass spectrometry
decomp.	decomposition	Hz	hertz ( $s^{-1}$ )
DFT	density functional theory	HPLC	high performance liquid chromatography
DME	1,2-dimethoxyethane	<i>i</i> -Bu	<i>iso</i> -butyl
DMF	<i>N,N</i> -dimethylformamide	<i>i</i> -Pr	<i>iso</i> -propyl
DMSO	dimethyl sulfoxide	IR	infrared light
Dipp	2,6-di- <i>iso</i> -propylphenyl	<i>J</i>	coupling constant (spectra)
dppp			

K	Kelvin	MS	mass spectrometry
kcal	kilocalorie(s)	M	metal
KC <sub>8</sub>	potassium graphite	<i>n</i>	normal
kJ	kilojoule(s)	NBE	norbornene
kPa	kilopascal	NBO	natural bond orbital
λ	lambda, wavelength	<i>n</i> -Bu	<i>normal</i> -butyl
LA	Lewis acid(s)	nep	neopentylglycolato
LB	Lewis base(s)	NHC	<i>N</i> -heterocyclic carbene
LC	liquid chromatography	nm	nanometer(s)
LED	light-emitting diode	NMP	<i>N</i> -methylpyrrolidone
LUMO	lowest unoccupied molecular orbital	NMR	nuclear magnetic resonance
<i>m</i>	meta	NPA	natural population analysis
m	meter	Nu	nucleophile
m	multiplet (spectra)	<i>o</i>	ortho
M	molar (mole per liter)	<i>p</i>	para
MALDI	matrix assisted laser desorption/ionization	PCM	polarizable continuum model
Me	methyl	Ph	phenyl
Mes	mesityl	pin	pinacolato
mg	milligram(s)	photocat.	photocatalyst
MHz	megahertz	ppm	parts per million (spectra)
min	minute(s)	PTLC	preparative thin layer chromatography
mm	millimeter(s)	py	pyridine
mmHg	millimeter of mercury	q	quartet (spectra)
μm	micrometer(s)	quant.	quantitative
mL	milliliter(s)	quint	quintet (spectra)
μL	microliter(s)	R <sup>2</sup>	coefficient of determination
mmol	millimole(s)	R <sub>f</sub>	retention factor
μmol	micromole(s)	RMSE	root mean squared error
mol	mole	rt	room temperature
mol%	mole percent	s	singlet (spectra)
m.p.	melting point	sat.	saturated
MPLC	medium pressure liquid chromatography	SCE	saturated calomel electrode
Ms	mesyl	SHE	standard hydrogen electrode
		sept	septet (spectra)
		SET	single-electron transfer

sex	sextet (spectra)	Tf	triflyl
S <sub>E</sub> Ar	electrophilic aromatic substitution	THF	tetrahydrofuran
S <sub>N</sub> Ar	nucleophilic aromatic substitution	TLC	thin layer chromatography
S <sub>N</sub> 1	unimolecular nucleophilic substitution	TMS	trimethylsilyl
S <sub>N</sub> 2	bimolecular nucleophilic substitution	tol	tolyl
t	triplet (spectra)	Ts	tosyl
t <sub>1/2</sub>	half-life time	TS	transition-state
<i>t</i> -Bu	<i>tertiary</i> -butyl	UV	ultraviolet
		V	volt
		V	volume
		vs.	versus

# **Chapter 1**

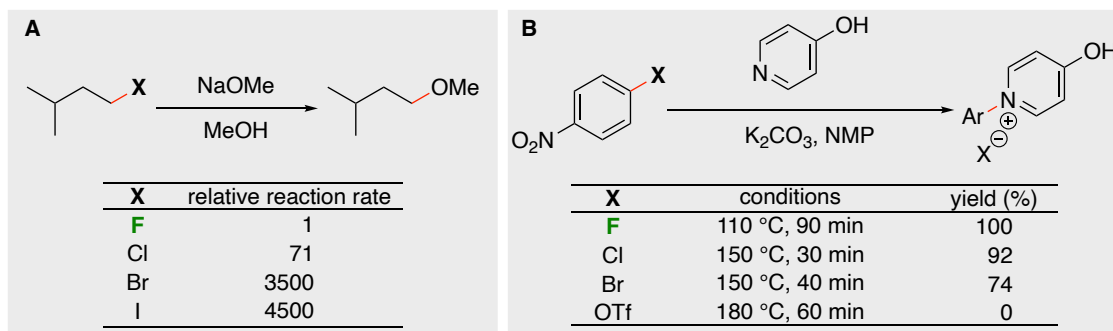
## **Introduction and General Summary**

Synthetic organic chemistry has enriched our modern lives by enabling the creation of a wide variety of valuable molecules such as pharmaceuticals, agrochemicals, and functional materials. Remarkable advances in synthetic technology in recent decades have made manufacturing processes more efficient and produced novel molecules that are difficult to synthesize by conventional methods. In order to ensure a stable supply of useful molecules for modern human life in the future, it is necessary to produce them massively and inexpensively while taking environmental impacts into consideration. In other words, the development of clean, selective, and highly efficient catalytic reactions has become essential science and technology in modern synthetic organic chemistry. In this regard, organocatalysts<sup>1</sup> and enzyme catalysts,<sup>2</sup> which have won the recent Nobel Prize in Chemistry, have attracted much attention in recent years, whereas transition-metal catalysts also still play indispensable roles in organic synthesis thanks to their versatile reactivity, chemoselectivity, and thermal stability.<sup>3</sup>

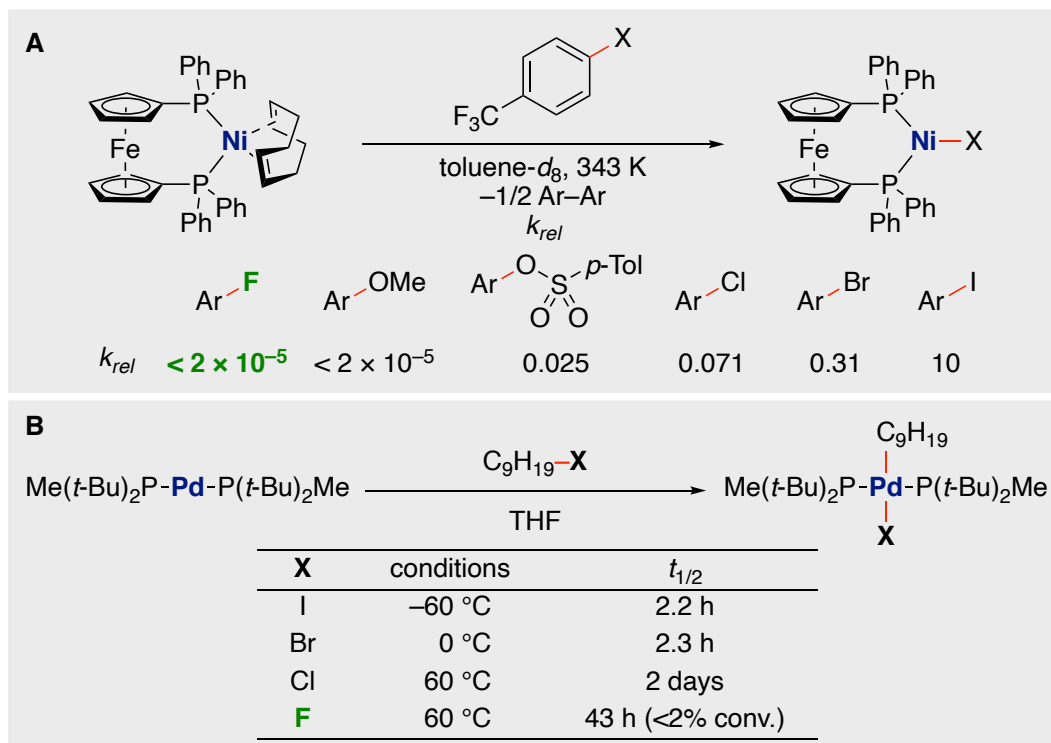
To date, transition metal-catalyzed reactions have focused mainly on introducing functional groups through activation of relatively weak  $\sigma$ -bonds such as C–Br, C–I, and C–OTs bonds. One of the greatest advances in Pd-catalyzed cross-coupling over the past two decades has been the development of ligands that facilitate elementary processes such as oxidative addition and reductive elimination. For example, Buchwald and co-workers have developed dialkyl(biaryl)phosphine ligands,<sup>4</sup> that allow the Suzuki–Miyaura reaction and Buchwald–Hartwig reaction using unactivated aryl chloride as substrates. Thus, the invention of new ligands has enabled the use of various organohalides in a wide range of transformations to broaden their scopes. To further enable the use of inert substrates, it is necessary to design novel catalysts based on an unconventional approach.





**Scheme 1-2.** Relative rates of nucleophilic substitution of organo(pseudo)halides.

In the reactivity of oxidative addition reactions of aryl halides (Scheme 1-3, A)<sup>9</sup> and alkyl halides (Scheme 1-3, B)<sup>10</sup> to low-valent transition metal complexes, organofluorine compound has been found to be the least reactive among different organo(pseudo)halides.

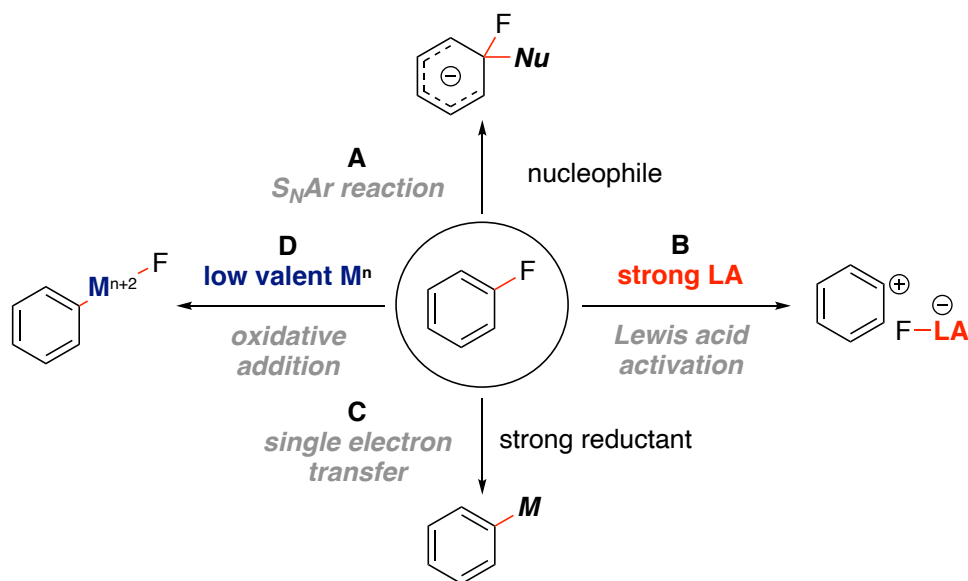
**Scheme 1-3.** Relative rates of oxidative addition of organo(pseudo)halides.

Catalytic transformations of C–F bonds are not only scientifically interesting but also important from the viewpoint of synthetic organic chemistry. For example, by taking advantage of the high stability of C–F bonds, which do not react under conventional reaction conditions, it is possible to convert C–F bonds at a late stage of synthesis. On the other hand, it is necessary to decompose and effectively utilize materials and persistent pollutants bearing C–F bonds through “breaking bond” in terms of sustainability, while modern catalysis has focused on “making new bonds”. To pursue these challenges, the author has studied the development of catalytic transformations of C–F bonds of aryl and alkyl fluorides using precisely designed transition metal complexes as catalysts as described in this thesis.

## 2. Aryl fluorides

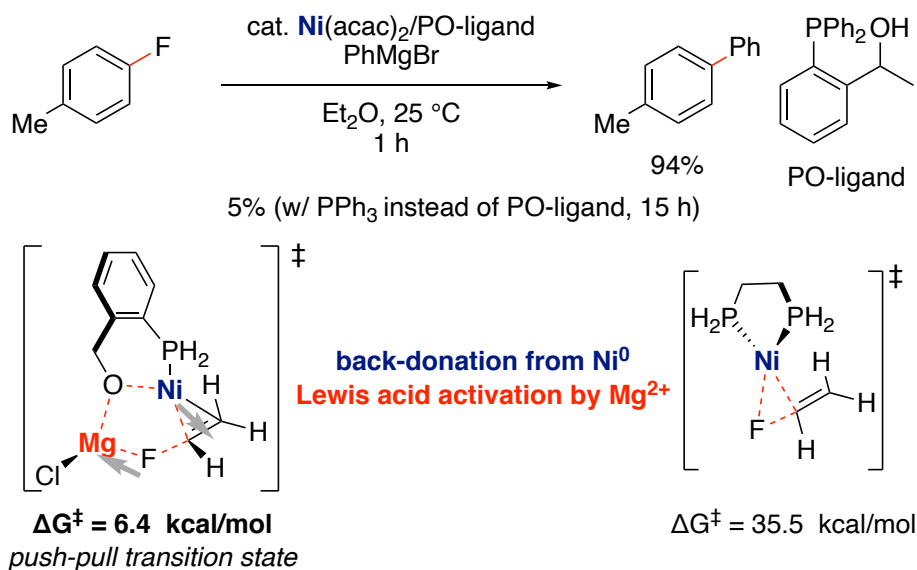
### Transformation of C(*sp*<sup>2</sup>)-F bonds

Although aryl fluorides are relatively more reactive in the S<sub>N</sub>Ar reactions than other aryl halides, harsh reaction conditions using strong bases are required for unactivated aryl fluorides.<sup>11</sup> In general, in order to carry out the S<sub>N</sub>Ar reactions of unactivated aryl fluorides under mild conditions, 1) the aromatic ring should be activated through coordination to an electron-deficient metal (*e.g.*, Cr(CO)<sub>3</sub> complexes,<sup>12</sup> Ru or Rh catalysts<sup>13</sup>) or 2) single-electron oxidation (*e.g.*, photocatalysts,<sup>14</sup> electrophotocatalysts,<sup>15</sup> oxidants<sup>16</sup>) is necessary to produce electrophilic radical cation species (Scheme 1-4, A). Aryl cations can also be generated from aryl fluorides by using strong Lewis acids such as silylium cations and aluminum compounds, which have a high fluoride ion affinity (FIA; Me<sub>3</sub>Si<sup>+</sup> 953 kJ/mol<sup>17</sup>, AlCl<sub>3</sub> 505 kJ/mol<sup>18</sup>) (Scheme 1-4, B). Single-electron reduction using strong reductant<sup>19</sup> ( $E^{\circ}_{\text{red}}$  vs. SCE: Li -3.2 V, Na -2.9 V, K -3.1 V)<sup>20</sup> can also convert the C(*sp*<sup>2</sup>)-F bonds of aryl fluorides ( $E^{\circ}_{\text{red}} \approx -2.97$  V vs. SCE)<sup>21</sup> (Scheme 1-4, C). Recently, hydrodefluorination<sup>22</sup> and defluorinative borylation<sup>23</sup> reactions have been developed by using photo-excited reductants. Many other transformations triggered by the oxidative addition of C-F bonds to low-valent metals have also been actively investigated (Scheme 1-4, D). This strategy is relevant to this thesis and described in more detail.

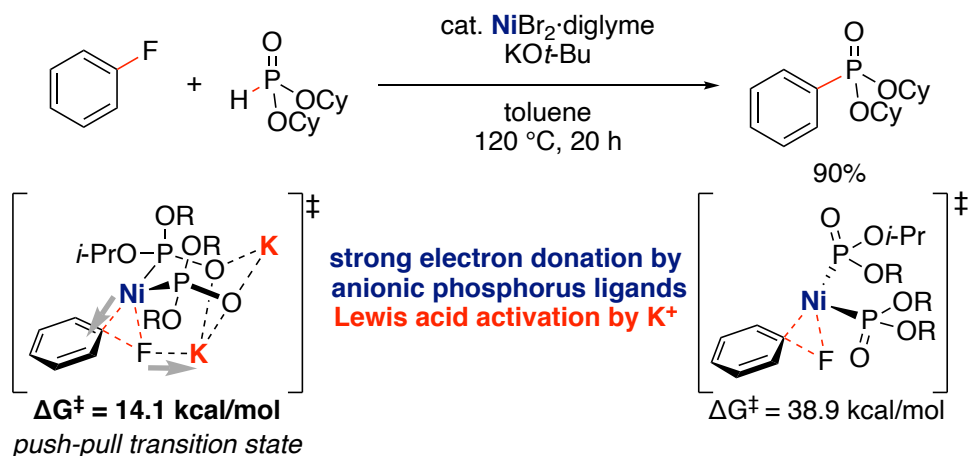
**Scheme 1-4.** General strategies for transformation of aryl fluorides.

The first catalytic conversion of unactivated aryl fluorides was invented five decades ago by Kumada, Tamao, and co-workers.<sup>24</sup> They reported the so-called KTC cross-coupling reaction of aryl fluorides by using an electron-rich Ni catalyst. Recently, Martin and co-workers isolated a complex derived from the oxidative addition of an aryl fluoride to a low-valent Ni complex.<sup>25</sup>

Nakamura and co-workers developed an efficient catalytic system based on Ni(acac)<sub>2</sub> and a PO-ligand, which bears a hydroxyl group, for the KTC coupling reactions with aryl fluorides (Scheme 1-5).<sup>26</sup> A Lewis acidic Mg cation is located near the Ni catalyst center, and the C(sp<sup>2</sup>)-F bond is cleaved through a cooperative activation mechanism by Lewis acidic metal and transition-metal. More specifically, the fluorine atom coordinates to the Mg cation and the C(sp<sup>2</sup>)-F bond is activated through electron-donation from the Ni center (push-pull mechanism).

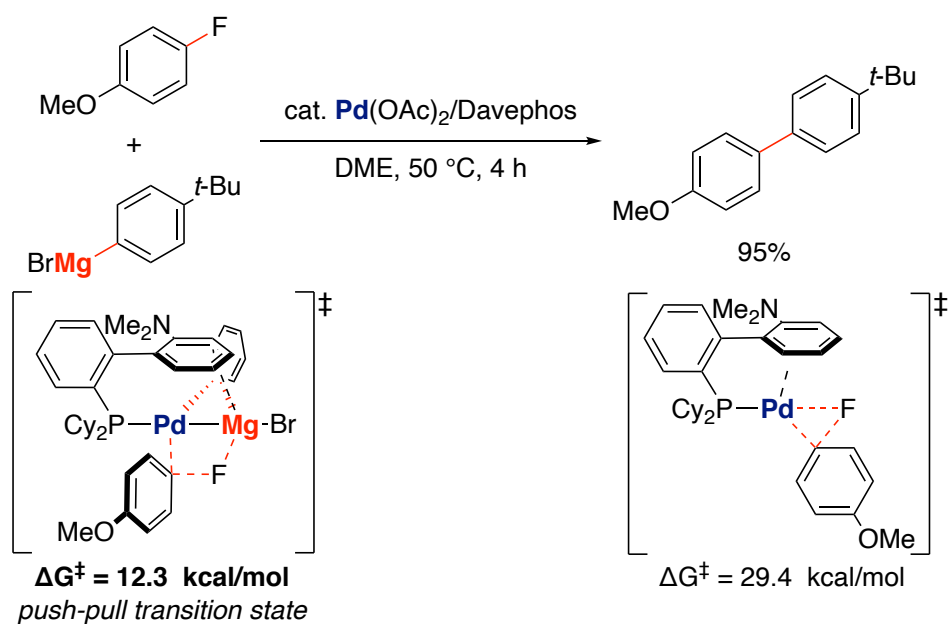
**Scheme 1-5.** Ni-catalyzed KTC coupling reaction through a push-pull mechanism.

This report has led to a series of studies utilizing the push-pull strategy by bringing Lewis acidic metals close to a transition metal center by using well-designed ligands such as a diaminophosphine oxide ligand.<sup>27</sup> In addition to the KTC reaction, phosphonylation<sup>28</sup> and silylation<sup>29</sup> reactions of aryl fluorides using a Ni catalyst/Lewis acidic metals have been developed (Scheme 1-6).

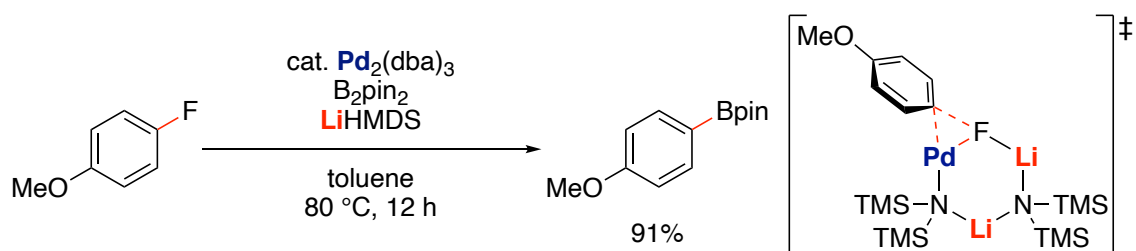
**Scheme 1-6.** Ni-catalyzed defluorophosphonylation of aryl fluorides.

Although some Pd catalysts have also been developed for catalytic transformations of C–F bonds, they require harsh reaction conditions and directing groups.<sup>30</sup> By utilizing the push-pull mechanism, the KTC coupling<sup>31</sup> reaction under mild conditions has been achieved by Pd catalysts (Scheme 1-7).

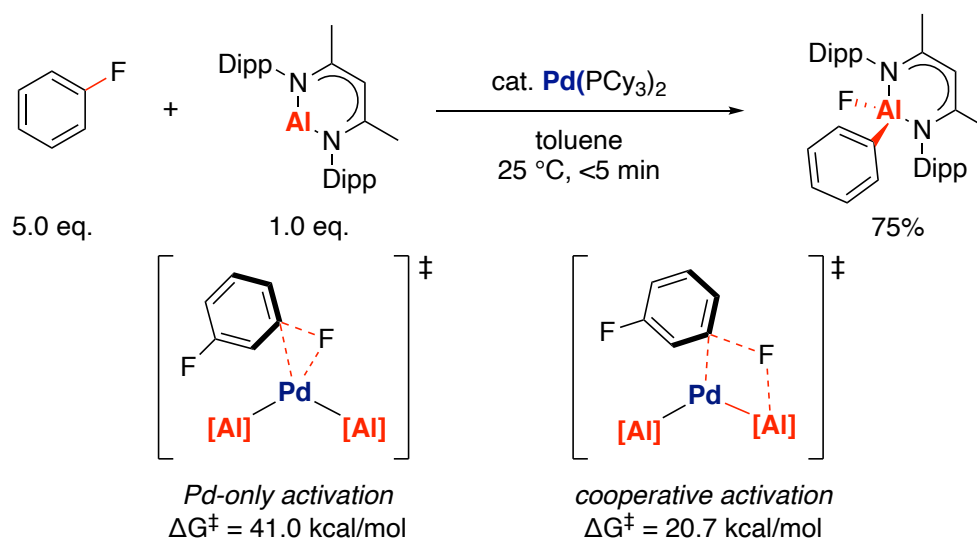
**Scheme 1-7.** Pd-catalyzed KTC coupling reaction with aryl fluorides.



Recently, Cao and co-workers developed Pd/LiHMDS catalysts, which are effective for the borylation<sup>32</sup> and the Sonogashira coupling<sup>33</sup> reactions through C–F bond activation (Scheme 1-8). In general, a distortion energy becomes significantly higher in the transition state of the C–F bond activation due to its high bond dissociation energy. They show that the 3+6-membered-ring activation mode is highly effective in the transition state to overcome the high strain energy.<sup>34</sup>

**Scheme 1-8.** Pd-catalyzed borylation of aryl fluorides.

Crimmin and co-workers have recently developed the Pd-catalyzed aluminium of aryl fluorides with an Al(I) reagent (Scheme 1-9).<sup>35</sup> Cooperative activation of the C–F bonds by Pd and Al is highly effective to allow the reaction to proceed at even  $-50\text{ }^\circ\text{C}$  and high site-selectivity with polyfluoroarenes.

**Scheme 1-9.** Pd-catalyzed aluminium of aryl fluorides.

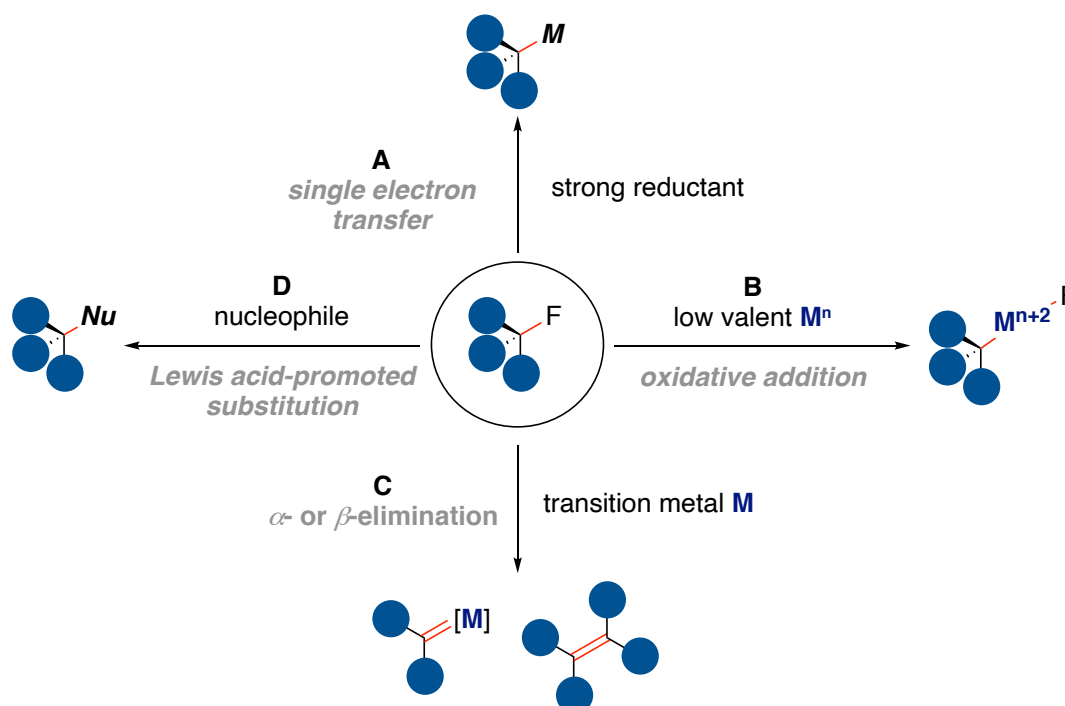


### 3. Alkyl fluorides

#### Transformation of C(sp<sup>3</sup>)-F bonds

Alkyl fluorides are extremely stable compounds and are generally difficult to further transform. Strong reductants such as alkaline metals and activated magnesium can reduce alkyl fluorides (Scheme 1-10, A).<sup>36</sup> Other strategies include (B) oxidative addition reaction to a low-valent metal center, (C)  $\alpha$ - and  $\beta$ -fluorine elimination through transition metal intermediates, and (D) nucleophilic substitution reactions promoted by Lewis acids (Scheme 1-10).

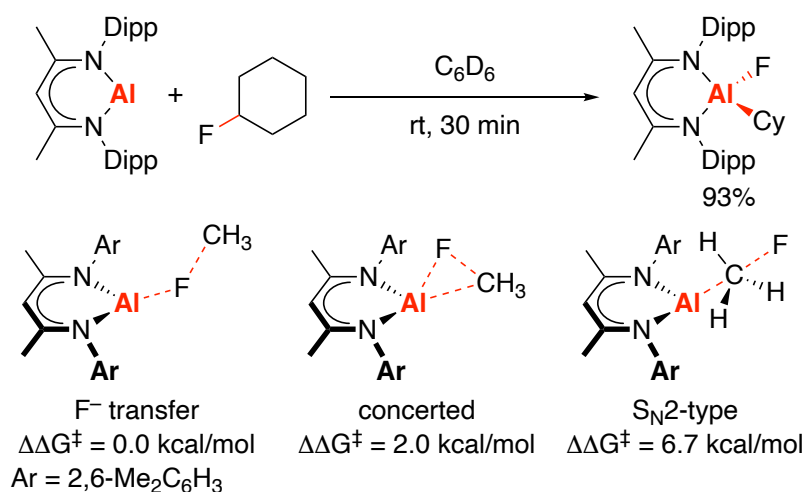
**Scheme 1-10.** General strategies for transformations of alkyl fluorides.



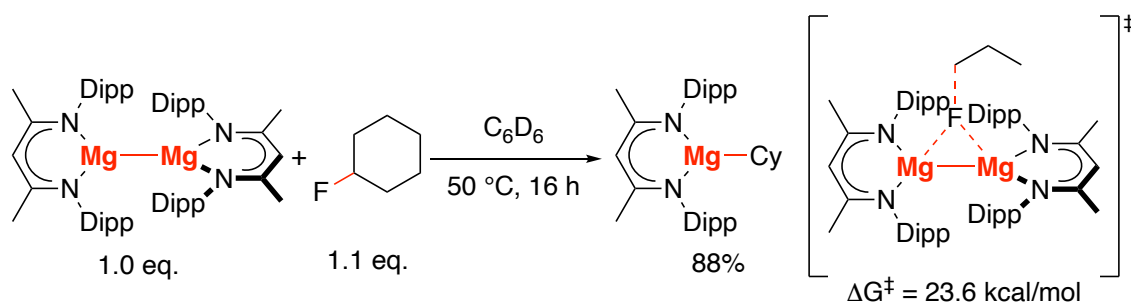
### 3-1. Oxidative addition of C(sp<sup>3</sup>)–F bonds

The direct oxidative addition reaction of a C(sp<sup>3</sup>)–F bond of simple alkyl fluorides has been achieved by using an Al(I) complex (Scheme 1-11).<sup>37</sup> Nikonov and co-workers reported that this reaction proceeded at –60 °C. Their theoretical calculations have revealed that a stepwise fluoride ion transfer mechanism is favored for the cleavage process.<sup>38</sup>

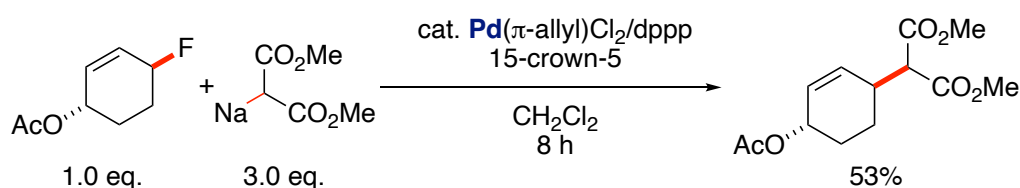
**Scheme 1-11.** Oxidative addition of fluorocyclohexane to the Al(I) center.



Crimmin and co-workers reported the formation of alkylmagnesium species through C–F bond cleavage by a dimeric Mg(I)–Mg(I) complex (Scheme 1-12).<sup>39</sup> Their computational studies have revealed that the C–F bond cleavage step proceeds in a unique frontside S<sub>N</sub>2 reaction mechanism. Here, not only the interaction between σ<sub>(Mg–Mg)</sub>-bond and σ\*<sub>(C–F)</sub>-bond, but also coordination of the F atom to the σ\*<sub>(Mg–Mg)</sub>-bond is supposedly important. Qualitatively, the organic group acts like a leaving group to bear a carbanion-like character.

**Scheme 1-12.** C(*sp*<sup>3</sup>)-F bond cleavage enabled by a dimeric Mg(I) complex.

Transition-metal catalyzed substitution reactions of allylic fluorides have been developed (Scheme 1-13).<sup>40</sup> More recently, the asymmetric desymmetrization of a benzylic difluoromethylene moiety was developed by Hartwig and co-workers.<sup>41</sup>

**Scheme 1-13.** Pd-catalyzed allylic substitution of allyl fluorides.

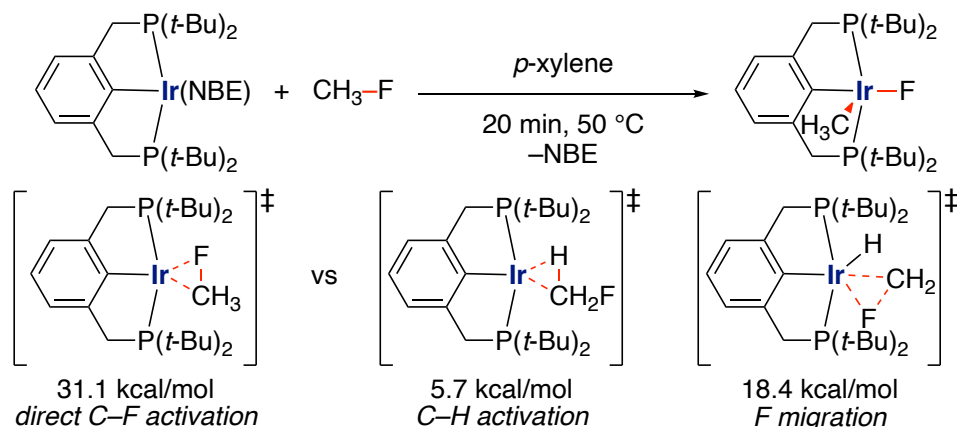
Ogoshi and co-workers have reported hydrodefluorination of benzotrifluorides catalyzed by a bis-NHC Ni complex.<sup>42</sup> They have successfully characterized the oxidative addition complex.

### 3-2. $\alpha$ -Elimination and $\beta$ -elimination

As mentioned above, the oxidative addition of C(*sp*<sup>3</sup>)-F bonds is not feasible, whereas different modes of C(*sp*<sup>3</sup>)-F bond cleavage by transition metal-catalysis can be possible through  $\alpha$ - and  $\beta$ -elimination reactions.<sup>43</sup> Krogh-Jespersen, Goldman, and co-workers reported a formal oxidative addition reaction of alkyl fluorides to a PCP-pincer

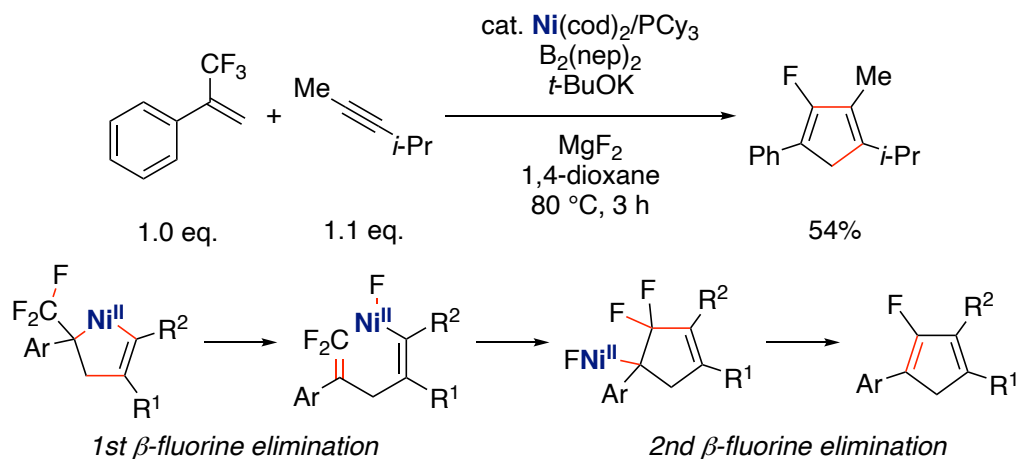
Ir complex (Scheme 1-14).<sup>44</sup> In this reaction, the C(sp<sup>3</sup>)-H bond at the  $\alpha$ -position of fluorine is cleaved first, and  $\alpha$ -fluorine elimination takes place to give a carbene complex. Subsequent hydrogen atom transfer gives a formal oxidative addition complex.

**Scheme 1-14.** Net oxidative addition of fluoromethane through  $\alpha$ -fluorine elimination.



Ichikawa and co-workers have described a Ni-catalyzed defluorinative [3 + 2] cycloaddition reaction, in which cyclic products are obtained *via* double  $\beta$ -fluorine eliminations (Scheme 1-15).<sup>45</sup>

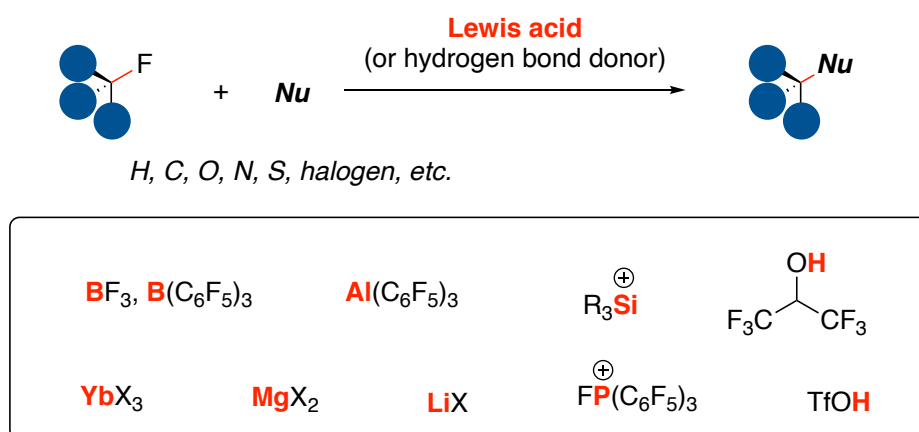
**Scheme 1-15.** [3 + 2]-Cycloaddition reaction through double  $\beta$ -fluorine eliminations.



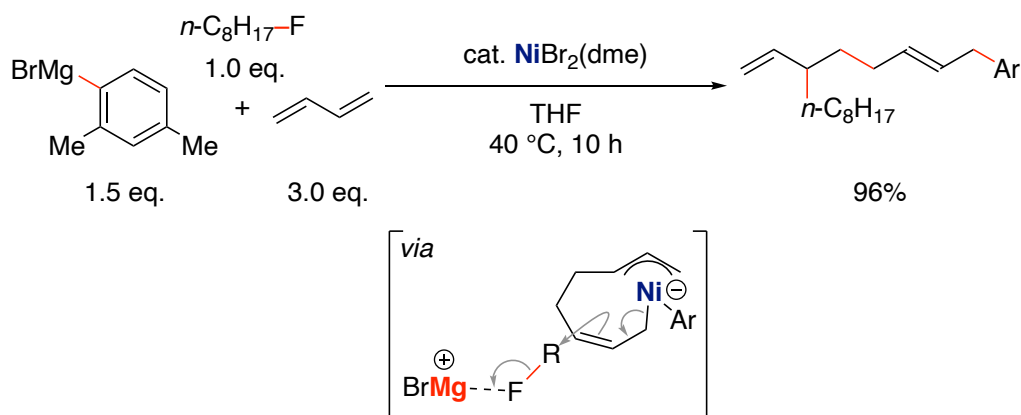
### 3-3. Lewis acid-promoted nucleophilic substitution reactions

Lewis acids such as boron, aluminum, silylium cations, phosphonium cations, and hydrogen-bond donors have been reported to abstract fluorine atoms from alkyl fluorides, allowing the S<sub>N</sub>1-type reaction to proceed (Scheme 1-16).<sup>46</sup> It has also been reported that halogen exchange reactions can proceed by metal halides such as MgI<sub>2</sub> and YbI<sub>3</sub> via S<sub>N</sub>2 or S<sub>N</sub>i mechanisms.

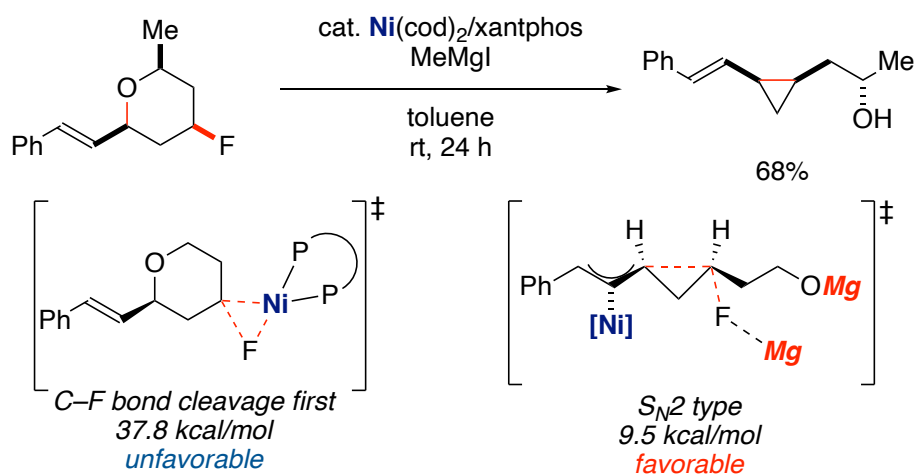
**Scheme 1-16.** Lewis acid-catalyzed/mediated substitution reactions.



Lewis acid-promoted and transition metal-catalyzed substitution reactions of alkyl fluorides have also been described. Kambe and co-workers have reported that an anionic transition-metal/magnesium cation system is effective for the cross-coupling reaction of alkyl fluorides (Scheme 1-17).<sup>47</sup> In this system, a Lewis acidic magnesium cation located near a transition-metal ate-complex as a counter ion binds to fluorine to assist the activation of C(sp<sup>3</sup>)-F bond by the nucleophilic transition metal center in an S<sub>N</sub>2 manner.

**Scheme 1-17.** Ni-catalyzed dimerizative alkylarylation of 1,3-butadiene.

Jarvo and co-workers have demonstrated a Ni-catalyzed cross-electrophile coupling reaction of alkyl fluorides (Scheme 1-18).<sup>48</sup> In this reaction, a Ni  $\pi$ -allyl complex generated upon C–O bond cleavage undergoes an intramolecular  $\text{S}_{\text{N}}2$  reaction to activate the  $\text{C}(\text{sp}^3)\text{-F}$  bond coordinating to a magnesium cation rather than direct oxidative addition of the  $\text{C}(\text{sp}^3)\text{-F}$  bond to a low-valent Ni complex.

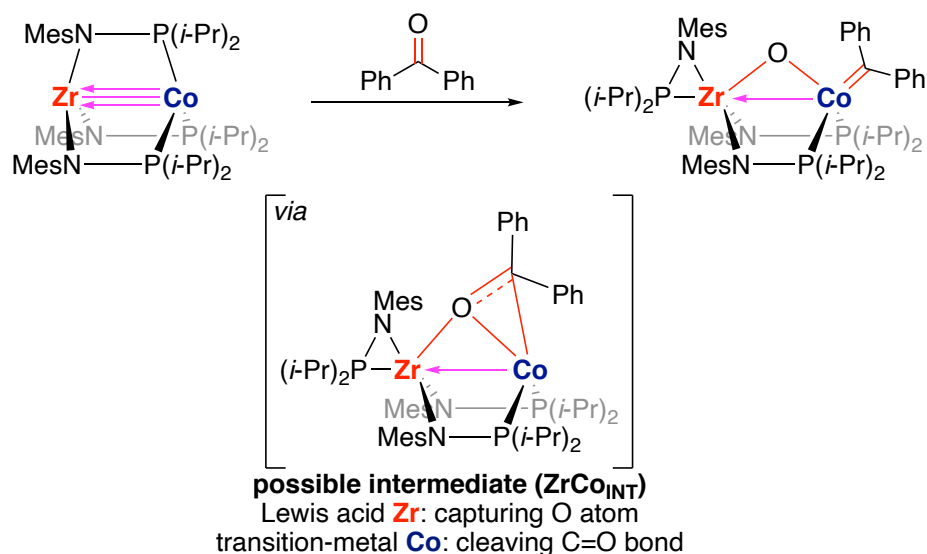
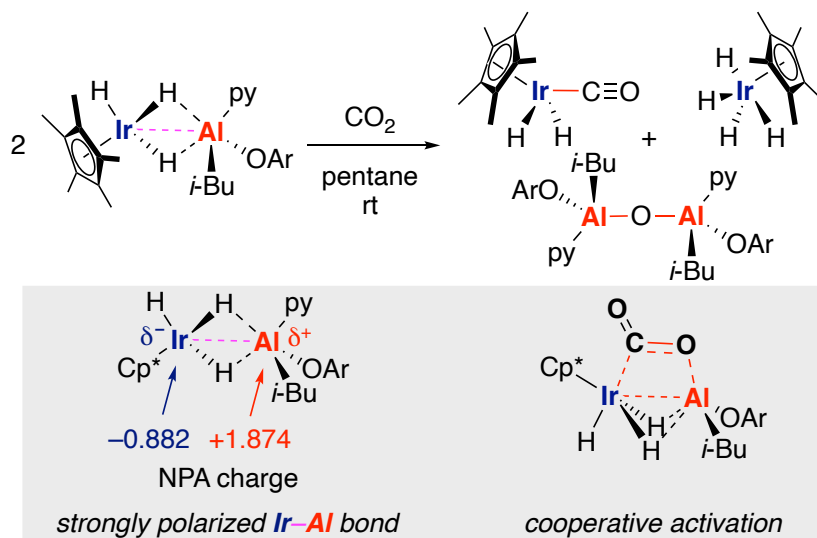
**Scheme 1-18.** Ni-catalyzed intramolecular cross-electrophile coupling.

#### 4. Polarized metal–metal bonds in inert bond activation

The combination of a Lewis acid and an electron-rich transition metal has found to be effective to achieve C–F bond transformation reactions in many cases as described above. For more efficient catalytic conversions of C–F bonds, it can be necessary not only to place such Lewis acidic metals close to the transition metal center, but also to make the transition metal center electron-richer to promote the bond cleavage steps. Therefore, the author has envisioned that by connecting a Lewis acidic metal and a transition metal, the strong  $\sigma$ -donicity of the electropositive metal would generate the electron-rich transition metal complex, and a cooperative action of these two metals would facilitate the activation of C–F bonds. Therefore, the author has focused on the potential of heterobimetallic complexes,<sup>49</sup> which have a Lewis acidic metal and an electron-rich transition metal for activating inert C–F bonds.

Thomas and co-workers have demonstrated that a heterobimetallic Zr–Co complex can cleave the carbonyl C=O double bond of benzophenone to form Co-carbene complex (Scheme 1-19).<sup>50</sup> They have proposed that the oxygen atom of benzophenone initially coordinate to the Lewis acidic Zr center to give ketyl radicals through a single-electron transfer. Afterward, the C=O bond cleavage by the Zr–Co bond proceeds through possible intermediate **ZrCo<sub>INT</sub>** to give the Co-carbene complex.

Camp and co-workers have found that a bimetallic Al–Ir complex activates the C=O double bond of carbon dioxide (Scheme 1-20).<sup>51</sup> Theoretical calculations have indicated that the metal–metal bond is polarized in an  $\text{Al}^+ \text{--} \text{Ir}^-$  form and the C=O bond can be activated in a cooperative manner across the polarized bond. The reactivity of the metal–metal bonds derived from a Lewis acidic metal and a late transition metal in activating small molecules has also been reported in many other studies.<sup>49</sup>

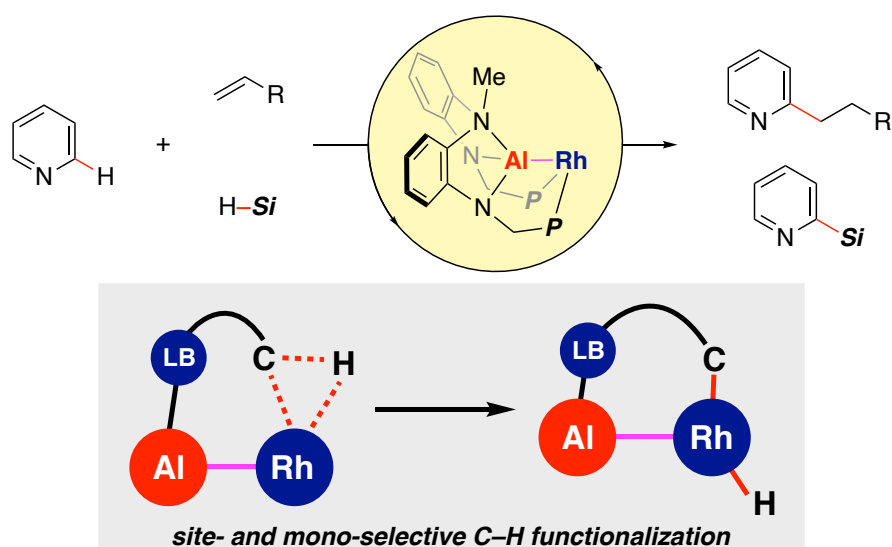
**Scheme 1-19.** Carbonyl C=O bond activation by a bimetallic Zr–Co complex.**Scheme 1-20.** Activation of carbon dioxide by a bimetallic Al–Ir complex.

Despite these interesting stoichiometric reactivity associated with heterobimetallic complexes, there have been only a few reports of catalytic transformations involving cooperative activation of inert bonds by polarized metal–metal bonds. The author's group has developed X-type group 13 metalloligands,<sup>52</sup> and catalytic

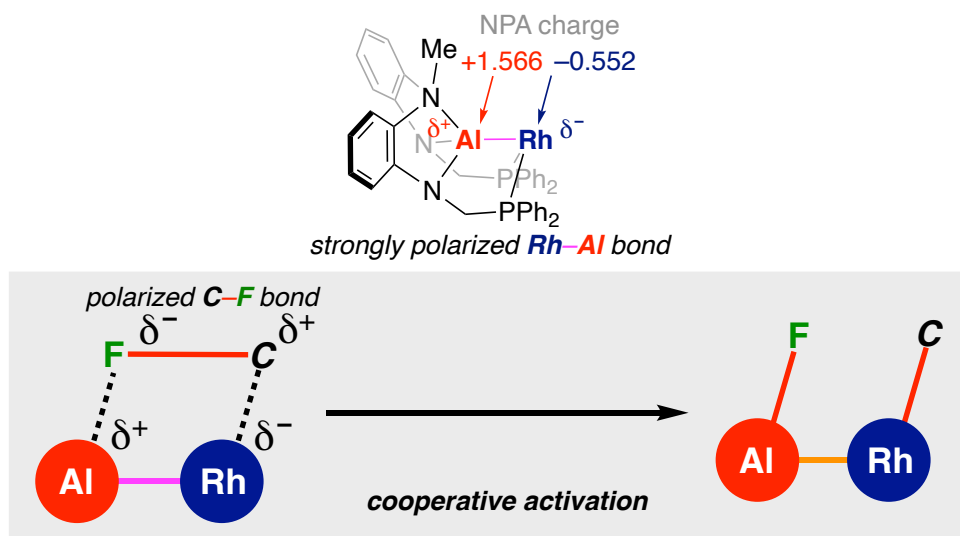


C–H alkylation and silylation reactions at the C2-position of pyridines using their Rh complexes (Scheme 1-21).<sup>53</sup> The X-type PAIP-pincer ligands are characterized by a high Lewis acidity due to the vacant p-orbital of Al and strong  $\sigma$ -donicity thanks to its high electronegativity. As a result, a pyridine substrate can be captured at the Al center, and the adjacent electron-rich Rh can activate the C–H bond at C2-position through oxidative addition.

**Scheme 1-21.** Catalytic C–H functionalization by an Al–Rh bimetallic complex.



The author's group has also investigated the electronic structure of the Al–Rh bimetallic complex by theoretical calculations and shown that the Al–Rh bond is highly polarized in an Al<sup>+</sup>–Rh<sup>−</sup> form (Scheme 1-22).<sup>54</sup> The author has envisioned that such unusual reversed E<sup>+</sup>–TM<sup>−</sup> bond polarization (E = group 13 element; TM = transition-metal) could allow the cleavage of polarized strong bonds such as C–F bonds to enable novel catalytic transformation of C–F bonds.

**Scheme 1-22.** Polarization of Al–Rh bonding for cooperative C–F bond activation.

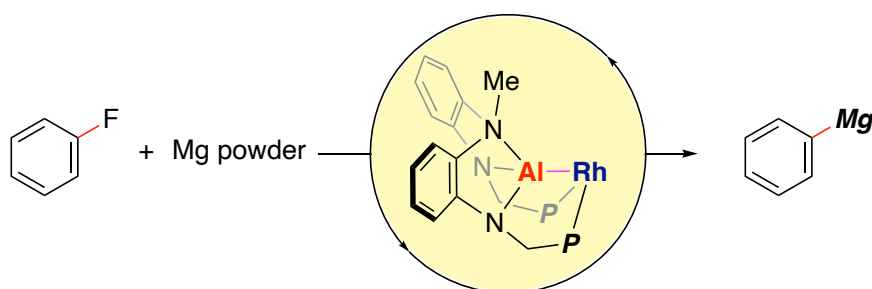
## 5. Overview of this Thesis

The author has focused on the unique property of the Al–Rh heterobimetallic complexes to develop catalytic transformations of C–F bonds through their cooperative activation by the highly polarized metal–metal bonding. He has found catalytic transformations proceed under mild conditions, which have been not trivial with conventional methods, by the bimetallic Al–Rh catalysts. The author has taken advantage of the bimetallic activation of C–F bonds to convert aryl fluorides to highly reactive arylmagnesium (Grignard) reagents. Both theoretical calculations and stoichiometric experiments have proved the mode of the cooperative activation of C–F bonds across the Al–Rh bond. The unique mode of C–F activation allows controlling a site-selectivity in C–F bond activation and formal cross-electrophile coupling reactions using aryl fluorides. Finally, the cooperative activation can also be applied to C( $sp^3$ )–F bonds of alkyl fluorides to develop their catalytic magnesiation reactions.

### 5-1. Magnesiumation of C(*sp*<sup>2</sup>)-F bonds of aryl fluorides catalyzed by Al-Rh bimetallic complexes (Chapter 2)

In Chapter 2, the author describes the magnesiumation reaction of C(*sp*<sup>2</sup>)-F bonds of aryl fluorides catalyzed by Al-Rh bimetallic complexes (Scheme 1-23). As mentioned above, the cleavage of C-F bonds is usually difficult due to their high chemical stability. Conventional methods to magnesiumate C(*sp*<sup>2</sup>)-F bonds have required a stoichiometric amount of highly reactive and pyrophoric reagents. The author demonstrates the strongly polarized Al-Rh bond readily activates a C(*sp*<sup>2</sup>)-F bond of aryl fluorides under mild conditions in a cooperative manner, that has fully been proved by theoretical calculations and stoichiometric experiments.

**Scheme 1-23.** Magnesiumation of aryl fluorides catalyzed by Al-Rh complexes (Chapter 2).

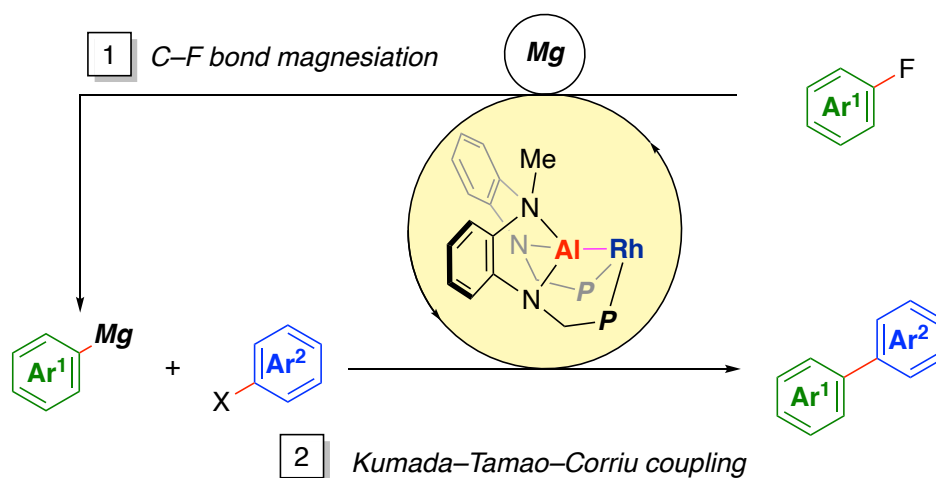


### 5-2. Kumada-Tamao-Corriu cross-coupling reaction catalyzed by Al-Rh bimetallic complexes (Chapter 3)

The author shows the Kumada-Tamao-Corriu (KTC) cross-coupling reaction can also be catalyzed by Al-Rh bimetallic complexes in Chapter 3 (Scheme 1-24). The reaction has been used widely in organic synthesis due to practicality and availability of organomagnesium reagents. In this study, the author shows that the Al-Rh complexes-catalyzes magnesiumation of aryl fluorides and then the KTC coupling reaction of

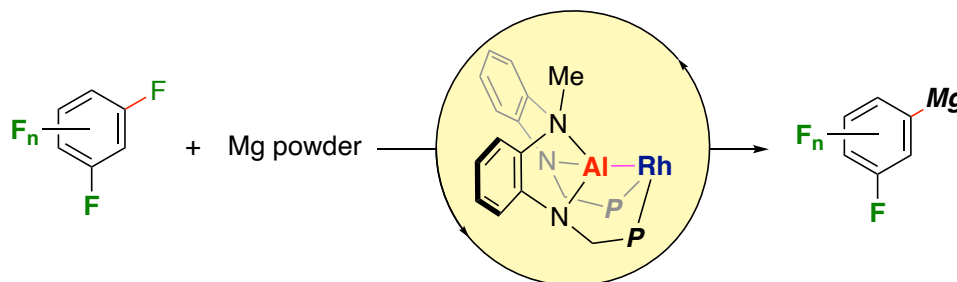
arylmagnesiums thus formed with added aryl halides to furnish unsymmetrical biaryls. This method allows to use aryl fluorides, which have been uncommon as a source of arylmagnesium reagents, to participate in the KTC coupling reactions.

**Scheme 1-24.** The Kumada–Tamao–Corriu cross-coupling reaction catalyzed by Al–Rh complexes (Chapter 3).



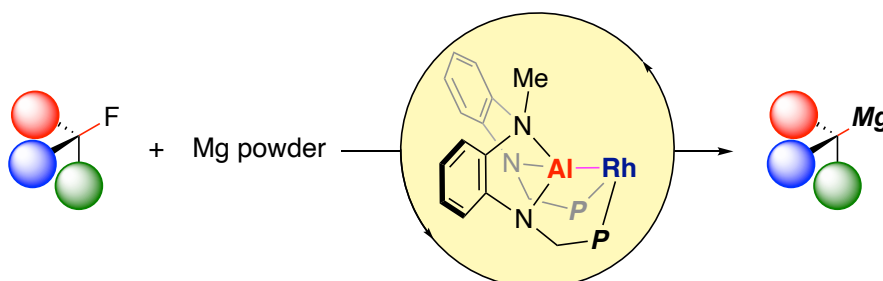
### 5-3. Site-selective magnesiation of C(sp<sup>2</sup>)–F bond of multi-fluorinated arenes catalyzed by Al–Rh bimetallic complexes (Chapter 4)

Chapter 4 shows catalyst-controlled site-selective magnesiation of a C(sp<sup>2</sup>)–F bond of multi-fluorinated arenes, taking advantage of the steric repulsion between arene substituents and the Al–Rh catalyst (Scheme 1-25). Fluorine-containing arylmagnesium reagents thus formed are shown to be useful to access some of fluorine-containing materials and drugs through the site-selective magnesiation reaction.

**Scheme 1-25.** Site-selective magnesiation of multi-fluorinated arenes (Chapter 4).

#### 5-4. Magnesiation of $C(sp^3)$ -F bonds of alkyl fluorides catalyzed by Al-Rh bimetallic complexes (Chapter 5)

In Chapter 5, the author describes that the Al-Rh bimetallic complexes catalyze the magnesiation of  $C(sp^3)$ -F bonds of alkyl fluorides using Mg powder (Scheme 1-26). The catalytic magnesiation also works with secondary and tertiary alkyl fluorides, which have been highly challenging to be reacted by conventional methods. The cooperative C-F activation by the polarized Al-Rh bond is thus shown to be a general strategy to allow novel catalytic transformations of fluoroorganic molecules.

**Scheme 1-26.** Magnesiation of alkyl fluorides catalyzed by Al-Rh complexes (Chapter 5).

**References and notes**

- (1) (a) MacMillan, D. W. *Nature* **2008**, *455*, 304. (b) Xiang, S.-H.; Tan, B. *Nat. Commun.* **2020**, *11*, 3786. (c) Hargittai, I. *Struct. Chem.* **2022**, *33*, 303.
- (2) (a) Arnold, F. H. *Angew. Chem. Int. Ed.* **2019**, *58*, 14420. (b) Arnold, F. H. *Angew. Chem. Int. Ed.* **2018**, *57*, 4143.
- (3) (a) Yorimitsu, H.; Kotori, M.; Patil, N. T. *Chem. Rec.* **2021**, *21*, 3335. (b) Johansson Seechurn, C.C.C.; Kitching, M. O.; Colacot, T. J.; Snieckus, V. *Angew. Chem. Int. Ed.* **2012**, *51*, 5062.
- (4) (a) Martin, R.; Buchwald, S. L. *Acc. Chem. Res.* **2008**, *41*, 1461. (b) Sather, A. C.; Buchwald, S. L. *Acc. Chem. Res.* **2016**, *49*, 2146. (c) Ingoglia, B. T.; Wagen, C. C.; Buchwald, S. L. *Tetrahedron* **2019**, *75*, 4199. (d) Kashihara, M.; Nakao, Y. *Acc. Chem. Res.* **2021**, *54*, 2928.
- (5) (a) Blanksby, S. J.; Ellison, G. B. *Acc. Chem. Res.* **2003**, *36*, 255. (b) Yu, D.-G.; Li, B.-J.; Shi, Z.-J. *Acc. Chem. Res.* **2010**, *43*, 1486. (c) Hiyama, T. *Organofluorine Compounds: Chemistry and Applications*, Springer, Berlin, 2000.
- (6) Pauling, L. *J. Am. Chem. Soc.* **1932**, *54*, 3570.
- (7) O'Hagan, D. *Chem. Soc. Rev.* **2008**, *37*, 308.
- (8) You, F.; Twieg, R. J. *Tetrahedron Lett.* **1999**, *40*, 8759.
- (9) Bajo, S.; Laidlaw, G.; Kennedy, A. R.; Sproules, S.; Nelson, D. J. *Organometallics* **2017**, *36*, 1662.
- (10) Hills, I. D.; Netherton, M. R.; Fu, G. C. *Angew. Chem. Int. Ed.* **2003**, *42*, 5749.
- (11) Diness, F.; Fairlie, D. *Angew. Chem. Int. Ed.* **2012**, *51*, 8012.
- (12) Rosillo, M.; Domínguez, G.; Pérez-Castells, J. *Chem. Soc. Rev.* **2007**, *36*, 1589.
- (13) (a) Kang, Q.-K.; Lin, Y.; Li, Y.; Shi, H. *J. Am. Chem. Soc.* **2020**, *142*, 3706. (b)

- Kang, Q.-K.; Lin, Y.; Li, Y.; Xu, L.; Li, K.; Shi, H. *Angew. Chem. Int. Ed.* **2021**, *60*, 20391.
- (14) Pistritto, V. A.; Schutzbach-Horton, M. E.; Nicewicz, D. A. *J. Am. Chem. Soc.* **2020**, *142*, 17187.
- (15) Huang, H.; Lambert, T. H. *Angew. Chem. Int. Ed.* **2020**, *59*, 658.
- (16) Shin, N. Y.; Tsui, E.; Reinhold, A.; Scholes, G. D.; Bird, M. J.; Knowles, R. R. *J. Am. Chem. Soc.* **2022**, *144*, 21783.
- (17) Erdmann, P.; Leitner, J.; Schwarz, J.; Greb, L. *ChemPhysChem* **2020**, *21*, 987.
- (18) Suzuki, N.; Fujita, T.; Amsharov, K. Y.; Ichikawa, J. *Chem. Commun.* **2016**, *52*, 12948.
- (19) (a) Meijs, G. F.; Bunnett, J. F.; Beckwith, A. L. J. *J. Am. Chem. Soc.* **1986**, *108*, 4899. (b) Guijarro, D.; Yus, M. *Tetrahedron* **2000**, *56*, 1135. (c) Rieke, R. D.; Bales, S. E. *J. Chem. Soc., Chem. Commun.* **1973**, 879.
- (20) Matsuura, N.; Umemoto, K.; Takeuchi, Z. *Bull. Chem. Soc. Jpn.* **1974**, *47*, 813.
- (21) Andrieux, C. P.; Blocman, C.; Savéant, J. M. *J. Electroanal. Chem. Interfacial Electrochem.* **1979**, *105*, 413.
- (22) (a) Ding, T.-H.; Qu, J.-P.; Kang, Y.-B. *Org. Lett.* **2020**, *22*, 3084. (b) Glaser, F.; Larsen, C. B.; Kerzig, C.; Wenger, O. S. *Photochem. Photobiol. Sci.* **2020**, *19*, 1035. (c) Toriumi, N.; Yamashita, K.; Iwasawa, N. *Chem. Eur. J.* **2021**, *27*, 12635. (d) Moore, J. T.; Dorantes, M. J.; Pengmei, Z.; Schwartz, T. M.; Schaffner, J.; Apps, S. L.; Gaggioli, C. A.; Das, U.; Gagliardi, L.; Blank, D. A.; Lu, C. C. *Angew. Chem. Int. Ed.* **2022**, *61*, e202205575.
- (23) Wang, S.; Wang, H.; König, B. *Chem* **2021**, *7*, 1653.
- (24) Kiso, Y.; Tamao, K.; Kumada, M. *J. Organomet. Chem.* **1973**, *50*, C12.

- (25) Liu, X.-W.; Echavarren, J.; Zarate, C.; Martin, R. *J. Am. Chem. Soc.* **2015**, *137*, 12470.
- (26) (a) Yoshikai, N.; Mashima, H.; Nakamura, E. *J. Am. Chem. Soc.* **2005**, *127*, 17978.  
(b) Yoshikai, N.; Yatsuda, H.; Nakamura, E. *J. Am. Chem. Soc.* **2009**, *131*, 9590.
- (27) Jin, Z.; Li, Y.-J.; Ma, Y.-Q.; Qiu, L.-L.; Fang, J.-X. *Chem. Eur. J.* **2012**, *18*, 446.
- (28) You, Z.; Masuda, Y.; Iwai, T.; Higashida, K.; Sawamura, M. *J. Org. Chem.* **2022**, *87*, 14731.
- (29) Cui, B.; Jia, S.; Tokunaga, E.; Shibata, N. *Nat. Commun.* **2018**, *9*, 4393.
- (30) (a) Dankwardt, J. W. *J. Organomet. Chem.* **2005**, *690*, 932. (b) Widdowson, D. A.; Wilhelm, R. *Chem. Commun.* **1999**, 2211. (c) Widdowson, D. A.; Wilhelm, R. *Chem. Commun.* **2003**, 578. (d) Sabater, S.; Mata, J. A.; Peris, E. *Nat. Commun.* **2013**, *4*, 2553. (e) Lucht, B. L.; Poss, M. J.; King, M. A.; Richmond, T. G. *J. Chem. Soc., Chem. Commun.* **1991**, 400. (f) Gianetti, T. L.; Bergman, R. G.; Arnold, J. *Chem. Sci.* **2014**, *5*, 2517.
- (31) Wu, C.; McCollom, S. P.; Zheng, Z.; Zhang, J.; Sha, S.-C.; Li, M.; Walsh, P. J.; Tomson, N. C. *ACS Catal.* **2020**, *10*, 7934.
- (32) Zhao, X.; Wu, M.; Liu, Y.; Cao, S. *Org. Lett.* **2018**, *20*, 5564.
- (33) He, J.; Yang, K.; Zhao, J.; Cao, S. *Org. Lett.* **2019**, *21*, 9714.
- (34) Li, X.-X.; Wang, J.-S.; You, X.-X.; Zhong, R.-L.; Su, Z.-M. *J. Org. Chem.* **2022**, *87*, 16039.
- (35) Rekhroukh, F.; Chen, W.; Brown, R. K.; White, A. J. P.; Crimmin, M. R. *Chem. Sci.* **2020**, *11*, 7842.
- (36) (a) Guijarro, D.; Martínez, P.; Yus, M. *Tetrahedron* **2003**, *59*, 1237. (b) Ashby, E. C.; Yu, S. H.; Beach, R. G. *J. Am. Chem. Soc.* **1970**, *92*, 433. (c) Rieke, R. D.; Bales,



- S. E. *J. Am. Chem. Soc.* **1974**, *96*, 1775.
- (37) (a) Crimmin, M. R.; Butler, M. J.; White, A. J. P. *Chem. Commun.* **2015**, *51*, 15994.  
(b) Chu, T.; Boyko, Y.; Korobkov, I.; Nikonov, G. I. *Organometallics* **2015**, *34*, 5363.
- (38) Pitsch, C. E.; Wang, X. *Chem. Commun.* **2017**, *53*, 8196.
- (39) Coates, G.; Ward, B. J.; Bakewell, C.; White, A. J. P.; Crimmin, M. R. *Chem. Eur. J.* **2018**, *24*, 16282.
- (40) (a) Hazari, A.; Gouverneur, V.; Brown, J. M. *Angew. Chem, Int. Ed.* **2009**, *48*, 1296.  
(b) Blessley, G.; Holden, P.; Walker, M.; Brown, J. M.; Gouverneur, V. *Org. Lett.* **2012**, *14*, 2754.
- (41) Butcher, T. W.; Yang, J. L.; Amberg, W. M.; Watkins, N. B.; Wilkinson, N. D.; Hartwig, J. F. *Nature* **2020**, *583*, 548.
- (42) Iwamoto, H.; Imiya, H.; Ohashi, M.; Ogoshi, S. *J. Am. Chem. Soc.* **2020**, *142*, 19360.
- (43) Karimzadeh-Younjali, M.; Wendt, O. F. *Helv. Chim. Acta* **2021**, *104*, e2100114.
- (44) Choi, J.; Wang, D. Y.; Kundu, S.; Choliy, Y.; Emge, T. J.; Krogh-Jespersen, K.; Goldman, A. S. *Science* **2011**, *332*, 1545.
- (45) (a) Fujita, T.; Arita, T.; Ichitsuka, T.; Ichikawa, J. *Dalton Trans.* **2015**, *44*, 19460.  
(b) Ichitsuka, T.; Fujita, T.; Arita, T.; Ichikawa, J. *Angew. Chem. Int. Ed.* **2014**, *53*, 7564. (c) Ichitsuka, T.; Fujita, T.; Ichikawa, J. *ACS Catal.* **2015**, *5*, 5947.
- (46) (a) Vasilopoulos, A.; Golden, D. L.; Buss, J. A.; Stahl, S. S. *Org. Lett.* **2020**, *22*, 5753. (b) Jaiswal, A. K.; Goh, K. K. K.; Sung, S.; Young, R. D. *Org. Lett.* **2017**, *19*, 1934. (c) Champagne, P. A.; Benhassine, Y.; Desroches, J.; Paquin, J. *Angew. Chem. Int. Ed.* **2014**, *53*, 13835. (d) Caputo, C. B.; Hounjet, L. J.; Dobrovetsky, R.; Stephan, D. W. *Science* **2013**, *341*, 1374. (e) Stahl, T.; Klare, H. F. T.; Oestreich,

- M. *ACS Catal.* **2013**, *3*, 1578. (f) Dryzhakov, M.; Richmond, E.; Li, G.; Moran, J. *J. Fluorine Chem.* **2017**, *193*, 45. (g) Willcox, D. R.; Nichol, G. S.; Thomas, S. P. *ACS Catal.* **2021**, *11*, 3190. (h) Wang, F.; Nishimoto, Y.; Yasuda, M. *J. Am. Chem. Soc.* **2021**, *143*, 20616.
- (47) Iwasaki, T.; Min, X.; Fukuoka, A.; Kuniyasu, H.; Kambe, N. *Angew. Chem. Int. Ed.* **2016**, *55*, 5550.
- (48) (a) Erickson, L. W.; Lucas, E. L.; Tollefson, E. J.; Jarvo, E. R. *J. Am. Chem. Soc.* **2016**, *138*, 14006. (b) Xu, Z.; Yang, Y.; Jiang, J.; Fu, Y. *Organometallics* **2018**, *37*, 1114.
- (49) (a) Charles, R. M.; Brewster, T. P. *Coord. Chem. Rev.* **2021**, *433*, 213765. (b) Bauer, J.; Braunschweig, H.; Dewhurst, R. D. *Chem. Rev.* **2012**, *112*, 4329. (c) Mankad, N. P. *Chem. Commun.* **2018**, *54*, 1291. (d) Stephan, D. W. *Coord. Chem. Rev.* **1989**, *95*, 41. (e) Govindarajan, R.; Deolka, S.; Khusnutdinova, J. R. *Chem. Sci.* **2022**, *13*, 14008. (f) Chatterjee, B.; Chang, W. C.; Jena, S.; Werlé, C. *ACS Catal.* **2020**, *10*, 14024. (g) Navarro, M.; Moreno, J. J.; Pérez-Jiménez, M.; Campos, J. *Chem. Commun.* **2022**, *58*, 11220. (h) Wang, Q.; Brooks, S. H.; Liu, T.; Tomson, N. C. *Chem. Commun.* **2021**, *57*, 2839. (i) Jansen, G.; Schubart, M.; Findeis, B.; Gade, L. H.; Scowen, I. J.; McPartlin, M. *J. Am. Chem. Soc.* **1998**, *120*, 7239.
- (50) (a) Marquard, S. L.; Bezpalko, M. W.; Foxman, B. M.; Thomas, C. M. *J. Am. Chem. Soc.* **2013**, *135*, 6018. (b) Zhang, H.; Wu, B.; Marquard, S. L.; Litle, E. D.; Dickie, D. A.; Bezpalko, M. W.; Foxman, B. M.; Thomas, C. M. *Organometallics* **2017**, *36*, 3498. (c) Marquard, S. L.; Bezpalko, M. W.; Foxman, B. M.; Thomas, C. M. *Organometallics* **2014**, *33*, 2071. (d) Zhou, W.; Marquard, S. L.; Bezpalko, M. W.; Foxman, B. M.; Thomas, C. M. *Organometallics* **2013**, *32*, 1766. (e) Krogman, J.

- P.; Foxman, B. M.; Thomas, C. M. *J. Am. Chem. Soc.* **2011**, *133*, 14582.
- (51) Escomel, L.; Rosal, I. D.; Maron, L.; Jeanneau, E.; Veyre, L.; Thieuleux, C.; Camp, C. *J. Am. Chem. Soc.* **2021**, *143*, 4844.
- (52) (a) Hara, N.; Semba, K.; Nakao, Y. *ACS Catal.* **2022**, *12*, 1626. (b) Takaya, J. *Chem. Sci.* **2021**, *12*, 1964. (c) Komuro, T.; Nakajima, Y.; Takaya, J.; Hashimoto, H. *Coord. Chem. Rev.* **2022**, *473*, 214837.
- (53) (a) Hara, N.; Saito, T.; Semba, K.; Kuriakose, N.; Zheng, H.; Sakaki, S.; Nakao, Y. *J. Am. Chem. Soc.* **2018**, *140*, 7070. (b) Hara, N.; Uemura, N.; Nakao, Y. *Chem. Commun.* **2021**, *57*, 5957. (c) Hara, N.; Aso, K.; Li, Q.-Z.; Sakaki, S.; Nakao, Y. *Tetrahedron* **2021**, *95*, 132339.
- (54) (a) Hara, N.; Yamamoto, K.; Tanaka, Y.; Saito, T.; Sakaki, S.; Nakao, Y. *Bull. Chem. Soc. Jpn.* **2021**, *94*, 1859. (b) Li, Q.-Z.; Hara, N.; Semba, K.; Nakao, Y.; Sakaki, S. *Top. Catal.*, **2022**, *65*, 392.

## **Chapter 2**

### **Magnesiumation of Aryl Fluorides Catalyzed by a Rhodium–Aluminum Complex**

The author reports the magnesiumation of aryl fluorides catalyzed by an Al–Rh heterobimetallic complex. The author shows that the complex is highly reactive to cleave the C–F bonds across the polarized Al–Rh bond under mild conditions. The reaction allows the use of an easy-to-handle magnesium powder to generate a range of arylmagnesium reagents from aryl fluorides, which are conventionally inert to such metalation compared with other aryl halides.

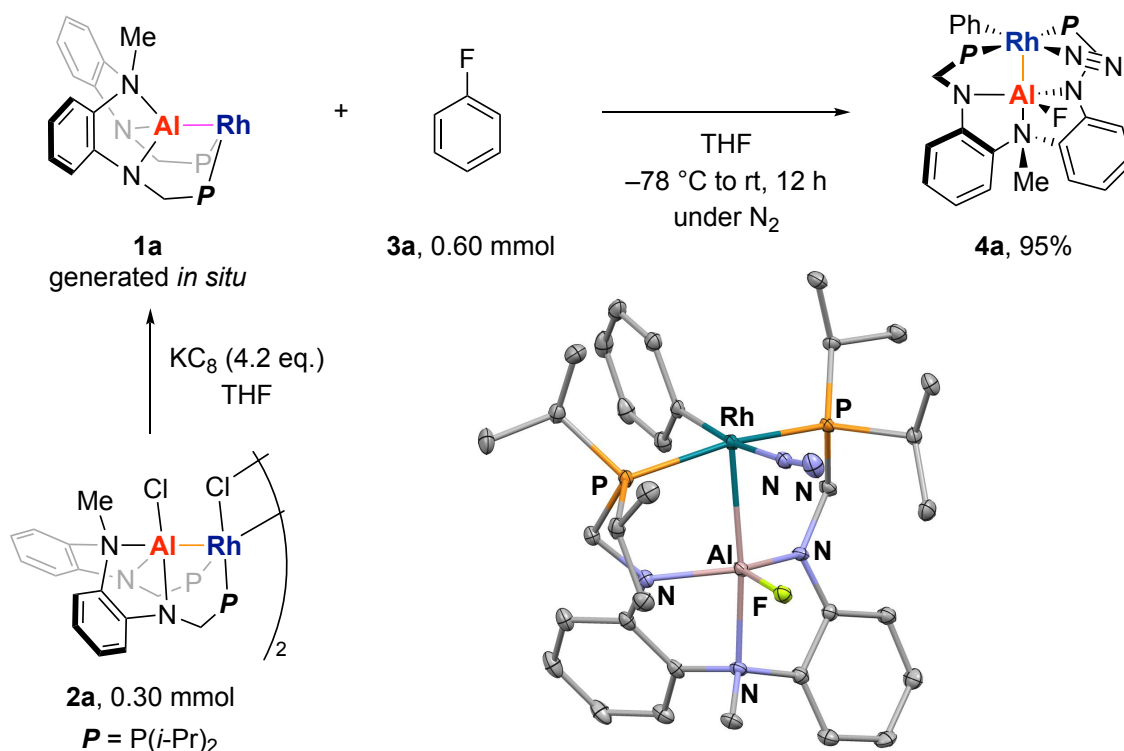
## Introduction

Complexes that contain metal–metal bonds have received considerable attention in organometallic chemistry due to their unique electronic properties, which differ significantly from those of single-metal systems, especially with respect to achieving novel organic transformations.<sup>1</sup> Among complexes with metal–metal bonds, heterobimetallic metal–metal bonding motifs are particularly reactive towards the cleavage of conventionally inert bonds due to their inherent polarization. In a pioneering study, Bergman showed that Zr–Ir complexes can activate a variety of thermodynamically strong bonds including O–H and N–H bonds.<sup>2</sup> B–Rh<sup>3</sup> and Si–Rh<sup>4</sup> manifolds have been reported to effectively activate C–F bonds<sup>5</sup> in perfluorinated organic molecules such as pentafluoropyridine and hexafluorobenzene. Moreover, a Zr–Co complex realizes the challenging activation of the C=O bond in benzophenone to afford a cobalt carbene complex.<sup>6</sup> However, catalytic transformations that include these bond-activation events remain elusive. Recently, the author's group has developed an Al–Rh heterobimetallic complex in which an X-type Al moiety<sup>7</sup> is ligated to the Rh center, and demonstrated its reactivity in the alkylation of pyridines.<sup>8a</sup> An NBO analysis suggested a polarized Al<sup>δ+</sup>–Rh<sup>δ-</sup> bond, and this result prompted us to test the reactivity of such Al–Rh bonds in the context of cleaving  $\sigma$ -bonds, which usually exhibit high bond-dissociation energies. The author's group previously reported that the energy level of the orbital containing the Al–Rh bond in (Me<sub>2</sub>Al)Rh(PMe<sub>3</sub>)<sub>2</sub> was higher than those containing the B–Rh bond in (Me<sub>2</sub>B)Rh(PMe<sub>3</sub>)<sub>2</sub> and the Si–Rh bond in (Me<sub>3</sub>Si)Rh(PMe<sub>3</sub>)<sub>2</sub>.<sup>8b</sup> The author thus expected reactivity of the Al–Rh bonds toward the C–F bond activation higher than that of B–Rh and Si–Rh bonds based on these results. Herein, the author reports the activation of C–F bonds in fluor arenes by means of an Al–Rh bond under very mild conditions, which

results in an unprecedented catalytic magnesiation of fluoroarenes using easy-to-handle Mg powder.<sup>9</sup>

## Results and discussion

The reaction of Al–Rh complex **1a**, which was generated in situ by the reduction of Al–Rh complex **2a**<sup>8a</sup> with KC<sub>8</sub>, and fluorobenzene (**3a**) under N<sub>2</sub> resulted in the activation of the C–F bond at the Al–Rh bond to afford complex **4a** in 95% yield (Scheme 2-1). The solid-state structure of **4a** was determined unequivocally by single-crystal x-ray diffraction analysis. In **4a**, the Al(III) moiety coordinates to the Rh center as an electron-accepting Z-type ligand<sup>10</sup> with trigonal bipyramidal geometry. The Rh center adopts a square-pyramidal geometry stabilized by an end-on N<sub>2</sub> ligand. It is noteworthy that the C–F-bond activation proceeds even at –30 °C (Eq. S2-1, Figures S2-5 and S2-6). To the best of the author’s knowledge, these are the mildest hitherto reported conditions for the activation of unactivated C–F bonds by a homogeneous metal complex.



**Scheme 2-1.** C–F bond activation by Al–Rh complex **1a**.

To gain mechanistic insights into the C–F-bond activation by **1a**, the reaction pathway was theoretically modelled by DFT calculations (Figures 2-1, S2-12, and S2-13, Tables S2-2 and S2-3). The C2=C3 bond of fluorobenzene coordinates to the Rh atom and the F atom occupies the position close to the Al atom in Al–Rh  $\sigma$ -complex **1AD1**. The C–F bond of **1AD1** then changes its orientation to give adduct **1AD2**. The activation of the C–F bond occurs at the Al–Rh  $\sigma$ -bond in a cooperative fashion to afford Rh–phenyl complex **4b** via transition state **TS**. After isomerization, which includes a positional change of the Ph group, followed by coordination of N<sub>2</sub>, another Rh–phenyl complex **4a** is generated. The Gibbs energy of activation ( $\Delta G^{\ddagger}$ ) and the Gibbs energy of reaction ( $\Delta G^{\circ}$ ) were estimated to be 3.7 kcal mol<sup>-1</sup> and -63.5 kcal mol<sup>-1</sup>, respectively (blue line in Figure 2-1). The very small  $\Delta G^{\ddagger}$  stands in sharp contrast to the considerably large  $\Delta G^{\ddagger}$  required for the activation of the C–F bond by Rh alone (24.2 kcal mol<sup>-1</sup>; red lines in

Figure 2-1). The small  $\Delta G^\ddagger$  value obtained for the cooperative activation of the C–F bond matches well with the experimentally observed reaction, which proceeds at low temperature.

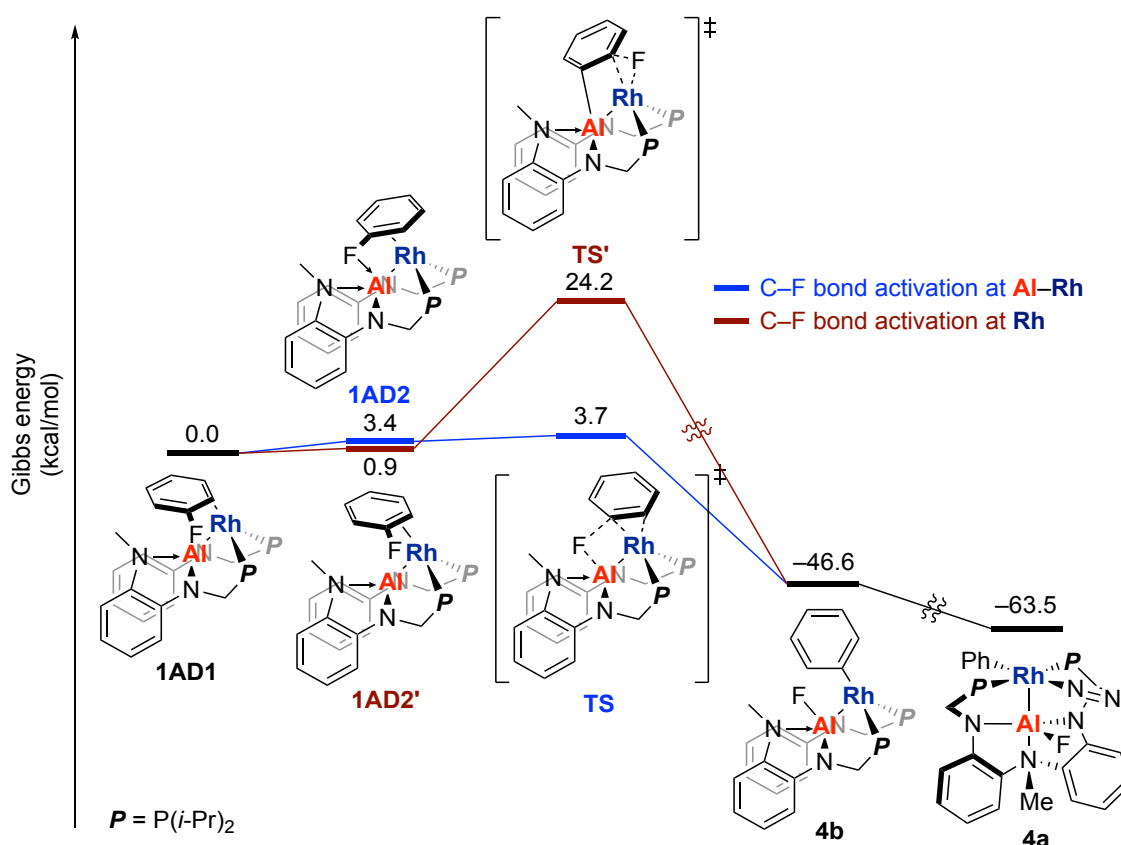
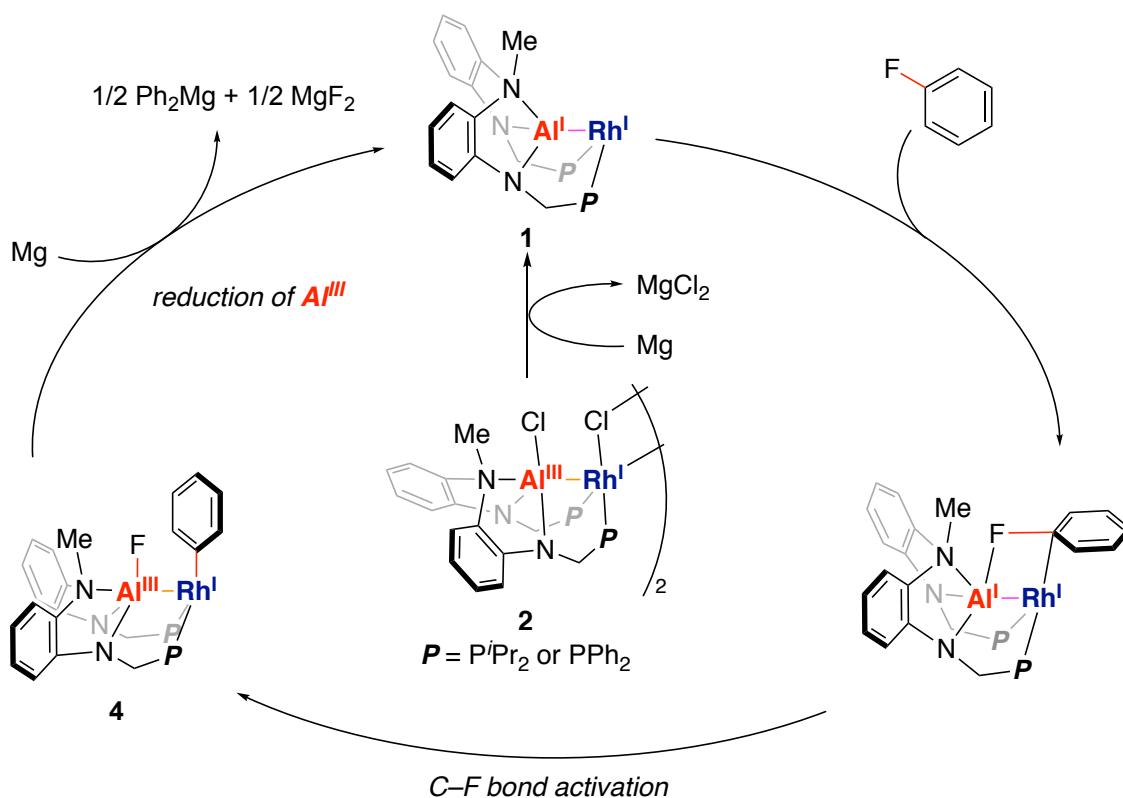


**Figure 2-1.** Energy diagram of the C–F bond activation of 3a by 1a.

Next, the author turned his attention to developing new catalytic transformations based on the unique reactivity of this Al–Rh manifold toward the activation of C–F bonds. The author's working hypothesis is shown in Scheme 2-2. The author anticipated that the C–F-bond activation would afford Z-type Al<sup>III</sup>–Rh<sup>I</sup> complex 4, which could potentially be reduced with Mg to realize a catalytic magnesiation of Ar–F bonds. The reduction potential of Mg metal should be sufficiently high to reduce the Al



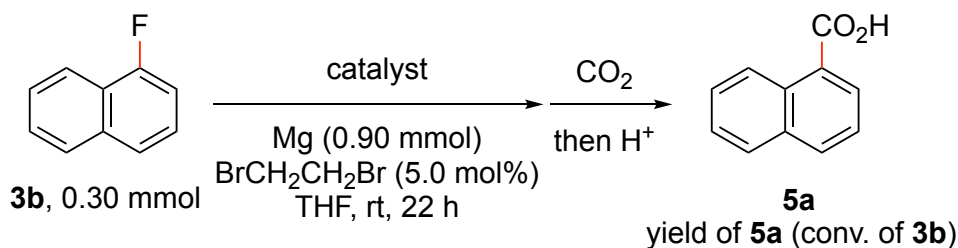
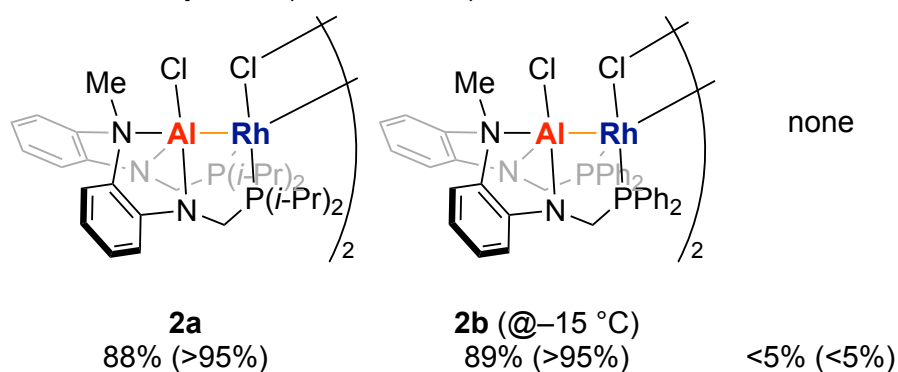
center of **4** ( $\text{Mg}^{2+}/\text{Mg} = -2.4 \text{ V}$ ;  $\text{Al}^{3+}/\text{Al} = -1.7 \text{ V}$  vs SHE).<sup>12</sup> In contrast to the magnesiation of Ar–X bonds ( $\text{X} = \text{I}, \text{Br}, \text{Cl}$ ),<sup>13</sup> that of Ar–F bonds is extremely difficult, even for highly dispersed Mg.<sup>14</sup> For example, the magnesiation of *p*-fluorotoluene proceeds only in moderate efficiency, even when a large excess of Rieke magnesium is used in refluxing THF.<sup>14a</sup> Although the magnesiation of the C–F bond with Mg(I)–Mg(I) complexes has recently been reported,<sup>5h–k</sup> precedents of the magnesiation of C–F bonds using readily available and easy-to-handle Mg powder remain elusive.



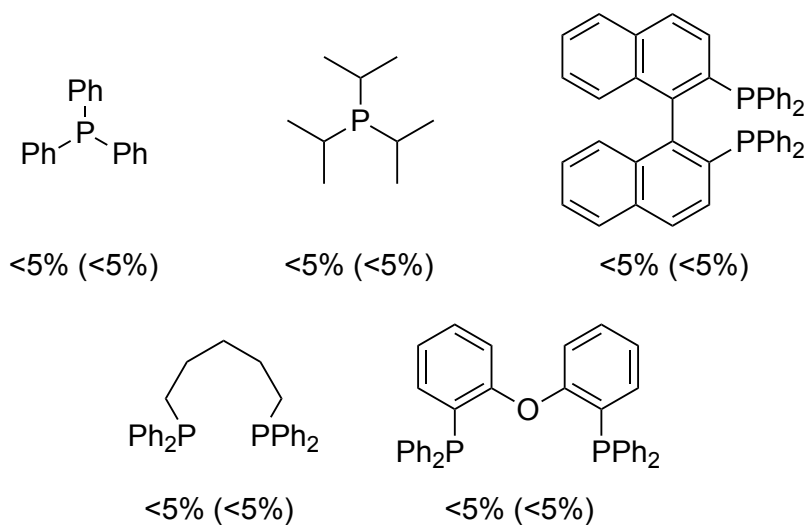
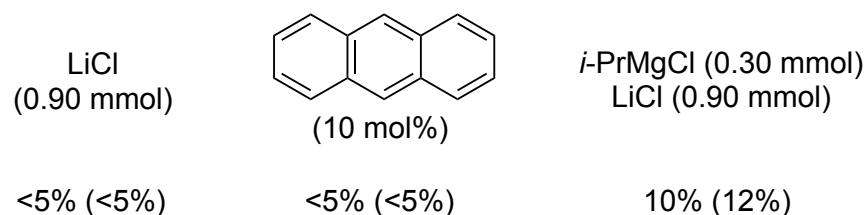
**Scheme 2-2.** A plausible catalytic cycle for the magnesiation of aryl fluorides using Al–Rh complexes such as **2**.

The proposed catalytic magnesiation of 1-fluoronaphthalene (**3b**, 0.30 mmol) with Mg powder (0.90 mmol), which was pre-activated upon treatment with 1,2-

dibromoethane (5.0 mol%), was attempted in the presence of various catalysts in THF at room temperature (Scheme 2-3). Gratifyingly, 1-naphthoic acid (**5a**) was obtained in 88% NMR yield using **2a** (5.0 mol% Rh) after quenching of the reaction with CO<sub>2</sub> (1 atm), followed by acidic work-up using 3 M HCl. Al–Rh complex **2b**, which bears phenyl groups on the phosphorus atoms instead of isopropyl groups, also furnished **5a** in high yield. The reaction did not proceed in the absence of an Al–Rh complex. Catalytic systems based on [RhCl(nbd)]<sub>2</sub> (5.0 mol% Rh; nbd = 2,5-norbornadiene)/phosphorus ligands (10 mol% P)/Et<sub>2</sub>AlCl (20 mol%) did not afford **5a**. Adding LiCl, which facilitates the magnesiation of C–Br bonds,<sup>15</sup> or adding a catalytic amount of anthracene, to generate magnesium anthracene,<sup>16</sup> did not show any effect. Using *i*-PrMgCl·LiCl led to the magnesiation of **3b** to afford **5a** in low yield, albeit that this approach is unsuitable for simple aryl fluorides such as **3a**.<sup>17</sup> Accordingly, it can be concluded that only Al–Rh complexes **2a** and **2b** catalyze the magnesiation of aryl fluorides.

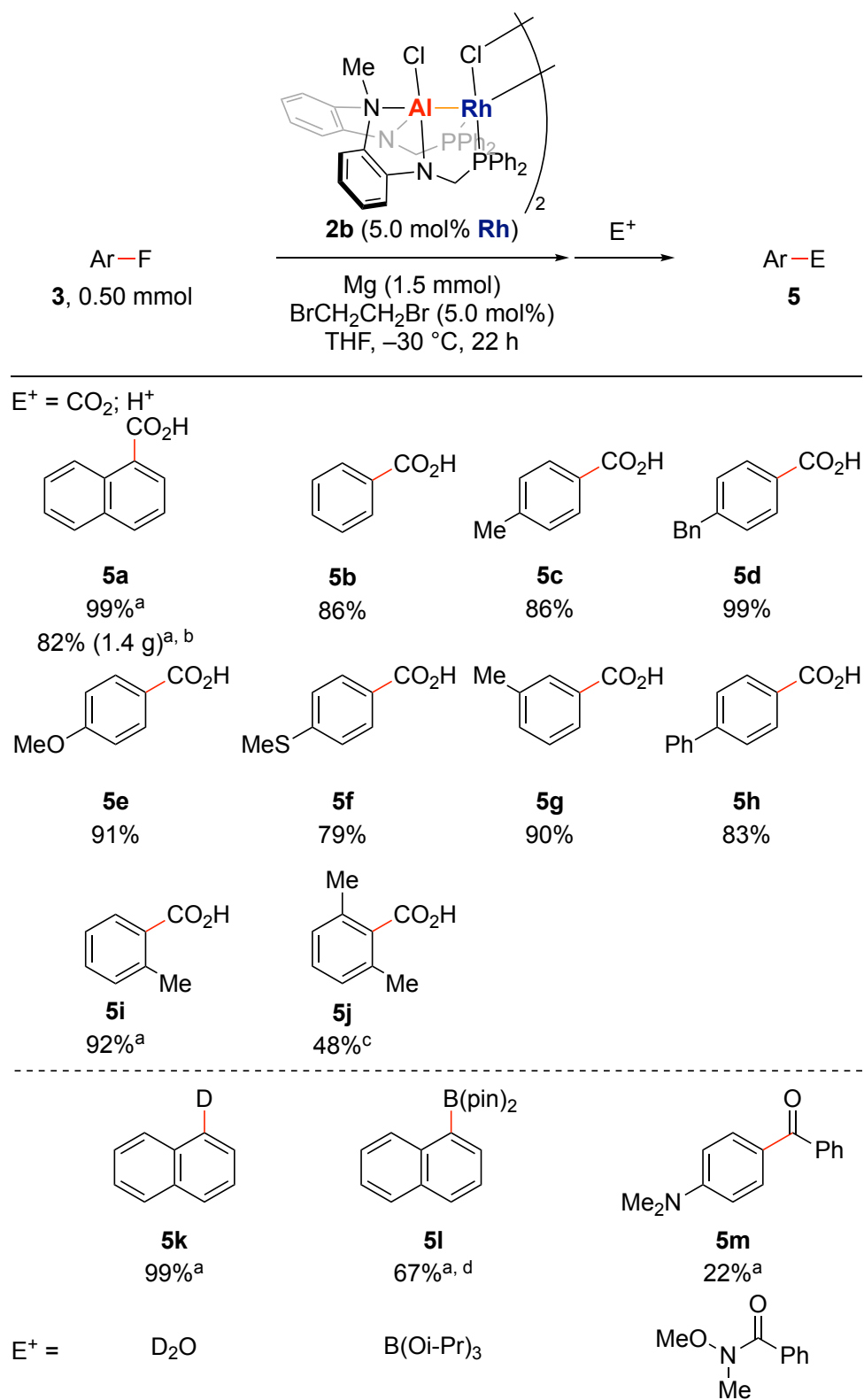
Scheme 2-3. Screening catalysts for the catalytic magnesiation of **3b**.**Al–Rh complexes (5.0 mol% Rh)*****in-situ*-generated catalysts**

**[RhCl(nbd)]<sub>2</sub>** (5.0 mol% Rh)/P ligand (10 mol% P)/Et<sub>2</sub>AlCl (20 mol%)

**others**

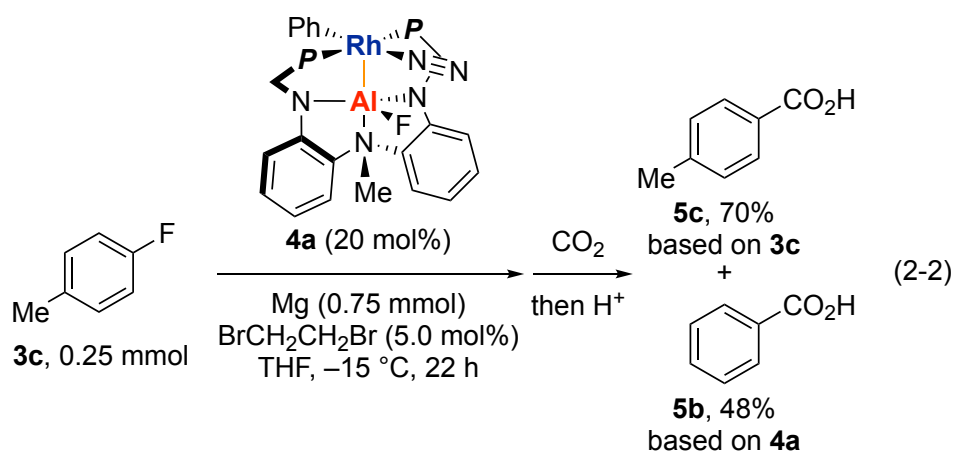
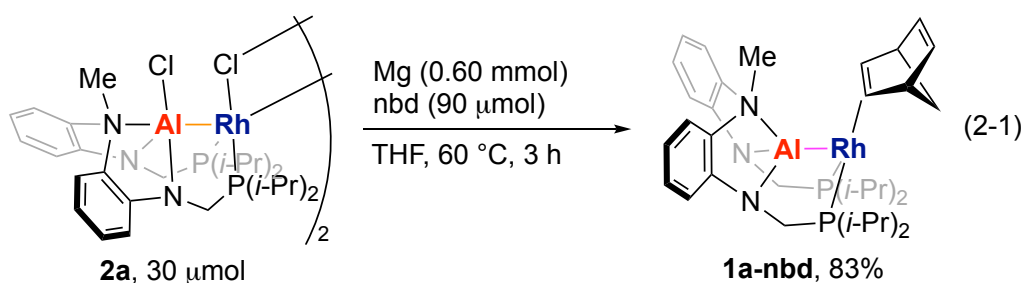
nbd = 2,5-norbornadiene

The magnesiation of various aryl fluorides **3** was examined at the 0.50-mmol-scale under the optimized conditions (Scheme 2-4). Under these conditions, 1-naphthoic acid (**5a**) was obtained from 1-fluoronaphthalene (**3b**) and isolated in 99% yield, while benzoic acid (**5b**) was isolated in 86% yield from the reaction involving fluorobenzene (**3a**). **5a** could be also prepared in 82% yield on a 10 mmol-scale. Electron-donating substituents at the *para*- or *meta*-position of fluorobenzene were tolerated to afford the corresponding benzoic acids (**5c–5g**) in good to high yield, whereas the reaction efficiency was decreased with 4-fluorobiphenyl (**3h**). It should also be noted here that the C–S bond of 4-fluorothioanisole (**3f**), which is easily functionalized by palladium or nickel catalysts,<sup>18</sup> was tolerated in this transformation. Sterically demanding 2-fluorotoluene (**3i**) and 2,6-dimethylfluorobenzene (**3j**) furnished the corresponding carboxylic acids (**5i** and **5j**) in 92% and 48% yield, respectively. D<sub>2</sub>O, B(O*i*-Pr)<sub>3</sub>, and *N*-methoxy-*N*-methylbenzamide<sup>19</sup> can also serve as quenching electrophiles to generate the corresponding deuterated, borylated, and acylated products (**5k–5m**).

Scheme 2-4. Scope of the reaction with respect to aryl fluorides **3**.

<sup>a</sup>Reaction was carried out at room temperature. <sup>b</sup>Reaction was run on a 10 mmol scale. <sup>c</sup>Reaction was carried out at 50 °C. <sup>d</sup>The pinacol ester was isolated after reacting with pinacol. pin = pinacolato

To evaluate the plausible catalytic cycle shown in Scheme 2-2, stoichiometric reactions were conducted. To gain insights into the reduction of **2** to **1** in Scheme 2-2, the reaction of **2a** (30  $\mu\text{mol}$ ) with Mg powder (0.60 mmol) in the presence of nbd (90  $\mu\text{mol}$ ) was examined. It proceeded at 60  $^{\circ}\text{C}$  to afford nbd-coordinated Al–Rh complex **1a-nbd** in high yield (Eq. 2-1). The catalytic magnesiation of *p*-fluorotoluene (**3c**, 0.25 mmol) with Mg powder (0.75 mmol) in the presence of **4a** (20 mol%, 50  $\mu\text{mol}$ ) afforded *p*-toluic acid (**5c**) in 70% yield (0.18 mmol) based on **3c** under concomitant formation of benzoic acid (**5b**) in 48% yield (24  $\mu\text{mol}$ ) based on **4a** (Eq. 2-2). These results support the generation of phenylmagnesium species from **4a** under the applied conditions, and thus corroborate the catalytic cycle proposed in Scheme 2-2. In fact, the formation of diphenylmagnesium was implied by  $^1\text{H}$  and  $^{13}\text{C}$  NMR spectroscopies of the crude mixture upon magnesiation of **3a** under the optimized conditions (Eq. S2-2, Figures S2-7, S2-8, and S2-9).<sup>20</sup>



**Conclusion**

In conclusion, the author has developed a catalytic magnesiation of Ar–F bonds through the C–F bond activation across the X-type heterobimetallic Al–Rh center. It is worth mentioning that the cooperative activation allows the functionalization of C–F bonds in unactivated fluoroarenes under very mild conditions. This is a rare example of successful applications of heterobimetallic catalysis. Further developments of catalytic functionalization of other strong polar  $\sigma$ -bonds by the heterobimetallic systems are currently under investigation.

## Experimental section

### General remarks compatible to all the experimental parts in the present thesis.

All manipulations of oxygen- and moisture-sensitive materials were conducted with a standard Schlenk technique under an argon atmosphere or in a glove box under a nitrogen atmosphere. Medium pressure liquid chromatography (MPLC) was performed with a Yamazen EPLC-W-Prep 2XY. Preparative recycling high performance liquid chromatography (HPLC) was performed with a SHIMADZU Prominence System equipped with COSMOSIL 5SL-II (Nacalai Tesque, 20 mm x 250 mm, spherical, 5  $\mu$ m) with hexane–EtOAc as an eluent. Recycling preparative HPLC (LC-908; column, JAIGEL-1H; solvent, CHCl<sub>3</sub>) was used. Analytical thin layer chromatography (TLC) was performed on Merck TLC silica gel 60 F<sub>254</sub> (0.25 mm) plates. Visualization was accomplished with UV light (254 nm).

Proton, boron, carbon, fluorine, and phosphorus nuclear magnetic resonance spectra (<sup>1</sup>H, <sup>2</sup>H, <sup>11</sup>B, <sup>13</sup>C, <sup>19</sup>F, and <sup>31</sup>P NMR) were recorded on a JEOL ECS-400 (<sup>1</sup>H NMR, 400 MHz; <sup>2</sup>H NMR 61 MHz; <sup>11</sup>B NMR, 128 MHz; <sup>13</sup>C NMR 101 MHz; <sup>19</sup>F NMR 376 Hz; <sup>31</sup>P NMR 162 MHz) spectrometer with solvent resonance as the internal standard (<sup>1</sup>H NMR, CDCl<sub>3</sub> at 7.26 ppm, C<sub>6</sub>D<sub>6</sub> at 7.16 ppm, (CD<sub>3</sub>)<sub>2</sub>SO at 2.49 ppm, CD<sub>2</sub>Cl<sub>2</sub> at 5.32 ppm, Acetone-*d*<sub>6</sub> at 2.05 ppm; <sup>13</sup>C NMR, CDCl<sub>3</sub> at 77.0 ppm, C<sub>6</sub>D<sub>6</sub> at 128.0 ppm, (CD<sub>3</sub>)<sub>2</sub>SO at 39.5 ppm, CD<sub>3</sub> of Acetone-*d*<sub>6</sub> at 29.8 ppm; <sup>19</sup>F NMR, CDCl<sub>3</sub>, DMSO-*d*<sub>6</sub>, and Acetone-*d*<sub>6</sub> at –162.20 ppm with C<sub>6</sub>F<sub>6</sub> as an internal standard). NMR data are reported as follows: chemical shift, multiplicity (s = singlet, d = doublet, t = triplet, q = quartet, quint = quintet, sext = sextet, sept = septet, br = broad, m = multiplet, vt = virtual triplet), coupling constants (Hz), and integration. High-resolution mass spectra were obtained with Thermo Fischer Scientific MS: Exactive Plus HPLC: UltiMate 3000 (ESI, APCI), JEOL JMS-

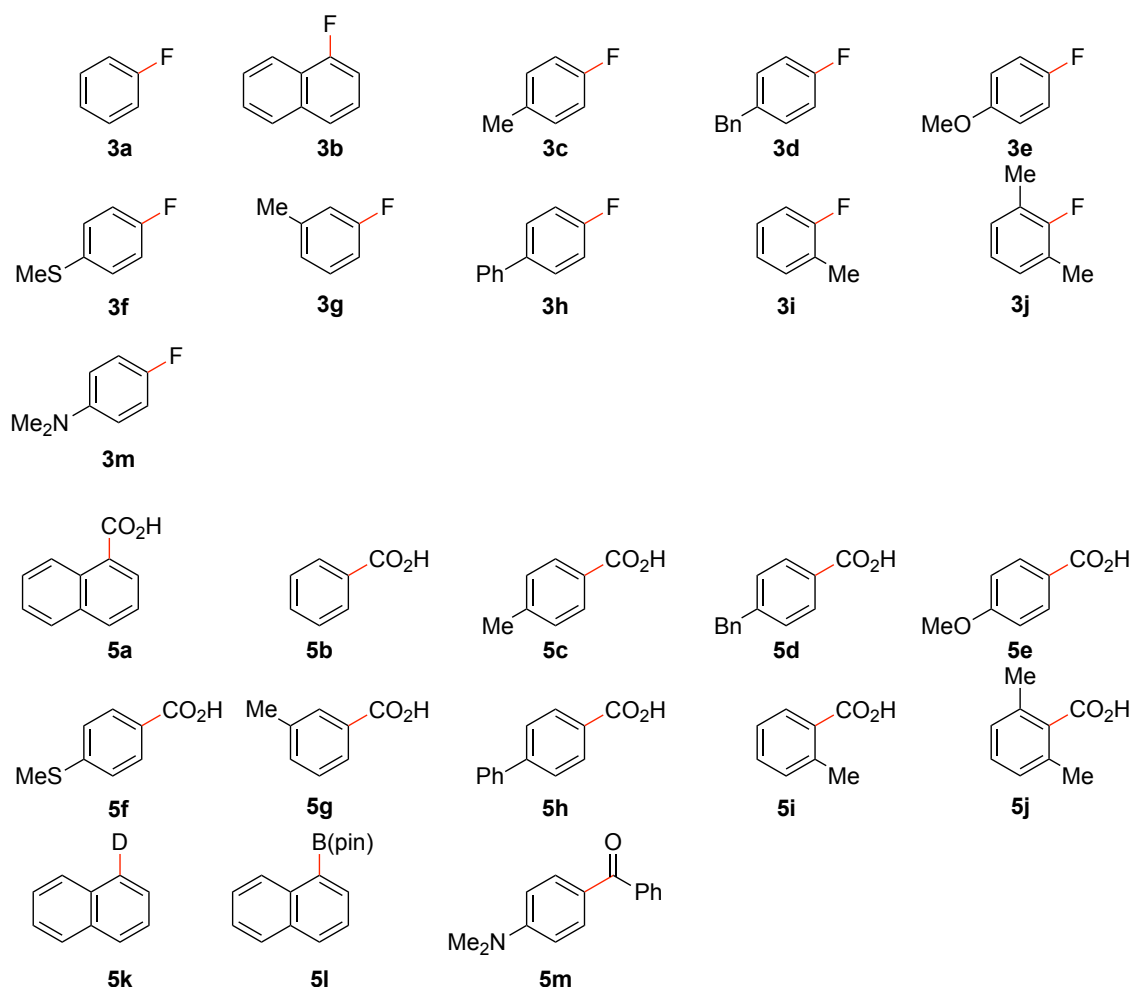


SX102A (EI), and Bruker Daltonics ultraflexXtreme (MALDI). Gas chromatography (GC) analyses were performed on a Shimadzu GC-2014 equipped with a BP1 column (SGE Analytical Science, 0.25 mm x 30 m, pressure = 149.0 kPa, detector = FID, 290 °C) with helium gas as a carrier. Elemental analyses were performed on a J-Science Micro corder JM11, and a YANACO Micro corder MT-5. IR analysis was performed on an Agilent Cary 630 FTIR spectrometer. Heating and stirring were performed with a KPI HHE-19G-US II and aluminum blocks.

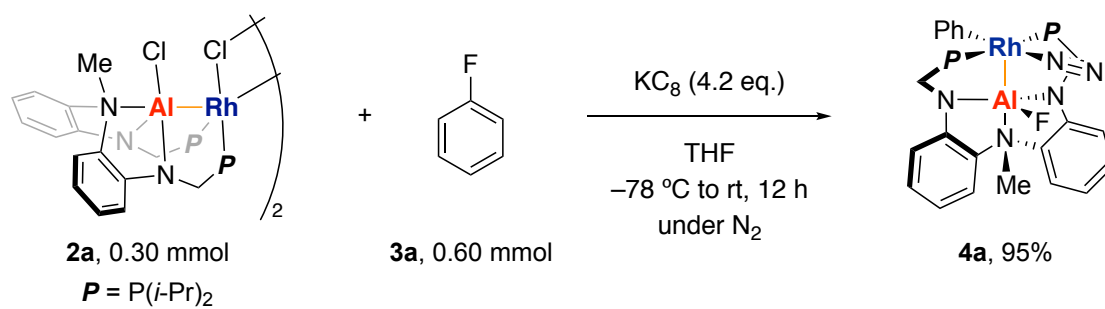
## Chemicals

Unless otherwise noted, commercially available chemicals were distilled under argon atmosphere in the presence of CaH<sub>2</sub> and stored in a glovebox. If commercially available chemicals are solids, the chemicals are used without purification. AlCl<sub>3</sub> (99.999%) was purchased from Aldrich and used without further purification. Pd/C and paraformaldehyde were purchased from Wako Pure Chemical Industries. These were used without further purification. Diphenylphosphine was purchased from Tokyo Chemical Industry Co., Ltd.. The aluminum–rhodium bimetallic complex **2a**<sup>8a</sup> was prepared according to literature procedures. [Rh(nbd)(μ-Cl)]<sub>2</sub> (nbd = 2,5-norbornadiene)<sup>21</sup> was synthesized following the reported procedures. Anhydrous hexane, toluene and THF were purchased from Kanto Chemical and purified by passage through activated alumina under positive argon pressure as described by Grubbs *et al.*<sup>22</sup> Magnesium powder used for reductant was purchased from Sigma-Aldrich (product number 13112) or Alfa Aesar (product number 10233). All other commercially available reagents were purchased from common sources (*e.g.* Tokyo Chemical Industry Co., Ltd., FUJIFILM Wako Pure Chemical Corporation, Sigma-Aldrich, Alfa-Aesar, Nacalai

Tesque INC. etc.).

Figure S2-1. List of fluoroarenes **3** and products **5** in this study.

## General Procedure for Scheme 2-1.



To a THF (5.0 mL) solution of **2a** (403 mg, 0.30 mmol) and fluorobenzene (**3a**, 58 mg, 0.60 mmol), a suspension of potassium graphite (176 mg, 1.3 mmol) in THF (5.0 mL) was slowly added at  $-78\text{ }^{\circ}\text{C}$ . The mixture was warmed up to room temperature and stirred for 12 h at the same temperature. After the reaction, THF was evaporated and benzene (10 mL) was added to the residue. After filtration through a KIRIYAMA filter paper (No. 5A), the filtrate was concentrated to afford a brown precipitate. The precipitate was washed with *n*-pentane (3.0 mL) x 2 and dried under reduced pressure to give **4a** as a brown solid in 95% yield. Yellow crystals of **4a** for X-ray crystallography were obtained from a saturated *n*-pentane solution of **4a** at  $-35\text{ }^{\circ}\text{C}$ . **4a**:  $^1\text{H}$  NMR (400 MHz,  $\text{C}_6\text{D}_6$ ,  $24\text{ }^{\circ}\text{C}$ ):  $\delta$  0.77 (q,  $J = 6.1\text{ Hz}$ , 6H), 0.95 (q,  $J = 7.0\text{ Hz}$ , 6H), 1.06 (q,  $J = 6.7\text{ Hz}$ , 6H), 1.25 (q,  $J = 6.7\text{ Hz}$ , 6H), 1.48 (br s, 2H), 2.42 (br s, 2H), 3.14 (s, 3H), 3.15 (d,  $J = 12.8\text{ Hz}$ , 2H), 3.30 (d,  $J = 12.8\text{ Hz}$ , 2H), 6.56–6.62 (m, 3H), 6.65–6.72 (m, 3H), 6.91 (t,  $J = 7.3\text{ Hz}$ , 1H), 7.19 (t,  $J = 7.3\text{ Hz}$ , 3H), 7.36 (d,  $J = 7.3\text{ Hz}$ , 2H), 7.68 (d,  $J = 7.3\text{ Hz}$ , 1H).  $^{13}\text{C}\{^1\text{H}\}$  NMR (101 MHz,  $\text{C}_6\text{D}_6$ ,  $24\text{ }^{\circ}\text{C}$ ):  $\delta$  18.0, 19.9 (two signals were overlapped), 20.2, 22.7 (d,  $J = 11.6\text{ Hz}$ ), 22.8 (d,  $J = 10.4\text{ Hz}$ ), 23.3 (d,  $J = 9.3\text{ Hz}$ ), 23.4 (d,  $J = 9.3\text{ Hz}$ ), 41.5 (d,  $J = 19.7\text{ Hz}$ ), 41.7 (d,  $J = 19.7\text{ Hz}$ ), 47.5 (d,  $J = 8.1\text{ Hz}$ ), 110.3, 114.3, 121.5, 123.0, 125.6, 127.9, 128.6, 132.0, 137.2, 137.7, 151.0 (t,  $J = 8.1\text{ Hz}$ ).  $^{31}\text{P}\{^1\text{H}\}$  NMR (162 MHz,  $\text{C}_6\text{D}_6$ ,  $24\text{ }^{\circ}\text{C}$ ):  $\delta$  39.9 (d,  $J_{\text{P-Rh}} = 144\text{ Hz}$ ).  $^{19}\text{F}\{^1\text{H}\}$  NMR (376 MHz, THF-*d*8,  $24\text{ }^{\circ}\text{C}$ ):  $\delta$   $-149$  (br). The signal of fluorine directly attached to the aluminum atom was broadened due to quadrupolar relaxation. IR (solid state):  $\nu_{\text{NN}} = 2214\text{ cm}^{-1}$ . m.p.  $170\text{ }^{\circ}\text{C}$  (decomp.). MALDI-MS  $\text{C}_{33}\text{H}_{48}\text{AlFN}_3\text{P}_2\text{Rh}^{*+}$ : Calcd. 697.2172, Found: 697.2172. Anal. Calcd.  $\text{C}_{33}\text{H}_{48}\text{AlFN}_5\text{P}_2\text{Rh}$ : C, 54.62; H, 6.67; N, 9.65. Found: C, 52.54; H, 7.04; N, 7.07. The experimental values did not agree with calculated values. This is because  $\text{N}_2$  ligand has come off during vacuum drying. IR spectrum of the crystals of **4a** that were dried in vacuo

at room temperature, the strength of absorption of  $\nu_{\text{NN}}$  ( $2214\text{ cm}^{-1}$ ) decreased.

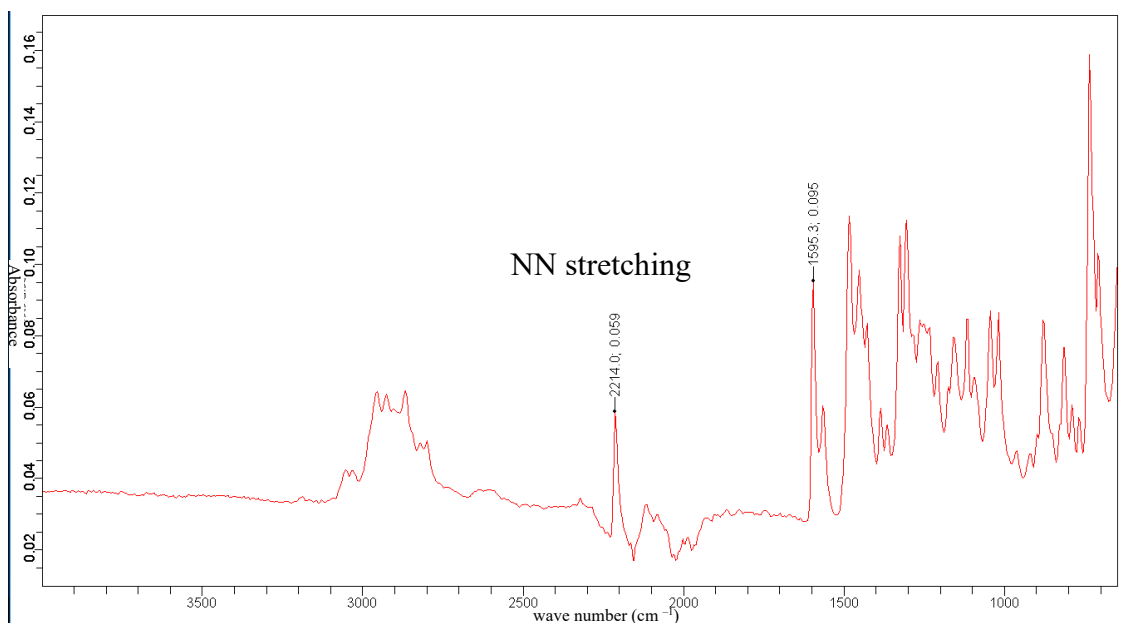


**Figure S2-2.** IR spectrum of complex **4a** in solid state.

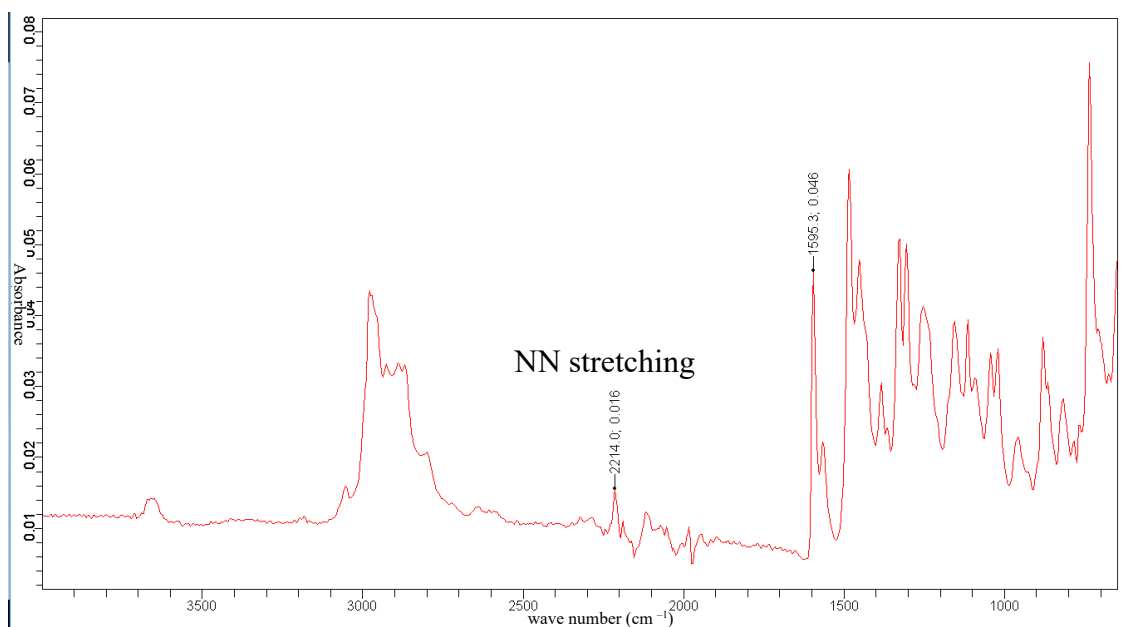
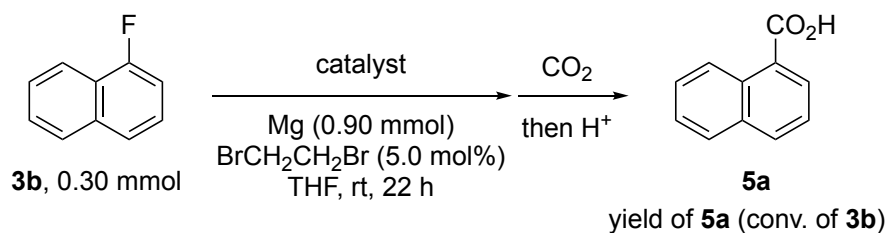


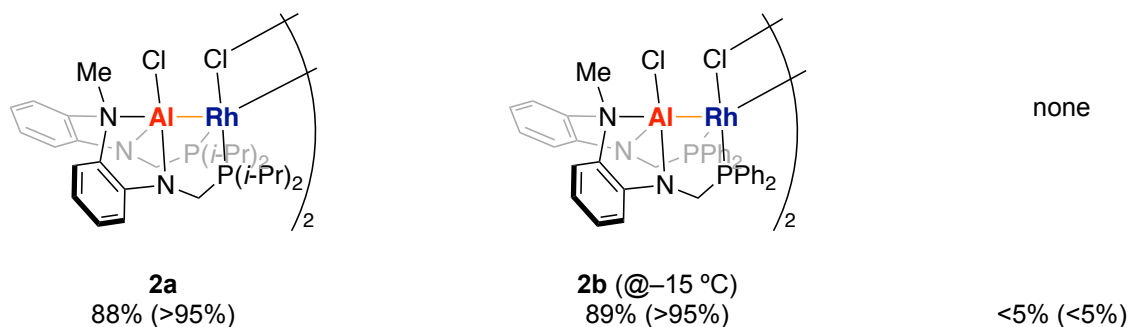
**Figure S2-3.** IR spectrum of complex **4a** in solid state after evacuation for 12 h.

## General procedures for Scheme 2-3.



*Al–Rh complexes:* In a glove box, a 4 mL vial with a stirring bar was charged with magnesium powder (22 mg, 0.90 mmol), THF (500  $\mu\text{L}$ ), and 1,2-dibromoethane (2.8 mg, 15  $\mu\text{mol}$ ), and the resulting mixture was stirred for 20 min at room temperature. 1-Fluoronaphthalene (**3b**, 44 mg, 0.30 mmol), catalyst (5.0 mol%Rh), and THF (500  $\mu\text{L}$ ) were put into the vial. The vial was taken out of the glove box and the mixture was stirred for 22 h at indicated temperature and then, stirred under atmospheric pressure of  $\text{CO}_2$  at room temperature for 30 min. To the mixture was added 3 M HCl aq. (2.0 mL). The mixture was extracted with EtOAc and combined organic layers were washed with  $\text{H}_2\text{O}$ . All of the volatiles were removed by rotary evaporator. Yield of **5a** was determined by  $^1\text{H}$  NMR spectroscopy with 1,3,5-trimethoxybenzene (50 mg, 0.30 mmol) as an internal standard.

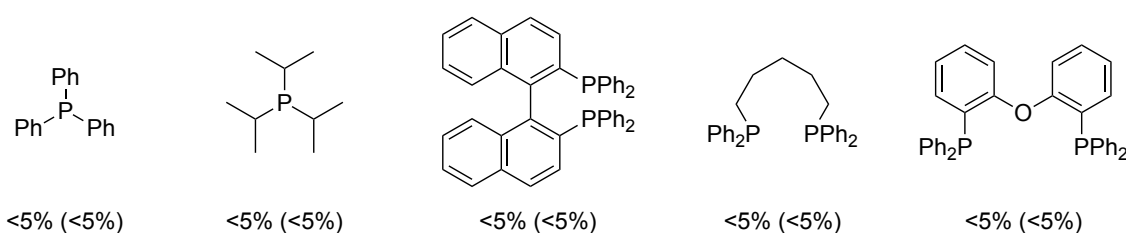
## Al–Rh complexes



*In-situ generated catalysts:* In a glove box, a 4 mL vial (*vial A*) with a stirring bar was charged with magnesium powder (22 mg, 0.90 mmol), THF (500  $\mu$ L), and 1,2-dibromoethane (2.8 mg, 15  $\mu$ mol), and the resulting mixture was stirred for 20 min at room temperature. Another vial (*vial B*) was charged with **3b** (44 mg, 0.30 mmol),  $[\text{Rh}(\text{nbd})(\mu\text{-Cl})_2]$  (3.5 mg, 8.0  $\mu$ mol, 2.5 mol%), a phosphine ligand (P/Rh = 2), and THF (500  $\mu$ L) and the resulting mixture was stirred for 10 min at room temperature. To *vial A* were added the solution in *vial B* and 1.03 M  $\text{Et}_2\text{AlCl}$  in *n*-hexane (15  $\mu$ L, 15  $\mu$ mol). The mixture was stirred for 22 h at room temperature and then, stirred under atmospheric pressure of  $\text{CO}_2$  at room temperature for 30 min. To the mixture was added 3 M HCl aq. (2.0 mL). The mixture was extracted with EtOAc and combined organic layers were washed with  $\text{H}_2\text{O}$ . All of the volatiles were removed by rotary evaporator. Yield of **5a** was determined by  $^1\text{H}$  NMR spectroscopy with 1,3,5-trimethoxybenzene (50 mg, 0.30 mmol) as an internal standard.

### *In-situ-generated catalysts*

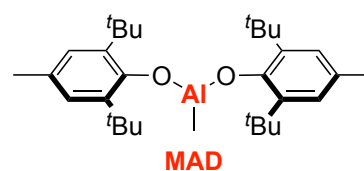
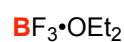
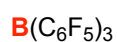
$[\text{Rh}(\text{nbd})(\mu\text{-Cl})_2]$  (5.0 mol%**Rh**)/P ligand (10 mol%P)/ $\text{Et}_2\text{AlCl}$  (20 mol%)



*Lewis acid catalysts:* In a glove box, a 4 mL vial with a stirring bar was charged with magnesium powder (22 mg, 0.90 mmol), THF (500  $\mu$ L), and 1,2-dibromoethane (2.8 mg, 15  $\mu$ mol), and the resulting mixture was stirred for 20 min at room temperature. **3b** (44 mg, 0.30 mmol), Lewis acid (30  $\mu$ mol) and THF (500  $\mu$ L) were put into the vial. The

mixture was stirred for 22 h at room temperature and then stirred under atmospheric pressure of CO<sub>2</sub> at room temperature for 30 min. To the mixture was added 3 M HCl aq. (2.0 mL). The mixture was extracted with EtOAc and combined organic layers were washed with H<sub>2</sub>O. All of the volatiles were removed by rotary evaporator. Yield of **5a** was determined by <sup>1</sup>H NMR spectroscopy with 1,3,5-trimethoxybenzene (50 mg, 0.30 mmol) as an internal standard.

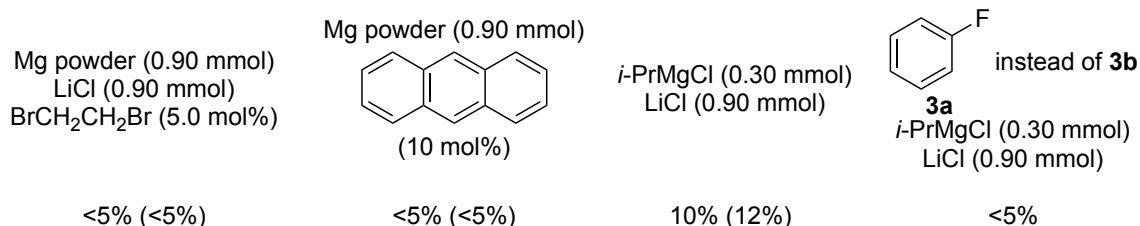
### Lewis acids



<5% (<5%)

*Others:* In a glove box, a 4 mL vial with a stirring bar was charged with magnesium source and an additive, and THF (500 μL). The resulting mixture was stirred for 20 min at the room temperature. **3b** (44 mg, 0.30 mmol) and THF (500 μL) were put into the vial. The mixture was stirred for 22 h at room temperature and then, stirred under atmospheric pressure of CO<sub>2</sub> at room temperature for 30 min. To the mixture was added 3 M HCl aq. (2.0 mL). The mixture was extracted with EtOAc and combined organic layers were washed with H<sub>2</sub>O. All of the volatiles were removed by rotary evaporator. Yield of **5a** was determined by <sup>1</sup>H NMR spectroscopy with 1,3,5-trimethoxybenzene (50 mg, 0.30 mmol) as an internal standard.

## Others

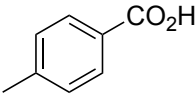
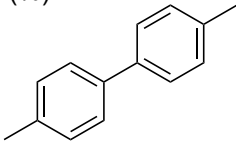


*Under argon atmosphere:* In a glove box, a 20 mL Schlenk tube with a stirring bar was charged with magnesium powder (22 mg, 0.90 mmol), THF (500  $\mu$ L), and 1,2-dibromoethane (2.8 mg, 15  $\mu$ mol), and the resulting mixture was stirred for 20 min at room temperature. 4-Fluorotoluene (**3c**, 44 mg, 0.30 mmol), **2b** (12 mg, 8.0  $\mu$ mol), and THF (500  $\mu$ L) were put into the Schlenk tube and then, the tube was taken out of the glove box. The tube was evacuated and refilled with argon gas for three times. The mixture was stirred for 22 h at  $-20$   $^{\circ}$ C and then, stirred under atmospheric pressure of CO<sub>2</sub> at room temperature for 30 min. To the mixture was added 3 M HCl aq. (2.0 mL). The mixture was extracted with EtOAc and combined organic layers were washed with H<sub>2</sub>O. All of the volatiles were removed by rotary evaporator. Yield of **5c** was determined by <sup>1</sup>H NMR spectroscopy with 1,3,5-trimethoxybenzene (50 mg, 0.30 mmol) as an internal standard. The corresponding product **5c** was obtained in 73% yield (68% yield under N<sub>2</sub> atmosphere).

*Magnesium property:* In a glove box, a 4 mL vial with a stirring bar was charged with indicated magnesium (22 mg, 0.90 mmol), THF (500  $\mu$ L), and 1,2-dibromoethane (2.8 mg, 15  $\mu$ mol), and the resulting mixture was stirred for 20 min at room temperature. **3c** (33 mg, 0.30 mmol), **2b** (12 mg, 8.0  $\mu$ mol), and THF (500  $\mu$ L) were put into the vial.



The mixture was stirred for 22 h at  $-20\text{ }^{\circ}\text{C}$  and then, stirred under atmospheric pressure of  $\text{CO}_2$  at room temperature for 30 min. To the mixture was added 3 M HCl aq. (2.0 mL). The mixture was extracted with EtOAc and combined organic layers were washed with  $\text{H}_2\text{O}$ . All of the volatiles were removed by rotary evaporator. Yield of *p*-toluic acid (**5c**) was determined by  $^1\text{H}$  NMR spectroscopy with 1,3,5-trimethoxybenzene (50 mg, 0.30 mmol) as an internal standard.

Supplier (product number)	NMR yield (%)	
		
Wako (138-13862) wash by HCl	16	0
Wako (134-13962)	30	61
Sigma Aldrich (13112)	80	8
Alfa Aesar (10233)	84	5

We investigated the purity of Mg powder (Sigma Aldrich; #13112) that stored in the glove box for 3 months because Mg could react with dinitrogen to generate magnesium nitride at high temperature.<sup>23</sup> Elemental Analysis, Mg powder: H, C, N were not detected.  $\text{Mg}_3\text{N}_2$ : Calcd. N, 27.76. Found: C, 0.15; H, 0.25; N, 24.99. According to the elemental analysis and the color of them, the Mg powder did not contain magnesium nitride.

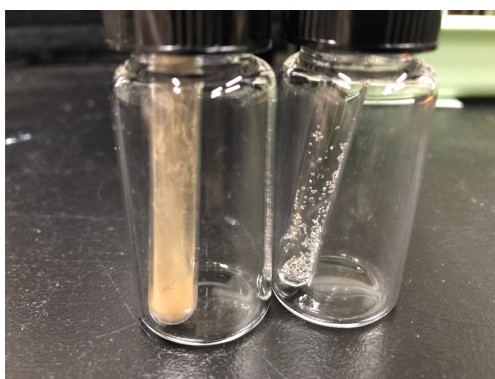
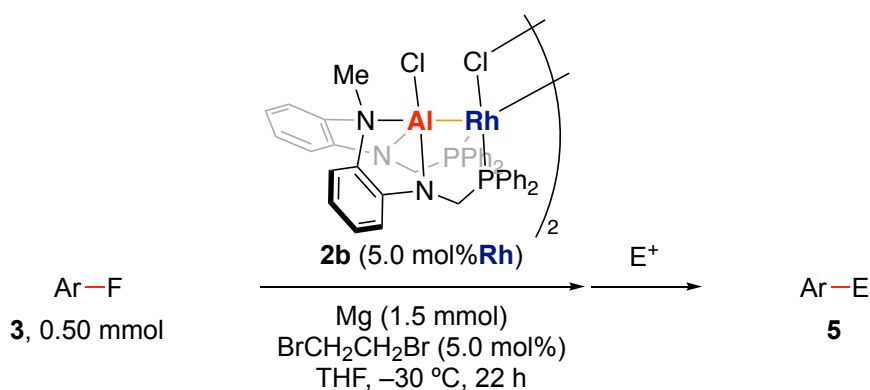
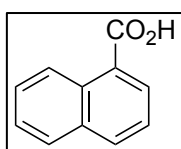


**Figure S2-4.** The picture of magnesium nitride (left) and magnesium powder (right).

## General procedures for Scheme 2-4.

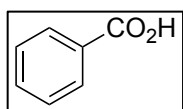


In a glove box, a 4 mL vial with a stirring bar was charged with magnesium powder (36 mg, 1.5 mmol), THF (500  $\mu\text{L}$ ), and 1,2-dibromoethane (4.7 mg, 25  $\mu\text{mol}$ ), and the resulting mixture was stirred for 20 min at room temperature. Aryl fluoride **3** (0.50 mmol), **2b** (20 mg, 13  $\mu\text{mol}$ ), and THF (1.0 mL) were put into the vial. The mixture was stirred for 22 h at  $-30\text{ }^\circ\text{C}$  and then, reacted with an indicated electrophile.

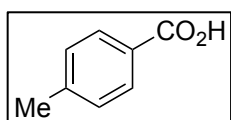


**1-Naphthoic acid (5a)**: The reaction of 1-fluoronaphthalene (**3b**, 73 mg, 0.50 mmol) at room temperature was followed by being stirred under atmospheric pressure of  $\text{CO}_2$  at room temperature for 30 min. To the mixture, 3 M HCl aq. (2.0 mL) was added. The mixture was extracted with EtOAc and combined organic layers were washed with  $\text{H}_2\text{O}$ . All of the volatiles were removed by rotary evaporator. After MPLC purification (Biotage<sup>®</sup> SNAP Ultra 25 g, *n*-hexane:EtOAc = 2:3), the title compound (85 mg, 0.50 mmol, 99%) was obtained as a white solid.  $R_f$  0.59 (*n*-hexane/EtOAc = 3:4).  $^1\text{H}$  NMR (400 MHz,  $\text{CDCl}_3$ ,  $24\text{ }^\circ\text{C}$ ):  $\delta$  7.54–7.60 (m, 2H), 7.67 (t,  $J = 7.6$  Hz, 1H), 7.93 (d,  $J = 7.8$  Hz, 1H), 8.11 (d,  $J = 8.2$  Hz, 1H), 8.43 (d,  $J = 6.9$  Hz, 1H), 9.10 (d,  $J = 8.4$  Hz, 1H).  $^{13}\text{C}\{^1\text{H}\}$  NMR (101 MHz,  $\text{CDCl}_3$ ,  $24\text{ }^\circ\text{C}$ ):  $\delta$  124.5,

125.5, 125.9, 126.3, 128.1, 128.7, 131.6, 131.9, 133.9, 134.6, 172.9. All the resonances of  $^1\text{H}$  and  $^{13}\text{C}$  NMR spectra were consistent with the reported values.<sup>24</sup>



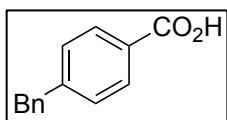
**Benzoic acid (5b):** The reaction of fluorobenzene (**3a**, 48 mg, 0.50 mmol) at  $-30\text{ }^\circ\text{C}$  was followed by being stirred under atmospheric pressure of  $\text{CO}_2$  at room temperature for 30 min. To the mixture, 3 M HCl aq. (2.0 mL) was added. The mixture was extracted with EtOAc and combined organic layers were washed with  $\text{H}_2\text{O}$ . All of the volatiles were removed by rotary evaporator. After MPLC purification (Biotage<sup>®</sup> SNAP Ultra 25 g, *n*-hexane:EtOAc = 2:3), the title compound (53 mg, 0.43 mmol, 86%) was obtained as a white solid.  $R_f$  0.53 (*n*-hexane/EtOAc = 3:4).  $^1\text{H}$  NMR (400 MHz,  $\text{CDCl}_3$ ,  $24\text{ }^\circ\text{C}$ ):  $\delta$  7.49 (t,  $J = 7.3$  Hz, 2H), 7.62 (t,  $J = 6.6$  Hz, 1H), 8.12 (d,  $J = 7.3$  Hz, 2H).  $^{13}\text{C}\{^1\text{H}\}$  NMR (101 MHz,  $\text{CDCl}_3$ ,  $24\text{ }^\circ\text{C}$ ):  $\delta$  128.5, 129.3, 130.2, 133.8, 172.3. All the resonances of  $^1\text{H}$  and  $^{13}\text{C}$  NMR spectra were consistent with the reported values.<sup>25</sup>



***p*-Toluic acid (5c):** The reaction of 4-fluorotoluene (**3c**, 55 mg, 0.50 mmol) at  $-30\text{ }^\circ\text{C}$  was followed by being stirred under atmospheric pressure of  $\text{CO}_2$  at room temperature for 30 min. To the mixture, 3 M HCl aq. (2.0 mL) was added. The mixture was extracted with EtOAc and combined organic layers were washed with  $\text{H}_2\text{O}$ . All of the volatiles were removed by rotary evaporator. After MPLC purification (25 g of silica gel, *n*-hexane:EtOAc = 2:3), the title compound (58 mg, 0.43 mmol, 86%) was obtained as a white solid.  $R_f$  0.56 (*n*-hexane/EtOAc = 3:4).  $^1\text{H}$  NMR (400 MHz,  $\text{CDCl}_3$ ,  $24\text{ }^\circ\text{C}$ ):  $\delta$  2.44 (s, 3H), 7.28 (d,  $J = 8.2$  Hz, 2H), 8.00 (d,  $J = 8.2$  Hz,

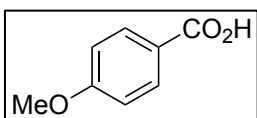
2H).  $^{13}\text{C}\{^1\text{H}\}$  NMR (101 MHz,  $\text{CDCl}_3$ , 24 °C):  $\delta$  21.7, 126.5, 129.2, 130.3, 144.6, 171.6.

All the resonances of  $^1\text{H}$  and  $^{13}\text{C}$  NMR spectra were consistent with the reported values.<sup>25</sup>



**4-Benzylbenzoic acid (5d):** The reaction of 1-benzyl-4-fluorobenzene (**3d**, 93 mg, 0.50 mmol) at  $-30$  °C was followed by

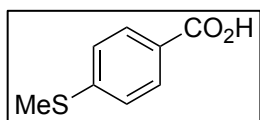
being stirred under atmospheric pressure of  $\text{CO}_2$  at room temperature for 30 min. To the mixture, 3 M HCl aq. (2.0 mL) was added. The mixture was extracted with EtOAc and combined organic layers were washed with  $\text{H}_2\text{O}$ . All of the volatiles were removed by rotary evaporator. After MPLC purification (25 g of silica gel, *n*-hexane:EtOAc = 1:1), the title compound (105 mg, 0.50 mmol, 99%) was obtained as a white solid.  $R_f$  0.59 (*n*-hexane/EtOAc = 3:4).  $^1\text{H}$  NMR (400 MHz,  $\text{CDCl}_3$ , 24 °C):  $\delta$  4.07 (s, 2H), 7.20 (d,  $J$  = 6.9 Hz, 2H), 7.25–7.34 (m, 5H), 8.06 (d,  $J$  = 8.2 Hz, 2H).  $^{13}\text{C}\{^1\text{H}\}$  NMR (101 MHz,  $\text{CDCl}_3$ , 24 °C):  $\delta$  42.0, 126.4, 127.2, 128.6, 129.0, 129.1, 130.5, 139.9, 147.6, 172.3. All the resonances of  $^1\text{H}$  and  $^{13}\text{C}$  NMR spectra were consistent with the reported values.<sup>26</sup>



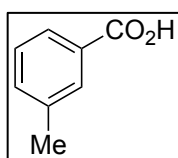
***p*-Anisic acid (5e):** The reaction of 4-fluoroanisole (**3e**, 63 mg, 0.50 mmol) at  $-30$  °C was followed by being stirred under atmospheric

pressure of  $\text{CO}_2$  at room temperature for 30 min. To the mixture, 3 M HCl aq. (2.0 mL) was added. The mixture was extracted with EtOAc and combined organic layers were washed with  $\text{H}_2\text{O}$ . All of the volatiles were removed by rotary evaporator. After MPLC purification (Biotage<sup>®</sup> SNAP Ultra 25 g, *n*-hexane:EtOAc = 2:3), the title compound (76 mg, 0.46 mmol, 91%) was obtained as a white solid.  $R_f$  0.44 (*n*-hexane/EtOAc = 3:4).  $^1\text{H}$  NMR (400 MHz,  $\text{CDCl}_3$ , 24 °C):  $\delta$  3.88 (s, 3H), 6.95 (d,  $J$  = 8.2 Hz, 2H), 8.07 (d,  $J$  = 8.2 Hz, 2H).  $^{13}\text{C}\{^1\text{H}\}$  NMR (101 MHz,  $\text{CDCl}_3$ , 24 °C):  $\delta$  55.5, 113.8, 121.7, 132.4, 164.1,

171.5. All the resonances of  $^1\text{H}$  and  $^{13}\text{C}$  NMR spectra were consistent with the reported values.<sup>25</sup>

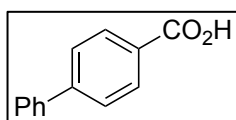


**4-(Methylthio)benzoic acid (5f):** The reaction of 4-fluorothioanisole (**3f**, 71 mg, 0.50 mmol) at  $-30\text{ }^\circ\text{C}$  was followed by being stirred under atmospheric pressure of  $\text{CO}_2$  at room temperature for 30 min. To the mixture, 3 M HCl aq. (2.0 mL) was added. The mixture was extracted with EtOAc and combined organic layers were washed with  $\text{H}_2\text{O}$ . All of the volatiles were removed by rotary evaporator. After MPLC purification (25 g of silica gel, *n*-hexane:EtOAc = 2:3), the title compound (67 mg, 0.40 mmol, 79%) was obtained as a pale yellow solid.  $R_f$  0.44 (*n*-hexane/EtOAc = 3:4). Yield of 4,4'-Bis(methylthio)-1,1'-biphenyl was estimated in 8% yield by  $^1\text{H}$  NMR spectroscopy with 1,3,5-trimethoxybenzene (6.1 mg, 36  $\mu\text{mol}$ ) as an internal standard. **5f**:  $^1\text{H}$  NMR (400 MHz,  $\text{CDCl}_3$ ,  $24\text{ }^\circ\text{C}$ ):  $\delta$  2.53 (s, 3H), 7.28 (d,  $J = 7.8$  Hz, 2H), 8.01 (d,  $J = 7.8$  Hz, 2H).  $^{13}\text{C}\{^1\text{H}\}$  NMR (101 MHz,  $\text{CDCl}_3$ ,  $24\text{ }^\circ\text{C}$ ):  $\delta$  14.8, 124.9, 125.2, 130.5, 146.8, 171.4.<sup>27a</sup> **4,4'-Bis(methylthio)-1,1'-biphenyl**:  $^1\text{H}$  NMR (400 MHz,  $\text{CDCl}_3$ ,  $24\text{ }^\circ\text{C}$ ):  $\delta$  2.52 (s, 6H), 7.32 (d,  $J = 7.3$  Hz, 4H), 7.50 (d,  $J = 7.3$  Hz, 4H).  $^{13}\text{C}\{^1\text{H}\}$  NMR (101 MHz,  $\text{CDCl}_3$ ,  $24\text{ }^\circ\text{C}$ ):  $\delta$  15.9, 127.0, 127.1, 137.3, 137.5.<sup>27b</sup> All the resonances of  $^1\text{H}$  and  $^{13}\text{C}$  NMR spectra were consistent with the reported values.<sup>27</sup>

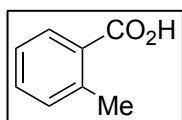


***m*-Toluic acid (5g):** The reaction of 3-fluorotoluene (**3g**, 55 mg, 0.50 mmol) at  $-30\text{ }^\circ\text{C}$  was followed by being stirred under atmospheric pressure of  $\text{CO}_2$  at room temperature for 30 min. To the mixture, 3 M HCl aq. (2.0 mL) was added. The mixture was extracted with EtOAc and combined organic layers were washed with  $\text{H}_2\text{O}$ . All of the volatiles were removed by rotary evaporator.

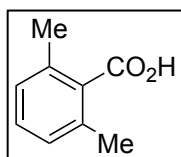
After MPLC purification (Biotage<sup>®</sup> SNAP Ultra 25 g, *n*-hexane:EtOAc = 2:3), the title compound (61 mg, 0.45 mmol, 90%) was obtained as a white solid.  $R_f$  0.56 (*n*-hexane/EtOAc = 3:4). <sup>1</sup>H NMR (400 MHz, CDCl<sub>3</sub>, 24 °C): δ 2.43 (s, 3H), 7.37 (t,  $J$  = 7.8 Hz, 1H), 7.43 (d,  $J$  = 7.3 Hz, 1H), 7.93 (d,  $J$  = 8.3 Hz, 1H), 7.94 (s, 1H). <sup>13</sup>C{<sup>1</sup>H} NMR (101 MHz, CDCl<sub>3</sub>, 24 °C): δ 21.3, 127.4, 128.4, 129.2, 130.7, 134.6, 138.3, 172.1. All the resonances of <sup>1</sup>H and <sup>13</sup>C NMR spectra were consistent with the reported values.<sup>25</sup>



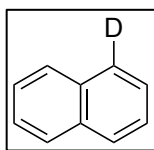
**4-Phenylbenzoic acid (5h):** The reaction of 4-fluorobiphenyl (**3h**, 86 mg, 0.50 mmol) at -30 °C was followed by being stirred under atmospheric pressure of CO<sub>2</sub> at room temperature for 30 min. To the mixture, 3 M HCl aq. (2.0 mL) was added. The mixture was extracted with EtOAc (40 mL) due to low solubility of **5h** and combined organic layers were washed with H<sub>2</sub>O. All of the volatiles were removed by rotary evaporator. Purification of the crude mixture by MPLC (25 g of silica gel, *n*-hexane:EtOAc = 3:4) gave the title compound (82 mg, 0.41 mmol, 83%) as a white solid.  $R_f$  0.37 (*n*-hexane/EtOAc = 3:4). Biphenyl was also isolated in 11% yield. **5h:** <sup>1</sup>H NMR (400 MHz, (CD<sub>3</sub>)<sub>2</sub>SO, 24 °C): δ 7.41 (t,  $J$  = 6.6 Hz, 1H), 7.49 (t,  $J$  = 7.1 Hz, 2H), 7.72 (d,  $J$  = 7.3 Hz, 2H), 7.79 (d,  $J$  = 7.3 Hz, 2H), 8.02 (d,  $J$  = 7.8 Hz, 2H). <sup>13</sup>C{<sup>1</sup>H} NMR (101 MHz, (CD<sub>3</sub>)<sub>2</sub>SO, 24 °C): δ 126.8, 127.0, 128.3, 129.1, 129.6, 130.0, 139.0, 144.3, 167.1.<sup>28a</sup> **Biphenyl:** <sup>1</sup>H NMR (400 MHz, CDCl<sub>3</sub>, 24 °C): δ 7.37 (t,  $J$  = 7.1 Hz, 2H), 7.47 (t,  $J$  = 7.3 Hz, 4H), 7.62 (d,  $J$  = 7.8 Hz, 4H). <sup>13</sup>C{<sup>1</sup>H} NMR (101 MHz, CDCl<sub>3</sub>, 24 °C): δ 127.15, 127.23, 128.7, 141.2.<sup>28b</sup> All the resonances of <sup>1</sup>H and <sup>13</sup>C NMR spectra were consistent with the reported values.<sup>28</sup>



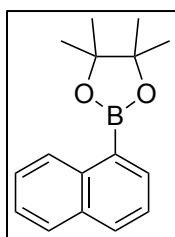
***o*-Toluic acid (5i):** The reaction of 2-fluorotoluene (**3i**, 55 mg, 0.50 mmol) at room temperature was followed by being stirred under atmospheric pressure of CO<sub>2</sub> at room temperature for 30 min. To the mixture, 3 M HCl aq. (2.0 mL) was added. The mixture was extracted with EtOAc and combined organic layers were washed with H<sub>2</sub>O. All of the volatiles were removed by rotary evaporator. After MPLC purification (Biotage<sup>®</sup> SNAP Ultra 25 g, *n*-hexane:EtOAc = 2:3), the title compound (62 mg, 0.46 mmol, 92%) was obtained as a white solid. R<sub>f</sub> 0.56 (*n*-hexane/EtOAc = 3:4). <sup>1</sup>H NMR (400 MHz, CDCl<sub>3</sub>, 24 °C): δ 2.64 (s, 3H), 7.23–7.28 (m, 2H), 7.43 (t, *J* = 7.3 Hz, 1H), 8.05 (d, *J* = 7.3 Hz, 1H), 12.03 (br s, 1H). <sup>13</sup>C{<sup>1</sup>H} NMR (101 MHz, CDCl<sub>3</sub>, 24 °C): δ 22.1, 125.9, 128.3, 131.6, 131.9, 132.9, 141.4, 172.9. All the resonances of <sup>1</sup>H and <sup>13</sup>C NMR spectra were consistent with the reported values.<sup>25</sup>



**2,6-Dimethylbenzoic acid (5j):** The reaction of 2-fluoro-1,3-dimethylbenzene (**3j**, 62 mg, 0.50 mmol) at 50 °C was followed by being stirred under atmospheric pressure of CO<sub>2</sub> at room temperature for 30 min. To the mixture, 3 M HCl aq. (2.0 mL) was added. The mixture was extracted with EtOAc and combined organic layers were washed with H<sub>2</sub>O. All of the volatiles were removed by rotary evaporator. After MPLC purification (Biotage<sup>®</sup> Sfär Silica High Capacity Duo 20 mm, 25 g, *n*-hexane:EtOAc = 2:3), the title compound (36 mg, 0.24 mmol, 48%) was obtained as a white solid. R<sub>f</sub> 0.44 (*n*-hexane/EtOAc = 3:4). <sup>1</sup>H NMR (400 MHz, CDCl<sub>3</sub>, 24 °C): δ 2.46, (s, 6H), 7.08 (d, *J* = 7.8 Hz, 2H), 7.24 (t, *J* = 8.0 Hz, 1H), 11.13 (br s, 1H). <sup>13</sup>C{<sup>1</sup>H} NMR (101 MHz, CDCl<sub>3</sub>, 24 °C): δ 20.1, 127.9, 129.9, 132.3, 135.6, 175.5. All the resonances of <sup>1</sup>H and <sup>13</sup>C NMR spectra were consistent with the reported values.<sup>29</sup>



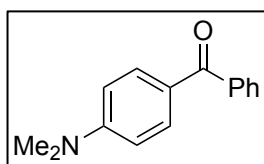
**Naphthalene-1-*d* (5k):** The reaction of 1-fluoronaphthalene (**3b**, 73 mg, 0.50 mmol) at room temperature was followed by addition of deuterium oxide (2.0 g, 100 mmol). Purification of the crude mixture by MPLC (25 g of silica gel, *n*-hexane) gave the title compound (64 mg, 0.50 mmol, 99%) as a white solid.  $R_f$  0.70 (*n*-hexane).  $^1\text{H}$  NMR (400 MHz,  $\text{CDCl}_3$ , 24 °C):  $\delta$  7.50 (d,  $J = 4.6$  Hz, 4H), 7.87 (t,  $J = 3.9$  Hz, 3H).  $^2\text{H}$  NMR (61 MHz,  $\text{CDCl}_3$ , 24 °C):  $\delta$  7.86 (s).  $^{13}\text{C}\{^1\text{H}\}$  NMR (101 MHz,  $\text{CDCl}_3$ , 24 °C):  $\delta$  125.7, 125.8, 127.5 (t,  $J = 26.0$  Hz), 127.9, 127.9, 127.9, 133.4, 133.5. All the resonances of  $^1\text{H}$  and  $^{13}\text{C}$  NMR spectra were consistent with the reported values.<sup>30</sup>



**4,4,5,5-Tetramethyl-2-(naphthalen-1-yl)-1,3,2-dioxaborolane (5l):** The reaction of 1-fluoronaphthalene (**3b**, 73 mg, 0.50 mmol) in the presence of triisopropyl borate (141 mg, 0.75 mmol) at room temperature was followed by addition of 3 M HCl aq. (2.0 mL). The mixture was extracted with EtOAc and combined organic layers were washed with  $\text{H}_2\text{O}$ . All of the volatiles were removed by rotary evaporator. A 15 mL vial with a stirring bar was charged with the resulting mixture, pinacol (65 mg, 0.55 mmol), and *n*-hexane (10 mL), and the resulting mixture was stirred for 24 h at room temperature. After evaporation of volatiles, purification of the crude mixture by MPLC (Biotage® Sfär Silica High Capacity Duo 20 mm, 25 g, *n*-hexane:EtOAc = 5:1) gave the title compound (85 mg, 0.34 mmol, 67%) as a white solid.  $R_f$  0.49 (*n*-hexane/EtOAc = 5:1).  $^1\text{H}$  NMR (400 MHz,  $\text{CDCl}_3$ , 24 °C):  $\delta$  1.45 (s, 12H), 7.50 (t,  $J = 7.3$  Hz, 2H), 7.57 (t,  $J = 7.6$  Hz, 1H), 7.86 (d,  $J = 7.8$  Hz, 1H), 7.96 (d,  $J = 7.8$  Hz, 1H), 8.12 (d,  $J = 6.4$  Hz, 1H), 8.81 (d,  $J = 8.2$  Hz, 1H).  $^{13}\text{C}\{^1\text{H}\}$  NMR (101 MHz,  $\text{CDCl}_3$ , 24 °C):  $\delta$  24.9, 83.7, 124.9, 125.4, 126.3, 128.3, 128.4, 131.6, 133.2,

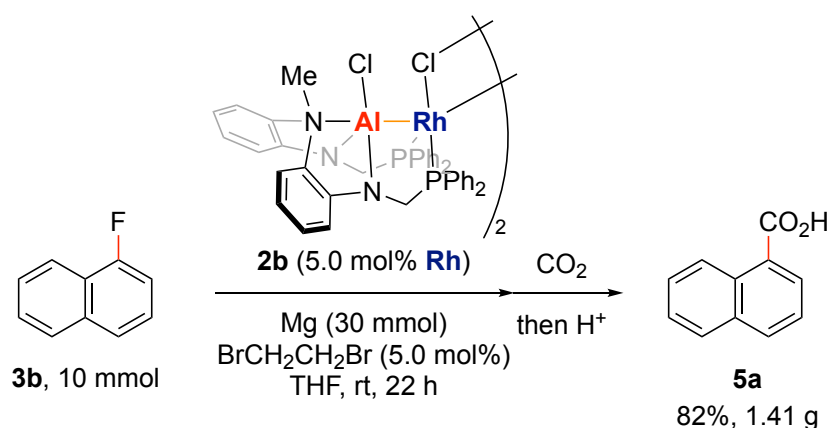


135.6, 136.9, the carbon directly attached to the boron atom was not detected due to quadrupolar relaxation.  $^{11}\text{B}\{^1\text{H}\}$  NMR (128 MHz,  $\text{CDCl}_3$ , 24 °C):  $\delta$  30.7. All the resonances of  $^1\text{H}$ ,  $^{11}\text{B}$  and  $^{13}\text{C}$  NMR spectra were consistent with the reported values.<sup>31</sup>



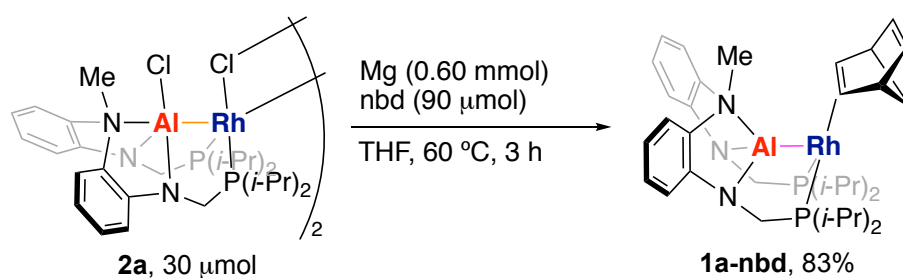
**4-Dimethylaminobenzophenone (5m):** The reaction of 1-fluoro-4-dimethyl-aminobenzene (**3k**, 70 mg, 0.50 mmol) at 50 °C was followed by addition of *N*-methoxy-*N*-methylbenzamide (165 mg, 1.0 mmol). After being stirred at room temperature for 3 h, purification of the mixture by MPLC (Biotage® Sfär Silica High Capacity Duo 20 mm, 25 g, *n*-hexane:EtOAc = 5:1) gave the title compound (25 mg, 0.11 mmol, 22%) as a yellow solid.  $R_f$  0.29 (*n*-hexane/EtOAc = 9:1).  $^1\text{H}$  NMR (400 MHz,  $\text{CDCl}_3$ , 24 °C):  $\delta$  3.07 (s, 6H), 6.68 (d,  $J = 7.8$  Hz, 2H), 7.45 (t,  $J = 7.3$  Hz, 2H), 7.52 (t,  $J = 7.3$  Hz, 1H), 7.73 (d,  $J = 7.8$  Hz, 2H), 7.81 (d,  $J = 8.2$  Hz, 2H).  $^{13}\text{C}\{^1\text{H}\}$  NMR (101 MHz,  $\text{CDCl}_3$ , 24 °C):  $\delta$  40.0, 110.5, 124.8, 128.0, 129.4, 131.1, 132.7, 139.3, 153.3, 195.1. All the resonances of  $^1\text{H}$  and  $^{13}\text{C}$  NMR spectra were consistent with the reported values.<sup>32</sup>

### Gram-scale synthesis



In a glove box, a 80 mL Schlenk tube with a stirring bar was charged with magnesium powder (730 mg, 30 mmol), THF (5.0 mL), and 1,2-dibromoethane (94 mg, 0.5 mmol), and the resulting mixture was stirred for 20 min at room temperature. **3b** (10 mmol), **2b** (404 mg, 0.25 mmol), and THF (15 mL) were put into the Schlenk tube. The Schlenk tube was taken out of the glove box and the mixture was stirred for 22 h at room temperature and then, stirred under atmospheric pressure of CO<sub>2</sub> at room temperature for 30 min. To the mixture was added 3 M HCl aq. (20 mL). The mixture was extracted with EtOAc and combined organic layers were washed with H<sub>2</sub>O. All of the volatiles were removed by rotary evaporator. The mixture was extracted with EtOAc and combined organic layers were washed with H<sub>2</sub>O. All of the volatiles were removed by rotary evaporator. After MPLC purification (40 g of silica gel, *n*-hexane:CH<sub>2</sub>Cl<sub>2</sub> = 1:2 then *n*-hexane:EtOAc = 3:4), the title compound (1.4 g, 8.2 mmol, 82%) was obtained as a white solid. R<sub>f</sub> 0.59 (*n*-hexane/EtOAc = 3:4).

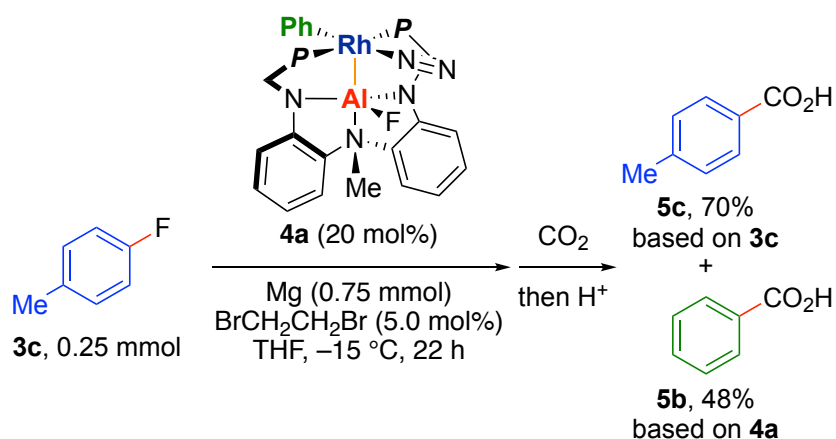
#### General procedures for Eq. 2-1.



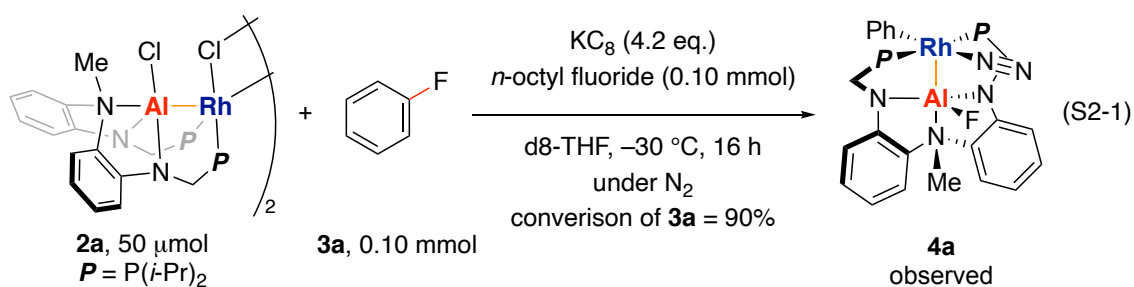
In a glove box, a 4 mL vial with a stirring bar was charged with **2a** (40 mg, 30  $\mu\text{mol}$ ), magnesium powder (15 mg, 0.60 mmol), 2,5-norbornadiene (nbd, 8.3 mg, 90  $\mu\text{mol}$ ), and THF (1.0 mL) and the resulting mixture was stirred for 3 h at 60 °C. After filtration through a KIRIYAMA filter paper (No. 5A), the filtrate was concentrated to

afford a brown precipitate. The precipitate was analyzed by  $^1\text{H}$  and  $^{31}\text{P}$  NMR spectroscopies. Spectroscopic data for **1a-nbd** match those previously reported in the literature.<sup>8a</sup>

### General procedures for Eq. 2-2.



In a glove box, a 4 mL vial with a stirring bar was charged with magnesium powder (18 mg, 0.75 mmol), THF (500  $\mu\text{L}$ ), and 1,2-dibromoethane (2.3 mg, 13  $\mu\text{mol}$ ) and the resulting mixture was stirred for 20 min at room temperature. **3c** (28 mg, 0.25 mmol), **4a** (36 mg, 50  $\mu\text{mol}$ ), and THF (500  $\mu\text{L}$ ) were put into the vial. The mixture was stirred for 22 h at -15 °C. The resulting mixture was stirred under CO<sub>2</sub> (1 atm) at room temperature for 30 min. To the mixture was added 3 M HCl (1.5 mL). The mixture was extracted with EtOAc and combined organic layers were washed with H<sub>2</sub>O. All of the volatiles were removed by rotary evaporator. The crude mixture was analyzed by  $^1\text{H}$  NMR spectroscopy with 1,3,5-trimethoxybenzene (13 mg, 76  $\mu\text{mol}$ ) as an internal standard. According to the  $^1\text{H}$  NMR spectrum, yields of *p*-toluic acid (**5c**) and benzoic acid (**5b**) were estimated in 70% yield (0.18 mmol) based on **3c** and 48% yield (24  $\mu\text{mol}$ ) based on **4a**, respectively.

Carbon–fluorine bond activation at  $-30\text{ }^{\circ}\text{C}$  (Eq. S2-1).

To a d8-THF (1.0 mL) solution of **2a** (71 mg, 50  $\mu\text{mol}$ ) and fluorobenzene (**3a**, 10 mg, 0.10 mmol), a suspension of potassium graphite (28 mg, 0.21 mmol) in d8-THF (2.0 mL) was slowly added at  $-78\text{ }^{\circ}\text{C}$ . After the reaction mixture was stirred at  $-30\text{ }^{\circ}\text{C}$  for 16 h,  $^{19}\text{F}$  NMR spectroscopy of the resulting mixture was measured at  $-30\text{ }^{\circ}\text{C}$ . Formation of **4a** was not confirmed by  $^{19}\text{F}$  NMR spectroscopy at  $-30\text{ }^{\circ}\text{C}$  because of broadness of the signal of **4a** at  $-30\text{ }^{\circ}\text{C}$ . However, we concluded that cooperative activation of the C–F bond of **3a** by in situ generated **1a** occurred at  $-30\text{ }^{\circ}\text{C}$  based on the results as follows: 1) When the same sample was measured at room temperature, **4a** was clearly observed (Figure S2-5). 2) The conversion of **3a** at  $-30\text{ }^{\circ}\text{C}$  was estimated in 90% by  $^{19}\text{F}$  NMR spectroscopy with *n*-octyl fluoride (13 mg, 0.10 mmol) as an internal standard (Figure S2-6). 3) The catalytic magnesiation of **3a** proceeded at  $-30\text{ }^{\circ}\text{C}$ .

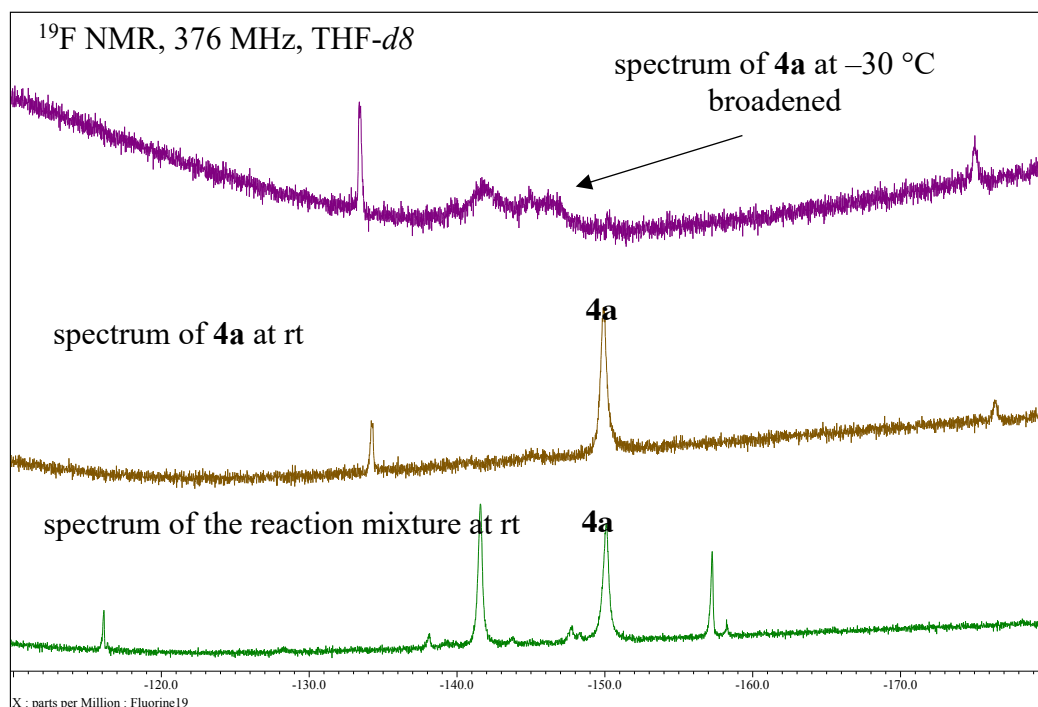


**Figure S2-5.**  $^{19}\text{F}$  NMR spectra of the reaction mixture related to Eq. S2-1 (green: measured at  $-30\text{ }^{\circ}\text{C}$ , brown: measured at room temperature) and **4a** (blue: measured at  $-30\text{ }^{\circ}\text{C}$ , purple: measured at room temperature).

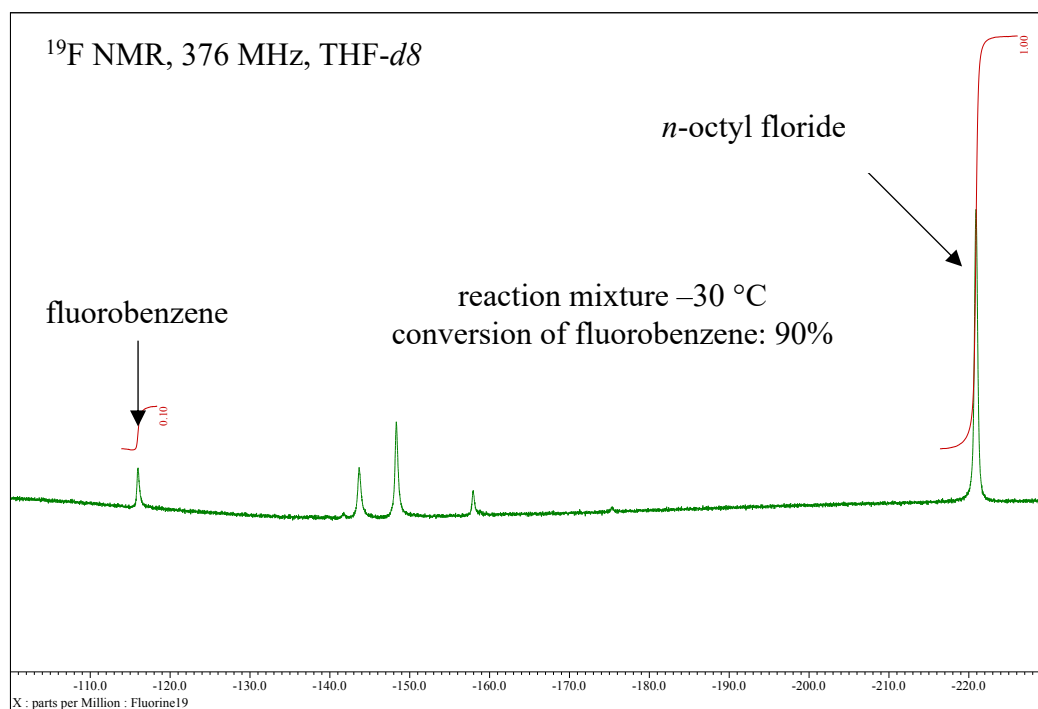
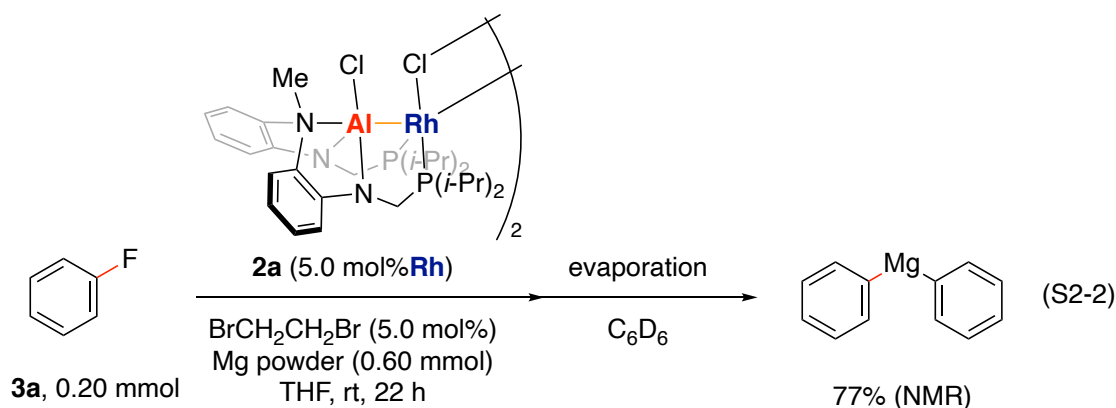


**Figure S2-6.** A  $^{19}\text{F}$  NMR spectrum of Eq. S2-1 with *n*-octyl fluoride as an internal standard.

**Identification of the generated organomagnesium species (Eq. S2-2).**



In a glove box, a 4 mL vial with a stirring bar was charged with magnesium powder (15 mg, 0.60 mmol), THF (500  $\mu$ L), and 1,2-dibromoethane (1.9 mg, 10  $\mu$ mol) and the resulting mixture was stirred for 20 min at room temperature. Fluorobenzene (**3a**, 19 mg, 0.20 mmol), **2a** (6.7 mg, 5.0  $\mu$ mol), and THF (500  $\mu$ L) were put into the vial. The mixture was stirred for 22 h at room temperature. All of the volatiles were removed. Internal standard (1,3,5-trimethoxybenzene, 39 mg, 0.23 mmol) and C<sub>6</sub>D<sub>6</sub> (500  $\mu$ L) were added to the resulting mixture. According to <sup>1</sup>H and <sup>13</sup>C NMR spectra of the mixture, generation of diphenylmagnesium (77% yield) was confirmed by comparing with <sup>1</sup>H and <sup>13</sup>C NMR spectra of independently synthesized diphenylmagnesium with **2a** (5.0 mol% Rh) or **4a** (5.0 mol% Rh) in C<sub>6</sub>D<sub>6</sub>.<sup>20a</sup> In addition, independently synthesized phenylmagnesium fluoride<sup>20b</sup> has very low solubility toward THF and C<sub>6</sub>D<sub>6</sub>.

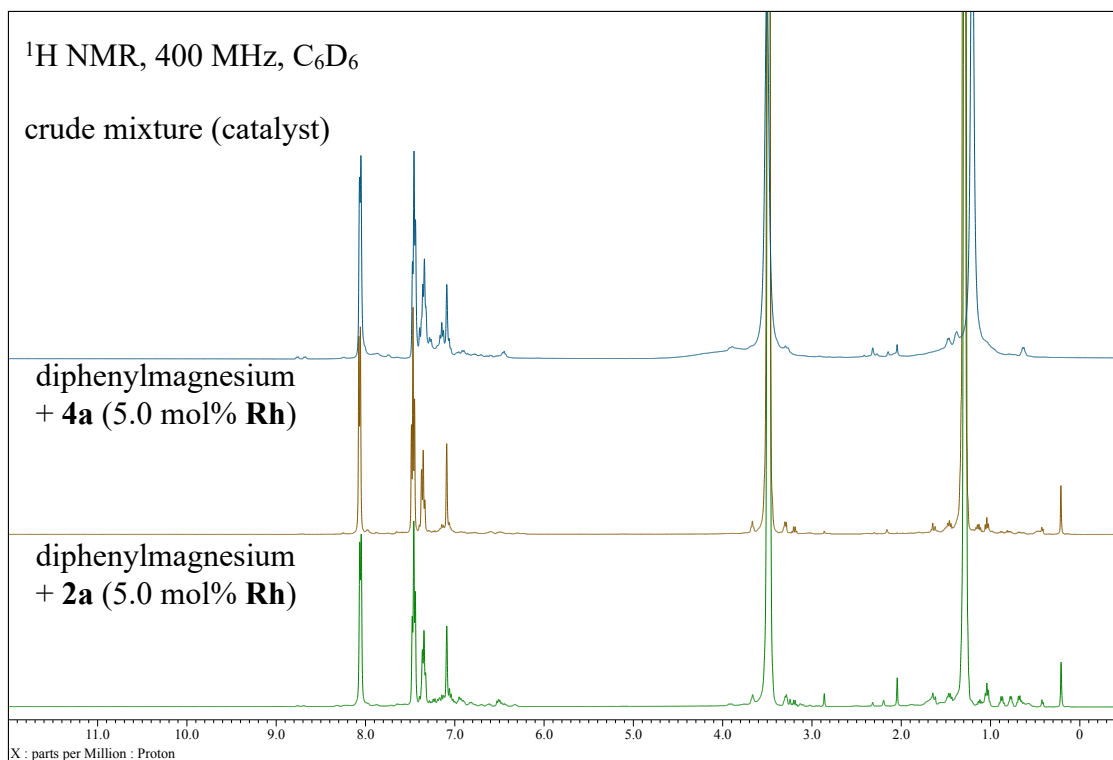


Figure S2-7.  $^1\text{H}$  NMR spectra related to Eq. S2-2.

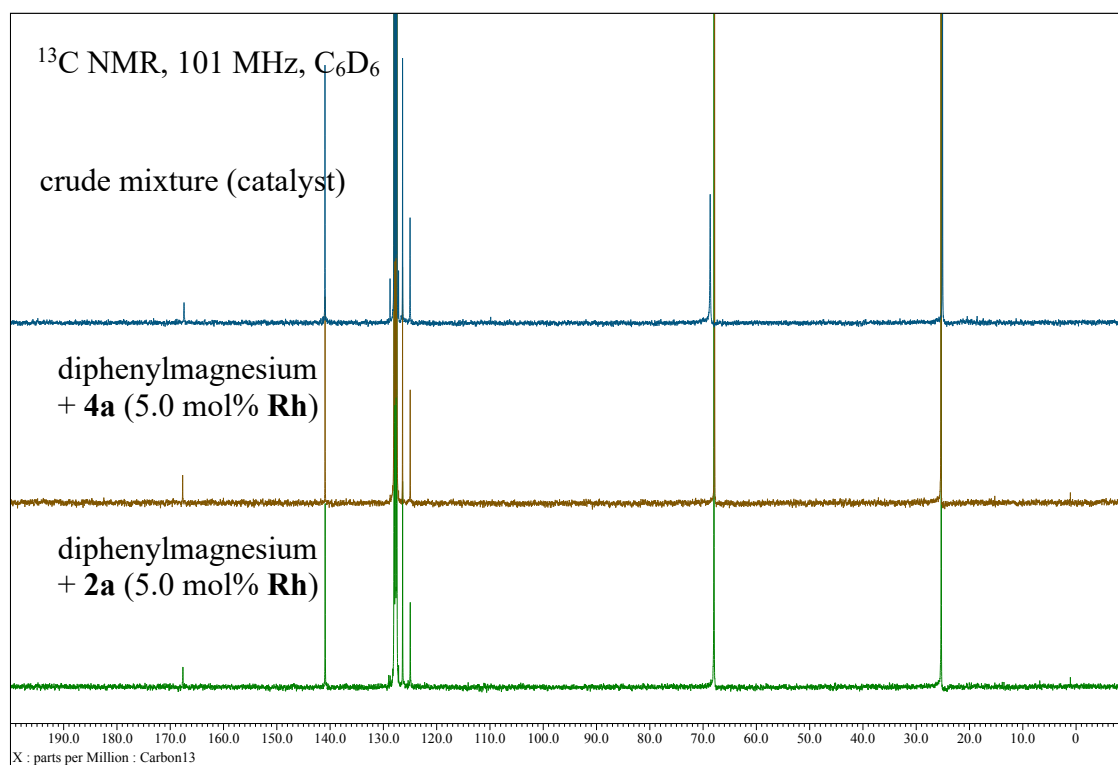
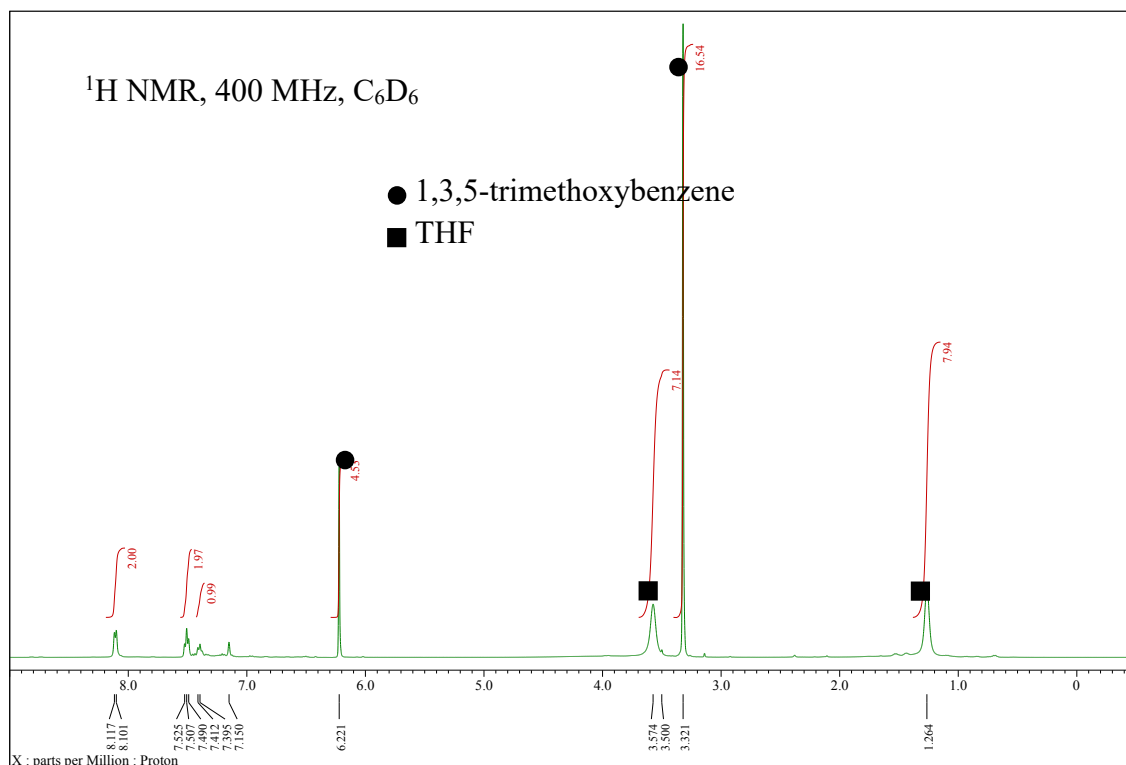
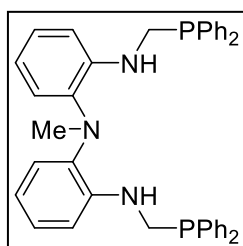


Figure S2-8.  $^{13}\text{C}$  NMR spectra related to Eq. S2-2.



**Figure S2-9.**  $^1\text{H}$  NMR spectrum of Eq. S2-2 with 1,3,5-trimethoxybenzene.

### Synthesis of Al–Rh complex 2b.

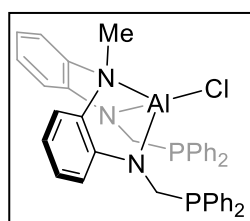


**PNNNP ligand (LH<sub>2</sub>):** Formaldehyde (0.60 g, 20 mmol) and diphenylphosphine (3.7 g, 20 mmol) were charged in an 80 mL Schlenk tube and the reaction mixture was stirred for 2 h at 100 °C. After being cooled to room temperature, to the reaction mixture was

added toluene (150 mL) and *N*-(2-aminophenyl)-*N*-methylbenzene-1,2-diamine (2.1 g, 10 mmol). The mixture was stirred for 16 h at 80 °C. After cooling the solution to room temperature, it was dried over MgSO<sub>4</sub>. After filtration of MgSO<sub>4</sub>, the filtrate was concentrated under reduced pressure. Diethyl ether (10 mL) x 2 was added and evaporated under reduced pressure to remove toluene. The desired product was obtained as light brown powder (5.5 g, 9.1 mmol, 91% yield). The obtained product was used in the next



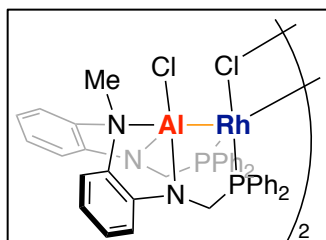
step without further purifications. crude NMR data:  $^1\text{H}$  NMR (400 MHz,  $\text{CDCl}_3$ , 24 °C):  $\delta$  2.67 (s, 3H,  $\text{NCH}_3$ ), 3.64 (s br, 4H,  $\text{PCH}_2\text{-NH}$ ), 4.37 (s br, 2H,  $\text{PCH}_2\text{-NH}$ ), 6.66 (d,  $J = 6.9$  Hz, 4H, overlapped one doublet signal (2H) and one triplet signal (2H)), 6.93 (d,  $J = 7.3$  Hz, 2H), 7.00 (t,  $J = 7.6$  Hz, 2H), 7.22–7.39 (20H).  $^{13}\text{C}\{^1\text{H}\}$  NMR (101 MHz,  $\text{CDCl}_3$ , 24 °C):  $\delta$  40.2, 43.6 (d,  $J_{\text{P-C}} = 9.3$  Hz), 110.8, 117.1, 121.6, 125.1, 128.5 (d,  $J_{\text{P-C}} = 6.9$  Hz), 128.7, 132.7 (d,  $J_{\text{P-C}} = 19$  Hz), 136.2, 136.8 (d,  $J_{\text{P-C}} = 14$  Hz), 142.0 (d,  $J_{\text{P-C}} = 6.9$  Hz).  $^{31}\text{P}\{^1\text{H}\}$  NMR (162 MHz,  $\text{CDCl}_3$ , 24 °C):  $\delta$  -18.8. HRMS-[ESI(+)] (m/z): Calcd. for  $[\text{C}_{39}\text{H}_{37}\text{N}_3\text{P}_2+\text{Na}]^+$ , 632.2353; found, 632.2355.



**L(AlCl):** To a  $\text{Et}_2\text{O}$  (60 mL) solution of  $\text{LH}_2$  (12 g, 20 mmol) in an 80 mL Schlenk tube, a solution of *t*-BuLi in pentane (1.53 M, 27 mL, 41 mmol) was added dropwise at room temperature. The

resulting solution was stirred for 15 min and then, it was added dropwise to a suspension of  $\text{AlCl}_3$  (2.6 g, 20 mmol) in toluene (60 mL) at room temperature. After stirring the reaction mixture for 3 h at room temperature, the solution was evaporated under reduced pressure and the target compound was extracted with toluene (ca. 200 mL). The toluene solution was evaporated again under reduced pressure, and the precipitate was washed by hexane (20 mL, 10 mL x 2) to afford  $\text{L(AlCl)}$  as a gray powder (7.0 g, 10 mmol, 53%).  $\text{L(AlCl)}$  was used in next step without further purifications. crude NMR data of  $\text{L(AlCl)}$ ;  $^1\text{H}$  NMR (400 MHz,  $\text{C}_6\text{D}_6$ , 24 °C):  $\delta$  2.76 (s, 3H,  $\text{NCH}_3$ ), 3.49 (d,  $J = 12.8$  Hz, 2H,  $\text{PCH}_2\text{-NH}$ ), 3.88 (d,  $J = 12.8$  Hz, 2H,  $\text{PCH}_2\text{-NH}$ ), 6.52 (t,  $J = 7.8$  Hz, 2H), 6.58 (d,  $J = 7.8$  Hz, 2H), 6.90–7.11 (m br, 16H), 7.37 (m br, 4H), 7.53 (m br, 4H).  $^{13}\text{C}\{^1\text{H}\}$  NMR (101 MHz,  $\text{C}_6\text{D}_6$ , 24 °C):  $\delta$  45.7, 47.1, 112.1, 115.5, 122.2, 128.7 (t,  $J_{\text{P-C}} = 3.5$  Hz), 128.8, 128.9 (t,

$J_{\text{P-C}} = 3.5$  Hz), 129.0, 129.5, 132.4 (t,  $J_{\text{P-C}} = 8.1$  Hz), 134.0 (t,  $J_{\text{P-C}} = 8.7$  Hz), 136.2, 136.9, 137.2, 149.3 (t,  $J_{\text{P-C}} = 8.7$  Hz).  $^{31}\text{P}\{^1\text{H}\}$  NMR (162 MHz,  $\text{C}_6\text{D}_6$ , 24 °C):  $\delta$  -18.8.



**2b**: To a toluene (2.0 mL) solution of  $[\text{Rh}(\text{nbd})(\mu\text{-Cl})_2]$  (688 mg, 1.5 mmol),  $\text{L}(\text{AlCl})$  (2.0 g, 3.0 mmol) in toluene (18 mL) was added dropwise at room temperature. The resulting deep dark-red solution was stirred at 80 °C for 16 h to generate dull yellow precipitates. The precipitates were collected by filtration and then, washed with toluene (2.0 mL) x 3, THF (2.0 mL) x 3, and pentane (2.0 mL) x 3 in this order. After drying it under reduced pressure, yellow crystals (1.5 g, 1.9 mmol, 62%, calculated as monomer) were obtained. m.p. 289 °C (decomp). Yellow crystals of **2b**, which are suitable for x-ray diffraction analysis and elemental analysis, were obtained from a saturated dichloromethane solution of **2b** at -35 °C. It was difficult to identify **2b** by NMR spectroscopies completely because it showed low solubility of **2b** toward common organic solvents and the signals from **2b** is almost broad since it may adopt unsymmetrical forms in solution similar to the almost same complex we previously reported.<sup>8a</sup>  $^1\text{H}$  NMR (400 MHz,  $\text{CD}_2\text{Cl}_2$ , 24 °C):  $\delta$  3.29 (br, 3H), 3.50 (s, 4H), 6.18 (br, 2H), 6.71 (br, 2H), 6.94–7.34 (m br, 16H), 7.40–7.92 (br, 8H).  $^{13}\text{C}$  NMR could not be measured because of low intensity of signals at room temperature.  $^{31}\text{P}\{^1\text{H}\}$  NMR (162 MHz,  $\text{CD}_2\text{Cl}_2$ , -80 °C):  $\delta$  48.6/60.0 ( $J_{\text{P-Rh}} = 161.3/161.3$  Hz,  $J_{\text{P-P}} = 39.2/39.2$  Hz), 50.9/58.3 ( $J_{\text{P-Rh}} = 174.4/170.0$  Hz,  $J_{\text{P-P}} = 34.9/34.9$  Hz). Anal. Calcd.  $\text{C}_{79}\text{H}_{72}\text{Cl}_6\text{N}_6\text{P}_4\text{Al}_2\text{Rh}_2$  (**2b** + 1.0 dichloromethane): C, 55.75; H, 4.26; N, 4.94. Found: C, 55.79; H, 4.52; N, 4.87.

**X-ray diffraction study and X-ray crystallographic analysis.**

The crystals of **2b** and **4a** were mounted on the CryoLoop (Hampton Research Corp.) with a layer of light mineral oil and placed in a nitrogen stream at 143(1) K. The X-ray structural determinations of **2b** were performed on a Rigaku/Saturn724+ CCD diffractometers using graphite-monochromated Mo K $\alpha$  radiation ( $\lambda = 0.71075 \text{ \AA}$ ) at 153 K, and processed using CrysAlis<sup>Pro</sup> (Agilent).<sup>33</sup> The X-ray structural determinations of **4a** were performed on a Rigaku/Saturn724+ CCD diffractometers using graphite-monochromated Mo K $\alpha$  radiation ( $\lambda = 0.71075 \text{ \AA}$ ) at 153 K, and processed using CrystalClear (Rigaku, Tokyo, Japan).<sup>34,35</sup> The structures were solved by a direct method and refined by full-matrix least-square refinement on  $F^2$ . The structure of **2b** was solved by SHELXT and refined by SHELXL.<sup>36,37</sup> The structure of **4a** was solved by SIR92<sup>38</sup> and refined by SHELXL (Version 2018/3).<sup>36,37</sup> Non-hydrogen atoms were anisotropically refined. Hydrogen atoms were included in the refinement on calculated positions riding on their carrier atoms. The function minimized was  $[\sum w(F_o^2 - F_c^2)^2]$  ( $w = 1 / [\sigma^2(F_o^2) + (aP)^2 + bP]$ ), where  $P = (\text{Max}(F_o^2, 0) + 2F_c^2) / 3$  with  $\sigma^2(F_o^2)$  from counting statistics. The function  $R1$  and  $wR2$  were  $(\sum ||F_o| - |F_c||) / \sum |F_o|$  and  $[\sum w(F_o^2 - F_c^2)^2 / \sum (wF_o^4)]^{1/2}$ , respectively. CCDC 2000480 (for **2b**) and 1999655 (for **4a**) contain the supplementary crystallographic data. These data can be obtained from The Cambridge Crystallographic Data Centre. A B alert in the CIF file of **4a** could not be solved because crystals require a long exposure time due to their low crystallinity.

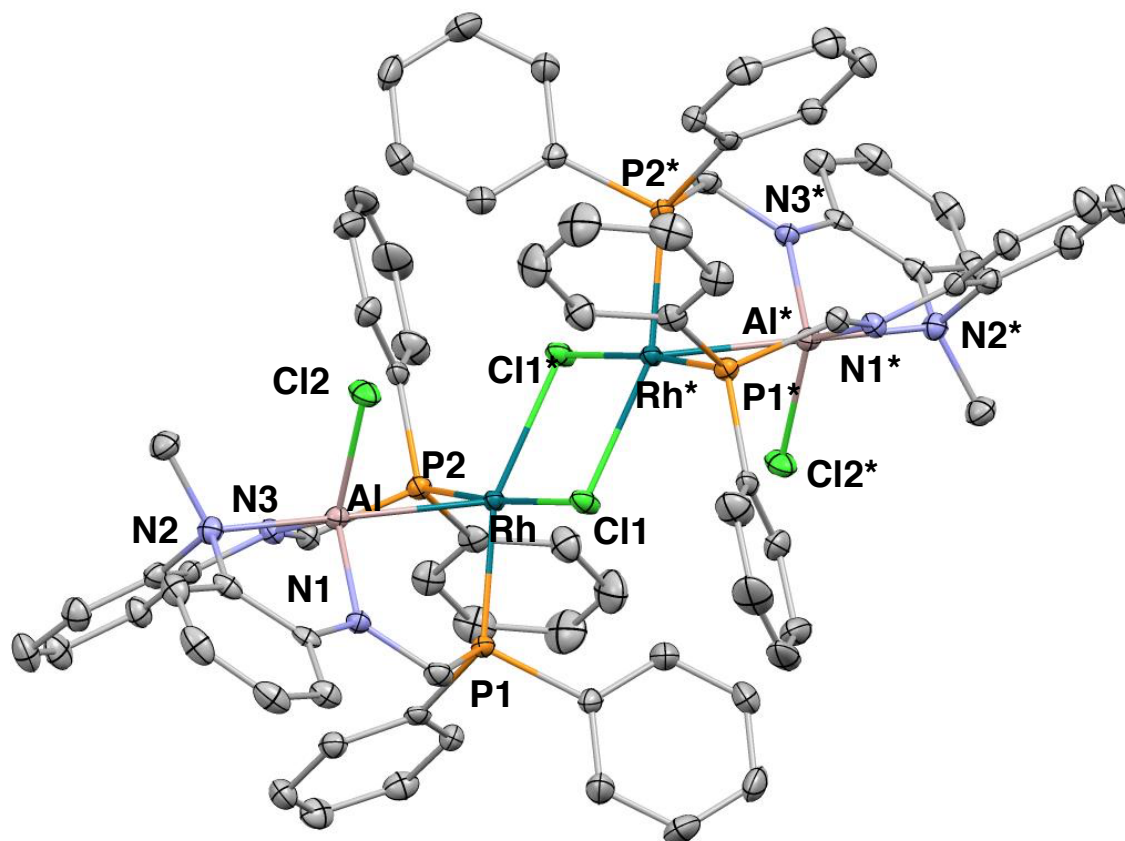


**Figure S2-10.** Crystal structure of **2b** (atomic displacement parameters set at 30% probability; all hydrogen atoms and solvent molecules are omitted for clarity). Selected bond lengths [ $\text{\AA}$ ] and angles [ $^\circ$ ]: Complex **2b**: Rh–Al 2.6117(9), Rh–P1 2.2198(9), Rh–P2 2.2124(8), Rh–Cl1 2.4468(9), Al–Cl2 2.182(2), Al–N1 1.863(2), Al–N2 2.152(2), Al–N3 1.868(3), P1–Rh–P2 97.31(3), N2–Al–Rh 177.21(8), N1–Al–N3 114.8(1).

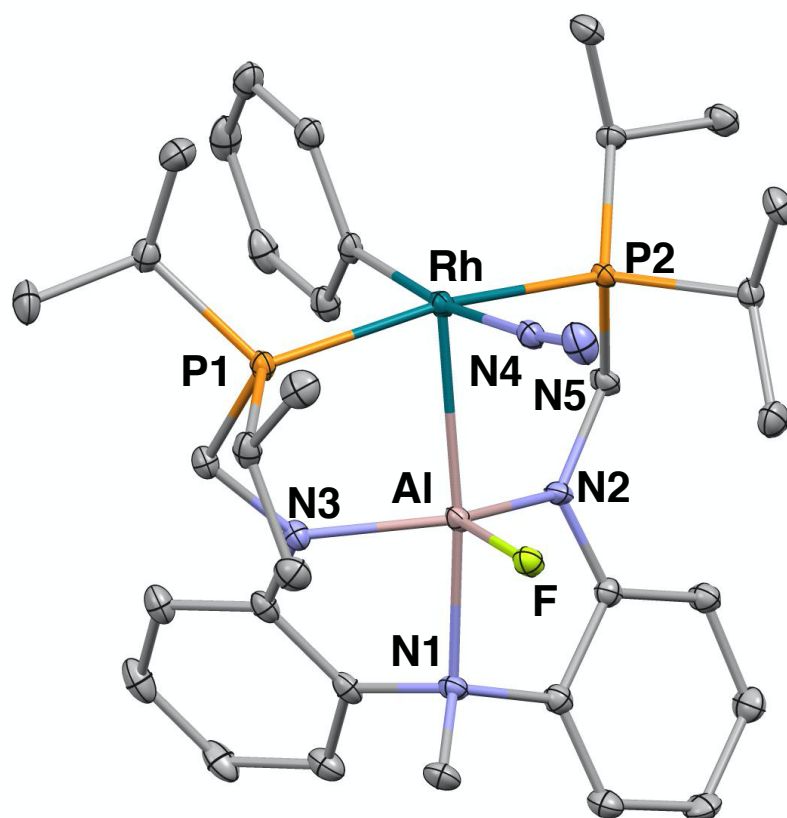


**Figure S2-11.** Crystal structure of **4a** (atomic displacement parameters set at 30% probability; all hydrogen atoms and solvent molecules are omitted for clarity). Selected bond lengths [ $\text{\AA}$ ] and angles [ $^\circ$ ]: Complex **4a**: Rh–Al 2.6098(8), Rh–P1 2.3342(8), Rh–P2 2.3090(8), Rh–C 2.039(3), Rh–N4 2.000(3), Al–F 1.687(2), Al–N1 2.105(2), Al–N2 1.883(2), Al–N3 1.873(2), N4–N5 1.090(4), P1–Rh–P2 164.58(3), Rh–Al–N1 172.88(7), N2–Al–N3 124.1(1).

**Table S2-1.** Crystallographic data of **2b** and **4a**.

compound	<b>2b</b>	<b>4a</b>
empirical formula	C <sub>78</sub> H <sub>70</sub> Al <sub>2</sub> Cl <sub>4</sub> N <sub>6</sub> P <sub>4</sub> Rh <sub>2</sub>	C <sub>33</sub> H <sub>48</sub> AlFN <sub>5</sub> P <sub>2</sub> Rh
formula weight	1616.91	725.61
crystal system	monoclinic	triclinic
space group	<i>P</i> 1 21/n 1 (#14)	<i>P</i> $\bar{1}$ (#2)
<i>a</i> , Å	14.3121(5)	10.079(2)
<i>b</i> , Å	19.2665(6)	11.873(2)
<i>c</i> , Å	15.4196(5)	15.392(3)
$\alpha$ , deg.	90	67.234(6)
$\beta$ , deg.	112.521(4)	80.582(7)
$\gamma$ , deg.	90	87.293(9)
<i>V</i> , Å <sup>3</sup>	3927.6(2)	1675.3(6)
<i>Z</i>	4	2
<i>D</i> calcd, g/cm <sup>-3</sup>	1.511	1.438
$\mu$ [Mo- <i>K</i> $\alpha$ ], mm <sup>-1</sup>	0.845	0.667
<i>T</i> , K	143	143
crystal size, mm	0.140 x 0.120 x 0.110	0.090 x 0.070 x 0.060
$\theta$ range for data collection (deg.)	2.552 to 25.350	3.20 to 27.50
no. of reflections measured	27345	13581
unique data	7179	7303
data / restraints / parameters	7179 / 0 / 461	7303 / 0 / 388
<i>R</i> 1 ( <i>I</i> > 2.0 $\sigma$ ( <i>I</i> ))	0.0356	0.0381
<i>wR</i> 2 ( <i>I</i> > 2.0 $\sigma$ ( <i>I</i> ))	0.0733	0.0768
<i>R</i> 1 (all data)	0.0495	0.0489
<i>wR</i> 2 (all data)	0.0787	0.0812
GOF on <i>F</i> <sup>2</sup>	1.031	1.006

a)  $R1 = (\sum||F_o| - |F_c||)/(\sum|F_o|)$  b)  $wR2 = [\{\sum w(F_o^2 - F_c^2)^2\}/\{\sum w(F_o^4)\}]^{1/2}$

**Computational details.**

Geometries were optimized by the DFT method with the B3PW91<sup>39</sup>-D3<sup>40</sup> functional in gas phase using small basis set system (BS-I). In BS-I, 6-31G(d)<sup>41</sup> basis sets were used for H, C, N, and F atoms and LANL2DZ<sup>42</sup> basis sets were used for Al, P, and Rh atoms with corresponding effective core potentials (ECPs), where one 3d polarization<sup>43</sup> function was added to Al and P atoms. The B3PW91-D3 functional was employed herein because the geometry of the Al–Rh complex could be reproduced well using this functional, as shown in Figure S2-12 and Table S2-2.

The potential energy was re-evaluated using the same functional with a better basis set system (BS-II); in BS-II, 6-311G(d)<sup>44</sup> basis sets were used for H, C, N, F, and P atoms, 6-311+G(2d)<sup>45</sup> basis set was used for Al atom, and the Stuttgart-Dresden-Bonn (SDB)<sup>46</sup> basis set (311111/22111/411/11) with the corresponding ECPs was used for Rh atom. Solvation effect of THF was considered using PCM model.<sup>47</sup> We selected the B3PW91-D3 functional for energy evaluation because the DFT calculation with this functional reproduced well the CCSD(T)-calculated energy changes in C–F bond activation by a model Al–Rh complex; the model reaction is shown in Figure S2-13 and the energy changes are presented in Table S2-3.

In this work, the discussion is presented using the Gibbs energy (298.15 K, 1 atm), where the translation entropy in solution was corrected with the method developed by Whitesides *et al.*<sup>48</sup> All these calculations were carried out with the Gaussian 16 program.<sup>49</sup>

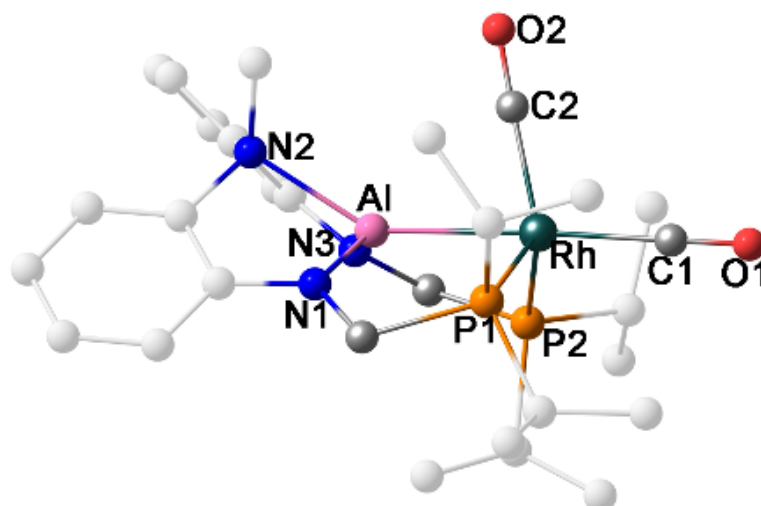


**Figure S2-12.** Rh(PAIP)(CO)<sub>2</sub> used for test calculation of geometry optimization.

**Table S2-2.** Comparison of optimized bond distances (Å) with the experimental values of Rh(PAIP)(CO)<sub>2</sub>.

	Rh-Al	Rh-P <sup>1</sup>	Rh-P <sup>2</sup>	Rh-C <sup>1</sup>	Rh-C <sup>2</sup>	Al-N <sup>1</sup>	Al-N <sup>2</sup>	Al-N <sup>3</sup>	C <sup>1</sup> -O <sup>1</sup>	C <sup>2</sup> -O <sup>2</sup>	RMSE
Exp.	2.439	2.362	2.344	1.935	1.874	1.812	2.094	1.837	1.139	1.149	
B3PW91	2.457	2.410	2.399	1.934	1.890	1.868	2.141	1.879	1.157	1.165	0.037
B3PW91-D3	2.435	2.381	2.368	1.931	1.891	1.861	2.118	1.873	1.158	1.166	0.025
B3LYP-D3	2.447	2.415	2.402	1.954	1.901	1.862	2.123	1.873	1.158	1.167	0.036
BP86-D3	2.448	2.389	2.390	1.932	1.896	1.884	2.112	1.875	1.175	1.183	0.035
ωB97XD	2.441	2.406	2.391	1.940	1.897	1.856	2.124	1.870	1.153	1.161	0.030
M06	2.466	2.454	2.429	1.964	1.913	1.860	2.116	1.871	1.157	1.165	0.048

As shown in Table S2-2, the RMSE (root mean squared error) by the B3PW91-D3 functional is the smallest, suggesting that this functional can be used for geometry optimization of the Al–Rh complex.



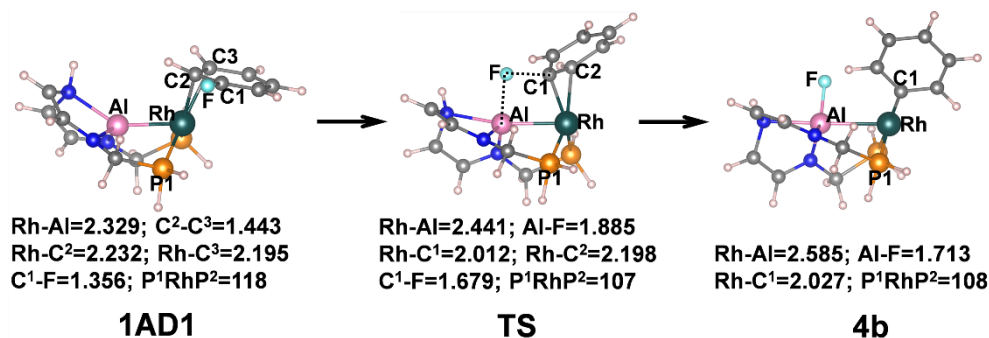


**Figure S2-13.** Geometry changes in a C–F bond cleavage of fluorobenzene using a model PAIP ligand.<sup>a</sup>

<sup>a</sup> In the model complex, phenyl groups on the N atoms were replaced with vinyl groups and *iso*-propyl groups on the P atoms were replaced with H atoms to reduce the size. The geometry of the other moiety was taken to be the same as the corresponding structure in the C–F bond activation of PhF by Rh(<sup>Me</sup>PAIP), in which *iso*-propyl groups on the P atoms were replaced with methyl groups for simplicity. Bond length is in angstrom and bond angle is in degree.

**Table S2-3.** Comparison of energy changes (kcal mol<sup>-1</sup>) between CCSD(T) and DFT calculations using various functionals in the model reaction shown in Figure S2-13.

	<b>1AD1</b>	<b>TS</b>	<b>4b</b>	<b>RMSE</b>
CCSD(T)	0.0	3.7	-40.9	Ref.
B3PW91	0.0	6.2	-38.0	2.7
B3PW91-D3	0.0	3.7	-40.7	0.1
B3LYP-D3	0.0	2.4	-45.8	3.6
BP86-D3	0.0	1.2	-37.8	2.8
ωB97XD	0.0	4.2	-43.6	2.0
M06	0.0	2.3	-41.9	1.2

As shown in Table S2-3, the RMSE is the smallest in the case of the B3PW91-D3 calculation in various DFT functionals examined here, suggesting that this functional is useful for investigating this C–F bond activation reaction.

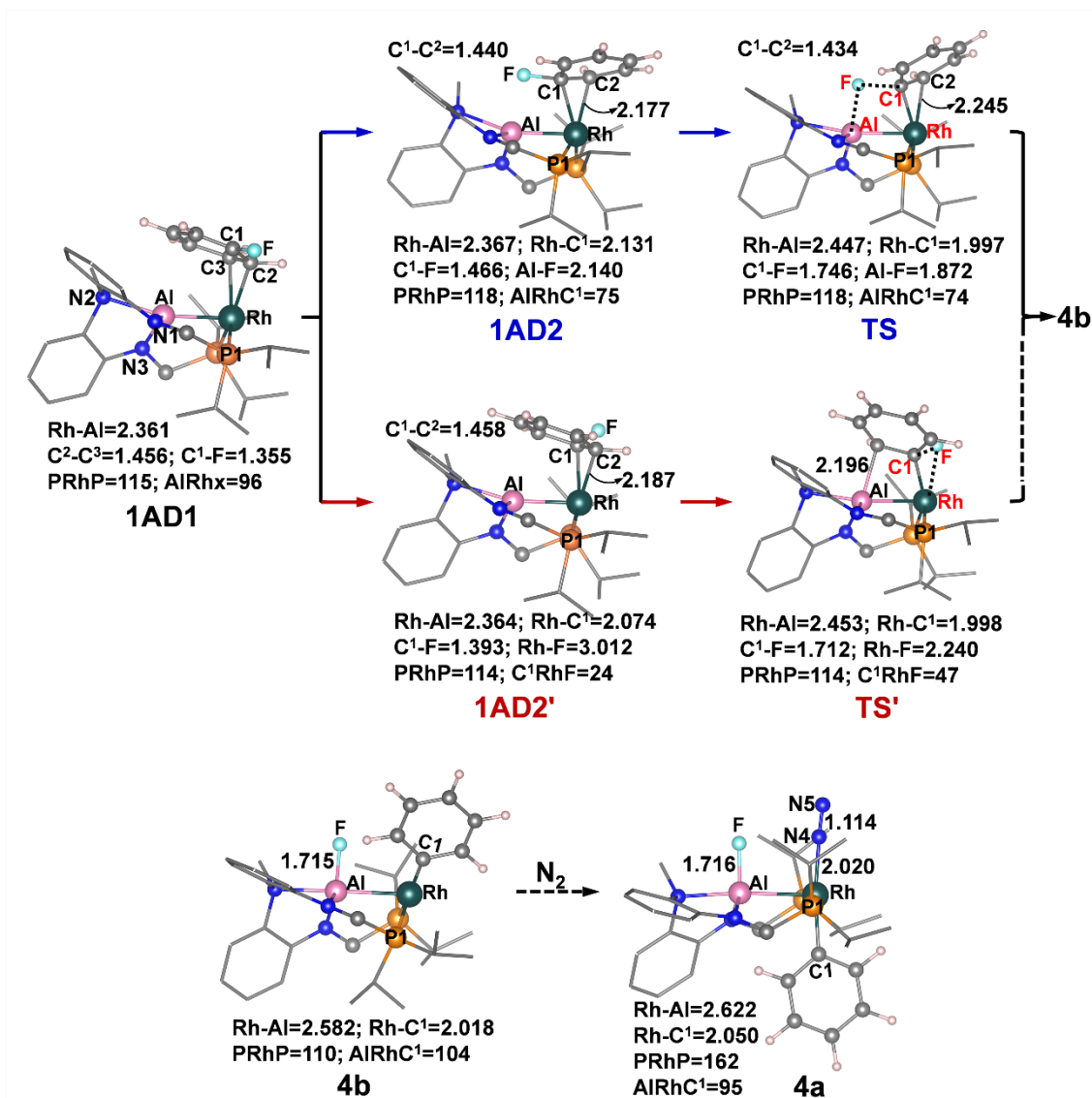


**Figure S2-14.** Geometry changes in the C–F bond activation of PhF by Rh(*i*-PrPAIP) complex, where the superscript *i*-Pr represents isopropyl phosphine. Bond length is in angstrom and bond angle is in degree.

## References and notes

- (1) (a) Powers, I. G.; Uyeda, C. *ACS Catal.* **2017**, *7*, 936. (b) Buchwalter, P.; Rosé, J.; Braunstein, P. *Chem. Rev.* **2015**, *115*, 28. (c) Wheatley, N.; Kalck, P. *Chem. Rev.* **1999**, *99*, 3379. (d) Gade, L. H. *Angew. Chem., Int. Ed.* **2000**, *39*, 2658. (e) Cooper, B. G.; Napoline, J. W.; Thomas, C. M. *Catal. Rev. Sci. Eng.* **2012**, *54*, 1. (f) Mankad, N. P. *Chem.-Eur. J.* **2016**, *22*, 5822. (g) Mankad, N. P. *Chem. Commun.* **2018**, *54*, 1291. (h) Rej, S.; Tsurugi, H.; Mashima, K. *Coord. Chem. Rev.* **2018**, *355*, 223. (i) Farley, C. M.; Uyeda, C. *Trends in Chemistry* **2019**, *1*, 497. (j) Sevin, A.; Hengtai, Y.; Chaquin, P. *J. Organomet. Chem.* **1984**, *262*, 391. (k) Thomas, C. M. *Comments Inorg. Chem.* **2011**, *32*, 14. (l) Trinquier, G.; Hoffmann, R. *Organometallics* **1984**, *3*, 370. (m) Moore, J. T.; Smith, N. E.; Lu, C. C. *Dalton Trans.* **2017**, *46*, 5689.
- (2) (a) Baranger, A. M.; Bergman, R. G. *J. Am. Chem. Soc.* **1994**, *116*, 3822. (b) Hanna, T. A.; Baranger, A. M.; Bergman, R. G. *J. Am. Chem. Soc.* **1995**, *117*, 11363.
- (3) (a) Braun, T.; Salomon, M. A.; Altenhöner, K.; Teltewskoi, M.; Hinze, S. *Angew. Chem., Int. Ed.* **2009**, *48*, 1818. (b) Teltewskoi, M.; Panetier, J. A.; Macgregor, S. A.; Braun, T. *Angew. Chem., Int. Ed.* **2010**, *49*, 3947.
- (4) (a) Aizenberg, M.; Milstein, D. *Science* **1994**, *265*, 359. (b) Raza, A. L.; Panetier, J. A.; Teltewskoi, M.; Macgregor, S. A.; Braun, T. *Organometallics* **2013**, *32*, 3795. (c) Raza, A. L.; Braun, T. *Chem. Sci.* **2015**, *6*, 4255.
- (5) (a) Liu, X.-W.; Echavarren, J.; Zarate, C.; Martin, R. *J. Am. Chem. Soc.* **2015**, *137*, 12470. (b) Yoshikai, N.; Matsuda, H.; Nakamura, E. *J. Am. Chem. Soc.* **2009**, *131*, 9590. (c) Nova, A.; Reinhold, M.; Perutz, R. N.; Macgregor, S. A.; McGrady, J. E. *Organometallics* **2010**, *29*, 1824. (d) Dugan, T. R.; Sun, X.-R.; Rybak-Akimova, E. V.; Olatunji-Ojo, O.; Cundari, T. R.; Holland, P. L. *J. Am. Chem. Soc.* **2011**, *133*,

12418. (e) Dugan, T. R.; Goldberg, J. M.; Brennessel, W. W.; Holland, P. L. *Organometallics* **2012**, *31*, 1349. (f) Asako, S.; Ilies, L.; Verma, P.; Ichikawa, S.; Nakamura, E. *Chem. Lett.* **2014**, *43*, 726. (g) Li, B. Z.; Qian, Y. Y.; Liu, J.; Chan, K. S. *Organometallics* **2014**, *33*, 7059. (h) Bakewell, C.; White, A. J. P.; Crimmin, M. R. *J. Am. Chem. Soc.* **2016**, *138*, 12763. (i) Bakewell, C.; Ward, B. J.; White, A. J. P.; Crimmin, M. R. *Chem. Sci.* **2018**, *9*, 2348. (j) Garçon, M.; Bakewell, C.; White, A. J. P.; Crimmin, M. R. *Chem. Commun.* **2019**, *55*, 1805. (k) Gentner, T. X.; Rösch, B.; Ballmann, G.; Langer, J.; Elsen, H.; Harder, S. *Angew. Chem., Int. Ed.* **2019**, *58*, 607. (l) Bakewell, C.; White, A. J. P.; Crimmin, M. R. *Angew. Chem., Int. Ed.* **2018**, *57*, 6638. (m) Coates, G.; Rekhroukh, F.; Crimmin, M. R. *Synlett* **2019**, *30*, 2233. (n) Kysliak, O.; Görls, H.; Kretschmer, R. *Chem. Commun.* **2020**, *56*, 7865. (o) Talavera, M.; Meißner, G.; Rachor, S. G.; Braun, T. *Chem. Commun.* **2020**, *56*, 4452. (p) Pietrasiak, E.; Lee, E. *Synlett* **2020**, *31*, 1349. (q) Amii, H.; Uneyama, K. *Chem. Rev.* **2009**, *109*, 2119. (r) Eisenstein, O.; Milani, J.; Perutz, R. N. *Chem. Rev.* **2017**, *117*, 8710.
- (6) Marquard, S. L.; Bezpalko, M. W.; Foxman, B. M.; Thomas, C. M. *J. Am. Chem. Soc.* **2013**, *135*, 6018.
- (7) (a) Green, M. L. H. *J. Organomet. Chem.* **1995**, *500*, 127. (b) Fischer, R. A.; Priermeier, T. *Organometallics* **1994**, *13*, 4306. (c) Anand, B. N.; Krossing, I.; Nöth, H. *Inorg. Chem.* **1997**, *36*, 1979. (d) Agou, T.; Yanagisawa, T.; Sasamori, T.; Tokitoh, N. *Bull. Chem. Soc. Jpn.* **2016**, *89*, 1184. (e) Takaya, J.; Iwasawa, N. *J. Am. Chem. Soc.* **2017**, *139*, 6074. (f) Hicks, J.; Mansikkamäki, A.; Vasko, P.; Goicoechea, J. M.; Aldridge, S. *Nat. Chem.* **2019**, *11*, 237. (g) Morisako, S.; Watanabe, S.; Ikemoto, S.; Muratsugu, S.; Tada, M.; Yamashita, M. *Angew. Chem., Int. Ed.* **2019**, *58*, 15031.

- (8) (a) Hara, N.; Saito, T.; Semba, K.; Kuriakose, N.; Zheng, H.; Sakaki, S.; Nakao, Y. *J. Am. Chem. Soc.* **2018**, *140*, 7070. (b) Kuriakose, N.; Zheng, J.-J.; Saito, T.; Hara, N.; Nakao, Y.; Sakaki, S. *Inorg. Chem.* **2019**, *58*, 4894.
- (9) Moore and Lu reported catalytic hydrogenolysis of aryl C–F bonds using a bimetallic rhodium–indium complex, see: Moore, J. T.; Lu, C. C. *J. Am. Chem. Soc.* **2020**, *142*, 11641.
- (10) (a) Amgoune, A. Bourissou, D. *Chem. Commun.* **2011**, *47*, 859. (b) You, D. Gabbai, F. P. *Trends in Chemistry* **2019**, *1*, 485. (c) Vollmer, M. V.; Xie, J.; Lu, C. C. *J. Am. Chem. Soc.* **2017**, *139*, 6570. (d) Devillard, M.; Nicolas, E.; Ehlers, A. W.; Backs, J.; Mallet-Ladeira, S.; Bouhadir, G.; Sloatweg, J. C.; Uhl, W.; Bourissou, D. *Chem. Eur. J.* **2015**, *21*, 74. (e) Cowie, B. E.; Tsao, F. A.; Emslie, D. J. H. *Angew. Chem., Int. Ed.* **2015**, *54*, 2165. (f) Rudd, P. A.; Liu, S.; Gagliardi, L.; Young V. G., Jr.; Lu, C. C. *J. Am. Chem. Soc.* **2011**, *133*, 20724. (g) Saito, T.; Hara, N.; Nakao, Y. *Chem. Lett.* **2017**, *46*, 1247.
- (11) Moore reported that Ru(dmpe)<sub>2</sub>H<sub>2</sub> (dmpe = Me<sub>2</sub>PCH<sub>2</sub>CH<sub>2</sub>PMe<sub>2</sub>) cleaved C–F bond of hexafluorobenzene at –78 °C. However, it was limited to C–F bonds of multi-fluorinated arenes. The reactions of di- or mono-fluorinated arenes were not reported, see: Whittlesey, M. K.; Perutz, R. N.; Moore, M. H. *Chem. Commun.* **1996**, 787.
- (12) *CRC Handbook of Chemistry and Physics*; 94th ed.; Haynes, W. M., Ed.; CRC Press: Boca Raton, 2013.
- (13) (a) *Main Group Metals in Organic Synthesis*; Yamamoto, H., Oshima, K., Eds.; Wiley-VCH: Weinheim, 2004. (b) Ziegler, D. S.; Wei, B.; Knochel, P. *Chem.-Eur. J.* **2019**, *25*, 2695.

- (14) (a) Rieke, R. D.; Bales, S. E. *J. Am. Chem. Soc.* **1974**, *96*, 1775. (b) Tjurina, L. A.; Kombarova, S. V.; Bumagin, N. A.; Beletskaya, I. P. *Metalloorganicheskaya Khimiya* **1990**, *3*, 48. (c) Tjurina, L. A.; Smirnov, V. V.; Barkovskii, G. B.; Nikolaev, E. N.; Esipov, S. E.; Beletskaya, I. P. *Organometallics* **2001**, *20*, 2449. (d) Speight, I. R.; Hanusa, T. P. *Molecules* **2020**, *25*, 570.
- (15) Piller, F. M.; Appukkuttan, P.; Gavryushin, A.; Helm, M.; Knochel P. *Angew. Chem., Int. Ed.* **2008**, *47*, 6802.
- (16) Bogdanović, B.; Liao, S.-T.; Mynott, R.; Schlichte, K.; Westeppe, U. *Chem. Ber.* **1984**, *117*, 1378.
- (17) Krasovskiy, A.; Knochel, P. *Angew. Chem., Int. Ed.* **2004**, *43*, 3333.
- (18) (a) Modha, S. G.; Mehta, V. P.; Van Der Eycken, E. V. *Chem. Soc. Rev.* **2013**, *42*, 5042. (b) Wang, L.; He, W.; Yu, Z. *Chem. Soc. Rev.* **2013**, *42*, 599. (c) Wenkert, E.; Ferreira, T. W.; Michelotti, E. L. *J. Chem. Soc., Chem. Commun.* **1979**, 637. (d) Okamura, H.; Miura, M.; Takei, H. *Tetrahedron Lett.* **1979**, *20*, 43.
- (19) Nahm, S.; Weinreb, S. M. *Tetrahedron Lett.* **1981**, *22*, 3815.
- (20) Generation of diphenylmagnesium<sup>20a</sup> was implied by comparing <sup>1</sup>H and <sup>13</sup>C NMR spectra of the crude mixture in C<sub>6</sub>D<sub>6</sub>, with those of independently synthesized diphenylmagnesium in the presence of **2a** or **4a** (5.0 mol% Rh). (a) Tang, H.; Richey, H. G. *Organometallics* **2001**, *20*, 1569. In addition, phenylmagnesium fluoride<sup>20b</sup> prepared independently showed very low solubility in THF and C<sub>6</sub>D<sub>6</sub>. (b) Ashby, E. C.; Nackashi, J. *J. Organomet. Chem.* **1974**, *72*, 11.
- (21) Abel, E. W.; Bennett, M. A.; Wilkinson, G. *J. Chem. Soc.* **1959**, 3178.
- (22) Pangborn, A. B.; Giardello, M. A.; Grubbs, R. H.; Rosen, R. K.; Timmers, F. J. *Organometallics* **1996**, *15*, 1518.

- (23) Glasson, D. R.; Jayaweera, S. A. A. *J. Appl. Chem.* **1968**, *18*, 65.
- (24) Correa, A.; Martin, R. *J. Am. Chem. Soc.* **2009**, *131*, 15974.
- (25) Murray, A. T.; Matton, P.; Fairhurst, N. W. G.; John, M. P.; Carbery, D. R. *Org. Lett.* **2012**, *14*, 3656.
- (26) Kraus, G. A. U.S. Patent WO 2013015918, January, 31, 2013.
- (27) (a) Gianetti, T. L.; Annen, S. P.; Santiso-Quinones, G.; Reiher, M.; Driess, M.; Grützmacher, H. *Angew. Chem. Int. Ed.* **2016**, *55*, 1854. (b) Kirai, N.; Yamamoto, Y. *Eur. J. Org. Chem.* **2009**, 1864.
- (28) (a) Wang, Z.-Q.; Tang, X.-S.; Yang, Z.-Q.; Yu, B.-Y.; Wang, H.-J.; Sang, W.; Yuan, Y.; Chen, C.; Verpoort, F. *Chem. Commun.* **2019**, *55*, 8591. (b) Liu, W.; Li, J.; Querard, P.; Li, C.-J. *J. Am. Chem. Soc.* **2019**, *141*, 6755.
- (29) Giri, R.; Maugel, N.; Li, J.-J.; Wang, D.-H.; Breazzano, S. P.; Saunders, L. B.; Yu, J.-Q. *J. Am. Chem. Soc.* **2007**, *129*, 3510.
- (30) Klein, P.; Lechner, V. D.; Schimmel, T.; Hintermann, L. *Chem. Eur. J.* **2020**, *26*, 176.
- (31) Kinuta, H.; Tobisu, M.; Chatani, N. *J. Am. Chem. Soc.* **2015**, *137*, 1593.
- (32) Schmink, J. R. Krska, S. W. *J. Am. Chem. Soc.* **2011**, *133*, 19574.
- (33) CrysAlisPRO: Agilent Technologies Ltd, Yarnton, Oxfordshire, England (2014).
- (34) Rigaku Corporation, 1999; and CrystalClear Software User's Guide, Molecular Structure Corporation, 2000.
- (35) Pflugrath, J. W. *Acta Crystallogr.* **1999**, *D55*, 1718.
- (36) Sheldrick, G. M. *Acta Crystallogr.* **2008**, *A64*, 112.
- (37) Sheldrick, G. M. *Acta Crystallogr.* **2015**, *C71*, 3.

- (38) Altomare, A.; Cascarano, G.; Giacobuzzo, C.; Guagliardi, A.; Bulra, M. C.; Polidori, G.; Camalli, M. *J. Appl. Cryst.* **1994**, *27*, 435.
- (39) (a) Becke, A. D. *Phys. Rev. A* **1988**, *38*, 3098. (b) Perdew, J. P.; Chevary, J. A.; Vosko, S. H.; Jackson, K. A.; Pederson, M. R.; Singh, D. J.; Fiolhais, C. *Phys. Rev. B* **1992**, *46*, 6671. (c) Becke, A. D. *J. Chem. Phys.* **1993**, *98*, 5648. (d) Perdew, J. P.; Burke, K.; Wang, Y. *Phys. Rev. B* **1996**, *54*, 16533.
- (40) Grimme, S.; Antony, J.; Ehrlich, S.; Krieg, H. *J. Chem. Phys.* **2010**, *132*, 154104.
- (41) (a) Ditchfield, R.; Hehre, W. J.; Pople, J. A. *J. Chem. Phys.* **1971**, *54*, 724. (b) Hehre, W. J.; Ditchfield, R.; Pople, J. A. *J. Chem. Phys.* **1972**, *56*, 2257. (c) Hariharan, P. C.; Pople, J. A. *Theoret. Chim. Acta* **1973**, *28*, 213.
- (42) (a) Wadt, W. R.; Hay, P. J. *J. Chem. Phys.* **1985**, *82*, 284. (b) Hay, P. J.; Wadt, W. R. *J. Chem. Phys.* **1985**, *82*, 299.
- (43) (a) Höllwarth, A.; Böhme, M.; Dapprich, S.; Ehlers, A. W.; Gobbi, A.; Jonas, V.; Köhler, K. F.; Stegmann, R.; Veldkamp, A.; Frenking, G. *Chem. Phys. Lett.* **1993**, *208*, 237. (b) Check, C. E.; Faust, T. O.; Bailey, J. M.; Wright, B. J.; Gilbert, T. M.; Sunderlin, L. S. *J. Phys. Chem. A* **2001**, *105*, 8111.
- (44) (a) Krishnan, R.; Binkley, J. S.; Seeger, R.; Pople, J. A. *J. Chem. Phys.* **1980**, *72*, 650. (b) McLean, A. D.; Chandler, G. S. *J. Chem. Phys.* **1980**, *72*, 5639. (c) Francl, M. M.; Pietro, W. J.; Hehre, W. J.; Binkley, J. S.; Gordon, M. S.; Defrees, D. J.; Pople, J. A. *J. Chem. Phys.* **1982**, *77*, 3654.
- (45) Spitznagel, G. W.; Clark, T.; Schleyer, P. v. R.; Hehre, W. J. *J. Comput. Chem.* **1987**, *8*, 1109.
- (46) (a) Andrae, D.; Häußermann, U.; Dolg, M.; Stoll, H.; Preuß, H. *Theor. Chim. Acta* **1990**, *77*, 123. (b) Martin, J. M. L.; Sundermann, A. *J. Chem. Phys.* **2001**, *114*, 3408.



- (47) (a) Miertuš, S.; Scrocco, E.; Tomasi, J. *Chem. Phys.* **1981**, *55*, 117. (b) Miertuš, S.; Tomasi, J. *Chem. Phys.* **1982**, *65*, 239. (c) Pascual-Ahuir, J. L.; Silla, E.; Tuñon, I. *J. Comput. Chem.* **1994**, *15*, 1127. (d) Tomasi, J.; Mennucci, B.; Cammi, R. *Chem. Rev.* **2005**, *105*, 2999.
- (48) Mammen, M.; Shakhnovich, E. I.; Deutch, J. M.; Whitesides, G. M. *J. Org. Chem.* **1998**, *63*, 3821.
- (49) Frisch, M. J.; Trucks, G. W.; Schlegel, H. B.; Scuseria, G. E.; Robb, M. A.; Cheeseman, J. R.; Scalmani, G.; Barone, V.; Petersson, G. A.; Nakatsuji, H.; Li, X.; Caricato, M.; Marenich, A. V.; Bloino, J.; Janesko, B. G.; Gomperts, R.; Mennucci, B.; Hratchian, H. P.; Ortiz, J. V.; Izmaylov, A. F.; Sonnenberg, J. L.; Williams-Young, D.; Ding, F.; Lipparini, F.; Egidi, F.; Goings, J.; Peng, B.; Petrone, A.; Henderson, T.; Ranasinghe, D.; Zakrzewski, V. G.; Gao, J.; Rega, N.; Zheng, G.; Liang, W.; Hada, M.; Ehara, M.; Toyota, K.; Fukuda, R.; Hasegawa, J.; Ishida, M.; Nakajima, T.; Honda, Y.; Kitao, O.; Nakai, H.; Vreven, T.; Throssell, K.; Montgomery, J. A., Jr.; Peralta, J. E.; Ogliaro, F.; Bearpark, M. J.; Heyd, J. J.; Brothers, E. N.; Kudin, K. N.; Staroverov, V. N.; Keith, T. A.; Kobayashi, R.; Normand, J.; Raghavachari, K.; Rendell, A. P.; Burant, J. C.; Iyengar, S. S.; Tomasi, J.; Cossi, M.; Millam, J. M.; Klene, M.; Adamo, C.; Cammi, R.; Ochterski, J. W.; Martin, R. L.; Morokuma, K.; Farkas, O.; Foresman, J. B.; Fox, D. J. *Gaussian 16*, revision B.01; Gaussian, Inc.: Wallingford, CT, 2016.

## **Chapter 3**

### **The Kumada–Tamao–Corriu Coupling Reaction Catalyzed by Rhodium–Aluminum Bimetallic Complexes**

Rhodium–aluminum bimetallic complexes catalyze the Kumada–Tamao–Corriu (KTC) cross-coupling reaction using aryl–magnesium compounds that are generated from the corresponding aryl fluorides or chlorides in situ by these catalysts. This method allows carrying out the challenging KTC coupling reaction using aryl fluorides as nucleophiles, which affords various biaryls.

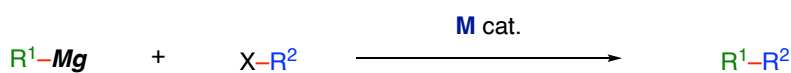
## Introduction

Transition-metal-catalyzed cross-coupling reactions are a powerful tool for the formation of C–C bonds.<sup>1</sup> Among these, cross-coupling reactions that use organomagnesium reagents, *i.e.*, the Kumada–Tamao–Corriu (KTC) cross-coupling reactions,<sup>2</sup> have become established as a key C–C-bond-forming reaction to prepare pharmaceuticals and functional materials<sup>3</sup> due to their practicality and the ease of access to organomagnesium reagents and the broad scope of readily available electrophiles (Scheme 3-1, A). Arylmagnesium compounds are usually prepared from the corresponding aryl iodides and bromides, while the commercially more readily available aryl chlorides and fluorides are less common starting materials.<sup>4</sup> In contrast with the high reactivity of C–I and C–Br bonds in a variety of reactions, C–Cl and C–F bonds often remain intact under comparatively milder reaction conditions due to their intrinsically higher bond-dissociation energy.<sup>5</sup> This lower reactivity provides access to multiply substituted arenes via subsequent KTC cross-coupling of C–Cl and C–F bonds after modifications of fluoro- and chloroarenes.

Recently, the author has reported that PAIP–Rh complexes catalyze the magnesiation of the C–F bonds of aryl fluorides to generate the corresponding aryl Grignard reagents (Scheme 3-1, B).<sup>6</sup> The author anticipated that the magnesiation and subsequent KTC cross-coupling reaction could both be catalyzed by the same PAIP–Rh complexes to allow rapid access to biaryls starting from aryl chlorides or fluorides (Scheme 3-1, C). Although KTC cross-coupling reactions catalyzed by Ni,<sup>2f-1</sup> Pd,<sup>2m,2n</sup> Fe,<sup>2o</sup> and other complexes<sup>2p,2q</sup> have been well established, Rh catalysis of the KTC cross-coupling reaction has been rare.<sup>7</sup> The Ozerov group has reported that a less-donating pincer POCOP ligand accelerates the reductive-elimination step to promote a Rh-

catalyzed KTC cross-coupling reaction.<sup>7a</sup>

### A Kumada–Tamao–Corriu (KTC) cross-coupling reaction

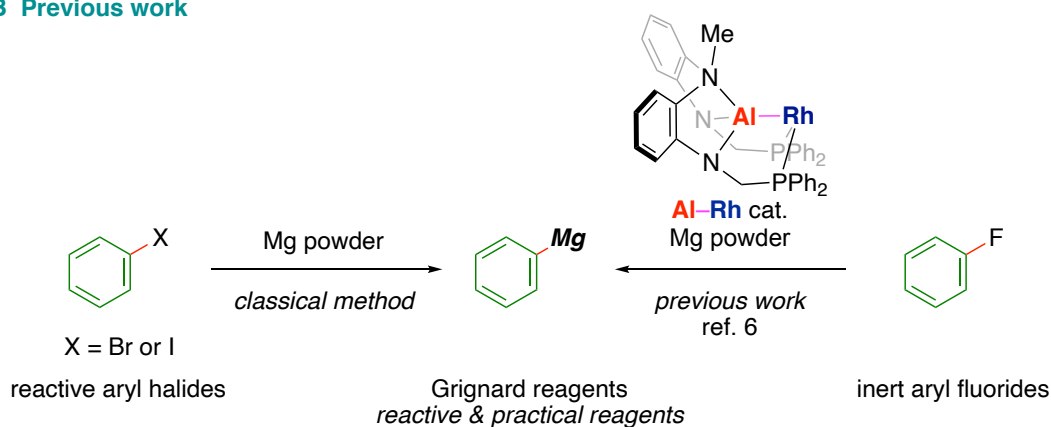


M = e.g., Ni, Pd, Fe

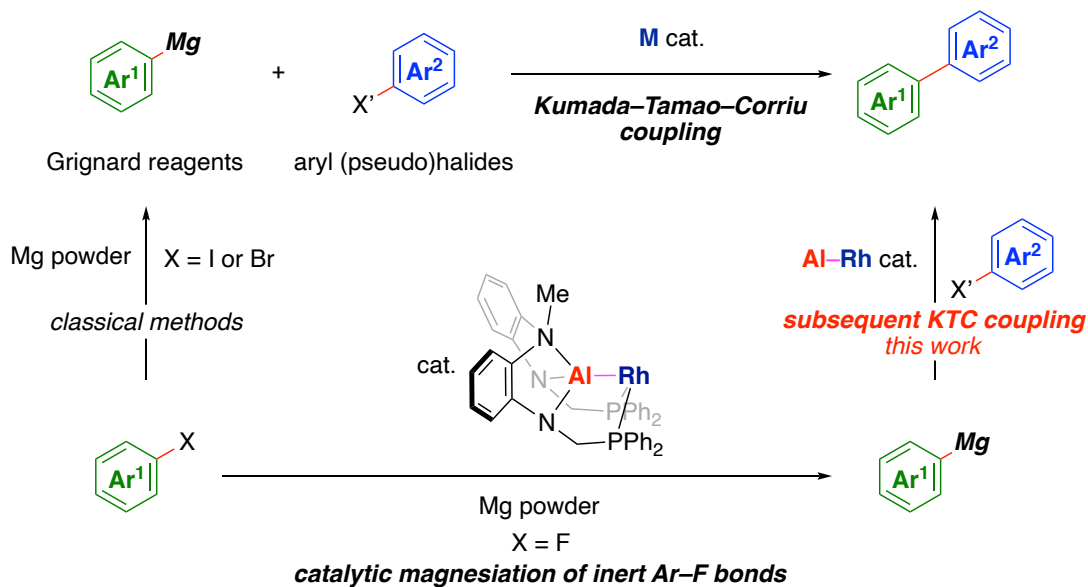
X = e.g., I, Br, Cl, F, pseudohalogen, OMe

R<sup>1</sup>, R<sup>2</sup> = aryl, heteroaryl, alkyl, alkenyl

### B Previous work



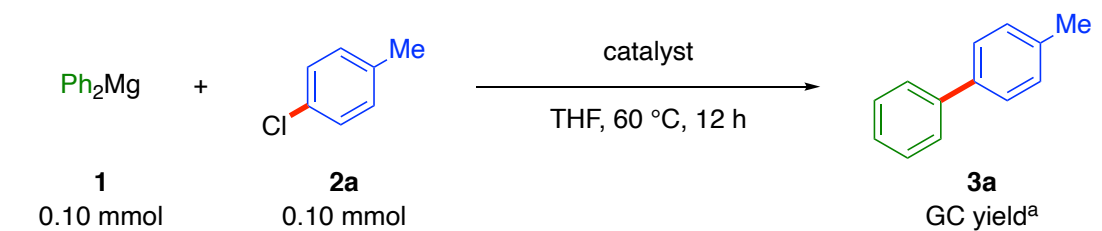
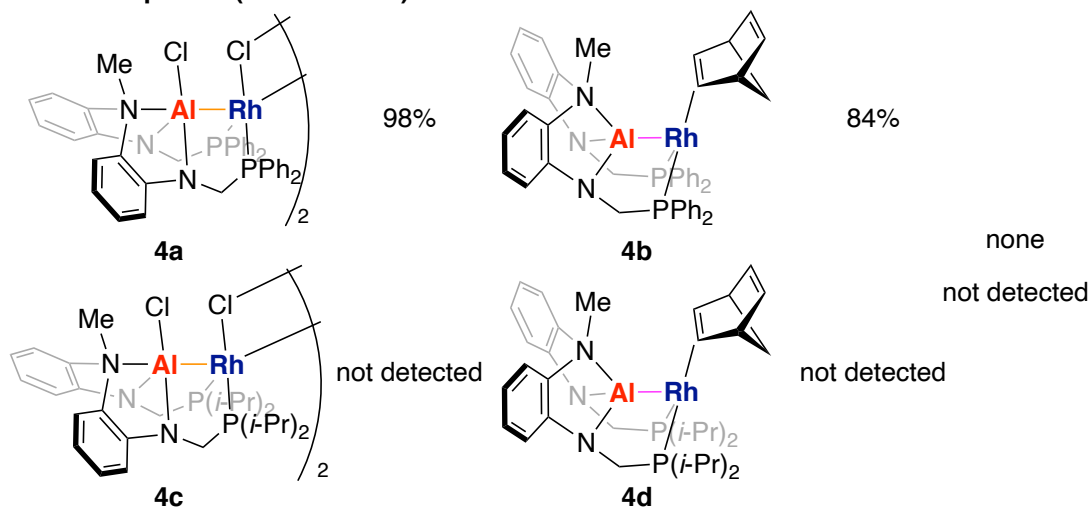
### C KTC coupling reaction for the formation of C(sp<sup>2</sup>)-C(sp<sup>2</sup>) bonds



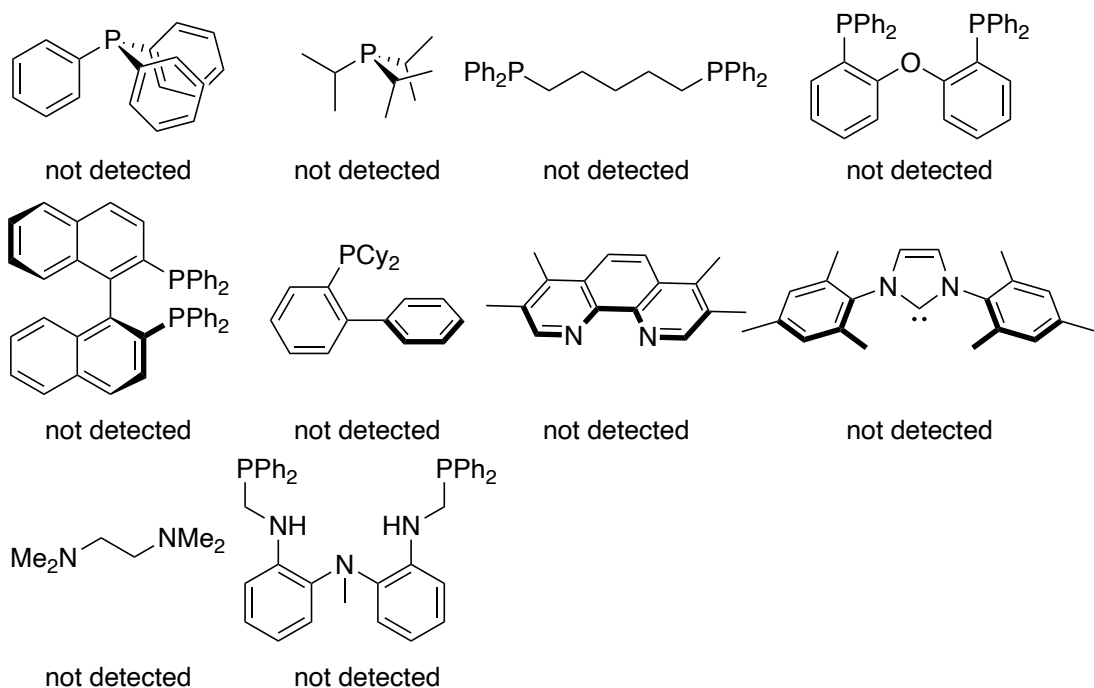
**Scheme 3-1.** Kumada–Tamao–Corriu cross-coupling reaction and working hypothesis of this work.

## Results and discussion

The author initially focused his efforts on the catalyst screening for the KTC cross-coupling reaction of diphenyl magnesium (**1**, 0.10 mmol, 1.0 eq.) with 4-chlorotoluene (**2a**, 0.10 mmol, 1.0 eq.) in THF at 60 °C for 12 h (Scheme 3-2, top). When Z-type PAIP–Rh complex **4a** (5.0 mol% of Rh) was used, cross-coupling product **3a** was obtained in 98% yield. X-type PAIP–Rh complex **4b** also catalyzed the KTC cross-coupling efficiently, whereas PAIP–Rh complexes **4c** and **4d**, which bear *i*-propyl groups instead of phenyl groups on the phosphorus atoms, did not furnish **3a**. These are because a less electron-rich rhodium center in **4a** and **4b** would facilitate reductive elimination to form a C–C bond.<sup>8</sup> The Ozerov group reported that C–C bond forming reductive elimination from a (PCP)Rh(III)Ph<sub>2</sub> complex is slower than oxidative addition of bromobenzene toward (PCP)Rh(I),<sup>7b</sup> and a less electron-donating pincer ligand is effective for the rhodium-catalyzed KTC cross-coupling reaction.<sup>7a</sup> The reaction did not proceed in the absence of the Al–Rh complexes. Catalytic systems based on [RhCl(nbd)]<sub>2</sub> (5.0 mol% of Rh; nbd = 2,5-norbornadiene)/ligand (10 mol% of L)/Et<sub>2</sub>AlCl (20 mol%) did not afford **3a** (Scheme 3-2, bottom). Accordingly, it can be concluded that the bimetallic Al–Rh complexes **4a** and **4b** are crucial for the KTC cross-coupling reaction.


**Al–Rh complexes (5.0 mol% Rh)**

**In-situ-generated catalysts**

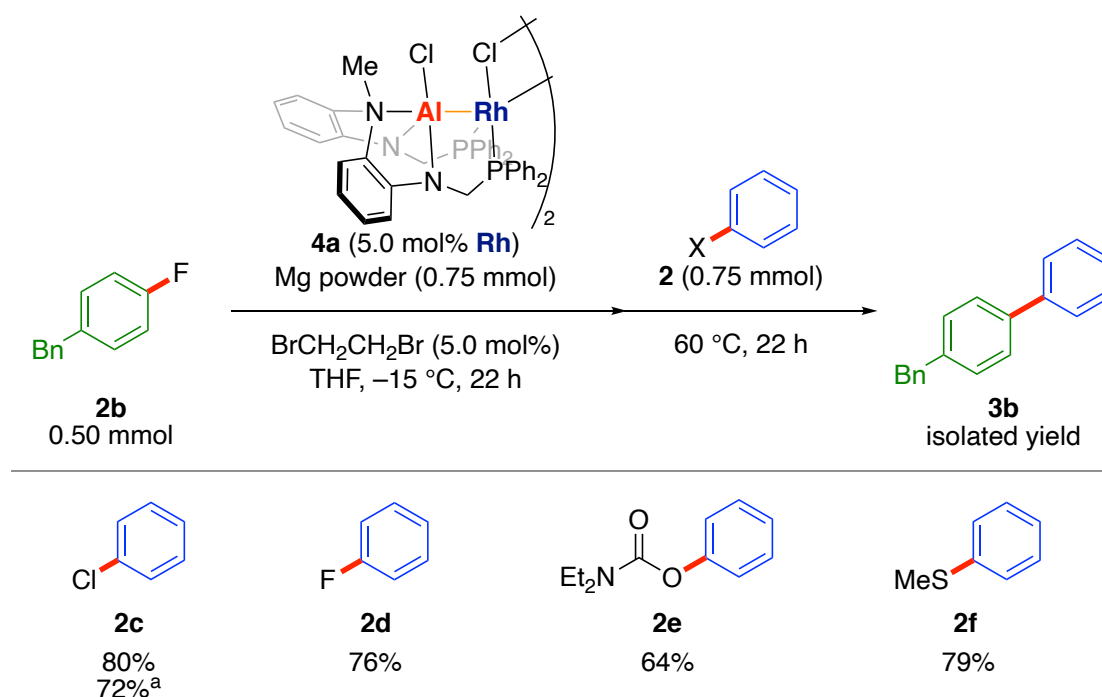
$[\text{RhCl}(\text{nbd})_2]$  (5.0 mol% Rh)/ligand (10 mol% L)/ $\text{Et}_2\text{AlCl}$  (20 mol%)



<sup>a</sup> Yield determined by GC (internal standard  $n\text{-C}_{13}\text{H}_{28}$ )

**Scheme 3-2.** Catalyst screening and control experiments.

The author then investigated the C–F-bond magnesiation/KTC cross-coupling reaction sequence using PAIP–Rh complex **4a** (Scheme 3-3). The magnesiation of 4-fluorodiphenylmethane (**2b**, 0.50 mmol, 1.0 eq.) with Mg powder (0.75 mmol, 1.5 eq.), which was preactivated upon treatment with 1,2-dibromoethane (5.0 mol%), was carried out in the presence of **4a** (5.0 mol% of Rh) in THF (0.33 M) at  $-15\text{ }^{\circ}\text{C}$  for 22 h. After filtration, the filtrate was treated with chlorobenzene (**2c**, 0.75 mmol, 1.5 eq.), and after stirring for 22 h at  $60\text{ }^{\circ}\text{C}$ , 4-benzylbiphenyl (**3b**) was isolated in 80% yield. **3b** could be also synthesized in 72% yield on a 1.0 mmol scale. Notably, less-reactive electrophiles, such as fluorobenzene (**2d**)<sup>2h-k,9</sup> and phenyl diethylcarbamate (**2e**),<sup>2i,10</sup> were also suitable under the applied conditions. Thioanisole (**2f**)<sup>11</sup> could also participate in the reaction as an electrophile.

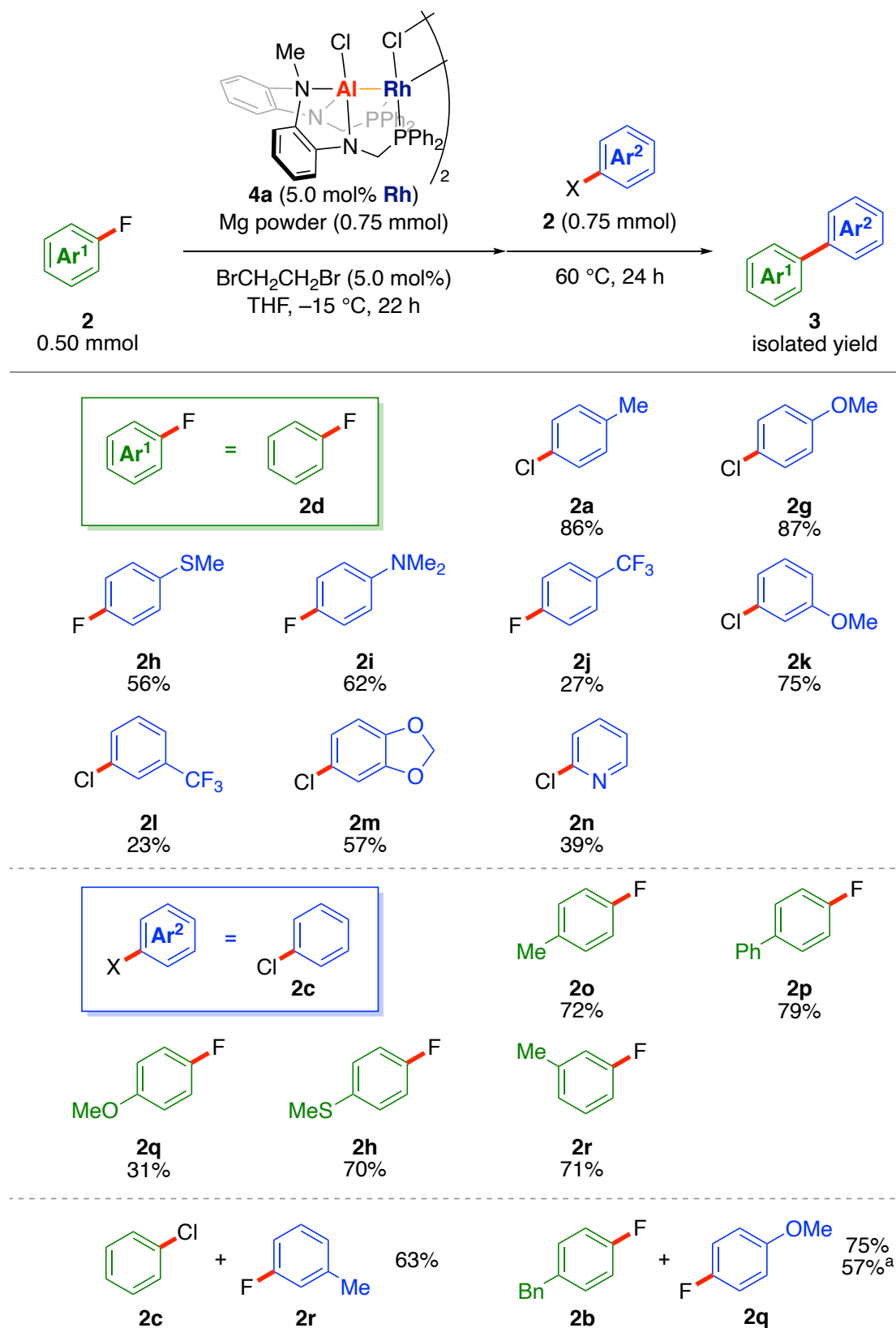


<sup>a</sup> Reaction was run on a 1.0 mmol scale

**Scheme 3-3.** Screening of leaving groups.

Subsequently, the author investigated the substrate scope (Scheme 3-4). Substituent effects on the benzene ring of electrophiles were investigated with fluorobenzene (**2d**) as a precursor of phenylmagnesium. Aryl halides that bear an electron-donating group at the *para*- or *meta*-positions (**2a**, **2g–i**, **2k**) were tolerated well and afforded the corresponding products **3** in good yield. It is worth noting here that the C–S bond of **2h**, which could potentially be functionalized under the applied conditions (**2f**, Scheme 3-3), remained intact. Electron-poor 4-trifluoromethylfluorobenzene (**2j**) and 3-trifluoromethylchlorobenzene (**2l**) gave the corresponding products in moderate yield. Aryl chloride **2m** and heteroaryl chloride **2n** are also viable electrophiles, demonstrating that the cyclic acetal and pyridine cores are compatible with catalysts that bear a strongly Lewis-acidic site. Next, the author surveyed scope of the arylmagnesium sources using chlorobenzene (**2c**) as an electrophile. Aryl fluorides bearing an electron-donating group at *para*- or *meta*-positions **2h**, **2o–r** were applicable under the optimized conditions. Furthermore, chlorobenzene (**2c**) could be used as a precursor of nucleophile to afford 3-methylbiphenyl in 63% yield after KTC cross-coupling with 3-fluorotoluene (**2r**). When the reaction of **2b** and **2q** was carried out without filtration to remove the residual Mg powder in a one-pot manner, the desired product was obtained in 57% yield with concomitant formation of 4,4'-dimethoxybiphenyl in 26% yield. In contrast, the standard conditions gave the desired product in 75% yield without formation of 4,4'-dimethoxybiphenyl.

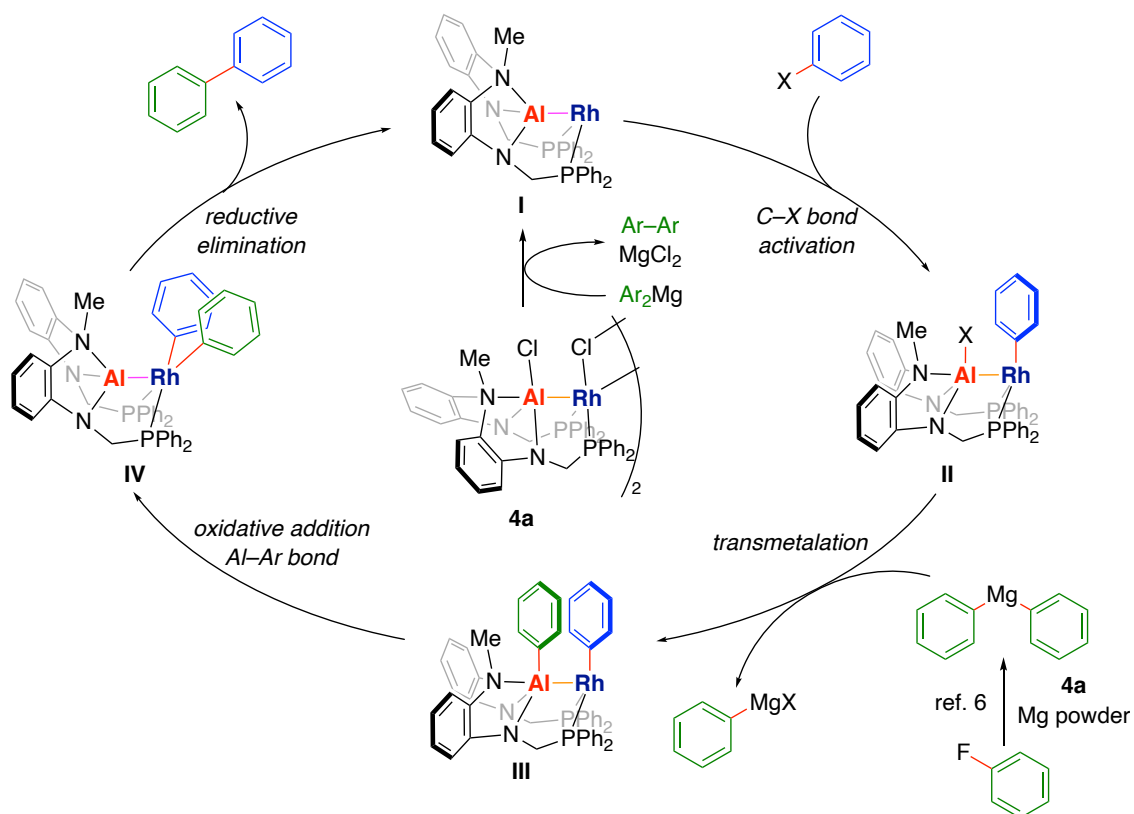




<sup>a</sup> Reaction was carried out without filtration.

**Scheme 3-4.** Substrate Scope.

A plausible catalytic cycle for the KTC cross-coupling is shown in Scheme 3-5. The cooperative activation of the C–X bond of the aryl halides by the Al–Rh bond of the active X-type complex **I** generates Z-type complex **II**.<sup>6</sup> Transmetalation of the *in-situ*-generated aryl Grignard reagent<sup>6</sup> with complex **II** could occur at the aluminum site to afford Z-type complex **III**, which bears two aryl–metal bonds. The oxidative addition of the Al–Ar bond toward the Rh center could afford X-type complex **IV**,<sup>12</sup> which gives biaryls through C–C bond-forming reductive elimination to regenerate the active Al–Rh complex **I**.



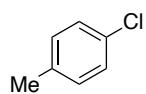
**Scheme 3-5.** Proposed Reaction Mechanism.

**Conclusion**

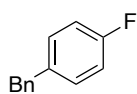
In conclusion, the author has developed a Kumada–Tamao–Corriu (KTC) cross-coupling reaction catalyzed by Al–Rh complexes. These Al–Rh complexes efficiently catalyze both the magnesiation of aryl fluorides or chlorides and the subsequent KTC cross-coupling with the resulting arylmagnesiums to afford a variety of biaryls. Further studies to reveal more information on the mechanism will be pursued to determine the details underlying the proposed transmetalation and the C–C-forming reductive elimination events at the bimetallic site.

## Experimental section

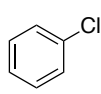
## aryl halides



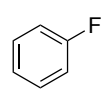
2a



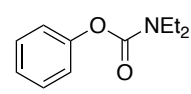
2b



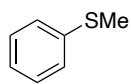
2c



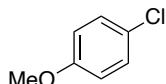
2d



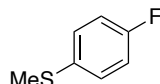
2e



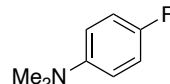
2f



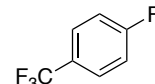
2g



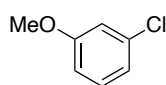
2h



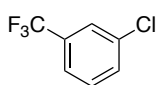
2i



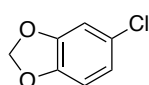
2j



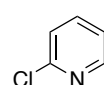
2k



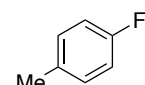
2l



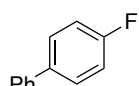
2m



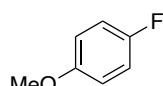
2n



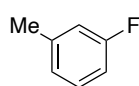
2o



2p

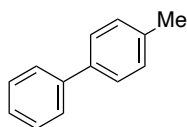


2q

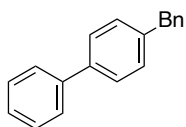


2r

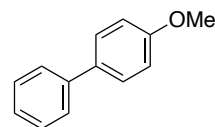
## products



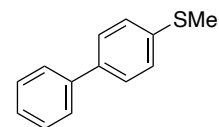
3a



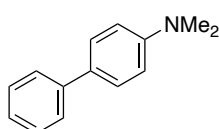
3b



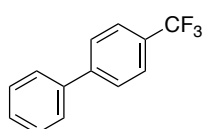
3c



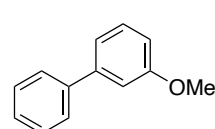
3d



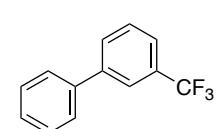
3e



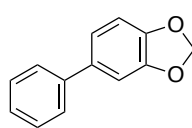
3f



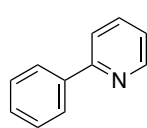
3g



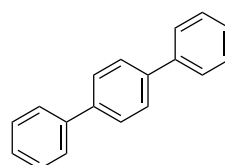
3h



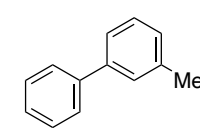
3i



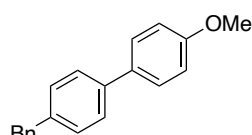
3j



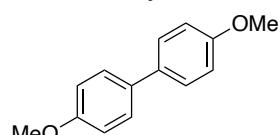
3k



3l



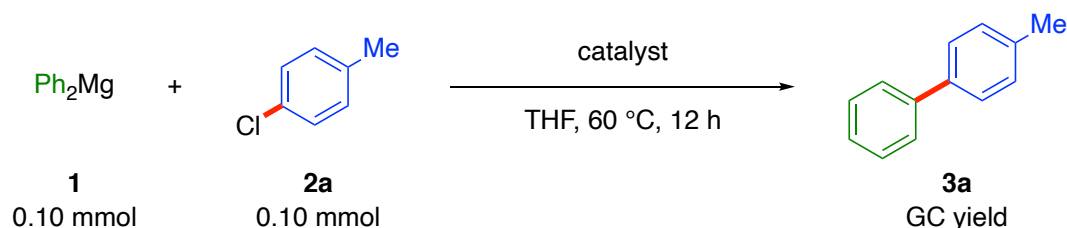
3m



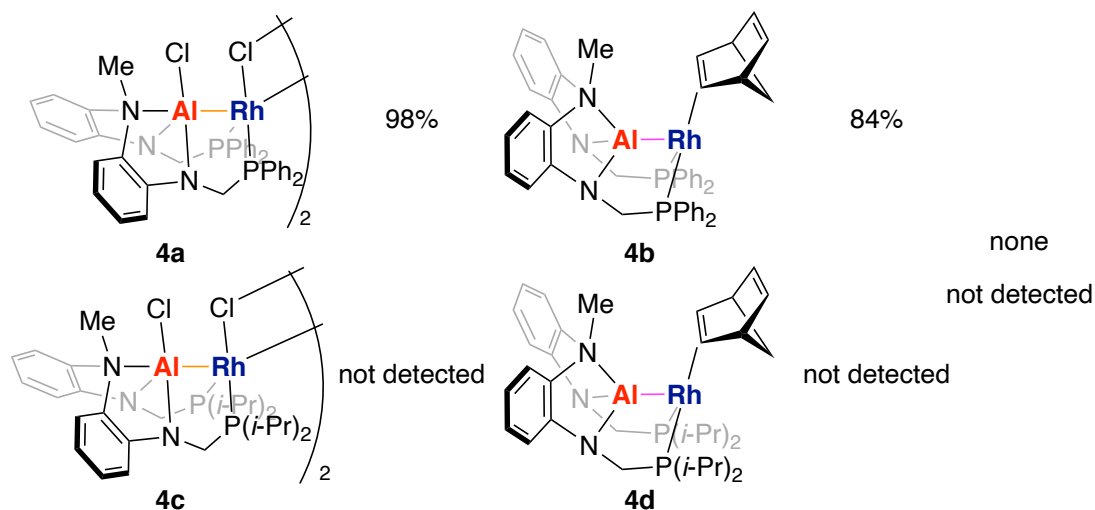
3n

Figure S3-1. A list of compounds in this study.

## General procedure for Scheme 3-2.



*Al–Rh complexes:* In a glove box, a 4 mL vial with a stirring bar was charged with diphenylmagnesium (**1**, 18 mg, 0.10 mmol, 1.0 eq.), 4-chlorotoluene (**2a**, 13 mg, 0.10 mmol, 1.0 eq.), catalyst (5.0 mol% of Rh), and THF (500  $\mu\text{L}$ ). The vial was taken out of the glove box and the mixture was stirred for 12 h at 60  $^\circ\text{C}$ . The yield of **3a** was determined by GC analysis of the crude mixture using the calibration curve with *n*-tridecane as an internal standard (Figure S3-2).

*Al–Rh complexes*

*In-situ-generated catalysts:* In a glove box, a 4 mL vial with a stirring bar was charged with  $[\text{Rh}(\text{nbd})(\mu\text{-Cl})_2]$  (1.2 mg, 2.5  $\mu\text{mol}$ , 2.5 mol%), an indicated ligand (number of coordination site (L)/Rh = 2, 10 mol% of L), and THF (200  $\mu\text{L}$ ). The resulting mixture

was stirred for 10 min at room temperature. To the vial, diphenylmagnesium (**1**, 18 mg, 0.10 mmol, 1.0 eq.), 4-chlorotoluene (**2a**, 13 mg, 0.10 mmol, 1.0 eq.), and 1.03 M Et<sub>2</sub>AlCl in *n*-hexane (19 μL, 20 μmol, 20 mol%) were added. The mixture was stirred for 12 h at 60 °C. The yield of **3a** was determined by GC analysis of reaction mixture using the calibration curve with *n*-tridecane as an internal standard (Figure S3-2).

### *In-situ-generated catalysts*

[Rh(nbd)(μ-Cl)]<sub>2</sub> (2.5 mol%)/ligand (10 mol% L)/Et<sub>2</sub>AlCl (20 mol%)

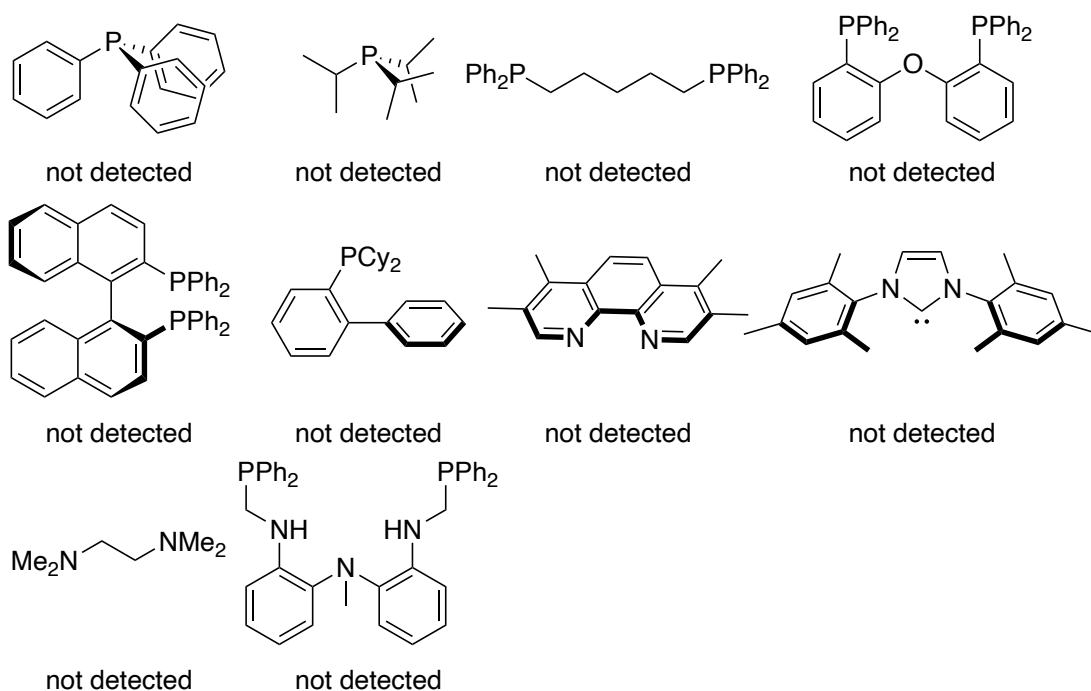


**Table S3-1.** Data for the GC calibration curve obtained using an authentic sample of 4-methylbiphenyl (**3a**).

mass (mg)		mass of <b>3a</b> /mass of C <sub>13</sub> H <sub>28</sub>	GC area		GC area of <b>3a</b> /GC area of C <sub>13</sub> H <sub>28</sub>
<b>3a</b>	C <sub>13</sub> H <sub>28</sub>		<b>3a</b>	C <sub>13</sub> H <sub>28</sub>	
8.5	5.0	1.70000	203361	135891	1.496500872
17.5	5.6	3.12500	327344	117253	2.791775051
33.7	6.1	5.52459	812102	158361	5.128169183

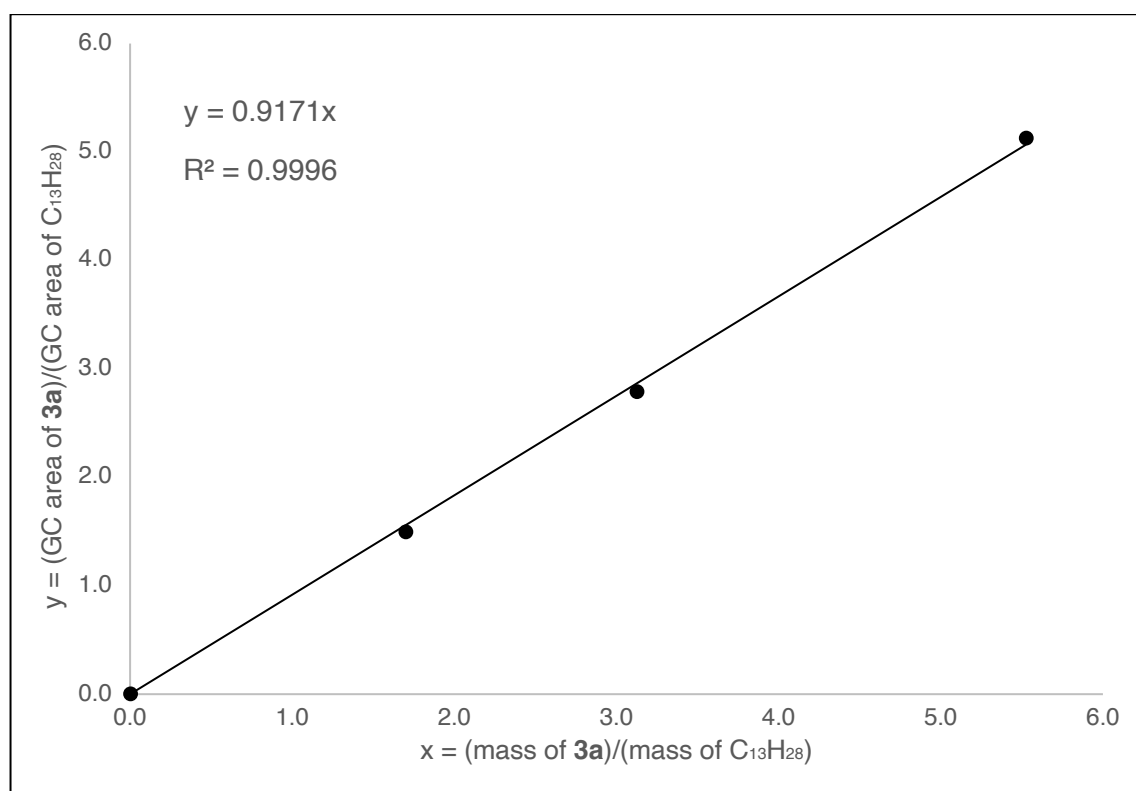
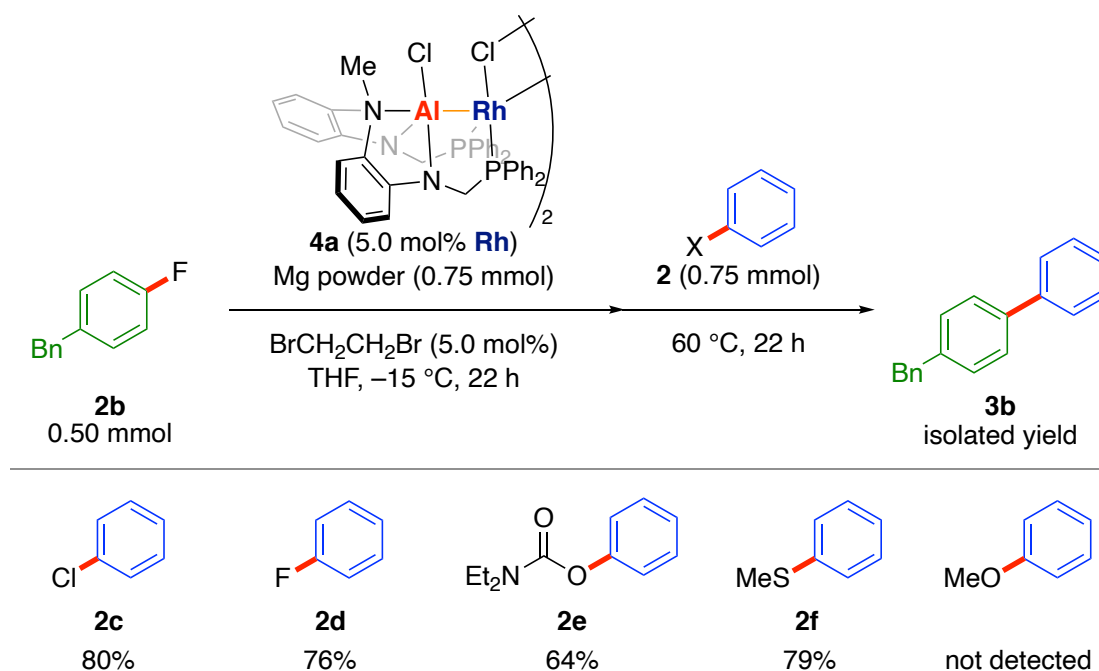


**Figure S3-2.** GC calibration curve to determine the yield of 4-methylbiphenyl (**3a**).

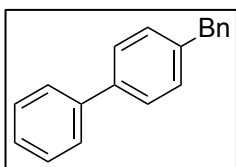
## General procedure for Scheme 3-3.



In a glove box, a 4 mL vial with a stirring bar was charged with magnesium powder (18 mg, 0.75 mmol, 1.5 eq.), THF (500  $\mu$ L), and 1,2-dibromoethane (4.7 mg, 25  $\mu$ mol, 5.0 mol%), and the resulting mixture was stirred for 20 min at room temperature. 4a (20 mg, 13  $\mu$ mol, 5.0 mol% of Rh) and THF (1.0 mL, 0.33 M) were added to the vial followed by 4-fluorodiphenylmethane (2b, 93 mg, 0.50 mmol, 1.0 eq.). The mixture was stirred at -15 °C for 22 h to generate 4-benzylphenylmagnesium. After that, insoluble solids of the resulting mixture were filtered through the Pasteur pipette filter, which is filled with a glass fiber filter (GB-100R ADVANTEC®), with THF (1.0 mL). The obtained filtrate was put into another 4 mL vial with a stirring bar and an indicated electrophile 2c-f (0.75 mmol, 1.5 eq.). The reaction mixture was stirred at 60 °C for 22 h. To the mixture, 3 M HCl aq. (2.0 mL) was carefully added. The organic layer was separated. The remained aqueous layer was extracted with EtOAc (4.0 mL) three times. All volatiles were removed in vacuo and the residue was purified by MPLC using

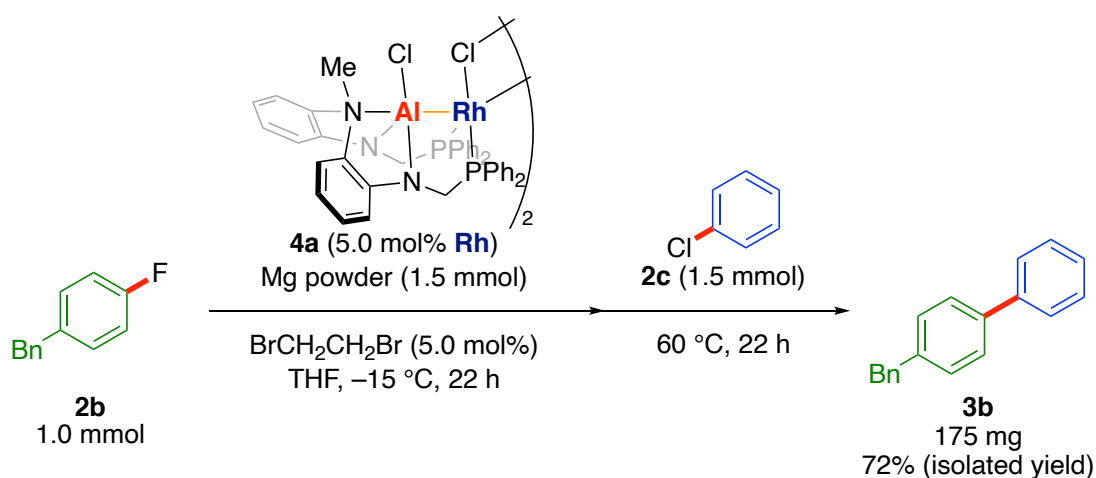


Biotage® Sfär Silica High Capacity Duo to obtain 4-benzylbiphenyl (**3b**).



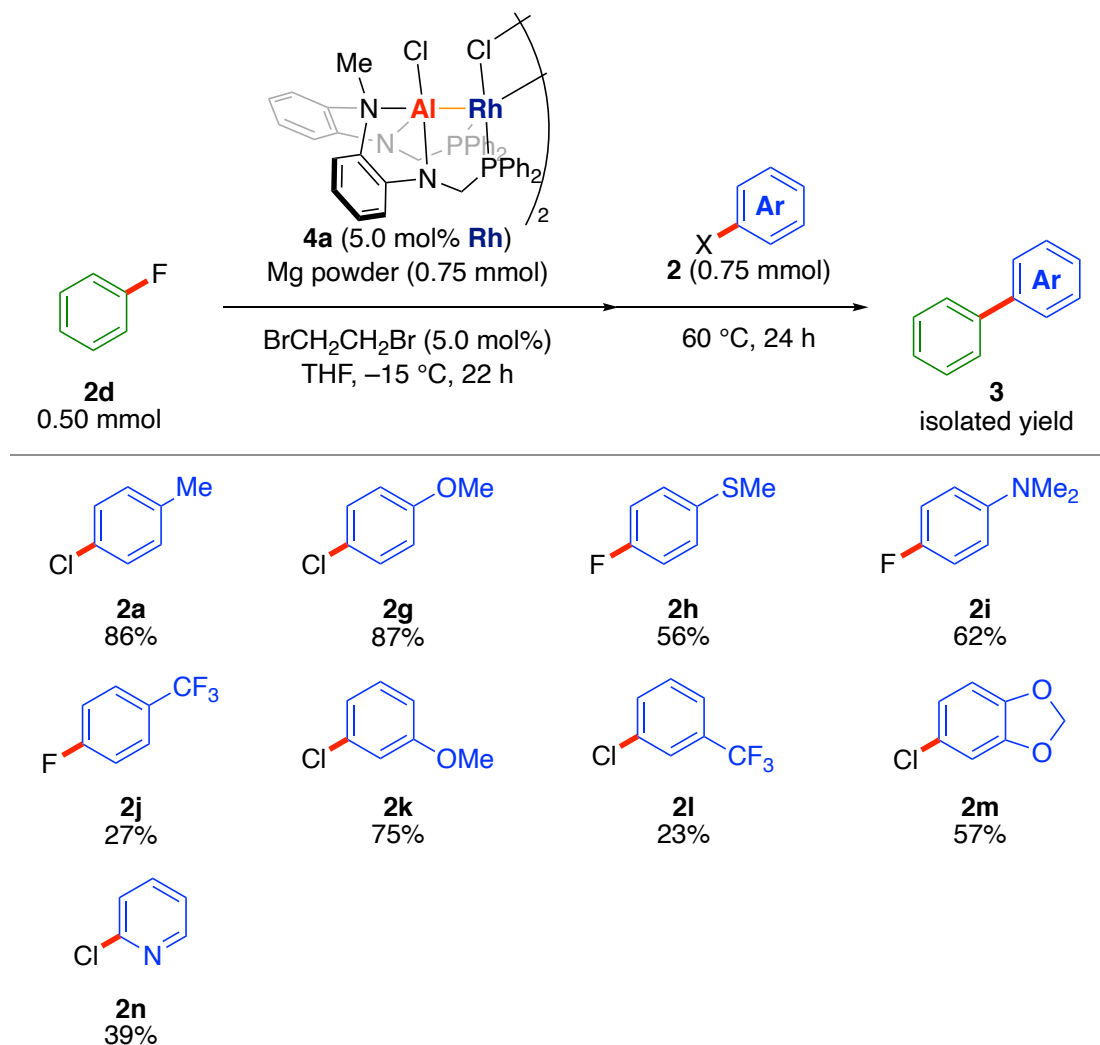
**4-benzylbiphenyl (3b):** The reaction of the generated Grignard reagent and chlorobenzene (**2c**, 84 mg, 0.75 mmol) followed by purification by MPLC (*n*-hexane) afforded the title compound (98 mg, 0.40 mmol, 80%) as a white powder.  $R_f$  0.23 (*n*-hexane).  $^1\text{H}$  NMR (400 MHz,  $\text{CDCl}_3$ ):  $\delta$  7.64 (d,  $J = 7.7$  Hz, 2H), 7.58 (d,  $J = 7.6$  Hz, 2H), 7.48 (t,  $J = 7.6$  Hz, 2H), 7.40–7.26 (m, 8H), 4.09 (s, 2H).  $^{13}\text{C}\{^1\text{H}\}$  NMR (101 MHz,  $\text{CDCl}_3$ ):  $\delta$  141.2, 140.4, 139.2, 129.5, 129.1, 128.9, 128.7, 127.4, 127.2, 127.2, 126.3, 41.7. All the resonances of  $^1\text{H}$  and  $^{13}\text{C}$  NMR spectra were consistent with the reported values.<sup>13</sup> The reaction with fluorobenzene (**2d**, 72 mg, 0.75 mmol, 1.5 eq.) afforded **3b** in 76% yield (93 mg, 0.38 mmol) as a white solid. The reaction with phenyl diethylcarbamate (**2e**, 145 mg, 0.75 mmol, 1.5 eq.) afforded **3b** in 64% yield (78 mg, 0.32 mmol) as a white solid. The reaction with thioanisole (**2f**, 93 mg, 0.75 mmol, 1.5 eq.) afforded **3b** in 79% yield (96 mg, 0.39 mmol) as a white solid. The reaction with anisole (81 mg, 0.75 mmol, 1.5 eq.) did not afford **3b**.

#### Procedures for the 1.0 mmol scale reaction.



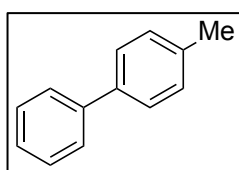
In a glove box, a 15 mL vial with a stirring bar was charged with magnesium powder (36 mg, 1.5 mmol, 1.5 eq.), THF (1.0 mL), and 1,2-dibromoethane (9.4 mg, 50  $\mu$ mol, 5.0 mol%), and the resulting mixture was stirred for 20 min at room temperature. A THF (2.0 mL, 0.33 M) solution of **4a** (40 mg, 25  $\mu$ mol, 5.0 mol% of Rh) and 4-fluorodiphenylmethane (**2b**, 186 mg, 1.0 mmol, 1.0 eq.) were added to the vial in this order. The mixture was stirred at  $-15$   $^{\circ}$ C for 22 h to generate 4-benzylphenylmagnesium and insoluble solids of the resulting mixture were filtered off through the Pasteur pipette filter, which is filled with a glass fiber filter (GB-100R ADVANTEC<sup>®</sup>), with THF (2.0 mL). The obtained filtrate was put into another 15 mL vial with a stirring bar and chlorobenzene **2c** (169 mg, 1.5 mmol, 1.5 eq.). The reaction mixture was stirred at 60  $^{\circ}$ C for 22 h. To the mixture, 3 M HCl aq. (3.0 mL) was carefully added. The organic layer was separated. The remained aqueous layer was extracted with EtOAc (8.0 mL) x 3. All volatiles of the combined organic layers were removed in vacuo and the residue was purified by MPLC using 20 g iLOK<sup>TM</sup>-SL. 4-Benzylbiphenyl (**3b**) was isolated (175 mg, 0.72 mmol, 72%) as a white powder.

## General procedure of Magnesiatioin and KTC coupling in Scheme 3-4.

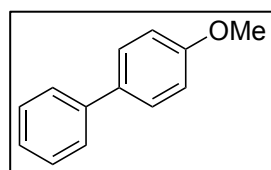


In a glove box, a 4 mL vial with a stirring bar was charged with magnesium powder (18 mg, 0.75 mmol, 1.5 eq.), THF (500  $\mu$ L), and 1,2-dibromoethane (4.7 mg, 25  $\mu$ mol, 5.0 mol%), and the resulting mixture was stirred for 20 min at room temperature. **4a** (20 mg, 13  $\mu$ mol, 5.0 mol% of Rh) and THF (1.0 mL, 0.33 M) were added to the vial followed by fluorobenzene (**2d**, 48 mg, 0.50 mmol, 1.0 eq.). The mixture was stirred at -15 °C for 22 h to generate diphenylmagnesium. Insoluble solids of the resulting mixture were filtered off through the Pasteur pipette filter, which is filled with a glass fiber filter (GB-100R ADVANTEC<sup>®</sup>), with THF (1.0 mL). The obtained filtrate was put into another

4 mL vial with a stirring bar and an indicated electrophile **2** (0.75 mmol, 1.5 eq.). The reaction mixture was stirred at 60 °C for 24 h. To the mixture, 3 M HCl aq. (2.0 mL) was carefully added. The organic layer was separated. The remained aqueous layer was extracted with EtOAc (4.0 mL) x 3. All volatiles were removed in vacuo and the residue was purified by MPLC using Biotage® Sfär Silica High Capacity Duo to obtain the corresponding product **3**.

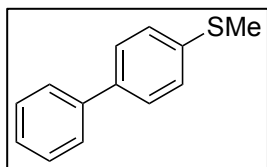


**4-Methylbiphenyl (3a)**: The reaction of in situ prepared phenylmagnesium and 4-chlorotoluene (**2a**, 95 mg, 0.75 mmol) followed by purification by MPLC (*n*-hexane) afforded the title compound (72 mg, 0.43 mmol, 86%) as a white powder.  $R_f$  0.52 (*n*-hexane).  $^1\text{H}$  NMR (400 MHz,  $\text{CDCl}_3$ ):  $\delta$  7.54 (d,  $J = 7.6$  Hz, 2H), 7.46 (d,  $J = 7.6$  Hz, 2H), 7.38 (t,  $J = 7.6$  Hz, 2H), 7.29 (d,  $J = 7.6$  Hz, 1H), 7.21 (d,  $J = 7.8$  Hz, 2H), 2.35 (s, 3H).  $^{13}\text{C}\{^1\text{H}\}$  NMR (101 MHz,  $\text{CDCl}_3$ ):  $\delta$  141.3, 138.5, 137.2, 129.6, 128.9, 127.1 (3 peaks were overlapped), 21.2. All the resonances of  $^1\text{H}$  and  $^{13}\text{C}$  NMR spectra were consistent with the reported values.<sup>2h</sup>

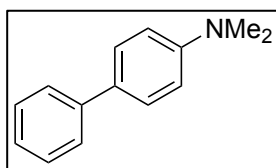


**4-Methoxybiphenyl (3c)**: The reaction of in situ prepared phenylmagnesium and 4-chloroanisole (**2g**, 107 mg, 0.75 mmol) followed by purification by MPLC (*n*-hexane/EtOAc = 95:5) afforded the title compound (80 mg, 0.44 mmol, 87%) as a white powder.  $R_f$  0.10 (*n*-hexane).  $^1\text{H}$  NMR (400 MHz,  $\text{CDCl}_3$ ):  $\delta$  7.54–7.50 (m, 4H), 7.39 (t,  $J = 7.6$  Hz, 2H), 7.29 (t,  $J = 7.4$  Hz, 1H), 6.96 (d,  $J = 8.2$  Hz, 2H), 3.81 (s, 3H).  $^{13}\text{C}\{^1\text{H}\}$  NMR (101 MHz,  $\text{CDCl}_3$ ):  $\delta$  159.3, 141.0, 133.9, 128.8, 128.3, 126.8, 126.8, 114.3, 55.4. All the resonances

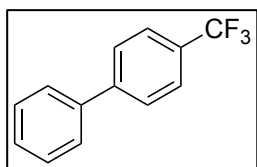
of  $^1\text{H}$  and  $^{13}\text{C}$  NMR spectra were consistent with the reported values.<sup>14</sup>



**4-Methylthiobiphenyl (3d):** The reaction of in situ prepared phenylmagnesium and 4-fluorothioanisole (**2h**, 107 mg, 0.75 mmol) followed by purification by MPLC (*n*-hexane) afforded the title compound (56 mg, 0.28 mmol, 56%) as a white powder.  $R_f$  0.25 (*n*-hexane).  $^1\text{H}$  NMR (400 MHz,  $\text{CDCl}_3$ ):  $\delta$  7.58 (d,  $J = 7.7$  Hz, 2H), 7.54 (d,  $J = 7.9$  Hz, 2H), 7.44 (t,  $J = 7.7$  Hz, 2H), 7.31–7.38 (m, 3H), 2.53 (s, 3H).  $^{13}\text{C}\{^1\text{H}\}$  NMR (101 MHz,  $\text{CDCl}_3$ ):  $\delta$  140.7, 138.2, 137.7, 128.9, 127.6, 127.3, 127.1, 127.0, 16.0. All the resonances of  $^1\text{H}$  and  $^{13}\text{C}$  NMR spectra were consistent with the reported values.<sup>11c</sup>

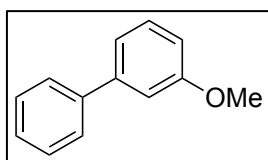


**4-*N,N*-Dimethylaminobiphenyl (3e):** The reaction of in situ prepared phenylmagnesium and 4-fluoro-*N,N*-dimethylaniline (**2i**, 104 mg, 0.75 mmol) followed by purification by MPLC (*n*-hexane/EtOAc = 9:1) afforded the title compound (61 mg, 0.31 mmol, 62%) as a white powder.  $R_f$  0.71 (*n*-hexane/EtOAc = 5:1).  $^1\text{H}$  NMR (400 MHz,  $\text{CDCl}_3$ ):  $\delta$  7.60–7.54 (m, 2H), 7.54–7.48 (m, 2H), 7.40 (t,  $J = 7.7$  Hz, 2H), 7.33–7.19 (m, 1H), 6.84–6.79 (m, 2H), 3.00 (s, 6H).  $^{13}\text{C}\{^1\text{H}\}$  NMR (101 MHz,  $\text{CDCl}_3$ ):  $\delta$  150.1, 141.4, 129.4, 128.8, 127.8, 126.4, 126.1, 112.9, 40.7. All the resonances of  $^1\text{H}$  and  $^{13}\text{C}$  NMR spectra were consistent with the reported values.<sup>15</sup>

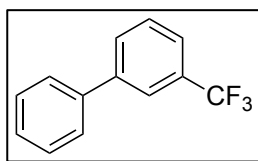


**4-Trifluoromethylbiphenyl (3f):** The reaction of in situ prepared phenylmagnesium and 4-fluorobenzotrifluoride (**2j**, 123 mg, 0.75 mmol) followed by purification by MPLC (*n*-hexane) afforded the

title compound (30 mg, 0.13 mmol, 27%) as a white powder.  $R_f$  0.72 (*n*-hexane).  $^1\text{H}$  NMR (400 MHz,  $\text{CDCl}_3$ ):  $\delta$  7.70 (s, 4H), 7.60 (d,  $J = 7.5$  Hz, 2H), 7.49 (d,  $J = 7.6$  Hz, 2H), 7.48–7.37 (m, 1H).  $^{13}\text{C}\{^1\text{H}\}$  NMR (101 MHz,  $\text{CDCl}_3$ ):  $\delta$  144.9, 139.9, 129.5 (q,  $J = 32.5$  Hz), 129.1, 128.3, 127.6, 127.4, 125.9 (q,  $J = 3.5$  Hz), 124.5 (q,  $J = 272.2$  Hz).  $^{19}\text{F}$  NMR (376 MHz,  $\text{CDCl}_3$ ):  $\delta$  -62.89. All the resonances of  $^1\text{H}$  and  $^{13}\text{C}$  NMR spectra were consistent with the reported values.<sup>14</sup>



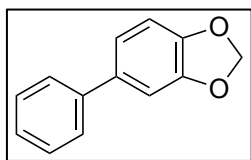
**3-Methoxybiphenyl (3g):** The reaction of in situ prepared phenylmagnesium and 3-chloroanisole (**2k**, 107 mg, 0.75 mmol) followed by purification by MPLC (*n*-hexane/EtOAc = 9:1) afforded the title compound (69 mg, 0.38 mmol, 75%) as a yellow oil.  $R_f$  0.30 (*n*-hexane).  $^1\text{H}$  NMR (400 MHz,  $\text{CDCl}_3$ ):  $\delta$  7.48 (d,  $J = 7.6$  Hz, 2H), 7.32 (t,  $J = 7.6$  Hz, 2H), 7.27–7.22 (m, 2H), 7.07 (d,  $J = 7.7$  Hz, 1H), 7.02 (bs, 1H), 6.79 (dd,  $J = 8.2, 2.4$  Hz, 1H), 3.74 (s, 3H).  $^{13}\text{C}\{^1\text{H}\}$  NMR (101 MHz,  $\text{CDCl}_3$ ):  $\delta$  160.1, 142.9, 141.2, 129.9, 128.9, 127.5, 127.3, 119.8, 113.0, 112.8, 55.4. All the resonances of  $^1\text{H}$  and  $^{13}\text{C}$  NMR spectra were consistent with the reported values.<sup>16</sup>



**3-Trifluoromethylbiphenyl (3h):** The reaction of in situ prepared phenylmagnesium and 3-chlorobenzotrifluoride (**2l**, 135 mg, 0.75 mmol) followed by purification by MPLC (*n*-hexane) afforded the title compound (26 mg, 0.12 mmol, 23%) as a yellow oil.  $R_f$  0.71 (*n*-hexane).  $^1\text{H}$  NMR (400 MHz,  $\text{CDCl}_3$ ):  $\delta$  7.85 (s, 1H), 7.78 (d,  $J = 7.6$  Hz, 1H), 7.62–7.54 (m, 4H), 7.49 (t,  $J = 7.6$  Hz, 2H), 7.41 (t,  $J = 7.4$  Hz, 1H).  $^{13}\text{C}\{^1\text{H}\}$  NMR (101 MHz,  $\text{CDCl}_3$ ):  $\delta$  142.2, 139.9, 131.3 (q,  $J = 32.2$  Hz) 130.6, 129.4, 129.1, 128.2, 127.3, 125.9 (q,  $J = 3.5$  Hz),

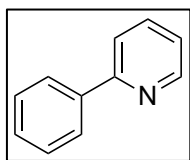
124.3 (q,  $J = 273.0$  Hz), 124.1 (q,  $J = 3.8$  Hz).  $^{19}\text{F}$  NMR (376 MHz,  $\text{CDCl}_3$ ):  $\delta -63.14$ .

All the resonances of  $^1\text{H}$  and  $^{13}\text{C}$  NMR spectra were consistent with the reported values.<sup>17</sup>



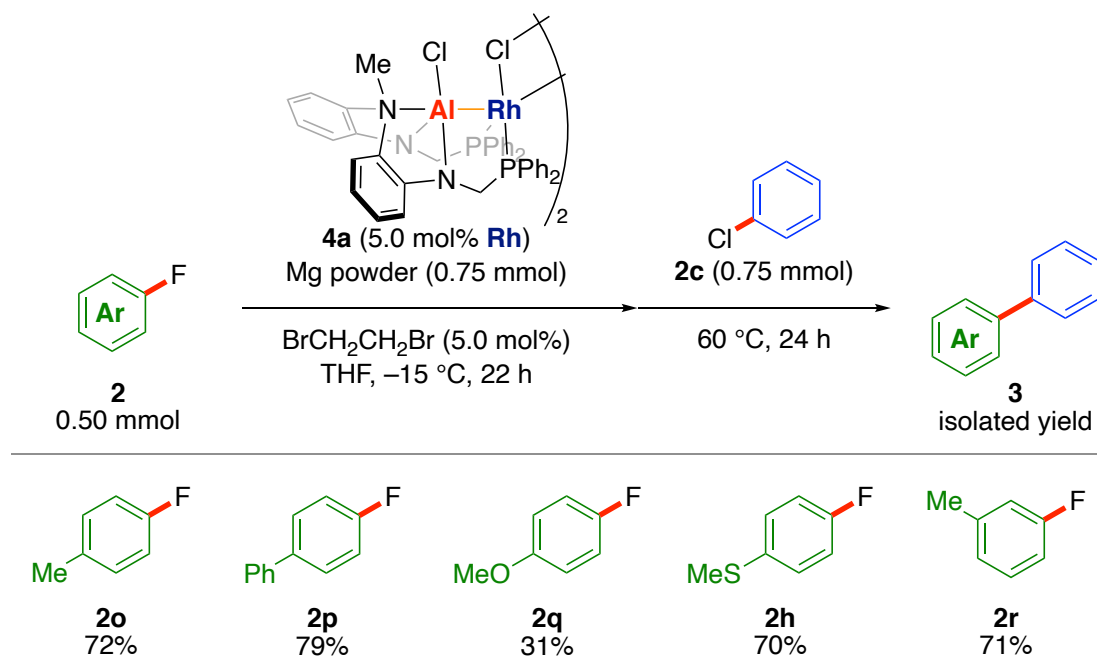
**5-Phenylbenzo[*d*][1,3]dioxole (3i):** The reaction of in situ prepared phenylmagnesium and 5-chlorobenzo[*d*][1,3]dioxole (**2m**, 117 mg, 0.75 mmol) followed by purification by MPLC (*n*-hexane/EtOAc =

9:1) afforded the title compound (57 mg, 0.29 mmol, 57%) as a yellow oil.  $R_f$  0.29 (*n*-hexane).  $^1\text{H}$  NMR (400 MHz,  $\text{CDCl}_3$ ):  $\delta$  7.53 (d,  $J = 7.5$  Hz, 2H), 7.42 (t,  $J = 7.8$  Hz, 2H), 7.33 (t,  $J = 7.3$  Hz, 1H), 7.09 (s, 1H), 7.08 (d,  $J = 8.0$  Hz, 1H), 6.90 (dd,  $J = 7.9, 1.9$  Hz, 1H), 6.01 (s, 2H).  $^{13}\text{C}\{^1\text{H}\}$  NMR (101 MHz,  $\text{CDCl}_3$ ):  $\delta$  148.2, 147.2, 141.1, 135.8, 128.9, 127.06, 127.03, 120.8, 108.7, 107.8, 101.3. All the resonances of  $^1\text{H}$  and  $^{13}\text{C}$  NMR spectra were consistent with the reported values.<sup>17</sup>



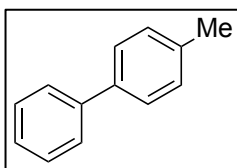
**2-Phenylpyridine (3j):** The reaction of in situ prepared phenylmagnesium and 2-chloropyridine (**2n**, 85 mg, 0.75 mmol) followed by purification by MPLC (*n*-hexane/EtOAc = 5:1) afforded the

title compound (30 mg, 0.19 mmol, 39%) as a colorless oil.  $R_f$  0.49 (*n*-hexane/EtOAc = 5:1).  $^1\text{H}$  NMR (400 MHz,  $\text{CDCl}_3$ ):  $\delta$  8.70 (dt,  $J = 5.0, 1.4$  Hz, 1H), 8.08–7.96 (m, 2H), 7.75–7.64 (m, 2H), 7.48 (dd,  $J = 8.3, 6.6$  Hz, 2H), 7.45–7.38 (m, 1H), 7.19 (td,  $J = 5.0, 3.1$  Hz, 1H).  $^{13}\text{C}\{^1\text{H}\}$  NMR (101 MHz,  $\text{CDCl}_3$ ):  $\delta$  157.4, 149.7, 139.4, 136.7, 128.9, 128.7, 126.9, 122.1, 120.5. All the resonances of  $^1\text{H}$  and  $^{13}\text{C}$  NMR spectra were consistent with the reported values.<sup>18</sup>

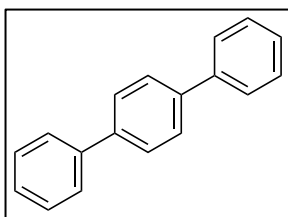


In a glove box, a 4 mL vial with a stirring bar was charged with magnesium powder (18 mg, 0.75 mmol, 1.5 eq.), THF (500  $\mu\text{L}$ ), and 1,2-dibromoethane (4.7 mg, 25  $\mu\text{mol}$ , 5.0 mol%), and the resulting mixture was stirred for 20 min at room temperature. **4a** (20 mg, 13  $\mu\text{mol}$ , 5.0 mol% of Rh) and THF (1.0 mL) were added to the vial followed by indicated aryl fluoride **2** (0.50 mmol, 1.0 eq.). The mixture was stirred at  $-15\text{ }^{\circ}\text{C}$  for 22 h to generate diarylmagnesium. Insoluble solids of the resulting mixture were filtered off through the Pasteur pipette filter, which is filled with a glass fiber filter (GB-100R ADVANTEC<sup>®</sup>), with THF (1.0 mL). The obtained filtrate was put into another 4 mL vial with a stirring bar and chlorobenzene (**2c**, 84 mg, 0.75 mmol, 1.5 eq.). The reaction mixture was stirred at  $60\text{ }^{\circ}\text{C}$  for 24 h. To the mixture, 3 M HCl aq. (2.0 mL) was carefully added. The organic layer was separated. The remained aqueous layer was extracted with EtOAc (4.0 mL) x 3. All volatiles were removed in vacuo and the residue was purified by MPLC using 20 g iLOK<sup>TM</sup>-SL to obtain the corresponding product **3**.

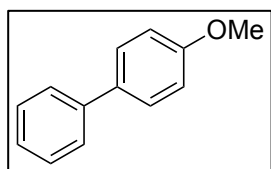




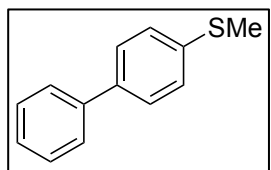
**4-Methylbiphenyl (3a):** The reaction with 4-fluorotoluene (**2o**, 55 mg, 0.50 mmol, 1.0 eq.) followed by purification by MPLC (*n*-hexane) afforded the title compound (60 mg, 0.36 mmol, 72%) as a white powder. All the resonances of  $^1\text{H}$  and  $^{13}\text{C}$  NMR spectra were consistent with the reported values.<sup>2h</sup>



***p*-Terphenyl (3k):** The reaction with 4-fluorobiphenyl (**2p**, 86 mg, 0.50 mmol) followed by purification by MPLC (*n*-hexane) afforded the title compound (91 mg, 0.40 mmol, 79%) as a white solid.  $R_f$  0.70 (*n*-hexane:EtOAc = 10:1).  $^1\text{H}$  NMR (101 MHz,  $\text{CDCl}_3$ ):  $\delta$  7.70 (s, 4H), 7.69–7.63 (m, 4H), 7.48 (t,  $J = 7.6$  Hz, 4H), 7.38 (tt,  $J = 6.6, 1.3$  Hz, 2H).  $^{13}\text{C}\{^1\text{H}\}$  NMR (101 MHz,  $\text{CDCl}_3$ ):  $\delta$  140.8, 140.3, 129.0, 127.6, 127.5, 127.2. All the resonances of  $^1\text{H}$  and  $^{13}\text{C}$  NMR spectra were consistent with the reported values.<sup>19</sup>

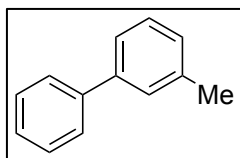


**4-Methoxybiphenyl (3c):** The reaction with 4-fluoroanisole (**2q**, 63 mg, 0.50 mmol) followed by purification by MPLC (*n*-hexane/EtOAc = 10:1) afforded the title compound (29 mg, 0.16 mmol, 31%) as a white solid. All the resonances of  $^1\text{H}$  and  $^{13}\text{C}$  NMR spectra were consistent with the reported values.<sup>14</sup>

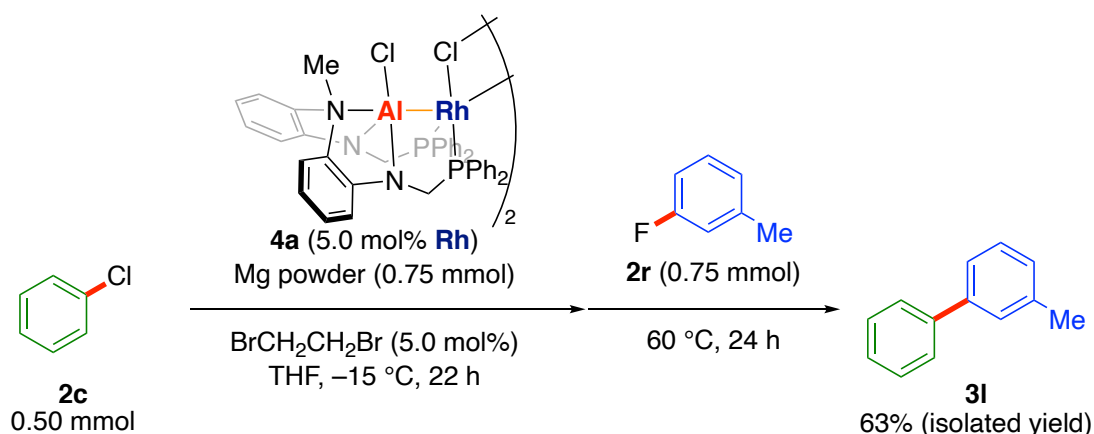


**4-Methylthiobiphenyl (3d):** The reaction with 4-fluorothioanisole (**2h**, 71 mg, 0.50 mmol) followed by purification by MPLC (*n*-hexane/EtOAc = 10:1) afforded the title compound (70 mg, 0.35 mmol, 70%) as a white solid. All the resonances of  $^1\text{H}$  and  $^{13}\text{C}$  NMR spectra were

consistent with the reported values.<sup>11c</sup>

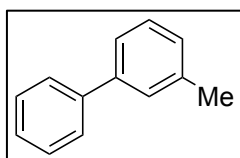


**3-Methylbiphenyl (3I):** The reaction with 3-fluorotoluene (**2r**, 55 mg, 0.50 mmol) followed by purification by MPLC (*n*-hexane) afforded the title compound (60 mg, 0.36 mmol, 71%) as a colorless liquid.  $R_f$  0.55 (*n*-hexane).  $^1\text{H}$  NMR (101 MHz,  $\text{CDCl}_3$ ):  $\delta$  7.63 (d,  $J = 7.6$  Hz, 2H), 7.49–7.43 (m, 4H), 7.37 (t,  $J = 7.5$  Hz, 2H), 7.21 (d,  $J = 7.4$  Hz, 1H), 2.46 (s, 3H).  $^{13}\text{C}\{^1\text{H}\}$  NMR (101 MHz,  $\text{CDCl}_3$ ):  $\delta$  141.5, 141.4, 138.5, 128.9, 128.82, 128.79, 128.1, 127.4, 127.3, 124.4, 21.7. All the resonances of  $^1\text{H}$  and  $^{13}\text{C}$  NMR spectra were consistent with the reported values.<sup>20</sup>



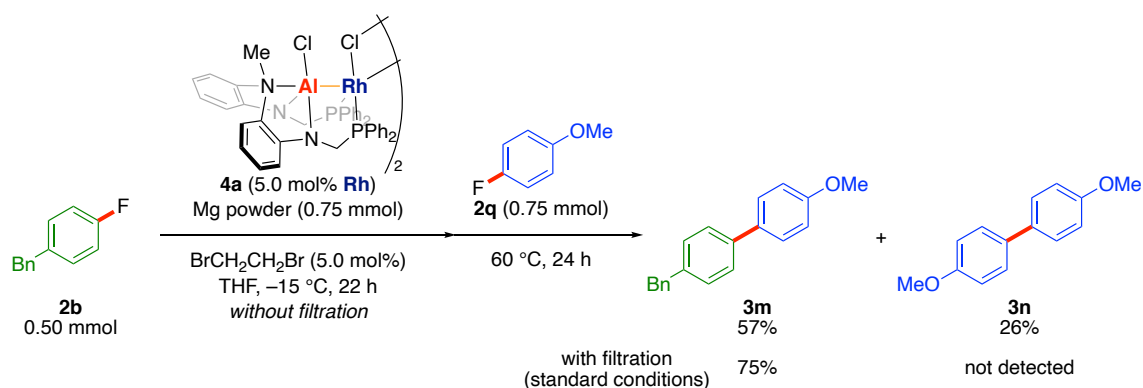
In a glove box, a 4 mL vial with a stirring bar was charged with magnesium powder (18 mg, 0.75 mmol, 1.5 eq.), THF (500  $\mu\text{L}$ ), and 1,2-dibromoethane (4.7 mg, 25  $\mu\text{mol}$ , 5.0 mol%), and the resulting mixture was stirred for 20 min at room temperature. **4a** (20 mg, 13  $\mu\text{mol}$ , 5.0 mol% of Rh) and THF (1.0 mL) were added to the vial followed by chlorobenzene (**2c**, 56 mg, 0.50 mmol, 1.0 eq.). The mixture was stirred at  $-15$  °C for 22 h to generate diphenylmagnesium. Insoluble solids of the resulting mixture were filtered off through the Pasteur pipette filter, which is filled with a glass fiber filter (GB-

100R ADVANTEC®), using THF (1.0 mL). The obtained filtrate was put into another 4 mL vial with a stirring bar and an indicated 3-fluorotoluene (**2r**, 83 mg, 0.75 mmol, 1.5 eq.). The reaction mixture was stirred at 60 °C for 24 h. To the mixture, 3 M HCl aq. (2.0 mL) was carefully added. The organic layer was separated. The remained aqueous layer was extracted with EtOAc (4.0 mL) x 3. All volatiles of the combined organic layers were removed in vacuo and the residue was purified by MPLC using Biotage® Sfär Silica High Capacity Duo to obtain 3-methylbiphenyl (**3l**).



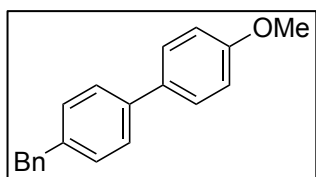
**3-Methylbiphenyl (3l):** The reaction purified by MPLC (*n*-hexane) afforded the title compound (53 mg, 0.32 mmol, 63%) as a colorless liquid. All the resonances of <sup>1</sup>H and <sup>13</sup>C NMR spectra were consistent with the reported values.<sup>20</sup>

### Procedures for the reaction with filtration.



In a glove box, a 4 mL vial with a stirring bar was charged with magnesium powder (18 mg, 0.75 mmol, 1.5 eq.), THF (500 μL), and 1,2-dibromoethane (4.7 mg, 25 μmol, 5.0 mol%), and the resulting mixture was stirred for 20 min at room temperature. **4a** (20 mg, 13 μmol, 5.0 mol% of Rh) and THF (1.0 mL) were added to the vial followed by 4-fluorodiphenylmethane (**2b**, 93 mg, 0.50 mmol, 1.0 eq.). The mixture was stirred at

–15 °C for 22 h to generate diarylmagnesium. Insoluble solids of the resulting mixture were filtered off through the Pasteur pipette filter, which is filled with a glass fiber filter (GB-100R ADVANTEC®), with THF (1.0 mL). The obtained filtrate was put into another 4 mL vial with a stirring bar and an indicated 4-fluoroanisole (**2q**, 95 mg, 0.75 mmol, 1.5 eq.). The reaction mixture was stirred at 60 °C for 24 h. To the mixture, 3 M HCl aq. (2.0 mL) was carefully added. The organic layer was separated. The remained aqueous layer was extracted with EtOAc (4.0 mL) x 3. All volatiles of the combined organic layers were removed in vacuo and the residue was purified by MPLC using 20 g iLOK™-SL to obtain 4-benzyl-4'-methoxybiphenyl (**3m**).



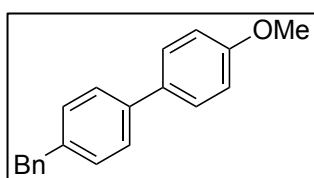
**4-Benzyl-4'-methoxybiphenyl (3m):** The reaction followed by purification by MPLC (*n*-hexane:EtOAc = 10:1) afforded the title compound (102 mg, 0.37 mmol, 75%) as a white solid.

$R_f$  0.45 (*n*-hexane:EtOAc = 10:1).  $^1\text{H}$  NMR (101 MHz,  $\text{CDCl}_3$ ):  $\delta$  7.51 (d,  $J = 8.7$  Hz, 2H), 7.48 (d,  $J = 8.2$  Hz, 2H), 7.38–7.27 (m, 2H), 7.27–7.17 (m, 5H), 6.97 (d,  $J = 8.7$  Hz, 2H), 4.02 (s, 2H), 3.85 (s, 3H).  $^{13}\text{C}$  { $^1\text{H}$ } NMR (101 MHz,  $\text{CDCl}_3$ ):  $\delta$  159.1, 141.2, 139.7, 138.8, 133.7, 129.4, 129.1, 128.6, 128.1, 126.9, 126.3, 114.3, 55.5, 41.7. All the resonances of  $^1\text{H}$  and  $^{13}\text{C}$  NMR spectra were consistent with the reported values.<sup>21</sup>

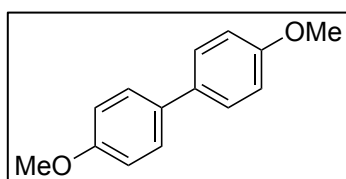
#### Procedures for the reaction without filtration.

In a glove box, a 4 mL vial with a stirring bar was charged with magnesium powder (18 mg, 0.75 mmol, 1.5 eq.), THF (500  $\mu\text{L}$ ), and 1,2-dibromoethane (4.7 mg, 25  $\mu\text{mol}$ , 5.0 mol%), and the resulting mixture was stirred for 20 min at room temperature. **4a** (20 mg, 13  $\mu\text{mol}$ , 5.0 mol% of Rh) and THF (1.0 mL) were added to the vial followed

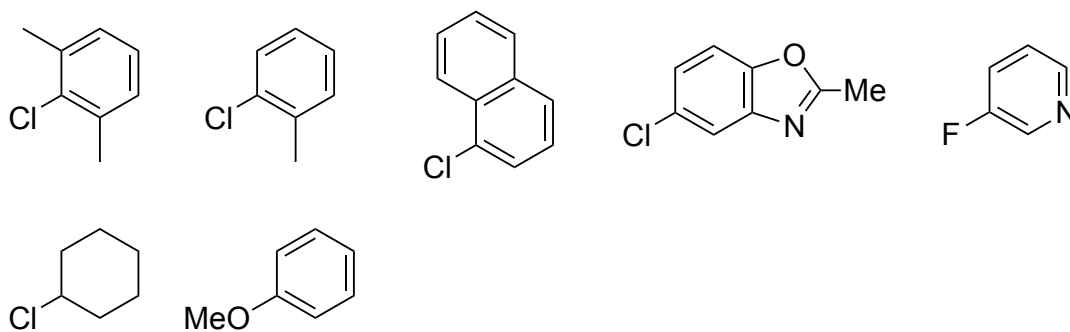
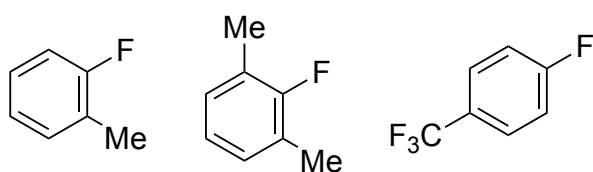
by 4-fluorodiphenylmethane (**2b**, 93 mg, 0.50 mmol, 1.0 eq.). The mixture was stirred at  $-15\text{ }^{\circ}\text{C}$  for 22 h to generate diarylmagnesium. To the resulting mixture, 4-fluoroanisole (**2q**, 95 mg, 0.75 mmol, 1.5 eq.) was added in a one-pot manner. The reaction mixture was stirred at  $60\text{ }^{\circ}\text{C}$  for 24 h. To the mixture, 3 M HCl aq. (2.0 mL) was carefully added. The organic layer was separated. The remained aqueous layer was extracted with EtOAc (4.0 mL) x 3. All volatiles of the combined organic layers were removed in vacuo and the residue was purified by MPLC using 20 g iLOK<sup>TM</sup>-SL and recycling preparative HPLC to isolate the cross-coupling product **3m** and the homo-coupling product **3n**.



**4-Benzyl-4'-methoxybiphenyl (3m)**: The reaction purified by MPLC (*n*-hexane:EtOAc = 10:1) followed by recycling preparative HPLC afforded the title compound (78 mg, 0.29 mmol, 57%) as a white solid.  $R_f$  0.45 (*n*-hexane:EtOAc = 10:1). All the resonances of  $^1\text{H}$  and  $^{13}\text{C}$  NMR spectra were consistent with the reported values.<sup>21</sup>



**4,4'-Dimethoxybiphenyl (3n)**: The reaction of in situ prepared 4-benzylphenyl magnesium from 4-fluorodiphenylmethane (**2b**, 93 mg, 0.50 mmol), and 4-fluoroanisole (**2q**, 95 mg, 0.75 mmol) followed by purification by MPLC (*n*-hexane:EtOAc = 10:1) and recycling preparative HPLC afforded the title compound (21 mg, 0.10 mmol, 26%) as a white solid.  $R_f$  0.40 (*n*-hexane:EtOAc = 10:1).  $^1\text{H}$  NMR (101 MHz,  $\text{CDCl}_3$ ):  $\delta$  7.48 (d,  $J = 8.7$  Hz, 4H), 6.96 (d,  $J = 8.9$  Hz, 4H), 3.85 (s, 6H).  $^{13}\text{C}\{^1\text{H}\}$  NMR (101 MHz,  $\text{CDCl}_3$ ):  $\delta$  158.8, 133.6, 127.9, 114.3, 55.5. All the resonances of  $^1\text{H}$  and  $^{13}\text{C}$  NMR spectra were consistent with the reported values.<sup>22</sup>

**Unsuccessful Electrophiles****Unsuccessful Arylmagnesium Precursors**

**References and notes**

- (1) For selected reviews on transition-metal-catalyzed C–C-bond-forming reactions, see: (a) Cordovilla, C.; Bartolomé, C.; Martínez-Ilarduya, J. M.; Espinet, P. *ACS Catal.* **2015**, *5*, 3040. (b) Trost, B. M. *Tetrahedron* **2015**, *71*, 5708. (c) Haas, D.; Hammann, J. M.; Greiner, R.; Knochel, P. *ACS Catal.* **2016**, *6*, 1540. (d) Miyaura, N.; Suzuki, A. *Chem. Rev.* **1995**, *95*, 2457. (e) Hazra, S.; Johansson Seechurn, C. C. C.; Handa, S.; Colacot, T. J. *ACS Catal.* **2021**, *11*, 13188. (f) Nakao, Y.; Hiyama, T. *Chem. Soc. Rev.* **2011**, *40*, 4893. (g) Jagtap, S. *Catalysts* **2017**, *7*, 267. (h) Chinchilla, R.; Nájera, C. *Chem. Rev.* **2007**, *107*, 874. (i) Littke, A. F.; Fu, G. C. *Angew. Chem., Int. Ed.* **2002**, *41*, 4176.
- (2) For selected reviews on Kumada–Tamao–Corriu coupling reactions, see: (a) Heravi, M. M.; Hajiabbasi, P. *Monatsh. Chem.* **2012**, *143*, 1575. (b) Heravi, M. M.; Zadsirjan, V.; Hajiabbasi, P.; Hamidi, H. *Monatsh. Chem.* **2019**, *150*, 535. (c) Terao, J.; Kambe, N. *Acc. Chem. Res.* **2008**, *41*, 1545. (d) Jana, R.; Pathak, T. P.; Sigman, M. S. *Chem. Rev.* **2011**, *111*, 1417. (e) Li, W.-N.; Wang, Z.-L. *RSC Adv.* **2013**, *3*, 25565. For pioneering reports and selected examples of Kumada–Tamao–Corriu coupling reactions, see: (f) Tamao, K.; Sumitani, K.; Kumada, M. *J. Am. Chem. Soc.* **1972**, *94*, 4374. (g) Corriu, R. J. P.; Masse, J. P. *J. Chem. Soc., Chem. Commun.* **1972**, 144. (h) Yoshikai, N.; Mashima, H.; Nakamura, E. *J. Am. Chem. Soc.* **2005**, *127*, 17978. (i) Yoshikai, N.; Matsuda, H.; Nakamura, E. *J. Am. Chem. Soc.* **2009**, *131*, 9590. (j) Inamoto, K.; Kuroda, J.; Sakamoto, T.; Hiroya, K. *Synthesis* **2007**, *18*, 2853. (k) Guo, W.-J.; Wang, Z.-X. *J. Org. Chem.* **2013**, *78*, 1054. (l) Vechorkin, O.; Proust, V.; Hu, X. *J. Am. Chem. Soc.* **2009**, *131*, 9756. (m) Hua, X.; Masson-Makdissi, J.; Sullivan, R. J.; Newman, S. G. *Org. Lett.* **2016**, *18*, 5312. (n) Martin,

- R.; Buchwald, S. L. *J. Am. Chem. Soc.* **2007**, *129*, 3844. (o) Hatakeyama, T.; Nakamura, M. *J. Am. Chem. Soc.* **2007**, *129*, 9844. (p) Coombs, J.; Perry, D.; Kwon, D.-H.; Thomas, C. M.; Ess, D. H. *Organometallics* **2018**, *37*, 4195. (q) Cong, X.; Tang, H.; Zeng, X. *J. Am. Chem. Soc.* **2015**, *137*, 14367.
- (3) (a) Herold, P.; Stutz, S.; Spindler, F. U.S. Patent WO 2002002508A1, January 10, 2002. (b) Linghu, X.; Wong, N.; Jost, V.; Fantasia, S.; Sowell, C. G.; Gosselin, F. *Org. Process Res. Dev.* **2017**, *21*, 1320. (c) Loewe, R. S.; Ewbank, P. C.; Liu, J.; Zhai, L.; McCullough, R. D. *Macromolecules* **2001**, *34*, 4324. (d) Giordano, C.; Coppi, L.; Minisci, F. Patent US5312975A, May 17, 1994. (e) Ishikawa, S.; Eguchi, H. Patent US6479709B1, November 12, 2002.
- (4) Aryl chlorides (10,128,540) and fluorides (10,975,993) are more accessible than aryl bromides (4,927,630) or iodides (808,292); the numbers in parenthesis refer to the number of commercially available aryl halides registered on SciFinder on February 9th, 2022.
- (5) *CRC Handbook of Chemistry and Physics*, 94th ed.; Haynes, W. M., Ed.; CRC Press: Boca Raton, FL, 2013.
- (6) Fujii, I.; Semba, K.; Li, Q.-Z.; Sakaki, S.; Nakao, Y. *J. Am. Chem. Soc.* **2020**, *142*, 11647.
- (7) (a) Timpa, S. D.; Fafard, C. M.; Herbert, D. E.; Ozerov, O. V. *Dalton Trans.* **2011**, *40*, 5426. (b) Gatard, S.; Çelenligil-Çetin, R.; Guo, C.; Foxman, B. M.; Ozerov, O. V. *J. Am. Chem. Soc.* **2006**, *128*, 2808. (c) Iwasaki, T.; Miyata, Y.; Akimoto, R.; Fujii, Y.; Kuniyasu, H.; Kambe, N. *J. Am. Chem. Soc.* **2014**, *136*, 9260. For selected examples on rhodium-catalyzed cross-coupling reactions using other organometallic nucleophiles, see: (d) Ueura, K.; Satoh, T.; Miura, M. *Org. Lett.*



- 2005, 7, 2229. (e) Hossain, K. M.; Takagi, K. *Chem. Lett.* **1999**, 1241. (f) Larock, R. C.; Narayanan, K.; Hershberger, S. S. *J. Org. Chem.* **1983**, 48, 4377.
- (8) Phosphines bearing phenyl groups are less electron-donating than those having *iso*-propyl groups. Tolman, C. A. *Chem. Rev.* **1977**, 77, 313.
- (9) (a) Aizenberg, M.; Milstein, D. *Science* **1994**, 265, 359. (b) Liu, X.-W.; Echavarren, J.; Zarate, C.; Martin, R. *J. Am. Chem. Soc.* **2015**, 137, 12470. (c) Niwa, T.; Ochiai, H.; Watanabe, Y.; Hosoya, T. *J. Am. Chem. Soc.* **2015**, 137, 14313. (d) Amii, H.; Uneyama, K. *Chem. Rev.* **2009**, 109, 2119.
- (10) (a) Quasdorf, K. W.; Antoft-Finch, A.; Liu, P.; Silberstein, A. L.; Komaromi, A.; Blackburn, T.; Ramgren, S. D.; Houk, K. N.; Snieckus, V.; Garg, N. K. *J. Am. Chem. Soc.* **2011**, 133, 6352. (b) Boit, T. B.; Bulger, A. S.; Dander, J. E.; Garg, N. K. *ACS Catal.* **2020**, 10, 12109. (c) Ogawa, H.; Yang, Z.-K.; Minami, H.; Kojima, K.; Saito, T.; Wang, C.; Uchiyama, M. *ACS Catal.* **2017**, 7, 3988. (d) Quasdorf, K. W.; Riener, M.; Petrova, K. V.; Garg, N. K. *J. Am. Chem. Soc.* **2009**, 131, 17748. (e) Silberstein, A. L.; Ramgren, S. D.; Garg, N. K. *Org. Lett.* **2012**, 14, 3796. (f) Hie, L.; Ramgren, S. D.; Mesganaw, T.; Garg, N. K. *Org. Lett.* **2012**, 14, 4182. (g) Mesganaw, T.; Fine Nathel, N. F.; Garg, N. K. *Org. Lett.* **2012**, 14, 2918. (h) Nishizawa, A.; Takahira, T.; Yasui, K.; Fujimoto, H.; Iwai, T.; Sawamura, M.; Chatani, N.; Tobisu, M. *J. Am. Chem. Soc.* **2019**, 141, 7261. (i) Mesganaw, T.; Silberstein, A. L.; Ramgren, S. D.; Fine Nathel, N. F.; Hong, X.; Liu, P.; Garg, N. K. *Chem. Sci.* **2011**, 2, 1766.
- (11) (a) Someya, C. I.; Weidauer, M.; Enthaler, S. *Catal. Lett.* **2013**, 143, 424. (b) Yamamoto, K.; Otsuka, S.; Nogi, K.; Yorimitsu, H. *ACS Catal.* **2017**, 7, 7623. (c) Bismuto, A.; Delcaillau, T.; Müller, P.; Morandi, B. *ACS Catal.* **2020**, 10, 4630. (d) Lou, J.; Wang, Q.; Wu, P.; Wang, H.; Zhou, Y.-G.; Yu, Z. *Chem. Soc. Rev.* **2020**, 49,

4307. (e) Gao, K.; Otsuka, S.; Baralle, A.; Nogi, K.; Yorimitsu, H.; Osuka, A. *J. Synth. Org. Chem., Jpn.* **2016**, *74*, 1119. (f) Nogi, K.; Yorimitsu, H. *Chem. – Asian J.* **2020**, *15*, 441. (g) Otsuka, S.; Nogi, K.; Yorimitsu, H. *Top. Curr. Chem.* **2018**, *376*, 13.
- (12) (a) Graziano, B. J.; Vollmer, M. V.; Lu, C. C. *Angew. Chem., Int. Ed.* **2021**, *60*, 15087. (b) Kim, J.; Kim, Y.-E.; Park, K.; Lee, Y. *Inorg. Chem.* **2019**, *58*, 11534. (c) Shih, W.-C.; Ozerov, O. V. *J. Am. Chem. Soc.* **2017**, *139*, 17297.
- (13) Schmink, J. R.; Leadbeater, N. E. *Org. Lett.* **2009**, *11*, 2575.
- (14) Li, J.-H.; Liu, W.-J. *Org. Lett.* **2004**, *6*, 2809
- (15) Ghalesahi, H. G.; Antonacci, G.; Madsen, R. *Eur. J. Org. Chem.* **2017**, 1331.
- (16) Shirakawa, E.; Hayashi, Y.; Itoh, K.; Watabe, R.; Uchiyama, N.; Konagaya, W.; Masui, S.; Hayashi, T. *Angew. Chem. Int. Ed.* **2012**, *51*, 218.
- (17) Guerra, R. R. G.; Martins, F. C. P.; Lima, C. G. S.; Gonçalves, R. H.; Leite, E. R.; Pereira-Filho, E. R.; Schwab, R. S. *Tetrahedron Letters* **2017**, *58*, 903.
- (18) Yang, J.; Li, P.; Wang, L. *Synthesis* **2011**, *8*, 1295.
- (19) Bolliger, J. L.; Frech, C. M. *Adv. Synth. Catal.* **2010**, *352*, 1075.
- (20) Wang, Z.-J.; Lv, J.-J.; Feng, J.-J.; Li, N.; Xu, X.; Wang, A.-J.; Qiu, R. *RSC Adv.* **2015**, *5*, 28467.
- (21) Ronson, T. O.; Carney, J. R.; Whitwood, A. C.; Taylor, R. J. K.; Fairlamb, I. J. S. *Chem. Commun.* **2015**, *51*, 3466.
- (22) Dzhevakov, P. B.; Topchiy, M. A.; Zharkova, D. A.; Morozov, O. S.; Asachenko, A. F.; Nechaev, M. S. *Adv. Synth. Catal.* **2016**, *358*, 977.

## **Chapter 4**

### **Site-Selective Magnesiumation of Multi-Fluorinated Arenes Catalyzed by Rhodium–Aluminum Bimetallic Complexes**

The author reports the site-selective C–F magnesiumation of multi-fluorinated arenes catalyzed by Rh–Al bimetallic complexes to prepare synthetically important fluorine-containing organomagnesium reagents. The author clarifies that the catalyst-control stems from steric and electronic environments of the substrates. The protocol has been applied to the efficient synthesis of fluorine-containing pharmaceuticals and liquid crystal molecules.

## Introduction

Fluorine is the most electronegative atom and able to form the strongest single bond with carbon.<sup>1</sup> These special features provide unique properties with fluorine-containing compounds. Fluoroarenes are often found as key structural motifs in pharmaceuticals,<sup>2</sup> agrochemicals,<sup>3</sup> and organic materials<sup>4</sup> (Scheme 4-1, A). In fact, 22% of small-molecule drugs registered globally in the past three decades contain fluorine atom,<sup>2a</sup> and the percentages are getting higher in recent years (2015: 34%, 2019: 43%).<sup>2a</sup> Hence, efficient methods to prepare substituted fluoroarenes are highly desired in modern organic synthesis.<sup>5</sup>

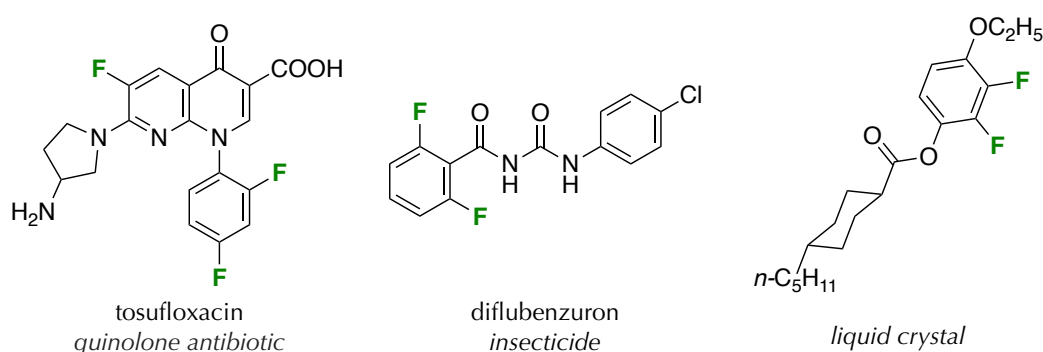
Fluorine-containing organometallic reagents are useful tools for the synthesis of fluorine-containing compounds thanks to diverse transformations available with their carbon–metal bonds.<sup>6</sup> Two complementary routes are potentially available to access these reagents (Scheme 4-1, B). Conventionally, fluorine-containing organometallics are prepared by the Balz–Schiemann reaction (step a)<sup>7</sup> followed by halogenation<sup>8</sup> (step b) and subsequent oxidative insertion,<sup>9</sup> halogen/metal exchange reaction,<sup>10</sup> or C–H bond metalation reactions (step c).<sup>11</sup> However, harsh reactions conditions for the Balz–Schiemann reaction and an issue of site-selectivity in the C–H bond metalation reaction have hampered their practical use.

The other route starting from perfluoroarenes can be more attractive according to the following reasons: 1) Perfluoroarenes such as hexafluorobenzene (C<sub>6</sub>F<sub>6</sub>) and pentafluoropyridine (C<sub>5</sub>F<sub>5</sub>N) can be transformed by aromatic nucleophilic substitution (S<sub>N</sub>Ar) reactions<sup>12</sup> and transition-metal catalyzed cross-coupling reactions<sup>13</sup> in a site-selective manner thanks to the relatively weakened C–F bonds in perfluoroarenes<sup>14</sup> (step d). 2) Perfluoroarenes can be prepared from upstream fluorine feedstocks such as F<sub>2</sub>/CoF<sub>2</sub>

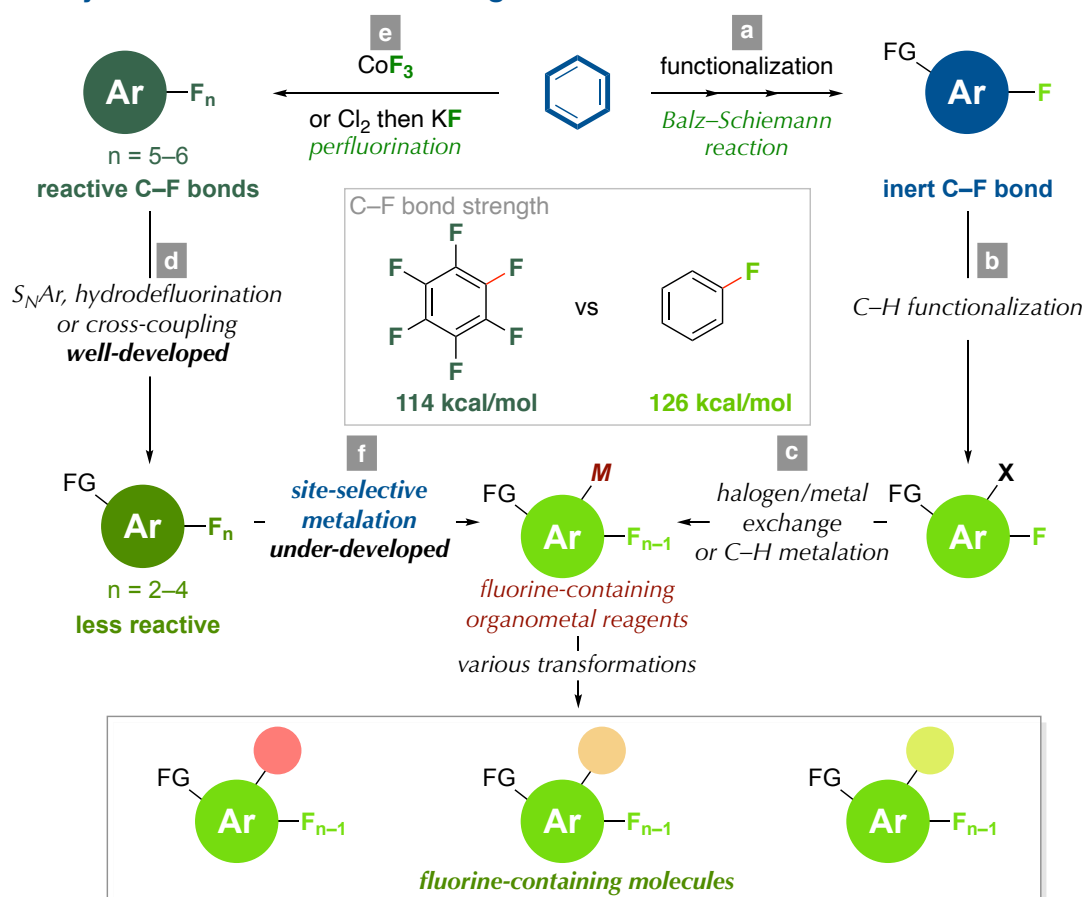
or KF through direct perfluorination of arenes using  $\text{CoF}_3$  (Fowler process)<sup>15</sup> or perchlorination with  $\text{Cl}_2$  followed by  $\text{S}_{\text{N}}\text{Ar}$  reaction with metal fluorides (Halex process)<sup>16</sup> (step e). However, this route has been hampered by a lack of site-selective C–F bond metalation (step f) of multi-fluoroarenes ( $\text{C}_6\text{F}_n\text{X}_{6-n}$ ;  $n = 2-4$ ).<sup>14</sup>

**Scheme 4-1.** Importance and synthetic strategies of functionalized aryl fluorides.

### A. Fluorine in Key Pharmaceutical, Agrochemical, and Material

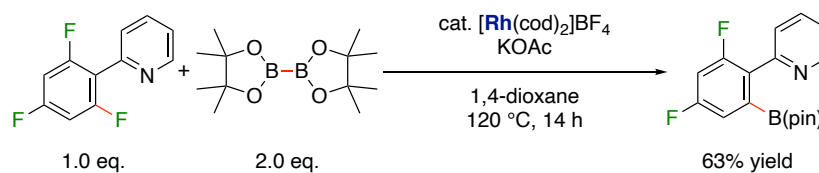
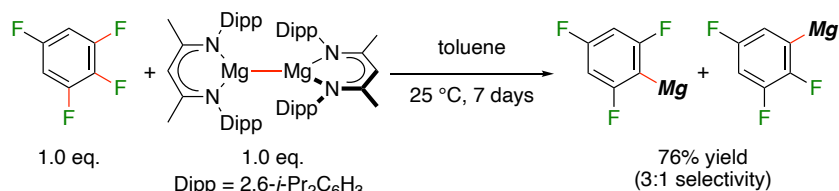
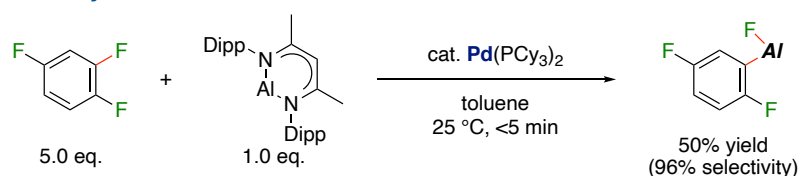
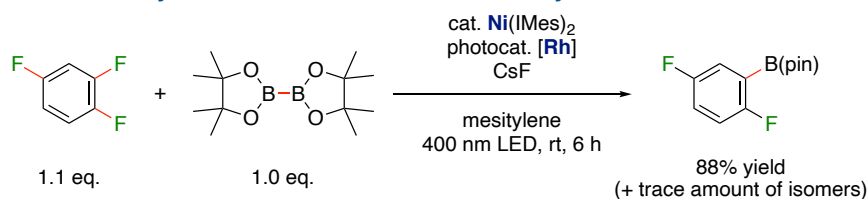


### B. Synthesis of Functionalized Organofluorides



Although site-selective C–F bond metalation reactions of multi-fluoroarenes were achieved through coordination of directing groups (Scheme 4-2, A),<sup>17</sup> the site-selectivity in their absence has been difficult to control. Recently, Crimmin and coworkers developed the site-selective magnesiation of fluoroarenes using a dimeric Mg(I)–Mg(I) reagent (Scheme 4-2, B)<sup>18</sup> and the alumination of multi-fluoroarenes using an Al(I) reagent by Pd catalysis (Scheme 4-2, C).<sup>19</sup> However, these systems require stoichiometric amounts of reactive Mg(I) or Al(I) reagents, which are prepared from alkaline metals. Marder and Radius group reported the site-selective photocatalytic C–F bond borylation of multi-fluoroarenes by Rh/Ni dual catalysis (Scheme 4-2, D).<sup>20</sup> They have achieved the high site-selectivity by promoting the rate-determining transmetalation step with the Rh photocatalyst at room temperature to afford fluorine-containing organoboron compounds.<sup>6</sup> Nevertheless, modest catalyst efficiency, especially for di- or tri-fluoroarenes, has been noted.

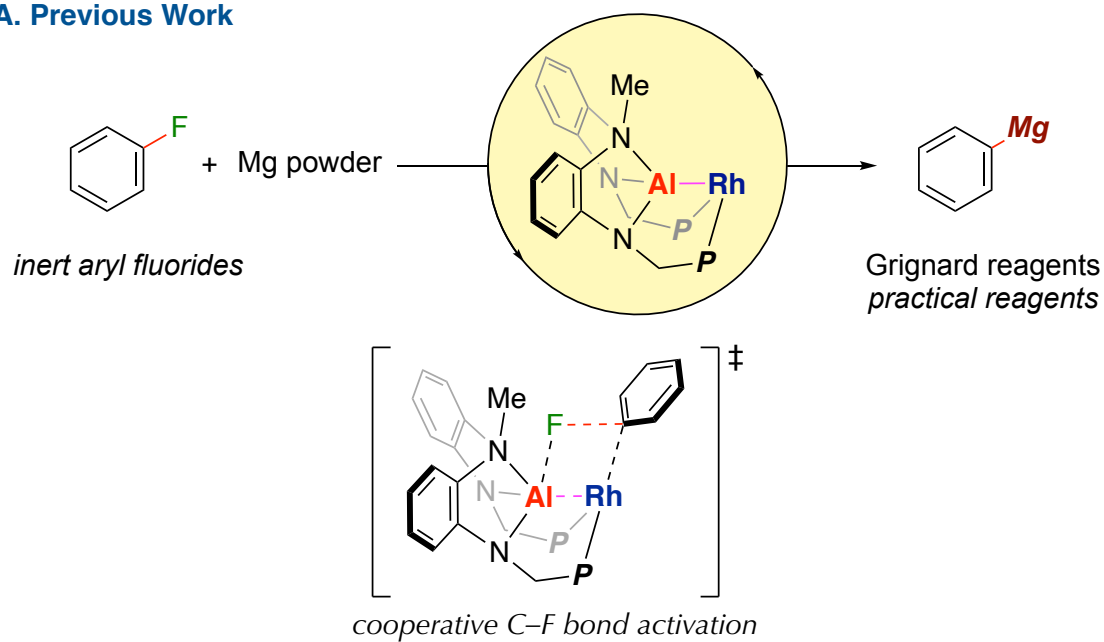
Scheme 4-2. Selected reports of site-selective metalation of multi-fluorinated arenes.

**A. Rh-Catalyzed *ortho*-Selective C–F Bond Borylation****B. Magnesium(I) Complex-Mediated Site-Selective C–F Bond Magnesiumation****C. Pd-Catalyzed Site-Selective C–F Bond Almination****D. Ni/Rh-Catalyzed Site-Selective C–F Bond Borylation**

Previously, the author has developed the magnesiumation of aryl fluorides catalyzed by Rh–Al bimetallic complexes through C–F bond activation cooperatively by the Rh–Al bond (Scheme 4-3, A).<sup>21</sup> The cooperative activation of C–F bond by the Rh–Al bond proceeds under very mild conditions, which can be beneficial for controlling the site-selectivity with multi-fluoroarenes, taking advantage of a steric repulsion between arene substituents and the ligand backbone of the Rh–Al complex.<sup>22</sup> Here, the author reports the undirected but site-selective magnesiumation of less hindered C–F bonds of multi-fluorinated arenes catalyzed by the Rh–Al bimetallic complexes (Scheme 4-3, B).

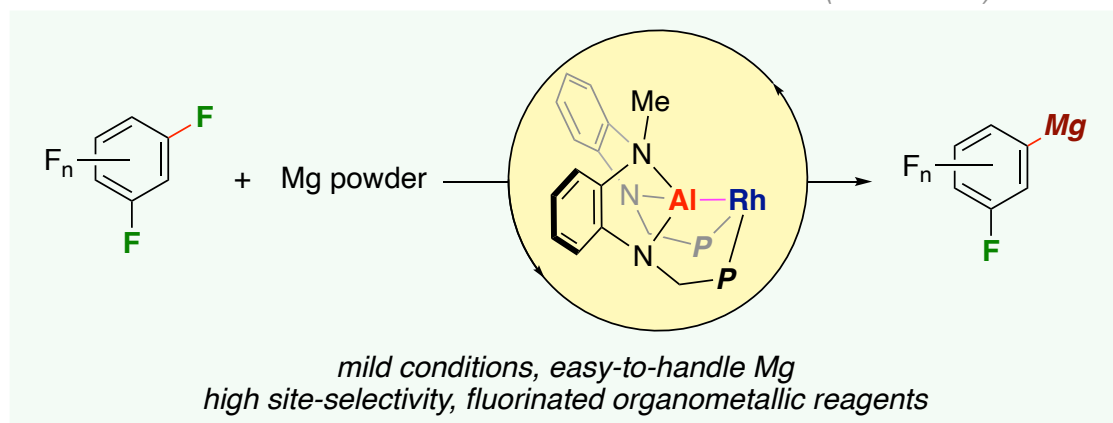
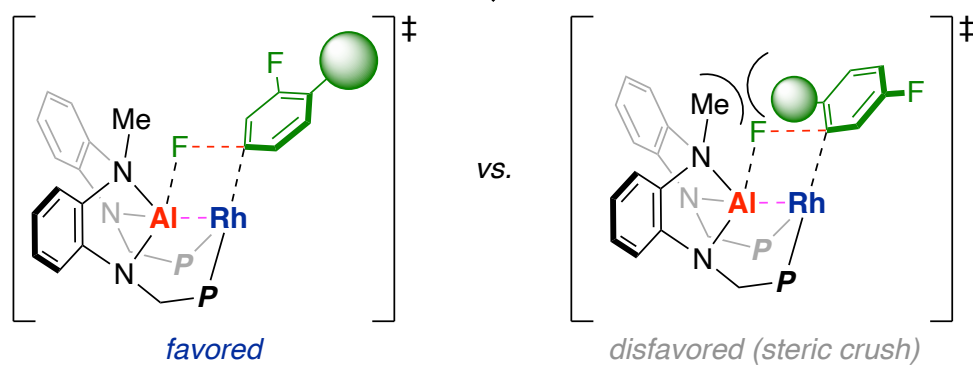
Scheme 4-3. Previous work and this work.

## A. Previous Work



*site-selective magnesiation*

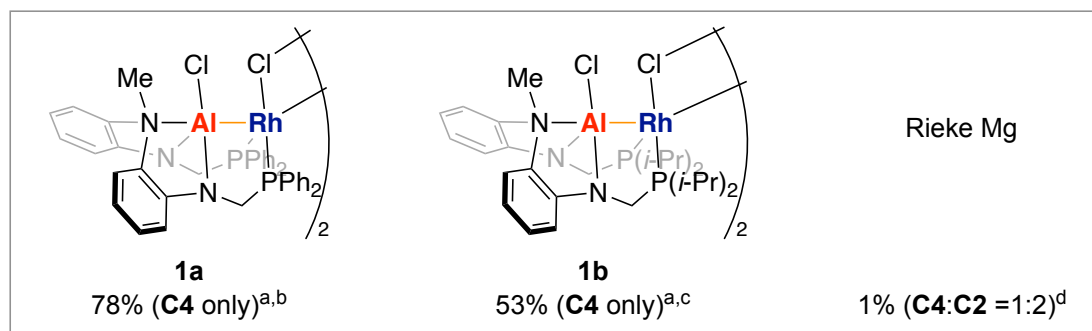
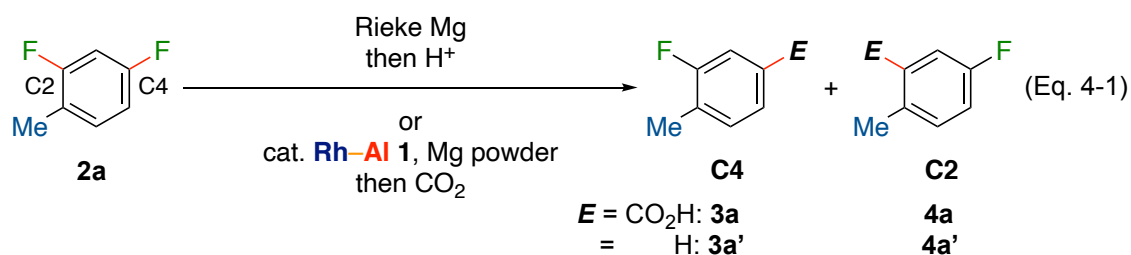
## B. This Work





## Results and discussion

The author examined the site-selective magnesiation of 2,4-difluorotoluene (**2a**, 0.50 mmol, 1.0 eq.) with Mg powder (1.5 mmol, 3.0 eq.), which was preactivated upon treatment with 1,2-dibromoethane (5.0 mol%), in the presence of Rh–Al complex **1a** (5.0 mol% Rh) in THF (1.5 mL, 0.33 M) at  $-15\text{ }^{\circ}\text{C}$  (Eq. 4-1). Interestingly, 3-fluoro-4-toluic acid (**3a**), was selectively obtained in 78% yield through C(4)–F functionalization without formation of C2-carboxylated product **4a** after quenching the reaction with  $\text{CO}_2$  followed by 3 M HCl aq. This result indicated that less sterically hindered C4-position underwent the magnesiation exclusively. Rh–Al complex **1b**, which bears *i*-Pr groups on the phosphorus atoms instead of phenyl groups, also gave **3a** in a site-selective manner, albeit in moderate yield. The observed site-selectivities were governed by the Rh–Al complexes. When the reaction was carried out with Rieke  $\text{Mg}^{23}$  in the absence of the catalyst, a mixture of 2-fluorotoluene (**3a'**) and 4-fluorotoluene (**4a'**) was obtained in low yield in a ratio of **3a'**:**4a'** = 1:2 after protonation with  $\text{NH}_4\text{Cl}$  aq. These results demonstrate the potential of the present catalytic method for the selective preparation of fluorine-containing building blocks from readily available multi-fluorinated arenes.

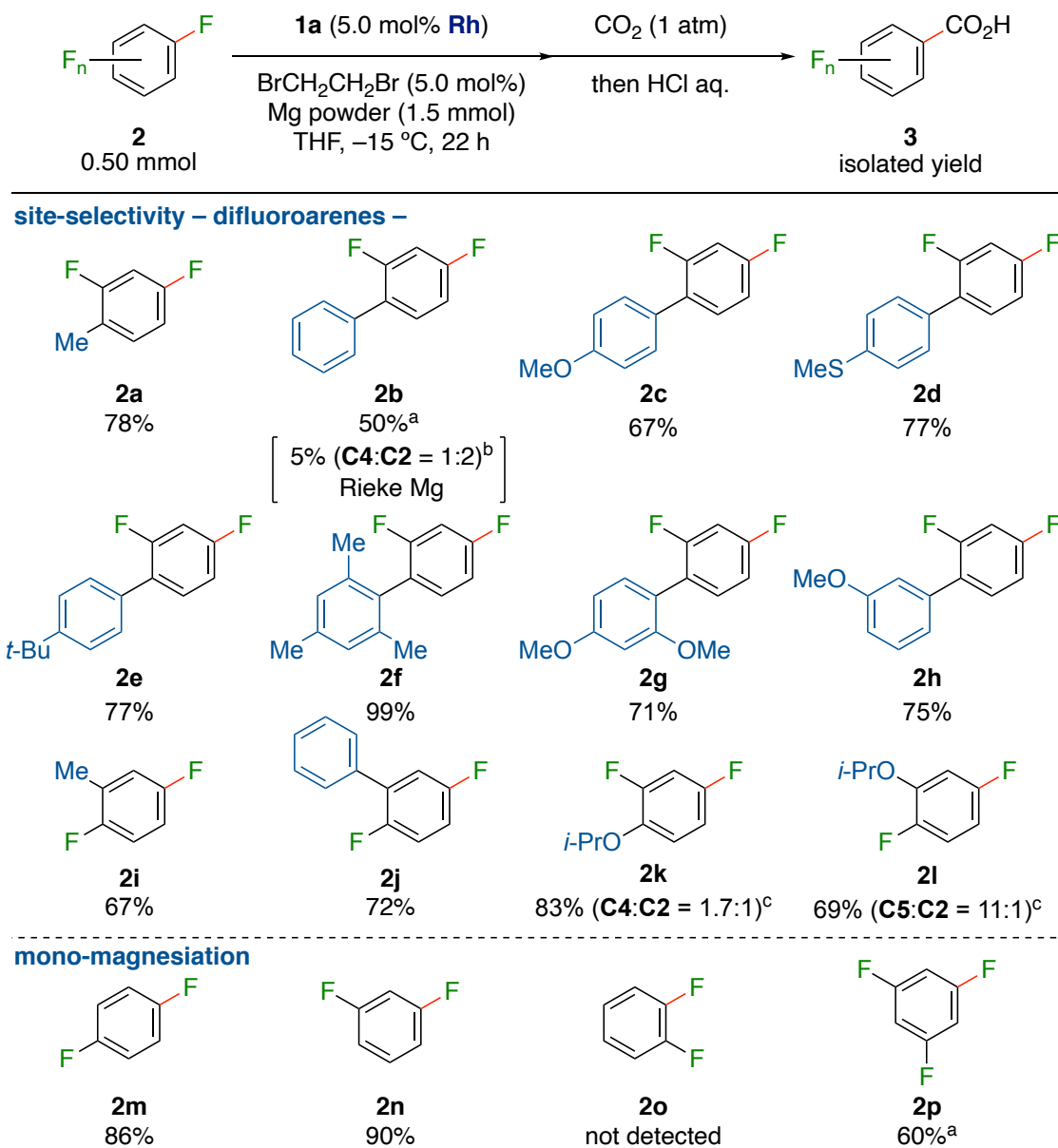


<sup>a</sup>**2a** (1.0 eq.), Mg powder (1.5 or 3.0 eq.), 1,2-dibromoethane (5.0 mol%), and **1** (5.0 mol% **Rh**) in THF at  $-15\text{ }^\circ\text{C}$  for 22 h. 3-Fluoro-4-toluic acid was obtained after carboxylation with  $\text{CO}_2$ . <sup>b</sup>Isolated yield. <sup>c</sup>The yield and site-selectivity were confirmed by  $^1\text{H}$  NMR spectroscopy. <sup>d</sup>**2a** (1.0 eq.) and Rieke Mg (1.0 eq.) in THF at  $80\text{ }^\circ\text{C}$  for 3 h. The yield and site-selectivity were confirmed by  $^{19}\text{F}$  NMR spectroscopy after protonation with  $\text{NH}_4\text{Cl}$ .

Next, the author investigated the scope of substrates in a 0.50 mmol scale under the optimized conditions using **1a** (Scheme 4-4). 2,4-Difluorobiphenyl (**2b**) afforded the C4-carboxylated product **3b** as a sole product in 50% yield. Again, the Rieke Mg conditions gave a mixture of isomers (**C4**:**C2** = 1:2) in 5% yield. Electron-rich or sterically demanding 2,4-difluorobiaryls **2c–2h** participated in the reaction to afford corresponding products **3c–3h** through the C–F functionalization at the less-hindered C4-position in good to high yield. It was worth noting that the electron-rich arenes and heteroatoms did not affect the site-selectivity. This protocol could also be applied to the C5-selective magnesiation of 2,5-difluoroarenes **2i** and **2j**. Although 2,5-difluoro-1-*iso*-propoxybenzene (**2l**) was preferentially magnesiated at the C5-position (**C5**:**C2** = 11:1), 2,4-difluoro-1-*iso*-propoxybenzene (**2k**) showed markedly decreased the selectivity, in which a mixture of isomers (**C4**:**C2** = 1.7:1) was obtained. In the case of **2k**, the reaction proceeded at the sterically demanding C2-position probably due to coordination of the

*iso*-propoxy group to the Lewis acidic Al center. However, in the case of **2l**, the C5-position was predominantly magnesiated. This was probably because the C–F bond at the C5-position of **2l** was electronically activated by the negative inductive effect of *Oi*-Pr (Hammett parameter;  $\sigma_m = 0.10$ ,  $\sigma_p = -0.45$ ),<sup>24</sup> whereas the C–F bond at C4-position of **2k** was electronically deactivated by a positive resonance effect of *Oi*-Pr. In addition to the site-selective magnesiation, the reactions of di- and tri-fluorobenzenes **2m–2p** proceeded in a mono-selective manner. For examples, 4-fluorobenzoic acid (**3m**) was selectively formed in 87% yield without forming products derived from further magnesiation. 1,3-Difluorobenzene (**2n**) and 1,3,5-trifluorobenzene (**2p**) afforded 3-fluorobenzoic acid (**3n**) in 99% yield and methyl 3,5-difluorobenzoate (**3p**) in 60% yield, respectively. On the other hand, 1,2-difluorobenzene (**2o**) gave a complex mixture and did not form the desired product.

Scheme 4-4. Substrate scope.

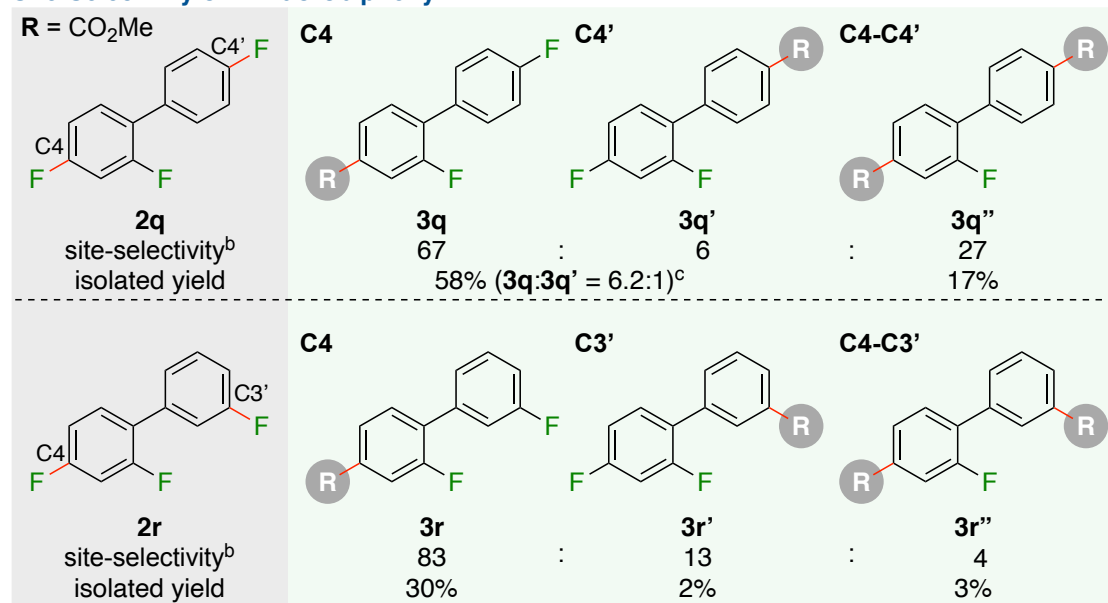
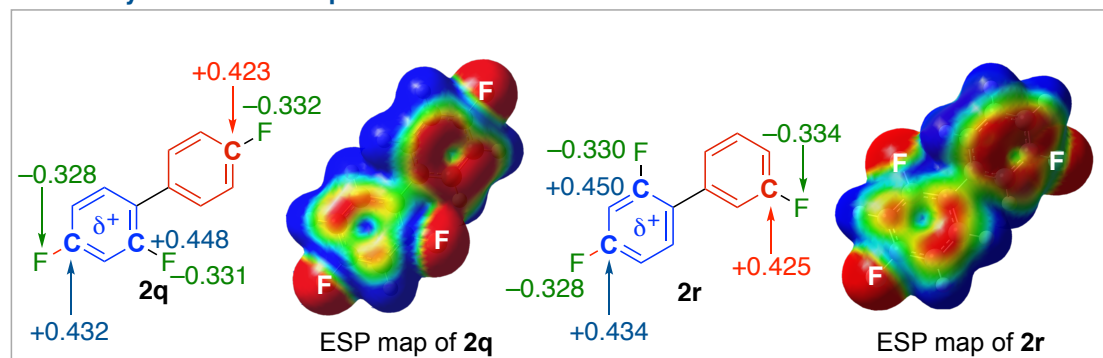


<sup>a</sup>The methyl esters were isolated after reacting with TMSCHN<sub>2</sub>. <sup>b</sup>Aryl fluoride (1.0 mmol) and Rieke Mg (1.0 mmol) without **1a** in THF (30 mL) at 80 °C for 3 h. Yield and site-selectivity were confirmed by gas chromatography after protonation with NH<sub>4</sub>Cl. <sup>c</sup>The reactions are carried out at -20 °C. Site-selectivity was estimated based on <sup>1</sup>H NMR analysis of a crude product.

The author then studied the reactions of trifluorobiphenyls **2q** and **2r** (Scheme 4-5). 2,4,4'-Trifluorobiphenyl (**2q**) was reacted preferentially at the C4-position to give **3q** with isomer **3q'** and double magnesiation product **3q''** being contaminated in the ratio

67:6:27 as estimated by  $^{19}\text{F}$  NMR spectroscopies of the crude product. The subsequent purification gave a mixture of **3q** and **3q'** in 58% yield (**3q:3q'** = 6.2:1), and **3q''** in 17% yield. A slightly better site-selectivity was observed (**3r:3r':3r''** = 83:13:4) when 2,3',4-trifluorobiphenyl (**2r**) was reacted. In both cases, the less sterically demanding and electron-deficient C–F bonds were activated. Calculated electrostatic potential (ESP) maps and the natural populations on the fluorinated carbons of **2q** and **2r** showed that the most reactive sites were the most positive. As reported previously,<sup>21</sup>  $\eta^2$ -coordination of the arene to the electron-rich Rh center precedes the C–F bond cleavage, and more electron-deficient arenes are preferred in the  $\eta^2$ -coordination to discriminate the reaction site. Rh–Al catalyst **1a** can thus selectively activate the C–F bond, which is sterically less hindered and more electrophilic.

## Scheme 4-5. Site-selectivity of trifluorobiphenyl.

Site-Selectivity of Trifluorobiphenyl<sup>a</sup>NBO Analysis and ESP Maps<sup>d</sup>

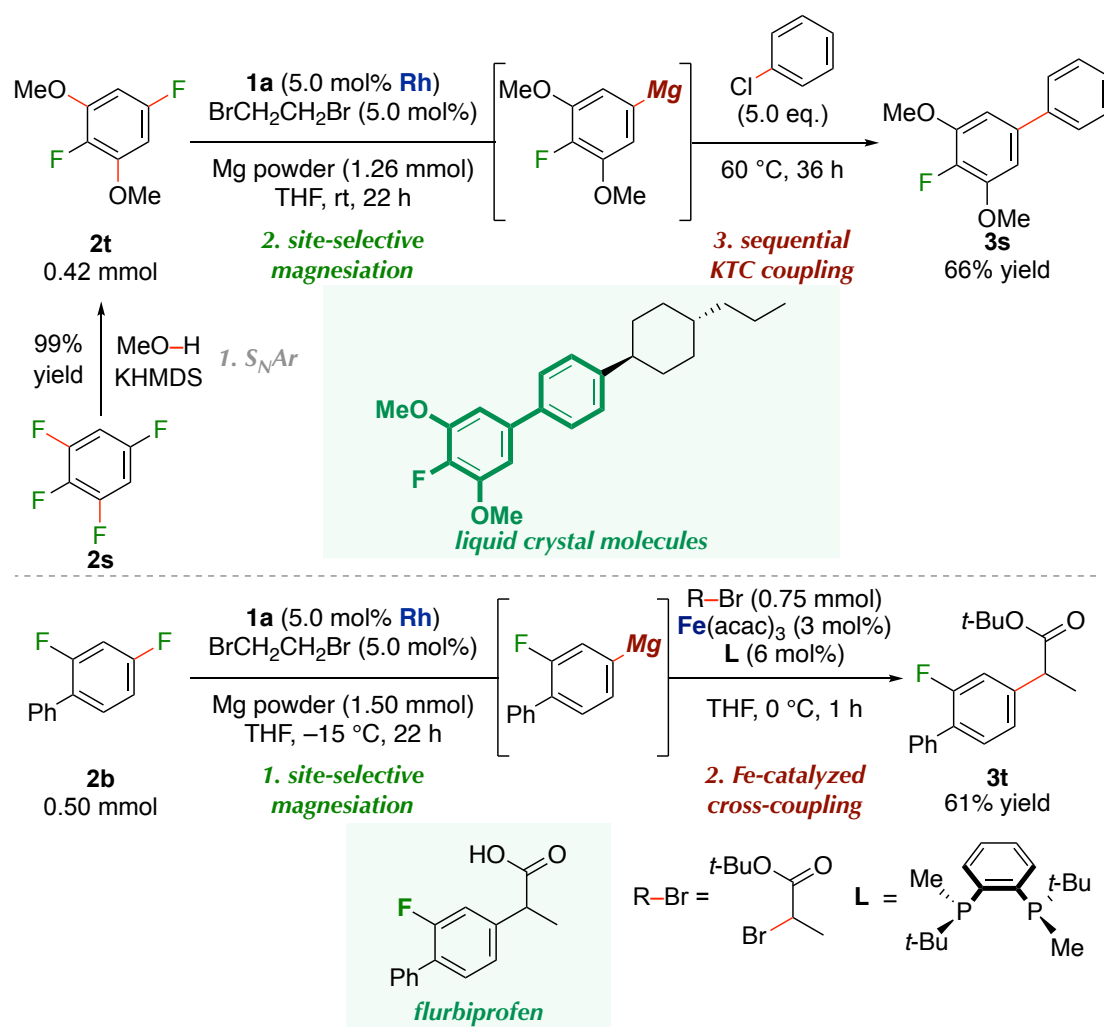
<sup>a</sup>Aryl fluoride **2** (0.50 mmol), Mg powder (1.5 mmol), which is activated using 1,2-dibromoethane (5.0 mol%) beforehand, and **1a** (5.0 mol% **Rh**) in THF (1.5 mL) at -30 °C for 22 h. The resulting mixture treated with CO<sub>2</sub> (1 atom). The methyl esters were isolated after reacting with TMSCHN<sub>2</sub>.

<sup>b</sup>The site-selectivity was estimated from <sup>19</sup>F NMR spectroscopy of the crude mixture. <sup>c</sup>The ratio was estimated from <sup>1</sup>H NMR spectroscopy of the purified mixture of **3q** and **3q'**. <sup>d</sup>The natural populations and ESP maps were calculated by using Gaussian 16 and B3LYP/6-31G(d). **2q** (-0.003000 au (red) to 0.024000 au (blue)) and **2r** (-0.002000 au (red) to 0.034000 au (blue)). Isovalue is 0.005000 au.

The synthetic utility of the site-selective magnesiation reaction can be demonstrated through the synthesis of a fluorine-containing liquid crystal molecule and a drug molecule (Scheme 4-6). 2,5-Difluoro-1,3-dimethoxybenzene (**2t**) was prepared through an aromatic nucleophilic substitution reaction of 1,2,3,5-tetrafluorobenzene (**2s**)

with MeOH,<sup>12b</sup> and then was subjected to the present magnesiation reaction. The less hindered C–F bond was reacted in a site-selective manner to give a fluoroarylmagnesium species, which was successfully transformed to a substructure **3s**, which can be found as a substructure of a liquid crystal molecule,<sup>25</sup> in 66% yield through the Kumada–Tamao–Corriu (KTC) cross-coupling reaction.<sup>26</sup> The magnesiation of **2b** was followed by the Fe-catalyzed cross-coupling reaction<sup>27</sup> with *tert*-butyl 2-bromopropionate gave a synthetic precursor **3t** in 61% yield (without Fe cat. 44%) of flurbiprofen, a nonsteroidal anti-inflammatory drug.<sup>28</sup>

**Scheme 4-6.** Synthetic application: materials and pharmaceuticals.



## Conclusion

In conclusion, the author has developed a site-selective magnesiation of multi-fluorinated arenes catalyzed by Rh–Al bimetallic complexes to prepare fluorinated arylmagnesium reactants, which allow rapid access to various fluoroarenes through diverse transformations of the Grignard reagents. It is worth mentioning that the catalyst could precisely recognize the steric and electronic environments of fluoroarene substrates to control the reaction site.

## Experimental section

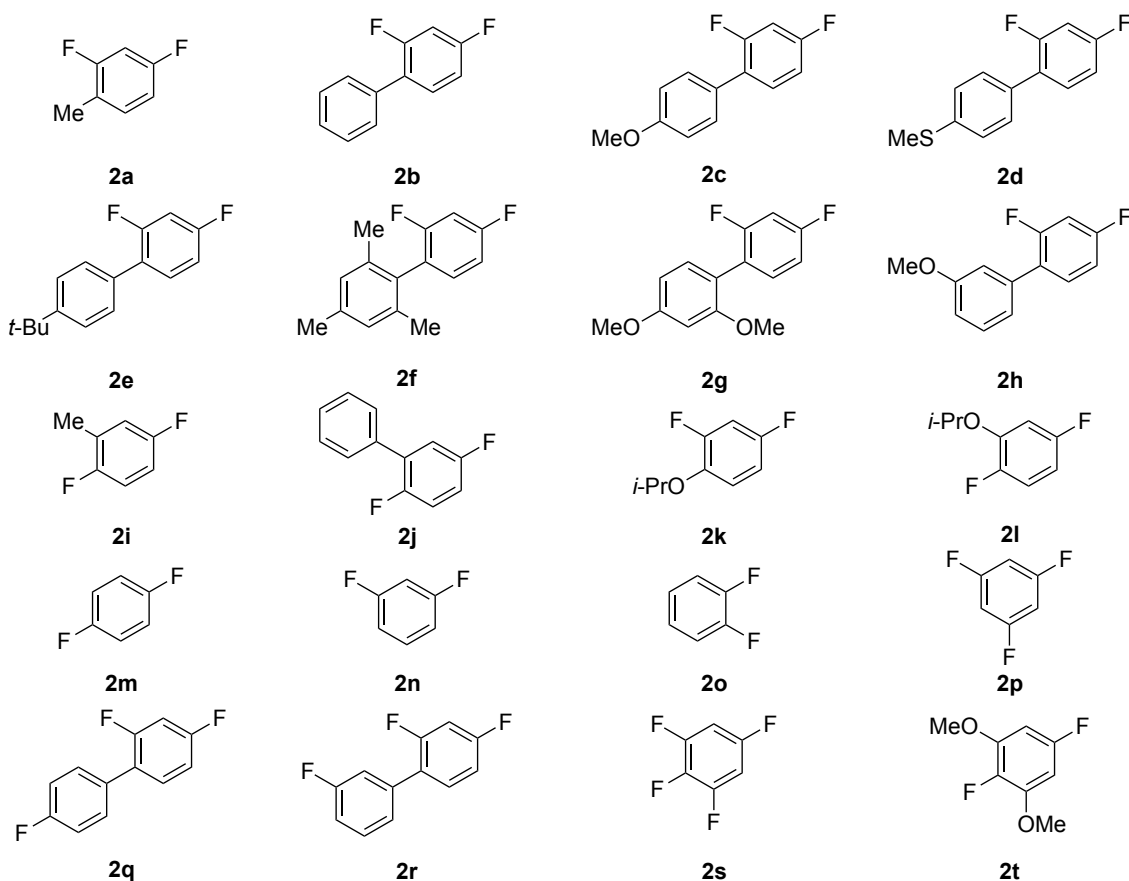


**Figure S4-1.** A list of aryl fluorides in this study.



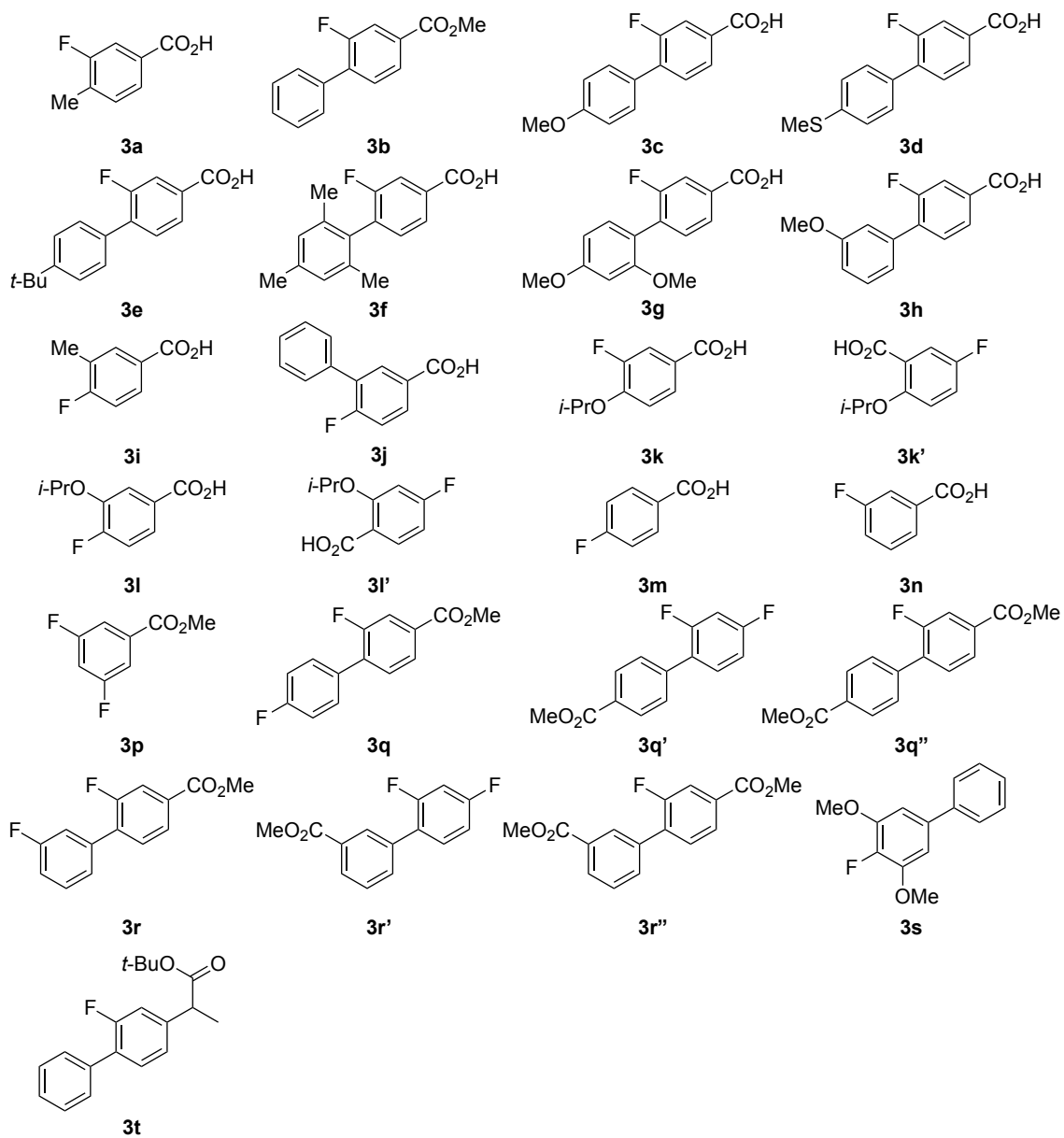
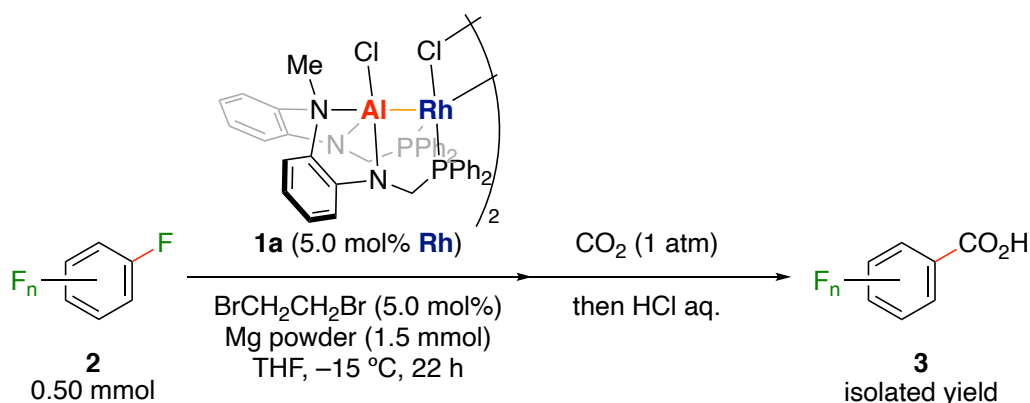
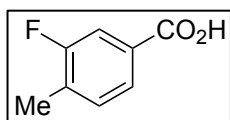


Figure S4-2. A list of products in this study.

## General procedure for Scheme 4-4.

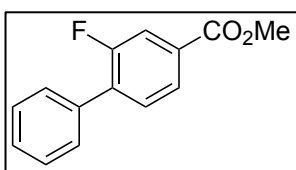


In a glove box, a 4 mL vial with a stirring bar was charged with magnesium powder (37 mg, 1.5 mmol, 3.0 eq.), THF (500  $\mu$ L), and 1,2-dibromoethane (4.7 mg, 25  $\mu$ mol, 5.0 mol%), and the resulting mixture was stirred for 20 min at room temperature. Aryl fluoride **2** (0.50 mmol, 1.0 eq.), **1a** (20 mg, 13  $\mu$ mol, 5.0 mol% of Rh), and THF (1.0 mL) were put into the vial. The mixture was stirred for 22 h at -15 °C and then, the resulting mixture was stirred under atmospheric pressure of CO<sub>2</sub> at room temperature for 20 min. To the mixture, 3 M HCl aq. (1.0 mL) was added. The mixture was extracted with EtOAc (4.0 mL) x 3 and combined organic layers were washed with H<sub>2</sub>O. All volatiles were removed in vacuo and the residue was purified by MPLC using Biotage<sup>®</sup> Sfar Silica High Capacity Duo to obtain the corresponding product **3**.

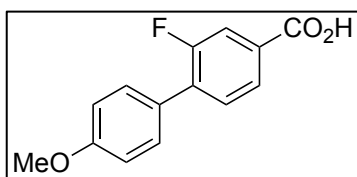


**3-Fuoro-4-toluic acid (3a):** The reaction of 2,4-difluorotoluene (**2a**, 64 mg, 0.50 mmol) was followed by being stirred under atmospheric pressure of CO<sub>2</sub>. After MPLC purification [silica gel, *n*-hexane/EtOAc (4:1 to 3:2 gradient)], the title compound (60 mg, 0.39 mmol, 78%) was obtained as a colorless solid.  $R_f$  0.42 [*n*-hexane/EtOAc (4:3)]. <sup>1</sup>H NMR (400 MHz, CDCl<sub>3</sub>):  $\delta$  7.80 (d,  $J$  = 7.7 Hz, 1H),

7.73 (d,  $J = 10.0$  Hz, 1H), 7.29 (t,  $J = 7.4$  Hz, 1H), 2.36 (s, 3H).  $^{13}\text{C}\{^1\text{H}\}$  NMR (101 MHz,  $\text{CDCl}_3$ ):  $\delta$  170.9 (d,  $J = 2.7$  Hz), 161.1 (d,  $J = 246.2$  Hz), 131.9 (d,  $J = 16.9$  Hz), 131.7 (d,  $J = 5.1$  Hz), 128.9 (d,  $J = 7.7$  Hz), 125.9 (d,  $J = 3.5$  Hz), 116.8 (d,  $J = 24.2$  Hz), 15.1 (d,  $J = 4.0$  Hz).  $^{19}\text{F}$  NMR (376 MHz,  $\text{CDCl}_3$ ):  $\delta$  -116.85. All the resonances of  $^1\text{H}$  NMR spectrum was consistent with the reported values.<sup>29</sup>

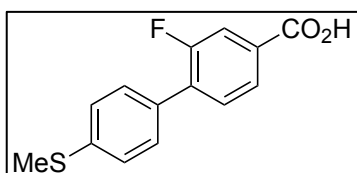


**Methyl 3-fluoro-4-phenylbenzoate (3b):** The reaction of 2,4-difluorobiphenyl (**2b**, 95 mg, 0.50 mmol) was followed by being stirred under atmospheric pressure of  $\text{CO}_2$ . To the mixture, 3 M HCl aq. (6.0 mL) was added. The mixture was extracted with EtOAc (4.0 mL) x 3 and combined organic layers were washed with  $\text{H}_2\text{O}$ . All volatiles were removed in vacuo and the residue was diluted with diethyl ether (4.0 mL) and methanol (2.0 mL). Trimethylsilyl diazomethane was added dropwise into the solution at room temperature until no bubbles appeared for 20 min. After the work-up using acetic acid to consume the residual trimethylsilyl diazomethane,<sup>30</sup> MPLC purification [silica gel, *n*-hexane/EtOAc (4:1)] afforded the title compound (58 mg, 0.25 mmol, 50%) as a colorless solid.  $R_f$  0.69 [*n*-hexane/EtOAc (4:1)].  $^1\text{H}$  NMR (400 MHz,  $\text{CDCl}_3$ ):  $\delta$  7.90 (d,  $J = 8.0$  Hz, 1H), 7.82 (d,  $J = 11.0$  Hz, 1H), 7.58 (d,  $J = 7.7$  Hz, 2H), 7.52 (t,  $J = 8.0$  Hz, 1H), 7.47 (t,  $J = 7.3$  Hz, 2H), 7.44 – 7.37 (m, 1H), 3.95 (s, 3H).  $^{13}\text{C}\{^1\text{H}\}$  NMR (101 MHz,  $\text{CDCl}_3$ ):  $\delta$  166.0 (d,  $J = 2.5$  Hz), 159.5 (d,  $J = 248.7$  Hz), 134.9, 133.8 (d,  $J = 13.0$  Hz), 131.1 (d,  $J = 8.0$  Hz), 130.9 (d,  $J = 3.8$  Hz), 129.1 (d,  $J = 3.3$  Hz), 128.7 (2 peaks were overlapped), 128.5, 125.6 (d,  $J = 3.8$  Hz), 117.5 (d,  $J = 25.2$  Hz), 52.5.  $^{19}\text{F}$  NMR (376 MHz,  $\text{CDCl}_3$ ):  $\delta$  -117.65. m.p. 65 °C. HRMS (APCI)  $m/z$ :  $[\text{M} + \text{H}]^+$  Calcd. for  $\text{C}_{14}\text{H}_{12}\text{F}_1\text{O}_2$  231.0816; Found, 231.0815.



**4-(4-Anisyl)-3-fluorobenzoic acid (3c):** The reaction of 2,4-difluoro-4'-methoxybiphenyl (**2c**, 110 mg, 0.50 mmol) was followed by being stirred under atmospheric pressure

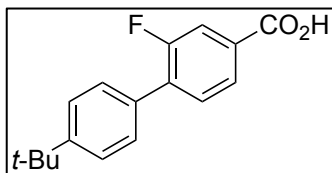
of CO<sub>2</sub>. After MPLC purification [*n*-hexane/EtOAc (4:1 to 3:2 gradient)], the title compound (82 mg, 0.33 mmol, 67%) was obtained as a colorless solid. R<sub>f</sub> 0.41 [*n*-hexane/EtOAc (4:3)]. <sup>1</sup>H NMR (400 MHz, DMSO-*d*<sub>6</sub>): δ 7.82 (d, *J* = 8.0 Hz, 1H), 7.73 (d, *J* = 11.4 Hz, 1H), 7.63 (t, *J* = 7.9 Hz, 1H), 7.55 (d, *J* = 8.0 Hz, 2H), 7.06 (d, *J* = 8.0 Hz, 2H), 3.81 (s, 3H). <sup>13</sup>C{<sup>1</sup>H} NMR (101 MHz, DMSO-*d*<sub>6</sub>): δ 166.1, 159.6, 158.7 (d, *J* = 246.3 Hz), 132.3 (d, *J* = 12.9 Hz), 131.3 (d, *J* = 7.7 Hz), 130.7 (d, *J* = 3.4 Hz), 130.2 (d, *J* = 2.8 Hz), 126.3, 125.7 (d, *J* = 2.3 Hz), 116.7 (d, *J* = 24.3 Hz), 114.3, 55.3. <sup>19</sup>F NMR (376 MHz, DMSO-*d*<sub>6</sub>): δ -117.40. m.p. 198 °C. HRMS (ESI) *m/z*: [M - H]<sup>-</sup> Calcd. for C<sub>14</sub>H<sub>10</sub>F<sub>1</sub>O<sub>3</sub>, 245.0619; Found, 245.0616.



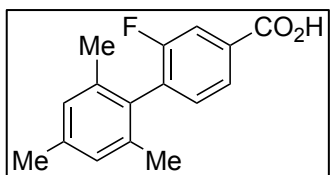
**3-Fluoro-4-(4-thiomethylphenyl)benzoic acid (3d):** The reaction of 2,4-difluoro-4'-thiomethylbiphenyl (**2d**, 118 mg, 0.50 mmol) was followed by being stirred under

atmospheric pressure of CO<sub>2</sub>. After MPLC purification [*n*-hexane/EtOAc (4:1 to 3:2 gradient)], the title compound (101 mg, 0.38 mmol, 77%) was obtained as a colorless solid. R<sub>f</sub> 0.34 [*n*-hexane/EtOAc (4:3)]. <sup>1</sup>H NMR (400 MHz, DMSO-*d*<sub>6</sub>): δ 7.84 (d, *J* = 8.0 Hz, 1H), 7.74 (d, *J* = 11.3 Hz, 1H), 7.65 (t, *J* = 8.0 Hz, 1H), 7.55 (d, *J* = 8.1 Hz, 2H), 7.38 (d, *J* = 8.0 Hz, 2H), 2.52 (s, 3H). <sup>13</sup>C{<sup>1</sup>H} NMR (101 MHz, DMSO-*d*<sub>6</sub>): δ 166.1, 158.8 (d, *J* = 247.3 Hz), 139.3, 132.0 (d, *J* = 12.8 Hz), 131.8 (d, *J* = 7.9 Hz), 130.8 (d, *J* = 3.1 Hz), 130.3, 129.3 (d, *J* = 2.5 Hz), 125.8, 125.8 (d, *J* = 2.4 Hz), 116.7 (d, *J* = 24.3 Hz), 14.4. <sup>19</sup>F NMR (376 MHz, DMSO-*d*<sub>6</sub>): δ -117.12. m.p. 214 °C. HRMS (ESI) *m/z*: [M -

$[H]^-$  Calcd. for  $C_{14}H_{10}F_1O_2S_1$  261.0391; Found, 261.0387.

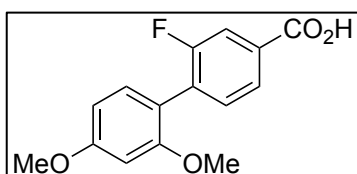


**4-(4-*tert*-Butylphenyl)-3-fluorobenzoic acid (3e):** The reaction of 2,4-difluoro-4'-*tert*-butylbiphenyl (**2e**, 123 mg, 0.50 mmol) was followed by being stirred under atmospheric pressure of  $CO_2$ . After MPLC purification [*n*-hexane/EtOAc (4:1 to 3:2 gradient)], the title compound (105 mg, 0.39 mmol, 77%) was obtained as a colorless solid.  $R_f$  0.50 [*n*-hexane/EtOAc (4:3)].  $^1H$  NMR (400 MHz,  $DMSO-d_6$ ):  $\delta$  7.84 (d,  $J = 8.0$  Hz, 1H), 7.75 (d,  $J = 11.3$  Hz, 1H), 7.66 (t,  $J = 7.9$  Hz, 1H), 7.53 (s, 4H), 1.32 (s, 9H).  $^{13}C\{^1H\}$  NMR (101 MHz,  $DMSO-d_6$ ):  $\delta$  166.1, 158.8 (d,  $J = 247.3$  Hz), 151.2, 132.4 (d,  $J = 12.9$  Hz), 131.8 (d,  $J = 7.6$  Hz), 131.1 (d,  $J = 28.7$  Hz), 131.0, 128.6 (d,  $J = 3.5$  Hz), 125.7 (d,  $J = 3.2$  Hz), 125.6, 116.7 (d,  $J = 24.3$  Hz), 34.4, 31.0.  $^{19}F$  NMR (376 MHz,  $DMSO-d_6$ ):  $\delta$  -117.25. m.p. 257 °C. HRMS (ESI)  $m/z$ :  $[M - H]^-$  Calcd. for  $C_{17}H_{16}F_1O_2$  271.1140; Found, 271.1138.



**3-Fluoro-4-mesitylbenzoic acid (3f):** The reaction of 1-mesityl-2,4-difluorobenzene (**2f**, 116 mg, 0.50 mmol) was followed by being stirred under atmospheric pressure of  $CO_2$ . After MPLC purification [*n*-hexane/EtOAc (4:1 to 3:2 gradient)], the title compound (128 mg, 0.50 mmol, 99%) was obtained as a colorless solid.  $R_f$  0.56 [*n*-hexane/EtOAc (4:3)].  $^1H$  NMR (400 MHz,  $DMSO-d_6$ ):  $\delta$  7.84 (d,  $J = 7.8$  Hz, 1H), 7.76 (d,  $J = 9.8$  Hz, 1H), 7.32 (t,  $J = 7.6$  Hz, 1H), 6.97 (s, 2H), 2.27 (s, 3H), 1.93 (s, 6H).  $^{13}C\{^1H\}$  NMR (101 MHz,  $DMSO-d_6$ ):  $\delta$  166.2 (d,  $J = 2.2$  Hz), 158.8 (d,  $J = 243.5$  Hz), 137.3, 135.5, 132.3 (d,  $J = 7.5$  Hz), 132.2 (d,  $J = 6.9$  Hz), 132.1 (d,  $J = 7.6$  Hz), 131.1, 128.1, 125.5 (d,  $J = 3.4$  Hz),

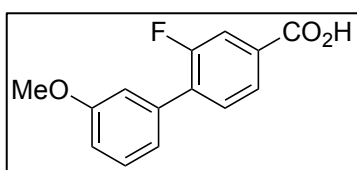
116.2 (d,  $J = 24.1$  Hz), 20.6, 19.9.  $^{19}\text{F}$  NMR (376 MHz,  $\text{DMSO-}d_6$ ):  $\delta -114.27$ . m.p.  $195$  °C. HRMS (ESI)  $m/z$ :  $[\text{M} - \text{H}]^-$  Calcd. for  $\text{C}_{16}\text{H}_{14}\text{F}_1\text{O}_2$  257.0983; Found, 257.0983.



**3-Fluoro-4-(2,4-dimethoxyphenyl)benzoic acid (3g):** The reaction of 2,4-difluoro-2',4'-dimethoxybiphenyl (**2g**, 125 mg, 0.50 mmol) was followed by being stirred under

atmospheric pressure of  $\text{CO}_2$ . After MPLC purification [ $n$ -hexane/EtOAc (4:1 to 3:2 gradient)], the title compound (98 mg, 0.36 mmol, 71%) was obtained as a colorless solid.

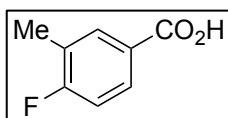
$R_f$  0.23 [ $n$ -hexane/EtOAc (4:3)].  $^1\text{H}$  NMR (400 MHz,  $\text{DMSO-}d_6$ ):  $\delta$  7.78 (d,  $J = 7.9$  Hz, 1H), 7.67 (d,  $J = 10.4$  Hz, 1H), 7.44 (t,  $J = 7.6$  Hz, 1H), 7.18 (d,  $J = 8.4$  Hz, 1H), 6.69 (s, 1H), 6.63 (d,  $J = 8.4$  Hz, 1H), 3.82 (s, 3H), 3.75 (s, 3H).  $^{13}\text{C}\{^1\text{H}\}$  NMR (101 MHz,  $\text{DMSO-}d_6$ ):  $\delta$  166.3 (d,  $J = 2.7$  Hz), 161.2, 159.2 (d,  $J = 246.4$  Hz), 157.6, 132.3 (d,  $J = 3.8$  Hz), 131.5 (d,  $J = 7.4$  Hz), 131.4, 130.5 (d,  $J = 15.9$  Hz), 125.0 (d,  $J = 3.4$  Hz), 116.0, 115.8, 105.3, 98.7, 55.6, 55.4.  $^{19}\text{F}$  NMR (376 MHz,  $\text{DMSO-}d_6$ ):  $\delta -112.97$ . m.p.  $209$  °C. HRMS (ESI)  $m/z$ :  $[\text{M} - \text{H}]^-$  Calcd. for  $\text{C}_{15}\text{H}_{12}\text{F}_1\text{O}_4$ , 275.0725; Found, 275.0725.



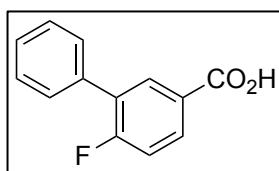
**3-Fluoro-4-(3-anisyl)benzoic acid (3h):** The reaction of 2,4-difluoro-3'-methoxybiphenyl (**2h**, 110 mg, 0.50 mmol) was followed by being stirred under atmospheric pressure

of  $\text{CO}_2$ . After MPLC purification [ $n$ -hexane/EtOAc (4:1 to 3:2 gradient)], the title compound (92 mg, 0.37 mmol, 75%) was obtained as a colorless solid.  $R_f$  0.20 [ $n$ -hexane/EtOAc (4:3)].  $^1\text{H}$  NMR (400 MHz,  $\text{DMSO-}d_6$ ):  $\delta$  7.84 (d,  $J = 8.0$  Hz, 1H), 7.75 (d,  $J = 11.4$  Hz, 1H), 7.68 (t,  $J = 7.9$  Hz, 1H), 7.42 (t,  $J = 7.9$  Hz, 1H), 7.16 (d,  $J = 7.8$  Hz, 1H), 7.13 (s, 1H), 7.03 (d,  $J = 8.4$  Hz, 1H), 3.81 (s, 3H).  $^{13}\text{C}\{^1\text{H}\}$  NMR (101 MHz,

DMSO- $d_6$ ):  $\delta$  166.1 (d,  $J = 2.5$  Hz), 159.4, 158.7 (d,  $J = 247.4$  Hz), 135.5, 132.4 (d,  $J = 13.1$  Hz), 132.1 (d,  $J = 7.5$  Hz), 131.2 (d,  $J = 3.3$  Hz), 129.8, 125.7 (d,  $J = 3.3$  Hz), 121.2 (d,  $J = 2.8$  Hz), 116.7 (d,  $J = 24.2$  Hz), 114.4 (d,  $J = 2.6$  Hz), 114.2, 55.2.  $^{19}\text{F}$  NMR (376 MHz, DMSO- $d_6$ ):  $\delta$  -116.82. m.p. 202 °C. HRMS (ESI)  $m/z$ :  $[\text{M} - \text{H}]^-$  Calcd. for  $\text{C}_{14}\text{H}_{10}\text{F}_1\text{O}_3$  245.0619; Found, 245.0618.



**4-Fluoro-3-toluic acid (3i):** The reaction of 2,5-difluorotoluene (**2i**, 64 mg, 0.50 mmol) was followed by being stirred under atmospheric pressure of  $\text{CO}_2$ . After MPLC purification [ $n$ -hexane/EtOAc (4:1 to 5:4 gradient)], the title compound (52 mg, 0.34 mmol, 67%) was obtained as a white solid.  $R_f$  0.47 [ $n$ -hexane/EtOAc (4:3)].  $^1\text{H}$  NMR (400 MHz, Acetone- $d_6$ ):  $\delta$  7.95 (d,  $J = 7.9$  Hz, 1H), 7.91 (t,  $J = 7.0$  Hz, 1H), 7.18 (t,  $J = 9.0$  Hz, 1H), 2.32 (s, 3H).  $^{13}\text{C}\{^1\text{H}\}$  NMR (101 MHz, Acetone- $d_6$ ):  $\delta$  166.8, 165.1 (d,  $J = 250.1$  Hz), 134.3 (d,  $J = 6.7$  Hz), 130.6 (d,  $J = 9.9$  Hz), 127.7 (d,  $J = 3.4$  Hz), 125.9 (d,  $J = 17.4$  Hz), 115.9 (d,  $J = 23.2$  Hz), 14.3.  $^{19}\text{F}$  NMR (376 MHz, Acetone- $d_6$ ):  $\delta$  -109.93. The resonance of  $^1\text{H}$  spectrum was consistent with the reported values. m.p. 159 °C. HRMS (ESI)  $m/z$ :  $[\text{M} - \text{H}]^-$  Calcd. for  $\text{C}_8\text{H}_6\text{F}_1\text{O}_2$  153.0357; Found, 153.0358.



**4-Fluoro-3-phenylbenzoic acid (3j):** The reaction of 2,5-difluorobiphenyl (**2j**, 95 mg, 0.50 mmol) was followed by being stirred under atmospheric pressure of  $\text{CO}_2$ . After MPLC purification [ $n$ -hexane/EtOAc (4:1 to 3:2 gradient)], the title compound (77 mg, 0.36 mmol, 72%) was obtained as a colorless solid.  $R_f$  0.32 [ $n$ -hexane/EtOAc (4:3)].  $^1\text{H}$  NMR (400 MHz, DMSO- $d_6$ ):  $\delta$  8.04 (d,  $J = 7.7$  Hz, 1H), 8.03–7.95 (m, 1H), 7.57 (d,  $J = 7.6$  Hz,

2H), 7.51 (t,  $J = 7.5$  Hz, 2H), 7.47–7.42 (m, 2H).  $^{13}\text{C}\{^1\text{H}\}$  NMR (101 MHz, DMSO- $d_6$ ):  $\delta$  166.3, 161.8 (d,  $J = 252.7$  Hz), 134.2, 132.1 (d,  $J = 4.8$  Hz), 130.9 (d,  $J = 9.7$  Hz), 128.83, 128.80, 128.5 (d,  $J = 14.2$  Hz), 128.3, 127.7 (d,  $J = 3.3$  Hz), 116.7 (d,  $J = 23.9$  Hz).  $^{19}\text{F}$  NMR (376 MHz, DMSO- $d_6$ ):  $\delta$  -111.81. m.p. 187 °C. HRMS (ESI)  $m/z$ :  $[\text{M} - \text{H}]^-$  Calcd. for  $\text{C}_{13}\text{H}_8\text{F}_1\text{O}_2$  215.0514; Found, 215.0515.

The reaction of 2,4-difluoro-1-*iso*-propoxybenzene (**2k**, 86 mg, 0.50 mmol) was carried out at -20 °C and followed by being stirred under atmospheric pressure of  $\text{CO}_2$ . MPLC purification [*n*-hexane/EtOAc (4:1 to 3:2 gradient)] gave a mixture of isomers **3k** and **3k'** (82 mg, 0.41 mmol, 83%) as a colorless solid. The site-selectivity was estimated based on  $^1\text{H}$  NMR analysis of the crude mixture (**3k**:**3k'** = 1.7:1, **Figure S4-1**).

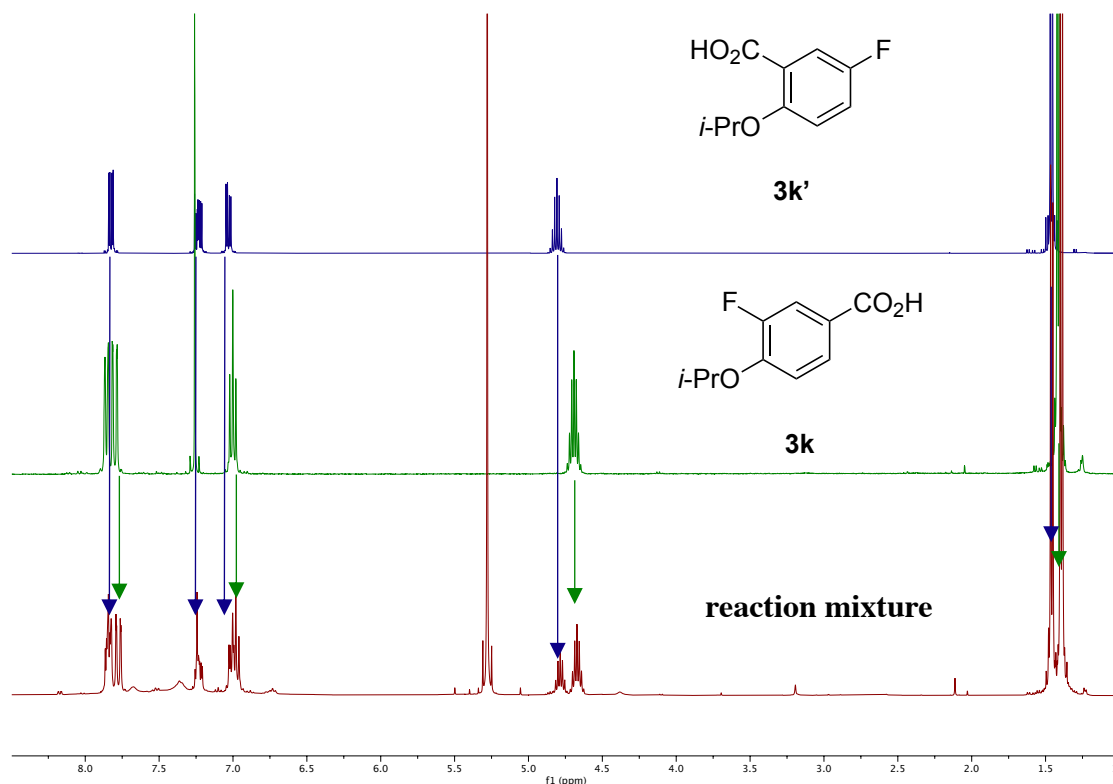
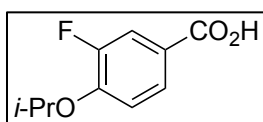
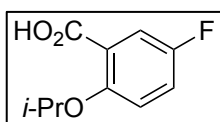


**Figure S4-1.**  $^1\text{H}$  NMR spectrum of the reaction mixture of **2k**.





**3-Fluoro-4-*iso*-propoxybenzoic acid (3k):**  $R_f$  0.40 [*n*-hexane/EtOAc (4:3)].  $^1\text{H}$  NMR (400 MHz,  $\text{CDCl}_3$ ):  $\delta$  7.86 (dd,  $J = 8.2, 1.5$  Hz, 1H), 7.80 (dd,  $J = 11.8, 2.1$  Hz, 1H), 7.00 (t,  $J = 8.2$  Hz, 1H), 4.69 (hept,  $J = 6.0$  Hz, 1H), 1.41 (d,  $J = 5.9$  Hz, 6H).  $^{13}\text{C}\{^1\text{H}\}$  NMR (101 MHz,  $\text{CDCl}_3$ ):  $\delta$  170.7, 152.5 (d,  $J = 262.4$  Hz), 151.2 (d,  $J = 26.7$  Hz), 127.5 (d,  $J = 3.0$  Hz), 121.7 (d,  $J = 4.1$  Hz), 118.3 (d,  $J = 20.2$  Hz), 115.0, 72.1, 22.0.  $^{19}\text{F}$  NMR (376 MHz,  $\text{CDCl}_3$ ):  $\delta$  -133.41. colorless solid. m.p. 168 °C. HRMS (ESI)  $m/z$ :  $[\text{M} - \text{H}]^-$  Calcd. for  $\text{C}_{10}\text{H}_{10}\text{F}_1\text{O}_3$  197.0619; Found, 197.0620.



**5-Fluoro-2-*iso*-propoxybenzoic acid (3k'):**  $R_f$  0.53 [*n*-hexane/EtOAc (4:3)].  $^1\text{H}$  NMR (400 MHz,  $\text{CDCl}_3$ ):  $\delta$  11.23 (br s, 1H), 7.83 (dd,  $J = 8.7, 3.3$  Hz, 1H), 7.24 (ddd,  $J = 9.1, 7.3, 3.4$  Hz, 1H), 7.03 (dd,  $J = 9.1, 4.1$  Hz, 1H), 4.81 (hept,  $J = 6.1$  Hz, 1H), 1.46 (d,  $J = 6.1$  Hz, 6H).  $^{13}\text{C}\{^1\text{H}\}$  NMR (101 MHz,  $\text{CDCl}_3$ ):  $\delta$  164.5 (d,  $J = 1.9$  Hz), 157.2 (d,  $J = 242.6$  Hz), 152.6 (d,  $J = 2.8$  Hz), 121.8 (d,  $J = 23.9$  Hz), 120.2 (d,  $J = 6.9$  Hz), 119.6 (d,  $J = 24.4$  Hz), 116.1 (d,  $J = 7.5$  Hz), 75.1, 22.0.  $^{19}\text{F}$  NMR (376 MHz,  $\text{CDCl}_3$ ):  $\delta$  -120.47. colorless solid. m.p. 59 °C. HRMS (ESI)  $m/z$ :  $[\text{M} - \text{H}]^-$  Calcd. for  $\text{C}_{10}\text{H}_{10}\text{F}_1\text{O}_3$  197.0619; Found, 197.0619.

The reaction of 2,5-difluoro-1-*iso*-propoxybenzene (**2l**, 86 mg, 0.50 mmol) was carried out at -20 °C and followed by being stirred under atmospheric pressure of  $\text{CO}_2$ . MPLC purification [*n*-hexane/EtOAc (4:1 to 3:2 gradient)] gave a mixture of isomers **3l** and **3l'** (68 mg, 0.34 mmol, 69%) as a colorless solid. The site-selectivity was estimated based on  $^1\text{H}$  NMR analysis of the crude mixture (**3l**:**3l'** = 11:1, **Figure S4-2**).

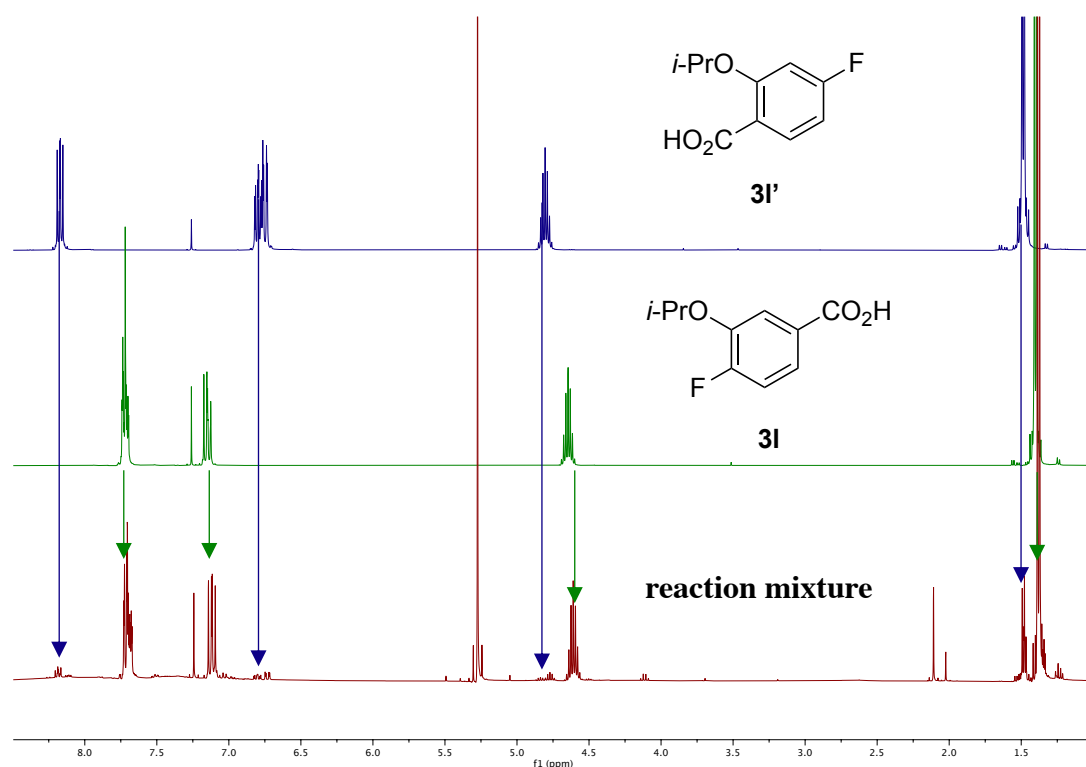
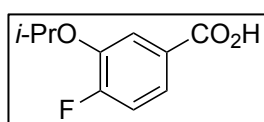
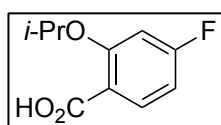


**Figure S4-2.**  $^1\text{H}$  NMR spectrum of the reaction mixture of **2I**.



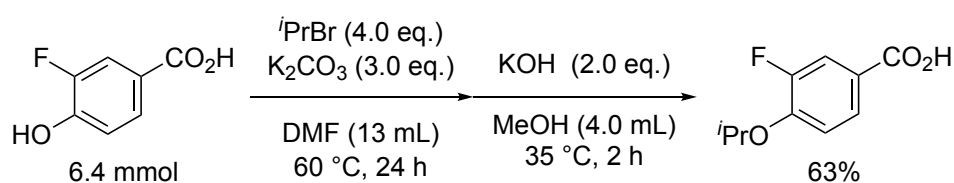
**4-Fluoro-3-iso-propoxybenzoic acid (3I):**  $R_f$  0.39 [*n*-hexane/EtOAc (4:3)].  $^1\text{H}$  NMR (400 MHz,  $\text{CDCl}_3$ ):  $\delta$  7.75–7.69 (m, 2H), 7.15 (dd,  $J = 10.7, 8.7$  Hz, 1H), 4.65 (hept,  $J = 6.0$  Hz, 1H), 1.40 (d,  $J = 6.2$  Hz, 6H).  $^{13}\text{C}\{^1\text{H}\}$  NMR (101 MHz,  $\text{CDCl}_3$ ):  $\delta$  171.7, 157.4 (d,  $J = 255.1$  Hz), 146.1 (d,  $J = 11.4$  Hz), 125.7 (d,  $J = 3.0$  Hz), 124.2 (d,  $J = 8.1$  Hz), 118.7 (d,  $J = 3.6$  Hz), 116.6 (d,  $J = 20.0$  Hz), 72.5, 22.0.  $^{19}\text{F}$  NMR (376 MHz,  $\text{CDCl}_3$ ):  $\delta$  -124.59. colorless solid. m.p. 135 °C. HRMS (ESI)  $m/z$ :  $[\text{M} - \text{H}]^-$  Calcd. for  $\text{C}_{10}\text{H}_{10}\text{F}_1\text{O}_3$  197.0619; Found, 197.0619.



**4-Fluoro-2-iso-propoxybenzoic acid (3I')**:  $R_f$  0.42 [*n*-hexane/EtOAc (4:3)].  $^1\text{H}$  NMR (400 MHz,  $\text{CDCl}_3$ ):  $\delta$  10.94 (br, 1H), 8.17 (dd,  $J = 8.8, 6.9$  Hz, 1H), 6.80 (ddd,  $J = 8.8, 7.6, 2.3$  Hz, 1H), 6.75 (dd,  $J = 10.3, 2.3$  Hz, 1H), 4.80

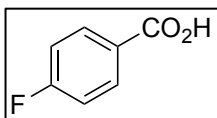
(hept,  $J = 6.1$  Hz, 1H), 1.49 (d,  $J = 6.1$  Hz, 6H).  $^{13}\text{C}\{^1\text{H}\}$  NMR (101 MHz,  $\text{CDCl}_3$ ):  $\delta$  166.6 (d,  $J = 255.6$  Hz), 164.8, 158.0 (d,  $J = 10.8$  Hz), 136.0 (d,  $J = 11.3$  Hz), 114.9 (d,  $J = 2.9$  Hz), 109.5 (d,  $J = 21.4$  Hz), 102.0 (d,  $J = 26.1$  Hz), 74.7, 22.0.  $^{19}\text{F}$  NMR (376 MHz,  $\text{CDCl}_3$ ):  $\delta$  -101.73. colorless solid. m.p. 81 °C. HRMS (ESI)  $m/z$ :  $[\text{M} - \text{H}]^-$  Calcd. for  $\text{C}_{10}\text{H}_{10}\text{F}_1\text{O}_3$  197.0619; Found, 197.0620.

### Synthesis of authentic samples.<sup>31,32</sup>

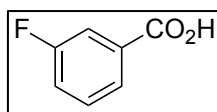


To a stirred suspension of 3-fluoro-4-hydroxybenzoic acid (1.0 g, 6.4 mmol) and  $\text{K}_2\text{CO}_3$  (2.7 g, 19 mmol) in anhydrous DMF (13 mL) was added 2-bromopropane (3.1 g, 26 mmol) dropwise at room temperature under nitrogen atmosphere. After the addition was completed, the suspension was stirred at 60 °C for 24 h. After the reaction, the mixture was cooled to room temperature, quenched with 10 mL water, and then evaporated to dryness. The resulting residue were reacted with KOH (0.72 g, 13 mmol) in MeOH (4.0 mL) at 35 °C for 2 h. After the reaction, the mixture was cooled to room temperature and evaporated to dryness. To the reaction mixture was added water (10 mL) followed by 3 M HCl aq. to acidify to pH = 1. The organic layer was extracted with  $\text{Et}_2\text{O}$  (5.0 mL) x 3 and combined organic layers were washed with  $\text{H}_2\text{O}$  followed by brine, and dried over anhydrous  $\text{MgSO}_4$ . Insoluble materials were filtered off and the filtrate was evaporated to dryness to afford **3k** as a colorless solid (0.80 g, 4.0 mmol, 63%). Other authentic samples **3k'**, **3l**, and **3l'** were also synthesized using the above procedure [**3k'**

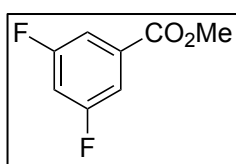
(1.1 g, 5.4 mmol, 84%), **3I** (0.90 g, 4.6 mmol, 71%), **3I'** (1.1 g, 5.3 mmol, 83%)].



**4-Fluorobenzoic acid (3m):** The reaction of 1,4-difluorobenzene (**2m**, 57 mg, 0.50 mmol) was followed by being stirred under atmospheric pressure of CO<sub>2</sub>. After MPLC purification [*n*-hexane/EtOAc (4:1 to 3:2 gradient)], the title compound (60 mg, 0.43 mmol, 86%) was obtained as a colorless solid. R<sub>f</sub> 0.34 [*n*-hexane/EtOAc (4:3)]. <sup>1</sup>H NMR (400 MHz, CDCl<sub>3</sub>): δ 8.14 (t, *J* = 6.8 Hz, 2H), 7.15 (t, *J* = 8.4 Hz, 2H). <sup>13</sup>C {<sup>1</sup>H} NMR (101 MHz, CDCl<sub>3</sub>): δ 171.3, 166.5 (d, *J* = 254.9 Hz), 133.1 (d, *J* = 9.4 Hz), 125.6 (d, *J* = 2.6 Hz), 115.9 (d, *J* = 22.1 Hz). <sup>19</sup>F NMR (376 MHz, CDCl<sub>3</sub>): δ -104.52. All the resonances of <sup>1</sup>H and <sup>13</sup>C NMR spectra were consistent with the reported values.<sup>33,34</sup>

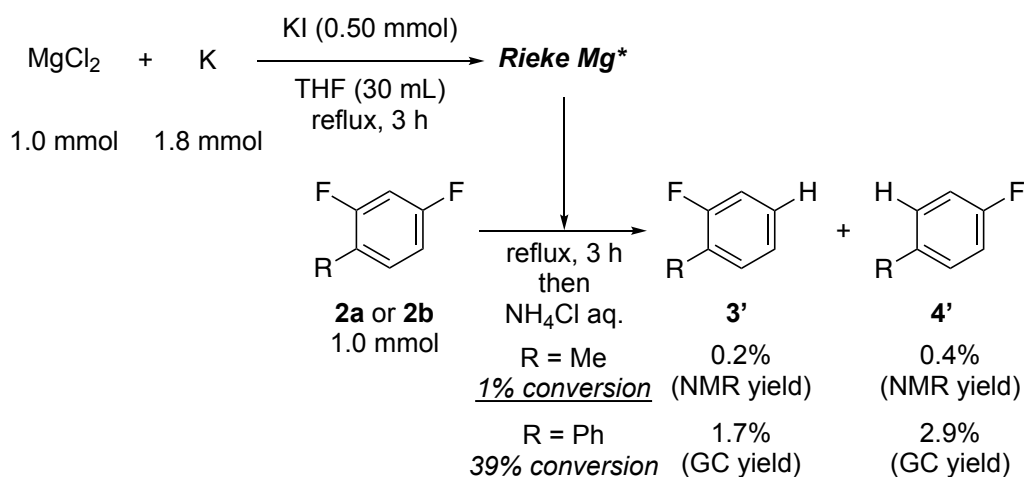


**3-Fluorobenzoic acid (3n):** The reaction of 1,3-difluorobenzene (**2n**, 57 mg, 0.50 mmol) was followed by being stirred under atmospheric pressure of CO<sub>2</sub>. After MPLC purification [*n*-hexane/EtOAc (4:1 to 3:2 gradient)], the title compound (63 mg, 0.45 mmol, 90%) was obtained as a colorless solid. R<sub>f</sub> 0.37 [*n*-hexane/EtOAc (4:3)]. <sup>1</sup>H NMR (400 MHz, CDCl<sub>3</sub>): δ 7.92 (d, *J* = 7.7 Hz, 1H), 7.80 (d, *J* = 9.2 Hz, 1H), 7.47 (q, *J* = 7.4 Hz, 1H), 7.33 (t, *J* = 8.4 Hz, 1H). <sup>13</sup>C {<sup>1</sup>H} NMR (101 MHz, CDCl<sub>3</sub>): δ 171.2, 162.7 (d, *J* = 247.4 Hz), 131.5 (d, *J* = 7.2 Hz), 130.4 (d, *J* = 7.9 Hz), 126.1 (d, *J* = 3.3 Hz), 121.2 (d, *J* = 21.3 Hz), 117.2 (d, *J* = 23.1 Hz). <sup>19</sup>F NMR (376 MHz, CDCl<sub>3</sub>): δ -112.48. All the resonances of <sup>1</sup>H and <sup>13</sup>C NMR spectra were consistent with the reported values.<sup>35</sup>



**Methyl 3,5-difluorobenzoate (3p):** The reaction of 1,3,5-trifluorobenzene (**2p**, 66 mg, 0.50 mmol) was followed by being stirred under atmospheric pressure of CO<sub>2</sub>. To the mixture, 3 M HCl aq. (6.0 mL) was added. The mixture was extracted with EtOAc (4.0 mL) x 3 and combined organic layers were washed with H<sub>2</sub>O. All volatiles were removed in vacuo and the residue was diluted with diethyl ether (4.0 mL) and methanol (2.0 mL). Trimethylsilyl diazomethane was added dropwise into the solution of the residue at room temperature until no bubbles appeared for 20 min. Acetic acid was added to consume the residual trimethylsilyl diazomethane.<sup>30</sup> After MPLC purification [silica gel, *n*-hexane/EtOAc (5:1)], the title compound (52 mg, 0.30 mmol, 60%) was obtained as a colorless liquid. *R*<sub>f</sub> 0.71 [*n*-hexane/EtOAc (4:1)]. <sup>1</sup>H NMR (400 MHz, CDCl<sub>3</sub>): δ 7.48 (br s, 2H), 6.95 (br s, 1H), 3.88 (s, 3H). <sup>13</sup>C {<sup>1</sup>H} NMR (101 MHz, CDCl<sub>3</sub>): δ 164.8 (br s), 162.9 (dd, *J* = 250.0, 11.9 Hz), 133.5 (t, *J* = 9.1 Hz), 112.6 (dd, *J* = 24.1, 9.2 Hz), 108.3 (t, *J* = 25.4 Hz), 52.6 (br s). <sup>19</sup>F NMR (376 MHz, CDCl<sub>3</sub>): δ -109.07. All the resonances of <sup>1</sup>H, <sup>13</sup>C and <sup>19</sup>F NMR spectra were consistent with the reported values.<sup>36</sup>

**Rieke magnesium conditions (Eq. 4-1).**<sup>23</sup>



Freshly cut potassium (70 mg, 1.8 mmol, 1.8 eq.), MgCl<sub>2</sub> (95 mg, 1.0 mmol, 1.0 eq.), KI (83 mg, 0.50 mmol, 0.50 eq.), and THF (30 ml) were placed in an oven-dried 80 mL Schlenk flask equipped with a condenser, a magnetic stirring bar, and N<sub>2</sub> atmosphere. After the mixture was stirred and heated to reflux for 3 h to ensure complete reaction of potassium, the mixture was then cooled to rt for 30 min. Aryl fluorides **2a** or **2b** were added into the dark grey Rieke Mg suspension. After refluxing for 3 h, the resulting mixture was quenched by sat. NH<sub>4</sub>Cl aqueous solution.

### 1. 2,4-Difluorotoluene (**2a**, R = Me).

The yields of products were estimated based on <sup>19</sup>F NMR analysis of a crude product (internal standard: C<sub>6</sub>F<sub>6</sub>). 2-Fluorotoluene (**3a'**) and 4-fluorotoluene (**4a'**) were observed in 0.2% and 0.4% yield, respectively (**3a'**:**4a'** = 1:2, **Figure S4-3**). 99% of starting material **2a** was recovered.

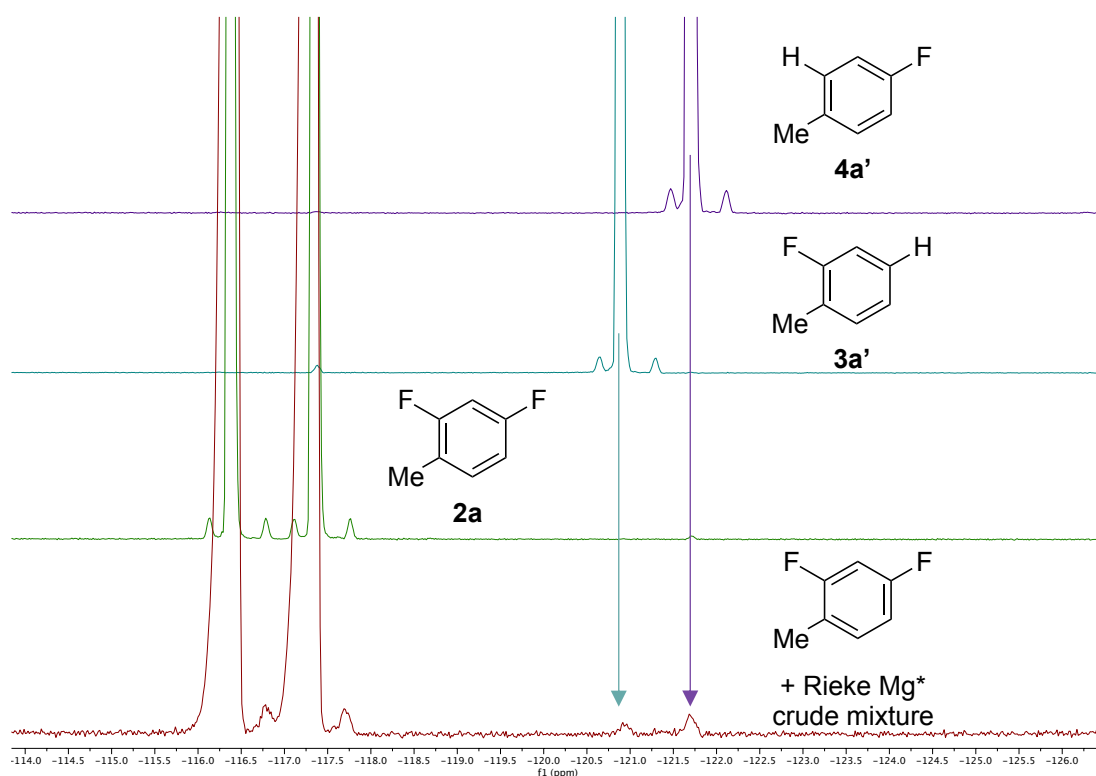


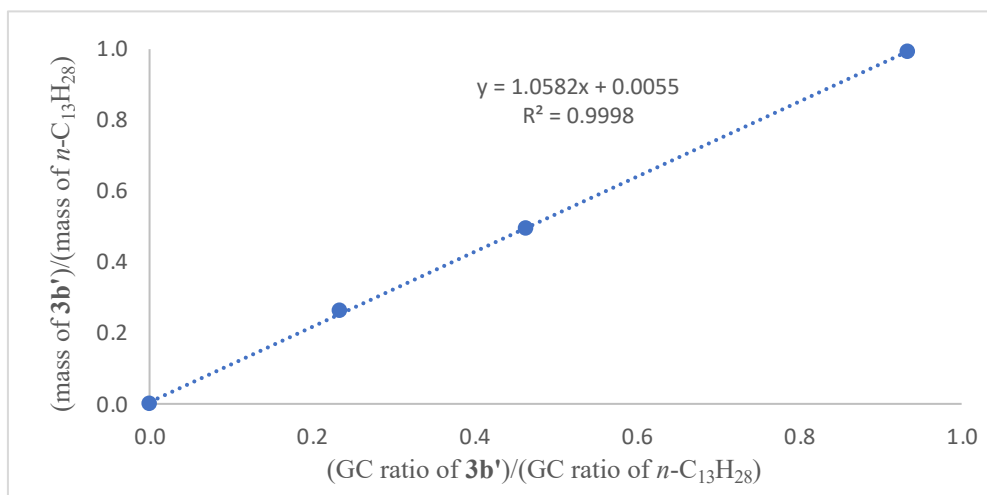
**Figure S4-3.**  $^{19}\text{F}$  NMR spectra of the reaction mixture of **2a** and Rieke Mg.

## 2. 2,4-Difluorobiphenyl (**2b**, R = Ph).

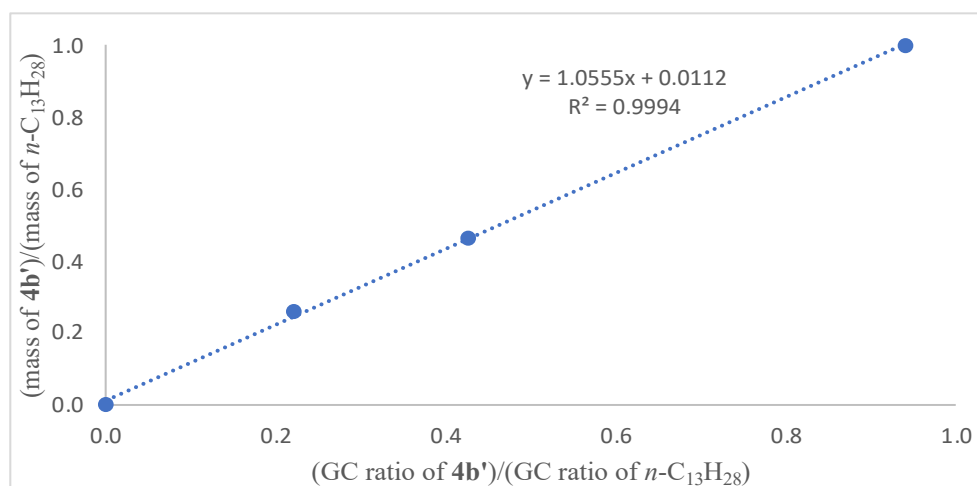
The yields of products were estimated by gas chromatography analysis (internal standard:  $\text{C}_{13}\text{H}_{28}$ ). 2-Fluorobiphenyl (**3b'**) and 4-fluorobiphenyl (**4b'**) were obtained in 1.7% and 2.9% yield, respectively (**3b'**:**4b'** = 37:63). 61% of starting material **2b** was recovered.

**Table S4-1.** Data for the GC calibration curve to determine yield of 2-fluorobiphenyl (**3b'**)

entry	mass (mg)		$y = \frac{\text{mmol of } \mathbf{3b'}}{\text{mmol of } C_{13}H_{28}}$	GC ratio		$x = \frac{\text{GC ratio of } \mathbf{3b'}}{\text{GC ratio of } C_{13}H_{28}}$
	<b>3b'</b>	$C_{13}H_{28}$		<b>3b'</b>	$C_{13}H_{28}$	
0	0	0	0	0	0	0
1	24.3	99.8	0.26068	18.996	81.004	0.23451
2	45.5	98.3	0.49555	31.630	68.370	0.46263
3	98.6	106.5	0.99120	48.276	51.724	0.93334

**Table S4-2.** Data for the GC calibration curve to determine yield of 4-fluorobiphenyl (**4b'**)

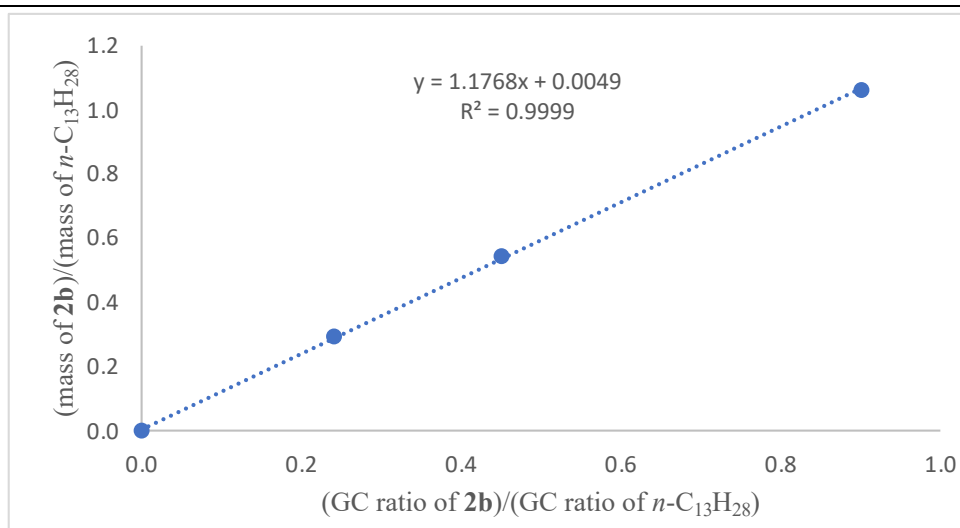
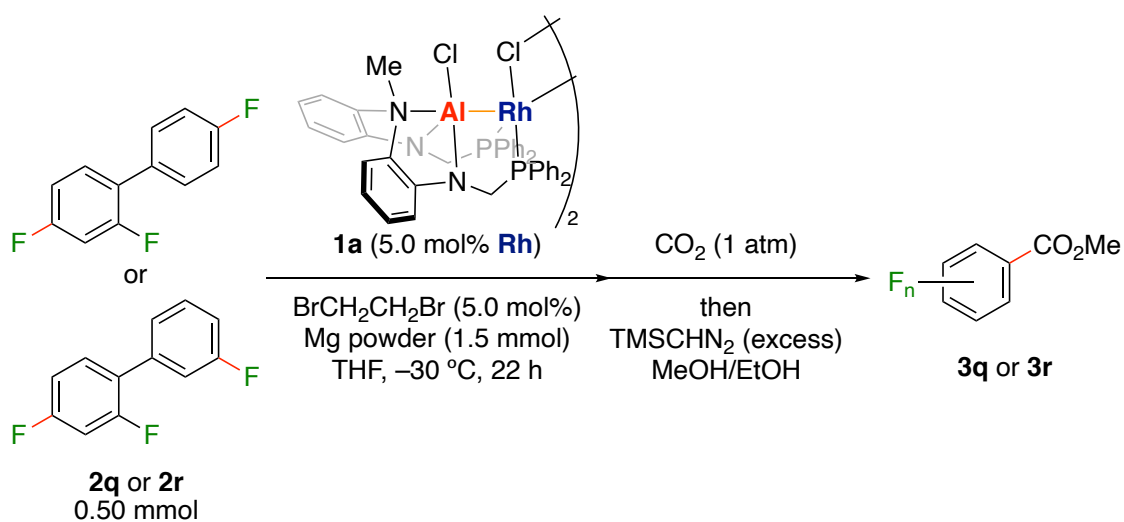
entry	mass (mg)		$y = \frac{\text{mmol of } \mathbf{4b'}}{\text{mmol of } C_{13}H_{28}}$	GC ratio		$x = \frac{\text{GC ratio of } \mathbf{4b'}}{\text{GC ratio of } C_{13}H_{28}}$
	<b>4b'</b>	$C_{13}H_{28}$		<b>4b'</b>	$C_{13}H_{28}$	
0	0	0	0	0	0	0
1	45.5	188.8	0.25801	18.107	81.893	0.22110
2	85.6	198.0	0.46285	29.889	70.111	0.42631
3	176.1	188.7	0.99913	48.446	51.554	0.93971





**Table S4-3.** Data for the GC calibration curve to determine yield of 2,4-difluorobiphenyl (**2b**)

entry	mass (mg)		$y = \frac{\text{mmol of } \mathbf{2b}}{\text{mmol of } C_{13}H_{28}}$	GC ratio		$x = \frac{\text{GC ratio of } \mathbf{2b}}{\text{GC ratio of } C_{13}H_{28}}$
	<b>2b</b>	$C_{13}H_{28}$		<b>2b</b>	$C_{13}H_{28}$	
0	0	0	0	0	0	0
1	50.5	184.9	0.29241	19.483	80.517	0.24198
2	95.4	188.3	0.54241	31.115	68.885	0.45170
3	192.9	194.3	1.06290	47.427	52.573	0.90212

**General procedure for Scheme 4-5.**

In a glove box, a 4 mL vial with a stirring bar was charged with magnesium powder (37 mg, 1.5 mmol, 3.0 eq.), THF (500  $\mu\text{L}$ ), and 1,2-dibromoethane (4.7 mg, 25

$\mu\text{mol}$ , 5.0 mol%), and the resulting mixture was stirred for 20 min at room temperature. Trifluorobiphenyl **2q** or **2r** (104 mg, 0.50 mmol, 1.0 eq.), **1a** (20 mg, 13  $\mu\text{mol}$ , 5.0 mol% of Rh), and THF (1.0 mL) were put into the vial. The mixture was stirred for 22 h at  $-30$   $^{\circ}\text{C}$  and then, the resulting mixture was stirred under atmospheric pressure of  $\text{CO}_2$  at room temperature for 20 min. To the mixture, 3 M HCl aq. (6.0 mL) was added. The mixture was extracted with EtOAc (4.0 mL) x 3 and combined organic layers were washed with  $\text{H}_2\text{O}$ . All volatiles were removed in vacuo and the residue was diluted with diethyl ether (6.0 mL) and methanol (2.0 mL). Trimethylsilyl diazomethane was added dropwise into the solution of the residue at room temperature until no bubbles appeared for 20 min. After addition of acetic acid to consume the residual trimethylsilyl diazomethane,<sup>30</sup> all volatiles were removed in vacuo and the residue was purified by MPLC using Biotage<sup>®</sup> Sfär Silica High Capacity Duo to obtain the corresponding product **3q** (**3q'** and **3q''**) or **3r** (**3r'** and **3r''**).

**Reaction of 2q:** MPLC purification [*n*-hexane/EtOAc (4:1 to 3:2 gradient)] gave a mixture of isomers **3q** and **3q'** (72 mg, 0.29 mmol, 58%, **3q:3q'** = 6.2:1) as a colorless solid (Figure S4-4). The dicarboxylated product **3q''** was isolated in 17% (25 mg, 0.087 mmol) as a colorless solid.

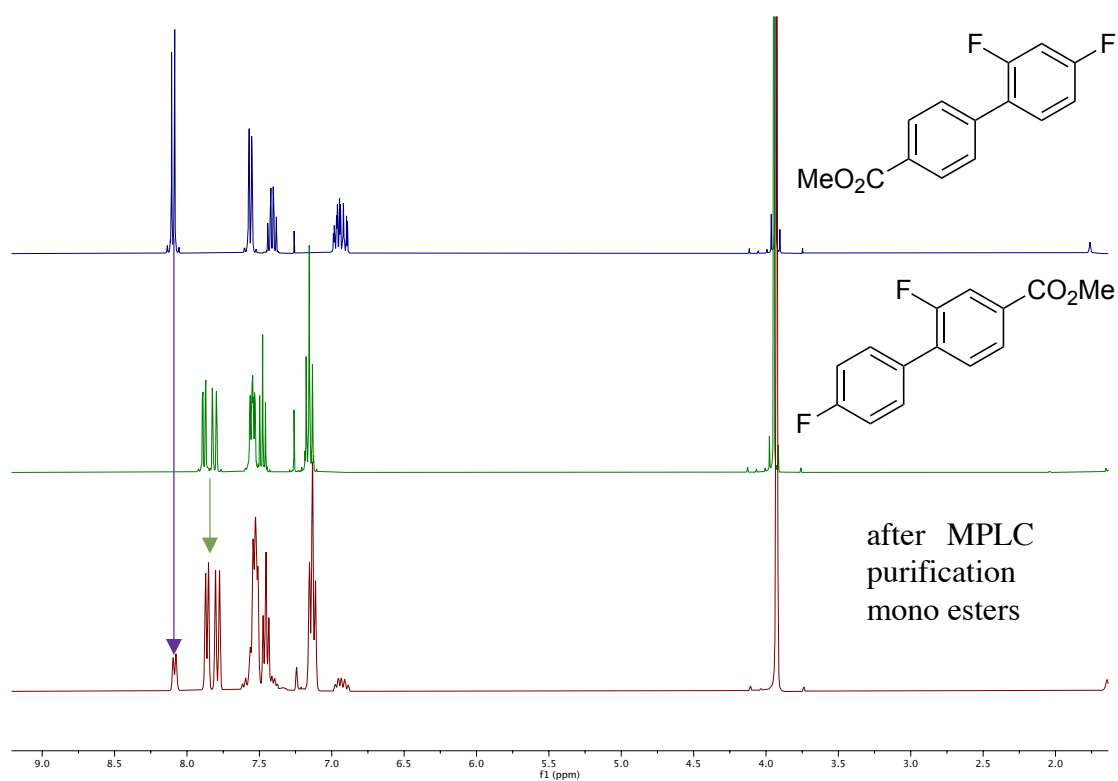


**Figure S4-4.**  $^1\text{H}$  NMR spectra of a mixture of isomers **3q** and **3q'** and the authentic samples.

The site-selectivity before isolation was estimated as  $\mathbf{3q:3q':3q''} = 67:6:27$  from  $^{19}\text{F}$  NMR spectrum of the crude mixture (Figure S4-5).

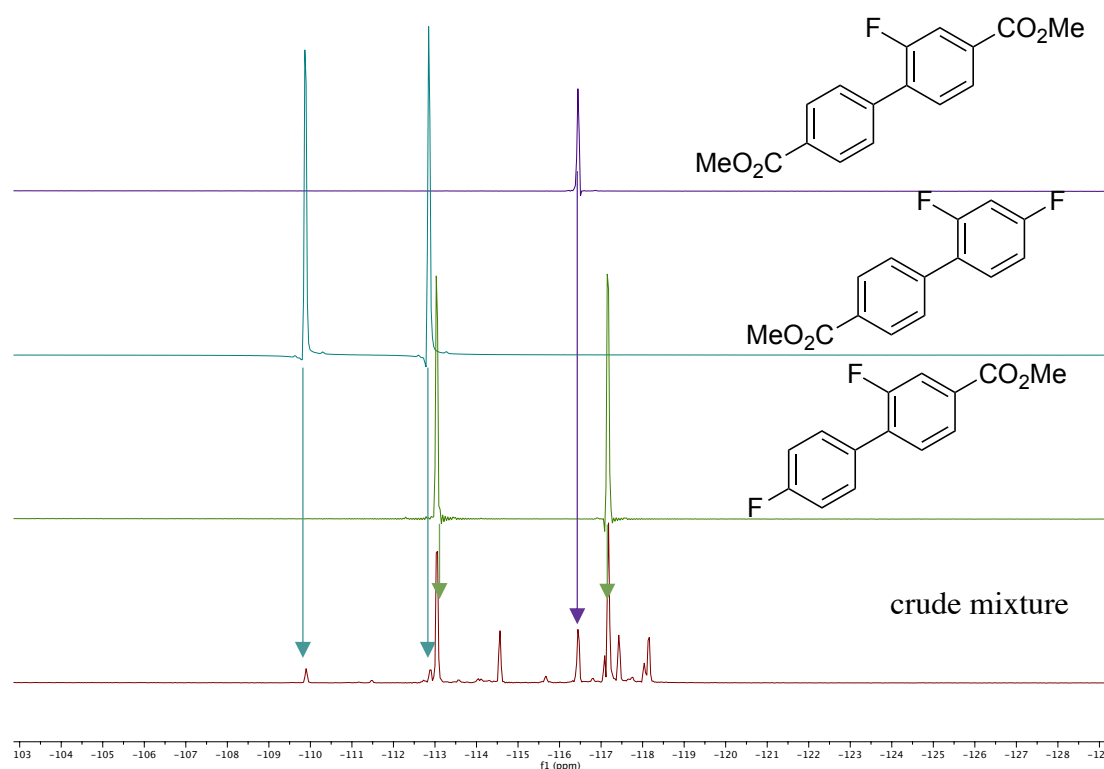
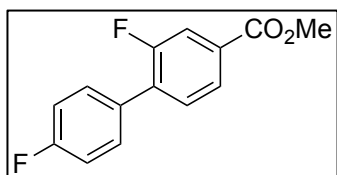


**Figure S4-5.**  $^{19}\text{F}$  NMR spectra of the reaction mixture of **2q** and the authentic samples.



**Methyl 2,4'-difluorobiphenyl-4-carboxylate (3q):**  $R_f$  0.68

[*n*-hexane/EtOAc (4:1)].  $^1\text{H}$  NMR (400 MHz,  $\text{CDCl}_3$ ):  $\delta$  7.88

(dd,  $J = 7.8, 1.7$  Hz, 1H), 7.81 (dd,  $J = 11.0, 1.7$  Hz, 1H), 7.55

(ddd,  $J = 8.9, 5.2, 1.8$  Hz, 2H), 7.48 (t,  $J = 7.9$  Hz, 1H), 7.24–7.10 (m, 2H), 3.95 (s, 3H).

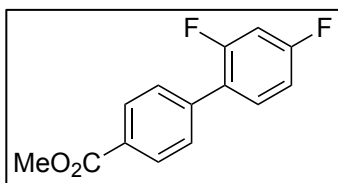
$^{13}\text{C}\{^1\text{H}\}$  NMR (101 MHz,  $\text{CDCl}_3$ ):  $\delta$  166.0 (d,  $J = 2.7$  Hz), 163.0 (d,  $J = 248.3$  Hz), 159.4

(d,  $J = 248.6$  Hz), 132.7 (d,  $J = 13.5$  Hz), 131.1 (d,  $J = 7.9$  Hz), 131.0 (d,  $J = 3.2$  Hz),

130.9, 130.7 (d,  $J = 3.4$  Hz), 125.7 (d,  $J = 3.7$  Hz), 117.5 (d,  $J = 25.0$  Hz), 115.8 (d,  $J =$

21.3 Hz), 52.6.  $^{19}\text{F}$  NMR (376 MHz,  $\text{CDCl}_3$ ):  $\delta$  -113.62, -117.74. colorless solid. m.p.

84 °C. HRMS (APCI)  $m/z$ :  $[\text{M} + \text{H}]^+$  Calcd. for  $\text{C}_{14}\text{H}_{11}\text{F}_2\text{O}_2$  249.0722; Found, 249.0721.



**Methyl 2',4'-difluorobiphenyl-4-carboxylate (3q')**:  $R_f$

0.68 [*n*-hexane/EtOAc (4:1)].  $^1\text{H NMR}$  (400 MHz,  $\text{CDCl}_3$ ):

$\delta$  8.10 (d,  $J = 8.6$  Hz, 2H), 7.56 (dd,  $J = 8.3, 1.8$  Hz, 2H), 7.41

(td,  $J = 8.7, 6.4$  Hz, 1H), 7.02–6.86 (m, 2H), 3.93 (s, 3H).  $^{13}\text{C}\{^1\text{H}\}$  NMR (101 MHz,

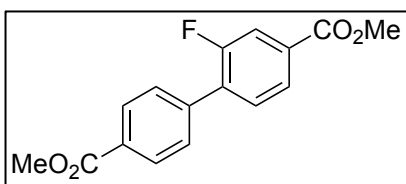
$\text{CDCl}_3$ ):  $\delta$  166.9, 162.8 (dd,  $J = 250.2, 11.6$  Hz), 159.9 (dd,  $J = 251.7, 11.8$  Hz), 139.6,

131.5 (dd,  $J = 9.6, 4.8$  Hz), 129.9, 129.4, 129.0 (d,  $J = 3.0$  Hz), 124.4 (dd,  $J = 13.4, 3.9$

Hz), 111.9 (dd,  $J = 21.4, 3.9$  Hz), 104.7 (t,  $J = 25.9$  Hz), 52.3.  $^{19}\text{F NMR}$  (376 MHz,

$\text{CDCl}_3$ ):  $\delta$  -110.42, -113.40. colorless solid. m.p. 92 °C. HRMS (APCI)  $m/z$ :  $[\text{M} + \text{H}]^+$

Calcd. for  $\text{C}_{14}\text{H}_{11}\text{F}_2\text{O}_2$  249.0722; Found, 249.0721.



**Dimethyl 2-fluorobiphenyl-4,4'-dicarboxylate**

**(3q'')**:  $R_f$  0.50 [*n*-hexane/EtOAc (4:1)].  $^1\text{H NMR}$  (400

MHz,  $\text{CDCl}_3$ ):  $\delta$  8.13 (dt,  $J = 8.0, 1.5$  Hz, 2H), 7.91 (dd,

$J = 8.0, 1.7$  Hz, 1H), 7.83 (dd,  $J = 11.0, 1.7$  Hz, 1H), 7.65 (dd,  $J = 8.3, 1.8$  Hz, 2H), 7.53

(t,  $J = 7.8$  Hz, 1H), 3.95 (s, 3H), 3.95 (s, 3H).  $^{13}\text{C}\{^1\text{H}\}$  NMR (101 MHz,  $\text{CDCl}_3$ ):  $\delta$  166.8,

165.8 (d,  $J = 2.7$  Hz), 159.5 (d,  $J = 250.2$  Hz), 139.4, 132.6 (d,  $J = 13.4$  Hz), 131.8 (d,  $J$

$= 7.7$  Hz), 130.8 (d,  $J = 3.4$  Hz), 130.1, 129.9, 129.2 (d,  $J = 3.5$  Hz), 125.8 (d,  $J = 3.7$  Hz),

117.6 (d,  $J = 24.7$  Hz), 52.6, 52.4.  $^{19}\text{F NMR}$  (376 MHz,  $\text{CDCl}_3$ ):  $\delta$  -117.07. colorless solid.

m.p. 140 °C. HRMS (APCI)  $m/z$ :  $[\text{M} + \text{H}]^+$  Calcd. for  $\text{C}_{16}\text{H}_{14}\text{F}_1\text{O}_4$  289.0871; Found,

289.0872.

**Reaction of 2r**: MPLC purification [*n*-hexane/EtOAc (4:1 to 3:2 gradient)] and HPLC

[*n*-hexane/EtOAc (98:2)] gave **3r** (37 mg, 0.15 mmol, 30%), **3r'** (2.3 mg, 0.010 mmol,

2%), and **3r''** (3.7 mg, 0.013 mmol, 3%) as a colorless solid.

The site-selectivity was estimated as  $3r:3r':3r'' = 83:13:4$  from  $^{19}\text{F}$  NMR spectrum of the crude mixture (Figure S4-6).

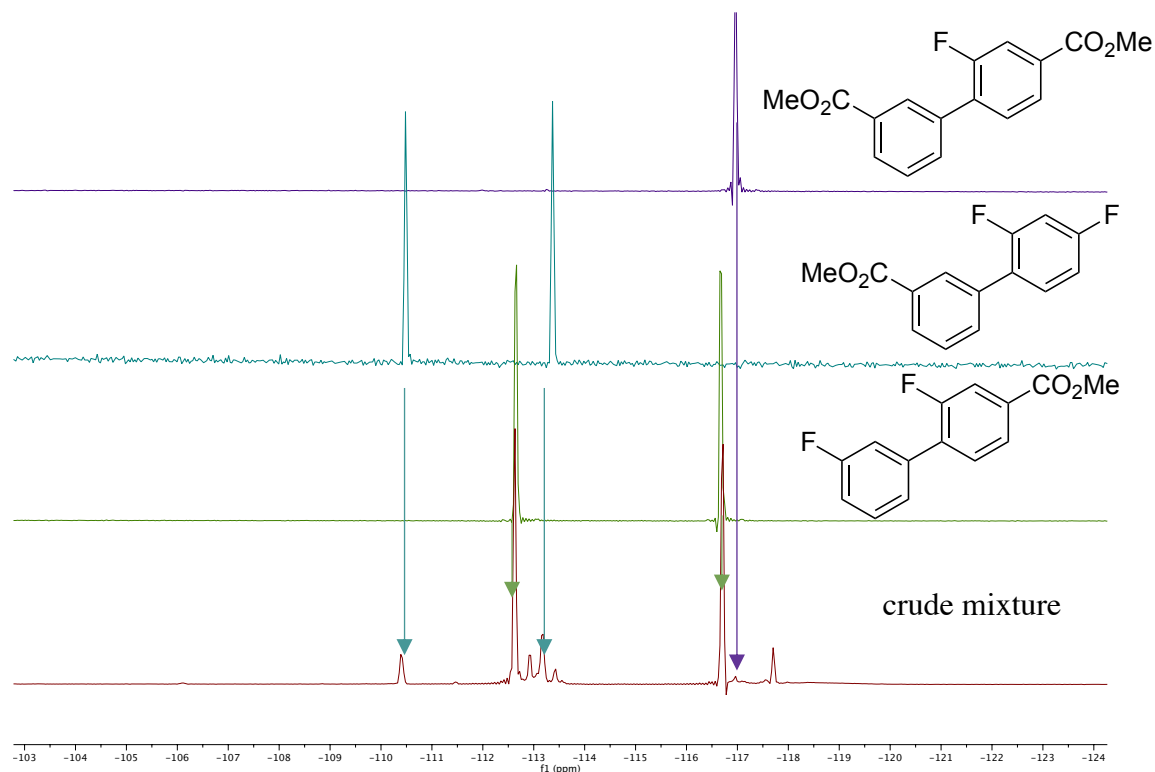
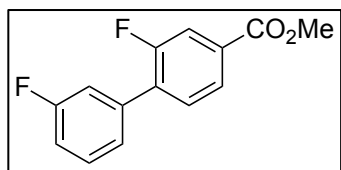


**Figure S4-6.**  $^{19}\text{F}$  NMR spectra of the reaction mixture of **2r** and the authentic samples.



**Methyl 2,3'-difluorobiphenyl-4-carboxylate (3r):**  $R_f$  0.65

[*n*-hexane/EtOAc (4:1)].  $^1\text{H}$  NMR (400 MHz,  $\text{CDCl}_3$ ):  $\delta$  7.89

(dd,  $J = 8.2, 1.8$  Hz, 1H), 7.82 (dd,  $J = 11.0, 1.8$  Hz, 1H), 7.51

(t,  $J = 7.8$  Hz, 1H), 7.43 (td,  $J = 8.0, 5.6$  Hz, 1H), 7.35 (dq,  $J = 7.6, 1.5$  Hz, 1H), 7.29 (ddt,

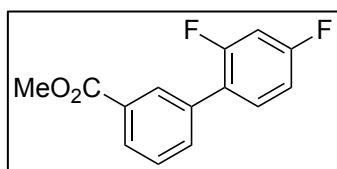
$J = 10.0, 3.0, 1.8$  Hz, 1H), 7.11 (tdd,  $J = 8.4, 2.7, 1.2$  Hz, 1H), 3.95 (s, 3H).  $^{13}\text{C}\{^1\text{H}\}$  NMR

(101 MHz,  $\text{CDCl}_3$ ):  $\delta$  165.9 (d,  $J = 2.3$  Hz), 162.9 (d,  $J = 246.2$  Hz), 159.5 (d,  $J = 249.9$

Hz), 136.9 (d,  $J = 7.8$  Hz), 132.5 (dd,  $J = 13.3, 1.9$  Hz), 131.7 (d,  $J = 7.7$  Hz), 130.7 (d,  $J$

$= 3.1$  Hz), 130.3 (d,  $J = 8.1$  Hz), 125.8 (d,  $J = 3.7$  Hz), 124.9 (dd,  $J = 3.8, 1.9$  Hz), 117.6

(d,  $J = 24.4$  Hz), 116.2 (dd,  $J = 22.9, 3.7$  Hz), 115.5 (d,  $J = 21.1$  Hz), 52.6.  $^{19}\text{F}$  NMR (376 MHz,  $\text{CDCl}_3$ ):  $\delta -113.25, -117.31$ . colorless solid. m.p.  $60$  °C. HRMS (APCI)  $m/z$ :  $[\text{M} + \text{H}]^+$  Calcd. for  $\text{C}_{14}\text{H}_{11}\text{F}_2\text{O}_2$  249.0722; Found, 249.0721.



**Methyl 2',4'-difluorobiphenyl-3-carboxylate (3r')**:  $R_f$

0.68 [*n*-hexane/EtOAc (4:1)].  $^1\text{H}$  NMR (400 MHz,  $\text{CDCl}_3$ ):

$\delta$  8.17 (s, 1H), 8.05 (d,  $J = 7.9$  Hz, 1H), 7.70 (d,  $J = 7.8$  Hz,

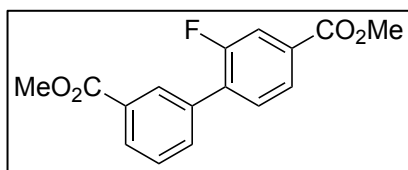
1H), 7.52 (t,  $J = 7.8$  Hz, 1H), 7.43 (q,  $J = 7.9$  Hz, 1H), 7.02–6.88 (m, 2H), 3.94 (s, 3H).

$^{13}\text{C}\{^1\text{H}\}$  NMR (101 MHz,  $\text{CDCl}_3$ ):  $\delta$  166.9, 162.7 (dd,  $J = 249.7, 12.0$  Hz), 159.9 (dd,  $J = 250.9, 12.1$  Hz), 135.4, 133.5 (d,  $J = 3.4$  Hz), 131.6 (dd,  $J = 9.6, 4.8$  Hz), 130.7, 130.1

(d,  $J = 2.1$  Hz), 129.0, 128.7, 124.5 (dd,  $J = 13.8, 4.2$  Hz), 111.9 (dd,  $J = 21.1, 3.8$  Hz),

104.6 (t,  $J = 25.9$  Hz), 52.4.  $^{19}\text{F}$  NMR (376 MHz,  $\text{CDCl}_3$ ):  $\delta -111.01, -113.99$ . colorless

solid. m.p.  $66$  °C. HRMS (APCI)  $m/z$ :  $[\text{M} + \text{H}]^+$  Calcd. for  $\text{C}_{14}\text{H}_{11}\text{F}_2\text{O}_2$  249.0722; Found, 249.0721.



**Dimethyl 2-fluorobiphenyl-3',4-dicarboxylate (3r'')**:

$R_f$  0.53 [*n*-hexane/EtOAc (4:1)].  $^1\text{H}$  NMR (400 MHz,

$\text{CDCl}_3$ ):  $\delta$  8.24 (q,  $J = 1.6$  Hz, 1H), 8.09 (dt,  $J = 7.8, 1.5$

Hz, 1H), 7.91 (dd,  $J = 8.2, 1.7$  Hz, 1H), 7.83 (dd,  $J = 11.0, 1.8$  Hz, 1H), 7.78 (dq,  $J = 7.9,$

1.5 Hz, 1H), 7.55 (td,  $J = 7.8, 1.7$  Hz, 2H), 3.95 (s, 3H), 3.95 (s, 3H).  $^{13}\text{C}\{^1\text{H}\}$  NMR (101

MHz,  $\text{CDCl}_3$ ):  $\delta$  166.9, 165.9 (d,  $J = 2.7$  Hz), 159.5 (d,  $J = 249.6$  Hz), 135.2, 133.6 (d,  $J$

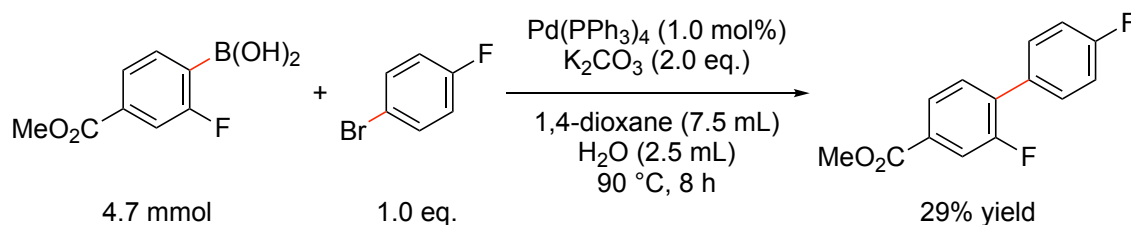
$= 4.0$  Hz), 132.7 (d,  $J = 13.5$  Hz), 131.6 (d,  $J = 7.5$  Hz), 130.9, 130.8, 130.2, 129.7, 128.9,

125.8 (d,  $J = 3.3$  Hz), 117.6 (d,  $J = 24.6$  Hz), 52.6, 52.5.  $^{19}\text{F}$  NMR (376 MHz,  $\text{CDCl}_3$ ):  $\delta$

$-117.58$ . colorless solid. m.p.  $99$  °C. HRMS (APCI)  $m/z$ :  $[\text{M} + \text{H}]^+$  Calcd. for  $\text{C}_{16}\text{H}_{14}\text{F}_1\text{O}_4$

289.0871; Found, 289.0872.

### Synthesis of authentic samples.



A 15 mL vial was charged with 1-bromo-4-fluorobenzene (0.81 g, 4.7 mmol, 1.0 eq.), 2-fluoro-4-methoxycarbonylphenylboronic acid (0.92 g, 4.7 mmol, 1.0 eq.), Pd(PPh<sub>3</sub>)<sub>4</sub> (54 mg, 47 μmol, 1.0 mol%) and K<sub>2</sub>CO<sub>3</sub> (1.3 g, 9.4 mmol, 2.0 eq.). Subsequently, 1,4-dioxane (7.5 mL) and H<sub>2</sub>O (2.5 mL) were introduced into the reaction vessel under N<sub>2</sub> atmosphere. The reaction mixture was stirred at 90 °C for 8 h. After completion of the reaction, it was allowed to cool to room temperature. The residue was purified by MPLC [*n*-hexane/EtOAc (4:1)] on silica gel to give the **3q** (0.34 g, 1.4 mmol, 29%) as a colorless solid. Other authentic samples **3q'**, **3q''**, **3r**, **3r'**, and **3r''** were also synthesized using the above procedure.

**3q'**: The reaction of methyl 4-bromobenzoate (1.0 g, 4.7 mmol, 1.0 eq.) and 2,4-difluorophenylboronic acid (0.88 g, 5.6 mmol, 1.2 eq.) gave **3q'** (1.1 g, 4.4 mmol, 94%) as a colorless solid.

**3q''**: The reaction of 2-fluoro-4-methoxycarbonylphenylboronic acid (0.92 g, 4.7 mmol, 1.0 eq.) and methyl 4-bromobenzoate (1.1 g, 4.9 mmol, 1.1 eq.) gave **3q''** (1.1 g, 3.7 mmol, 80%) as a colorless solid.

**3r**: The reaction of 1-bromo-3-fluorobenzene (0.82 g, 4.7 mmol, 1.0 eq.) and 2-fluoro-4-



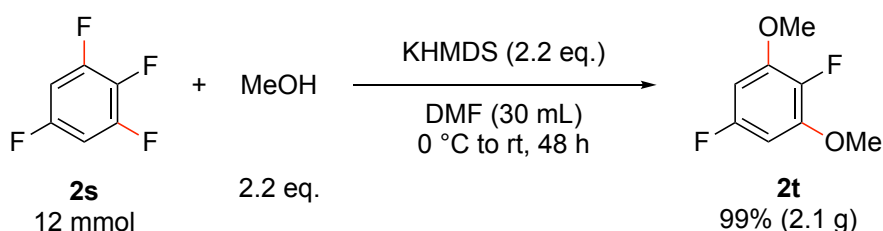
methoxycarbonylphenylboronic acid (0.92 g, 4.7 mmol, 1.0 eq.) gave **3r** (0.41 g, 1.7 mmol, 36%) as a colorless solid.

**3r'**: The reaction of methyl 3-bromobenzoate (1.0 g, 4.7 mmol, 1.0 eq.) and 2,4-difluorophenylboronic acid (0.88 g, 5.6 mmol, 1.2 eq.) gave **3r'** (1.1 g, 4.4 mmol, 96%) as a colorless solid.

**3r''**: The reaction of 2-fluoro-4-methoxycarbonylphenylboronic acid (0.92 g, 4.7 mmol, 1.0 eq.) and methyl 3-bromobenzoate (1.1 g, 4.9 mmol, 1.1 eq.) gave **3r''** (0.89 g, 3.1 mmol, 66%) as a colorless solid.

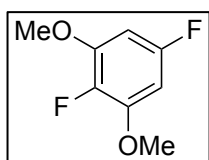
### General procedure for Scheme 4-6.

#### 1-1. Aromatic nucleophilic substitution of 1,2,3,5-tetrafluorobenzene.<sup>12b</sup>



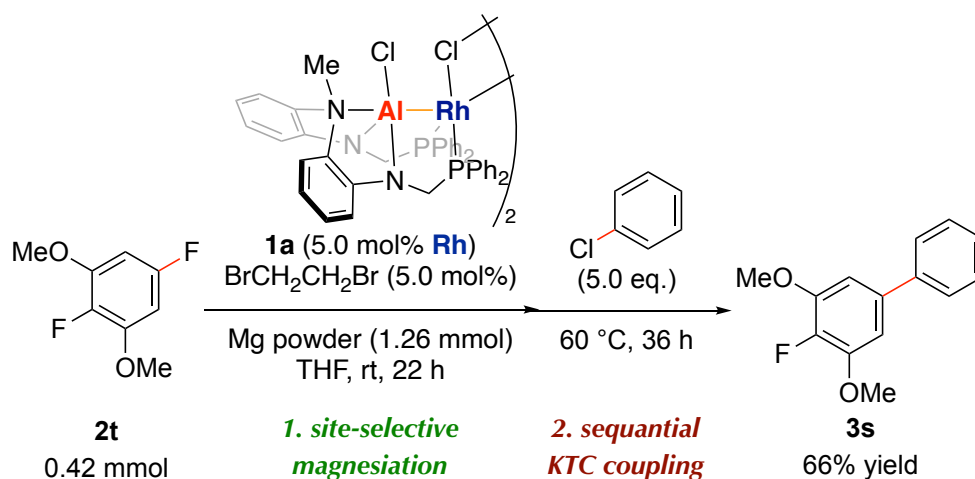
To a solution of methanol (0.85 g, 27 mmol) and 1,2,3,5-tetrafluorobenzene (**2s**, 1.8 g, 12 mmol) in anhydrous DMF (30 mL) at 0 °C, was added anhydrous KHMDS (27 mmol, 1.0 M in THF, 2.2 eq.) dropwise. The reaction was allowed to warm to room temperature, stirred for 48 h, and then quenched with sat. aq. NaHCO<sub>3</sub> (2.0 mL). The solvent was removed in vacuo and the residue was suspended in EtOAc (15 mL) and brine (5.0 mL), and the phases were separated. The aqueous phase was further extracted with EtOAc (15 mL). The combined organic phases were dried over Na<sub>2</sub>SO<sub>4</sub> and concentrated to afford the crude material. The residue was purified by MPLC on silica gel [*n*-hexane/EtOAc (99:1)] to give 2,5-difluoro-1,3-dimethoxybenzene (**2t**) in 99%

yield (2.1 g, 12 mmol) as a pale yellow solid.



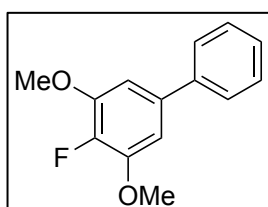
**2,5-Difluoro-1,3-dimethoxybenzene (2t):**  $R_f$  0.51 [*n*-hexane/EtOAc (95:5)].  $^1\text{H}$  NMR (400 MHz,  $\text{CDCl}_3$ ):  $\delta$  6.34 (dd,  $J = 10.1, 6.0$  Hz, 2H), 3.86 (s, 6H).  $^{13}\text{C}\{^1\text{H}\}$  NMR (101 MHz,  $\text{CDCl}_3$ ):  $\delta$  158.7 (dd,  $J = 240.6, 3.8$  Hz), 148.9 (dd,  $J = 12.4, 9.7$  Hz), 139.4 (dd,  $J = 239.5, 4.7$  Hz), 93.7 (d,  $J = 27.7$  Hz), 56.7.  $^{19}\text{F}$  NMR (376 MHz,  $\text{CDCl}_3$ ):  $\delta$  -115.70, -164.97. pale yellow solid. m.p. 95 °C. HRMS (APCI)  $m/z$ :  $[\text{M} + \text{H}]^+$  Calcd. for  $\text{C}_8\text{H}_9\text{F}_2\text{O}_2$  175.0565; Found, 175.0566.

### 1-2. Site-selective magnesiation and Kumada–Tamao–Corriu cross-coupling.



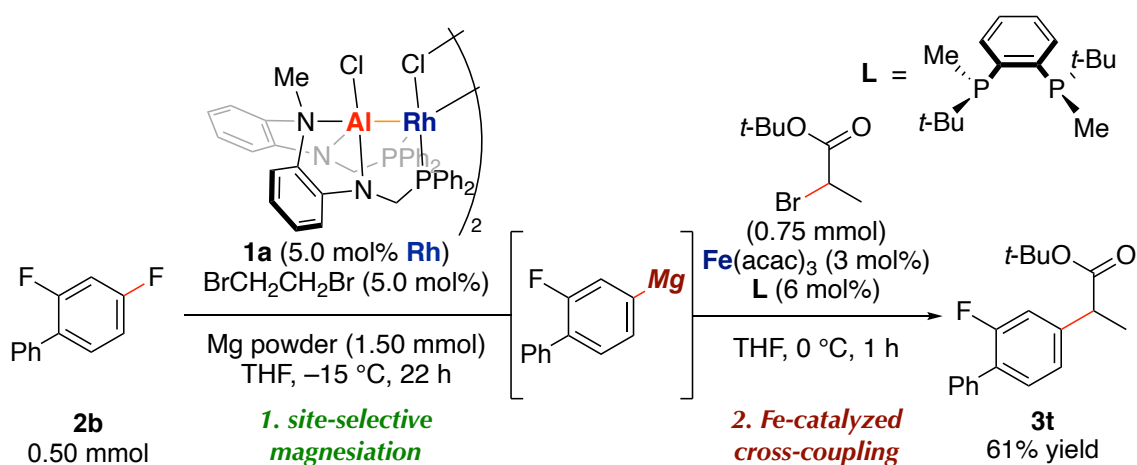
In a glove box, a 4 mL vial with a stirring bar was charged with magnesium powder (31 mg, 1.3 mmol, 3.0 eq.), THF (500  $\mu\text{L}$ ), and 1,2-dibromoethane (4.0 mg, 21  $\mu\text{mol}$ , 5.0 mol%), and the resulting mixture was stirred for 20 min at room temperature. **1a** (17 mg, 11  $\mu\text{mol}$ , 5.0 mol% of Rh) and THF (1.0 mL) were added to the vial followed by **2t** (73 mg, 0.42 mmol, 1.0 eq.). The mixture was stirred for 22 h at rt to generate the corresponding arylmagnesium. Insoluble solids of the resulting mixture were filtered off

through the Pasteur pipette filter, which is filled with a glass fiber filter (GB-100R ADVANTEC®), with THF (1.0 mL). The obtained filtrate was put into another 4 mL vial with a stirring bar and chlorobenzene (236 mg, 2.1 mmol, 5.0 eq.). The reaction mixture was stirred at 60 °C for 36 h. To the mixture, 3 M HCl aq. (2.0 mL) was carefully added. The organic layer was separated. The remained aqueous layer was extracted with EtOAc (4.0 mL) x 3. All volatiles were removed in vacuo and the residue was purified by MPLC using Biotage® Sfär Silica High Capacity Duo [*n*-hexane/EtOAc (100:0 to 95:5 gradient)] to obtain the title compound **3s** (64 mg, 0.28 mmol, 66%) as a colorless solid.



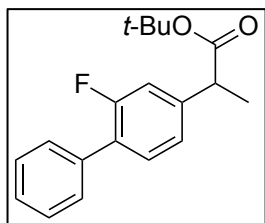
**3,5-Dimethoxy-4-difluorobiphenyl (3s):**  $R_f$  0.76 [*n*-hexane:EtOAc (9:1)].  $^1\text{H}$  NMR (400 MHz,  $\text{CDCl}_3$ ):  $\delta$  7.55 (d,  $J = 7.7$  Hz, 2H), 7.45 (t,  $J = 7.5$  Hz, 2H), 7.37 (t,  $J = 7.3$  Hz, 1H), 6.81 (dd,  $J = 7.2, 1.8$  Hz, 2H), 3.95 (s, 6H).  $^{13}\text{C}$  { $^1\text{H}$ } NMR (101 MHz,  $\text{CDCl}_3$ ):  $\delta$  148.6 (d,  $J = 8.5$  Hz), 142.4 (d,  $J = 244.9$  Hz), 141.0, 137.1 (d,  $J = 4.8$  Hz), 128.9, 127.6, 127.2, 105.2, 56.7.  $^{19}\text{F}$  NMR (376 MHz,  $\text{CDCl}_3$ ):  $\delta$  -155.07. colorless solid. m.p. 77 °C. HRMS (APCI)  $m/z$ :  $[\text{M} + \text{H}]^+$  Calcd. for  $\text{C}_{14}\text{H}_{14}\text{F}_2\text{O}_2$  233.0972; Found, 233.0971.

## 2. Site-selective magnesiation and Fe-catalyzed cross-coupling reaction.



In a glove box, a 4 mL vial with a stirring bar was charged with magnesium powder (37 mg, 1.5 mmol, 3.0 eq.), THF (500  $\mu$ L), and 1,2-dibromoethane (4.7 mg, 25  $\mu$ mol, 5.0 mol%), and the resulting mixture was stirred for 20 min at room temperature. **1a** (20 mg, 13  $\mu$ mol, 5.0 mol% of Rh) and THF (1.0 mL) followed by **2b** (95 mg, 0.50 mmol, 1.0 eq.) were added to the vial. The mixture was stirred for 22 h at room temperature to generate the corresponding arylmagnesium. Insoluble solids of the resulting mixture were filtered off through the Pasteur pipette filter, which is filled with a glass fiber filter (GB-100R ADVANTEC<sup>®</sup>), with THF (1.0 mL). The obtained filtrate was slowly added over 60 min using a syringe into a THF solution (1.0 mL) of Fe(acac)<sub>3</sub> (5.3 mg, 15  $\mu$ mol, 3.0 mol%), (*R,R*)-(+)-1,2-bis(*tert*-butylmethylphosphino)benzene (8.5 mg, 30  $\mu$ mol, 6.0 mol%), and *tert*-butyl 2-bromopropanoate (157 mg, 0.75 mmol, 1.5 eq.) at 0 °C.<sup>27</sup> After stirring for 10 min, the reaction was quenched by addition of 3 M HCl aq. (2.0 mL). The mixture was extracted with diethyl ether (4.0 mL) x 3 and combined organic layers were washed with H<sub>2</sub>O. After MPLC purification [*n*-hexane/EtOAc (100:0 to 95:5 gradient)], the title compound **3t** (92 mg, 0.31 mmol, 61%) was obtained as a

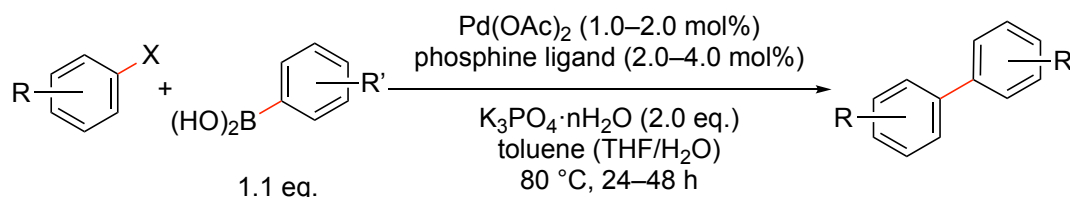
colorless solid.



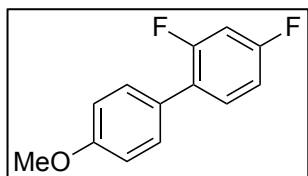
**tert-Butyl 2-(2-fluoro-[1,1'-biphenyl]-4-yl)propanoate (3t):**  $R_f$  0.69 [*n*-hexane/EtOAc (9:1)].  $^1\text{H}$  NMR (400 MHz,  $\text{CDCl}_3$ )  $\delta$  7.58–7.56 (m, 2H), 7.47–7.35 (m, 2H), 7.42–7.33 (m, 2H), 7.18–7.13 (m, 2H), 3.67 (q,  $J = 7.3$  Hz, 1H), 1.51 (d,  $J = 7.2$  Hz, 3H), 1.46 (s, 9H).

$^{13}\text{C}\{^1\text{H}\}$  NMR (101 MHz,  $\text{CDCl}_3$ )  $\delta$  173.3, 159.8 (d,  $J = 248.1$  Hz), 142.6 (d,  $J = 7.9$  Hz), 135.7, 130.7 (d,  $J = 3.6$  Hz), 129.1 (d,  $J = 3.3$  Hz), 128.5, 127.7, 127.5, 123.6 (d,  $J = 3.4$  Hz), 115.3 (d,  $J = 23.4$  Hz), 81.0, 46.1, 28.1, 18.5.  $^{19}\text{F}\{^1\text{H}\}$  NMR (376 MHz,  $\text{CDCl}_3$ )  $\delta$  –118.57. colorless solid. m.p. 47 °C. HRMS (ESI)  $m/z$ :  $[\text{M} + \text{Na}]^+$  Calcd. for  $\text{C}_{19}\text{H}_{21}\text{F}_1\text{O}_2\text{Na}$  323.1418; Found, 323.1419. All the resonances of  $^1\text{H}$  spectrum were consistent with the reported values.<sup>37</sup>

**General procedure for synthesis of multi-fluorinated arenes.**



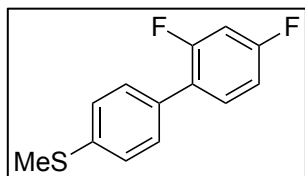
A reaction vessel was charged with aryl halide (1.0 eq.), arylboronic acid (1.0–1.3 eq.),  $\text{Pd(OAc)}_2$  (1.0–2.0 mol%), phosphine ligand (2.0–4.0 mol%,  $\text{PPh}_3$  for **2e**, **2j**; SPhos for **2f**, **2g**, **2h**, **2q**, **2r**; or dppf for **2c**, **2d**),  $\text{K}_3\text{PO}_4 \cdot n\text{H}_2\text{O}$  (2.0 eq.). Subsequently, toluene or toluene/THF/ $\text{H}_2\text{O}$  (3/1/1) were introduced into the reaction vessel under  $\text{N}_2$  atmosphere. The reaction mixture was stirred at 80 °C for 24–48 h. After completion of the reaction, it was allowed to cool to room temperature. The residue was purified by MPLC on silica gel to give the corresponding biaryls.



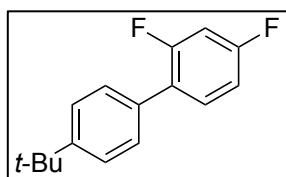
**2,4-Difluoro-4'-methoxybiphenyl (2c):** The reaction with 1-bromo-2,4-difluorobenzene (2.0 g, 10 mmol, 1.0 eq.) and 4-anisylboronic acid (1.9 g, 12 mmol, 1.2 eq.) was carried out.

After MPLC purification [*n*-hexane/EtOAc (100:0 to 95:5 gradient)], the title compound **2c** (1.4 g, 6.4 mmol, 61%) was obtained as a colorless solid.  $R_f$  0.74 [*n*-hexane/EtOAc (95:5)].  $^1\text{H}$  NMR (400 MHz,  $\text{CDCl}_3$ ):  $\delta$  7.45 (d,  $J$  = 8.1 Hz, 2H), 7.38 (dd,  $J$  = 8.3, 7.6 Hz, 1H), 7.00 (d,  $J$  = 6.4 Hz, 2H), 6.97–6.89 (m, 2H), 3.87 (s, 3H).  $^{13}\text{C}\{^1\text{H}\}$  NMR (101 MHz,  $\text{CDCl}_3$ ):  $\delta$  162.0 (dd,  $J$  = 248.0, 12.1 Hz), 159.8 (dd,  $J$  = 249.4, 11.7 Hz), 159.4, 131.2 (dd,  $J$  = 9.4, 4.9 Hz), 130.1 (d,  $J$  = 2.9 Hz), 127.4, 125.1 (dd,  $J$  = 13.9, 3.9 Hz), 114.1, 111.6 (dd,  $J$  = 21.1, 3.8 Hz), 104.4 (t,  $J$  = 26.0 Hz), 55.4.  $^{19}\text{F}$  NMR (376 MHz,  $\text{CDCl}_3$ ):  $\delta$  –112.85, –114.36. m.p. 71 °C. All the resonances of  $^1\text{H}$  and  $^{13}\text{C}$  NMR spectra were

consistent with the reported values.<sup>38</sup>

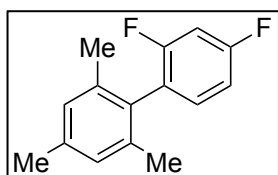


**2,4-Difluoro-4'-thiomethylbiphenyl (2d):** The reaction with 4-bromothioanisole (0.70 g, 3.5 mmol, 1.0 eq.) and 2,4-difluorophenylboronic acid (0.60 g, 3.8 mmol, 1.1 eq.) was carried out. After MPLC purification [*n*-hexane/EtOAc (100:0 to 95:5 gradient)], the title compound **2d** (0.60 g, 2.5 mmol, 73%) was obtained as a colorless solid.  $R_f$  0.68 [*n*-hexane/EtOAc (95:5)].  $^1\text{H}$  NMR (400 MHz,  $\text{CDCl}_3$ ):  $\delta$  7.43 (dt,  $J = 8.7, 1.9$  Hz, 2H), 7.40–7.35 (m, 1H), 7.32 (d,  $J = 8.3$  Hz, 2H), 6.98–6.87 (m, 2H), 2.53 (s, 3H).  $^{13}\text{C}\{^1\text{H}\}$  NMR (101 MHz,  $\text{CDCl}_3$ ):  $\delta$  162.3 (dd,  $J = 248.0, 11.9$  Hz), 159.8 (dd,  $J = 249.4, 11.8$  Hz), 138.5, 131.7, 131.3 (dd,  $J = 9.6, 4.8$  Hz), 129.4 (d,  $J = 2.1$  Hz), 126.5, 124.9 (dd,  $J = 13.6, 3.2$  Hz), 111.7 (dd,  $J = 21.3, 3.8$  Hz), 104.5 (t,  $J = 25.9$  Hz), 15.8.  $^{19}\text{F}$  NMR (376 MHz,  $\text{CDCl}_3$ ):  $\delta$  -112.02, -114.02. m.p. 99 °C. HRMS (EI)  $m/z$ :  $[\text{M}]^+$  Calcd. for  $\text{C}_{13}\text{H}_{10}\text{F}_2\text{S}_1$  236.0466; Found, 236.0464.

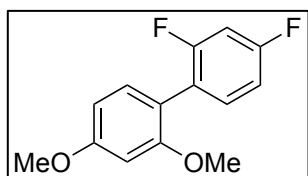


**2,4-Difluoro-4'-tert-butylbiphenyl (2e):** The reaction with 1-bromo-2,4-difluorobenzene (0.37 g, 1.9 mmol, 1.0 eq.) and 4-*tert*-butylphenylboronic acid (0.34 g, 1.9 mmol, 1.0 eq.) was carried out. After MPLC purification [*n*-hexane/EtOAc (100:0 to 99:1 gradient)], the title compound **2e** (0.43 g, 1.7 mmol, 91%) was obtained as a colorless solid.  $R_f$  0.89 [*n*-hexane/EtOAc (95:5)].  $^1\text{H}$  NMR (400 MHz,  $\text{CDCl}_3$ ):  $\delta$  7.57–7.32 (m, 5H), 7.00–6.86 (m, 2H), 1.38 (s, 9H).  $^{13}\text{C}\{^1\text{H}\}$  NMR (101 MHz,  $\text{CDCl}_3$ ):  $\delta$  162.2 (dd,  $J = 248.4, 12.1$  Hz), 159.9 (dd,  $J = 250.3, 11.9$  Hz), 150.9, 132.2, 131.5 (dd,  $J = 9.5, 5.1$  Hz), 128.7 (d,  $J = 2.5$  Hz), 125.6, 125.3 (dd,  $J = 13.8, 3.8$  Hz), 111.6 (dd,  $J = 21.0, 4.0$  Hz), 104.3 (dd,  $J = 26.0,$

25.1 Hz), 34.7, 31.5.  $^{19}\text{F}$  NMR (376 MHz,  $\text{CDCl}_3$ ):  $\delta$  -112.54, -114.14. m.p. 75 °C. All the resonances of  $^1\text{H}$  and  $^{13}\text{C}$  NMR spectra were consistent with the reported values.<sup>38</sup>



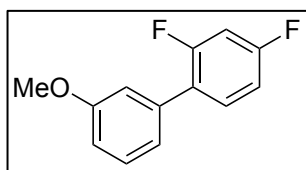
**1-Mesityl-2,4-difluorobenzene (2f):** The reaction with 1-bromo-2,4-difluorobenzene (3.0 g, 16 mmol, 1.0 eq.) and mesitylboronic acid (2.8 g, 17 mmol, 1.1 eq.) was carried out. After MPLC purification [*n*-hexane/EtOAc (100:0 to 99:1 gradient)], the title compound **2f** (1.3 g, 5.6 mmol, 36%) was obtained as a colorless oil.  $R_f$  0.81 [*n*-hexane/EtOAc (95:5)].  $^1\text{H}$  NMR (400 MHz,  $\text{CDCl}_3$ ):  $\delta$  7.15 (td,  $J$  = 8.4, 6.5 Hz, 1H), 7.02 (s, 2H), 7.01–6.91 (m, 2H), 2.39 (s, 3H), 2.08 (s, 6H).  $^{13}\text{C}\{^1\text{H}\}$  NMR (101 MHz,  $\text{CDCl}_3$ ):  $\delta$  162.4 (dd,  $J$  = 247.9, 11.9 Hz), 159.8 (dd,  $J$  = 247.2, 12.3 Hz), 137.8, 136.9, 132.3 (dd,  $J$  = 9.3, 5.3 Hz), 131.5, 128.3, 124.1 (dd,  $J$  = 18.1, 4.1 Hz), 111.5 (dd,  $J$  = 20.8, 3.8 Hz), 104.2 (t,  $J$  = 26.0 Hz), 21.2, 20.5.  $^{19}\text{F}$  NMR (376 MHz,  $\text{CDCl}_3$ ):  $\delta$  -110.92, -112.18 HRMS (EI)  $m/z$ :  $[\text{M}]^+$  Calcd. for  $\text{C}_{15}\text{H}_{14}\text{F}_2$  232.1058; Found, 232.1061. All the resonances of  $^1\text{H}$  NMR spectrum was consistent with the reported values.<sup>39</sup>



**2,4-Difluoro-2',4'-dimethoxybiphenyl (2g):** The reaction with 1-bromo-2,4-difluorobenzene (3.0 g, 16 mmol, 1.0 eq.) and 2,4-dimethoxyphenylboronic acid (3.1 g, 17 mmol, 1.1 eq.) was carried out. After MPLC purification [*n*-hexane/EtOAc (100:0 to 9:1 gradient)], the title compound **2g** (3.2 g, 13 mmol, 81%) was obtained as a colorless solid.  $R_f$  0.43 [*n*-hexane/EtOAc (95:5)].  $^1\text{H}$  NMR (400 MHz,  $\text{CDCl}_3$ ):  $\delta$  7.31 (q,  $J$  = 6.4 Hz, 1H), 7.17 (dd,  $J$  = 8.6, 3.1 Hz, 1H), 6.90 (dt,  $J$  = 12.4, 9.1 Hz, 2H), 6.59–6.57 (m, 2H), 3.86 (s, 3H), 3.80 (s, 3H).  $^{13}\text{C}\{^1\text{H}\}$  NMR (101 MHz,  $\text{CDCl}_3$ ):  $\delta$  162.2 (dd,  $J$  = 248.4, 11.3 Hz), 161.1, 160.2

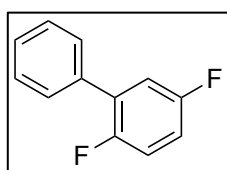


(dd,  $J = 249.5, 12.2$  Hz), 158.0, 132.7 (dd,  $J = 9.4, 5.0$  Hz), 131.8, 122.2 (dd,  $J = 16.3, 3.8$  Hz), 116.8, 110.9 (dd,  $J = 21.1, 3.8$  Hz), 104.5, 103.9 (t,  $J = 25.9$  Hz), 98.9, 55.7, 55.5.  $^{19}\text{F}$  NMR (376 MHz,  $\text{CDCl}_3$ ):  $\delta -110.49, -112.85$ . m.p.  $75^\circ\text{C}$ . HRMS (APCI)  $m/z$ :  $[\text{M} + \text{H}]^+$  Calcd. for  $\text{C}_{14}\text{H}_{13}\text{F}_2\text{O}_2$  251.0878; Found, 251.0882.



**2,4-Difluoro-3'-methoxybiphenyl (2h):** The reaction with 1-bromo-2,4-difluorobenzene (2.0 g, 10 mmol, 1.0 eq.) and 3-anisylboronic acid (1.7 g, 11 mmol, 1.1 eq.) was carried out.

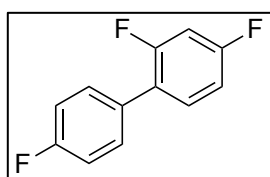
After MPLC purification [ $n$ -hexane/EtOAc (100:0 to 95:5 gradient)], the title compound **2h** (2.1 g, 9.5 mmol, 92%) was obtained as a colorless liquid.  $R_f$  0.69 [ $n$ -hexane/EtOAc (95:5)].  $^1\text{H}$  NMR (400 MHz,  $\text{CDCl}_3$ ):  $\delta$  7.32–7.22 (m, 2H), 6.99–6.96 (m, 2H), 6.84–6.77 (m, 3H), 3.72 (s, 3H).  $^{13}\text{C}\{^1\text{H}\}$  NMR (101 MHz,  $\text{CDCl}_3$ ):  $\delta$  162.4 (dd,  $J = 248.6, 11.7$  Hz), 159.8 (dd,  $J = 250.5, 11.8$  Hz), 159.7, 136.4, 131.5 (dd,  $J = 9.4, 4.9$  Hz), 129.6, 125.3 (dd,  $J = 13.5, 4.0$  Hz), 121.4, 114.8 (d,  $J = 2.9$  Hz), 113.3, 111.6 (dd,  $J = 21.0, 3.9$  Hz), 104.4 (t,  $J = 26.0$  Hz), 55.2.  $^{19}\text{F}$  NMR (376 MHz,  $\text{CDCl}_3$ ):  $\delta -111.90, -113.71$ . HRMS (EI)  $m/z$ :  $[\text{M}]^+$  Calcd. for  $\text{C}_{13}\text{H}_{10}\text{F}_2\text{O}_1$  220.0694; Found, 220.0697.



**2,5-Difluorobiphenyl (2j):** The reaction with 1-bromo-2,5-difluorobenzene (1.9 g, 10 mmol, 1.0 eq.) and phenylboronic acid (1.6 g, 13 mmol, 1.3 eq.) was carried out. After MPLC purification [ $n$ -hexane/EtOAc (100:0 to 99:1 gradient)], the title compound **2j** (1.5 g, 8.1 mmol, 81%)

was obtained as a colorless solid.  $R_f$  0.73 [ $n$ -hexane/EtOAc (95:5)].  $^1\text{H}$  NMR (400 MHz,  $\text{CDCl}_3$ ):  $\delta$  7.69 (dt,  $J = 8.1, 1.3$  Hz, 2H), 7.59 (tt,  $J = 8.1, 1.8$  Hz, 2H), 7.58–7.49 (m, 1H), 7.29 (ddd,  $J = 9.1, 6.1, 3.2$  Hz, 1H), 7.23 (td,  $J = 9.4, 4.6$  Hz, 1H), 7.11 (ddt,  $J = 9.1, 7.2,$

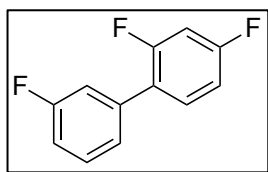
3.3 Hz, 1H).  $^{13}\text{C}\{^1\text{H}\}$  NMR (101 MHz,  $\text{CDCl}_3$ ):  $\delta$  158.9 (d,  $J = 241.7$  Hz), 155.8 (d,  $J = 243.4$  Hz), 134.9, 130.5 (dd,  $J = 16.1, 7.8$  Hz), 129.0 (d,  $J = 3.5$  Hz), 128.7, 128.3, 117.2 (dd,  $J = 27.0, 7.7$  Hz), 117.0 (dd,  $J = 25.3, 4.9$  Hz), 115.2 (dd,  $J = 24.0, 8.6$  Hz).  $^{19}\text{F}$  NMR (376 MHz,  $\text{CDCl}_3$ ):  $\delta$  -119.64, -124.68. All the resonances of  $^1\text{H}$  and  $^{13}\text{C}$  NMR spectra were consistent with the reported values.<sup>40</sup>



**2,4,4'-Trifluorobiphenyl (2q):** The reaction with 1-bromo-2,4-difluorobenzene (3.0 g, 16 mmol, 1.0 eq.) and 4-fluorophenylboronic acid (2.4 g, 17 mmol, 1.1 eq.) was carried out.

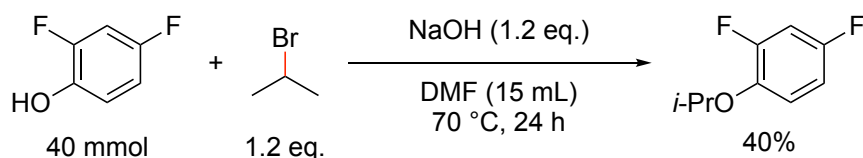
After MPLC purification [*n*-hexane/EtOAc (100:0 to 99:1 gradient)], the title compound **2q** (2.8 g, 13 mmol, 86%) was obtained as a colorless solid.  $R_f$  0.83 [*n*-hexane/EtOAc (95:5)].  $^1\text{H}$  NMR (400 MHz,  $\text{CDCl}_3$ ):  $\delta$  7.55–7.41 (m, 2H), 7.37 (td,  $J = 8.7, 6.4$  Hz, 1H), 7.22–7.07 (m, 2H), 7.01–6.85 (m, 2H).  $^{13}\text{C}\{^1\text{H}\}$  NMR (101 MHz,  $\text{CDCl}_3$ ):  $\delta$  162.6 (d,  $J = 247.3$  Hz), 162.4 (dd,  $J = 249.1, 11.7$  Hz), 159.8 (dd,  $J = 250.2, 11.6$  Hz), 131.4 (dd,  $J = 9.6, 4.8$  Hz), 131.1 (d,  $J = 3.4$  Hz), 130.7 (dd,  $J = 8.0, 2.4$  Hz), 124.5 (dd,  $J = 13.6, 3.8$  Hz), 115.6 (d,  $J = 21.6$  Hz), 111.8 (dd,  $J = 21.0, 3.9$  Hz), 104.6 (t,  $J = 26.1$  Hz).  $^{19}\text{F}$  NMR (376 MHz,  $\text{CDCl}_3$ ):  $\delta$  -111.78, -114.20, -114.91. m.p. 89 °C. HRMS (EI)  $m/z$ :  $[\text{M}]^{+}$  Calcd. for  $\text{C}_{12}\text{H}_7\text{F}_3$  208.0494; Found, 208.0499. All the resonances of  $^1\text{H}$  and  $^{19}\text{F}$  NMR spectra were consistent with the reported values.<sup>41</sup>

**2,3',4-Trifluorobiphenyl (2r):** The reaction with 1-bromo-2,4-difluorobenzene (1.0 g, 5.2 mmol, 1.0 eq.) and 3-fluorophenylboronic acid (0.65 g, 5.7 mmol, 1.1 eq.) was carried out. After MPLC purification [*n*-hexane/EtOAc (100:0 to 99:1 gradient)], the title

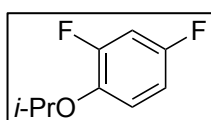


compound **2r** (1.0 g, 4.7 mmol, 91%) was obtained as a colorless solid.  $R_f$  0.83 [*n*-hexane/EtOAc (95:5)].  $^1\text{H}$  NMR (400 MHz,  $\text{CDCl}_3$ ):  $\delta$  7.44–7.37 (m, 2H), 7.29 (dq,  $J = 7.9, 1.4$  Hz, 1H), 7.23 (ddt,  $J = 10.2, 2.8, 1.6$  Hz, 1H), 7.08 (tdd,  $J = 8.3, 2.5, 0.9$  Hz, 1H), 7.01–6.89 (m, 2H).  $^{13}\text{C}\{^1\text{H}\}$  NMR (101 MHz,  $\text{CDCl}_3$ ):  $\delta$  162.9 (d,  $J = 245.5$  Hz), 162.7 (dd,  $J = 249.7, 11.9$  Hz), 159.8 (dd,  $J = 251.1, 11.5$  Hz), 137.1 (d,  $J = 8.2$  Hz), 131.5 (dd,  $J = 9.6, 4.7$  Hz), 130.1 (d,  $J = 8.5$  Hz), 124.7, 124.3 (d,  $J = 13.5$  Hz), 116.1 (dd,  $J = 22.5, 3.1$  Hz), 114.8 (d,  $J = 21.1$  Hz), 111.9 (dd,  $J = 21.1, 3.9$  Hz), 104.7 (t,  $J = 25.9$  Hz).  $^{19}\text{F}$  NMR (376 MHz,  $\text{CDCl}_3$ ):  $\delta$  -111.01, -113.53, -113.77. m.p. 30 °C. HRMS (EI)  $m/z$ :  $[\text{M}]^+$  Calcd. for  $\text{C}_{12}\text{H}_7\text{F}_3$  208.0494; Found, 208.0496. All the resonances of  $^1\text{H}$  NMR spectrum was consistent with the reported values.<sup>42</sup>

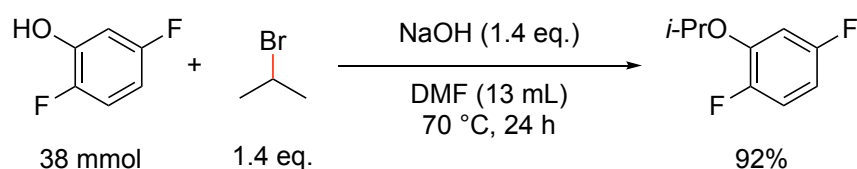
#### *iso*-Propoxide-substituted substrate synthesis.<sup>43</sup>



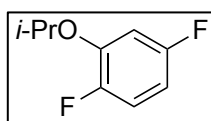
2,4-Difluorophenol (5.2 g, 40 mmol, 1.0 eq.), 2-bromopropane (5.9 g, 48 mmol, 1.2 eq.), and sodium hydroxide (1.9 g, 48 mmol, 1.2 eq.) were combined in DMF (15 mL) and heated at 70 °C. After 24 h, the reaction was cooled to room temperature. The product was extracted with diethyl ether, and then washed with water and brine. The combined organic layers were dried over  $\text{MgSO}_4$ . Removal of solvent under reduced pressure and vacuum distillation from  $\text{CaH}_2$  provided 2,4-difluoro-1-*iso*-propoxybenzene (**2k**) as a colorless liquid (2.7 g, 16 mmol, 40%, volatile).



**2,4-Difluoro-1-*iso*-propoxybenzene (2k):**  $R_f$  0.90 [*n*-hexane/EtOAc (95:5)].  $^1\text{H}$  NMR (400 MHz,  $\text{CDCl}_3$ ):  $\delta$  6.92 (td,  $J = 9.1, 5.5$  Hz, 1H), 6.82 (ddd,  $J = 11.4, 8.5, 3.0$  Hz, 1H), 6.74 (dddd,  $J = 9.4, 8.0, 3.2, 1.8$  Hz, 1H), 4.41 (hept,  $J = 6.1$  Hz, 1H), 1.32 (d,  $J = 6.1$  Hz, 6H).  $^{13}\text{C}\{^1\text{H}\}$  NMR (101 MHz,  $\text{CDCl}_3$ ):  $\delta$  156.9 (dd,  $J = 242.1, 10.5$  Hz), 154.0 (dd,  $J = 248.6, 12.0$  Hz), 142.3 (dd,  $J = 10.6, 3.7$  Hz), 119.3 (dd,  $J = 9.7, 3.1$  Hz), 110.5 (dd,  $J = 21.9, 4.5$  Hz), 104.9 (dd,  $J = 26.5, 22.8$  Hz), 73.6, 22.0.  $^{19}\text{F}$  NMR (376 MHz,  $\text{CDCl}_3$ ):  $\delta$  -119.92, -128.64. colorless liquid. HRMS (EI)  $m/z$ :  $[\text{M}]^+$  Calcd. for  $\text{C}_9\text{H}_{10}\text{F}_2\text{O}_1$  172.0694; Found, 172.0698.



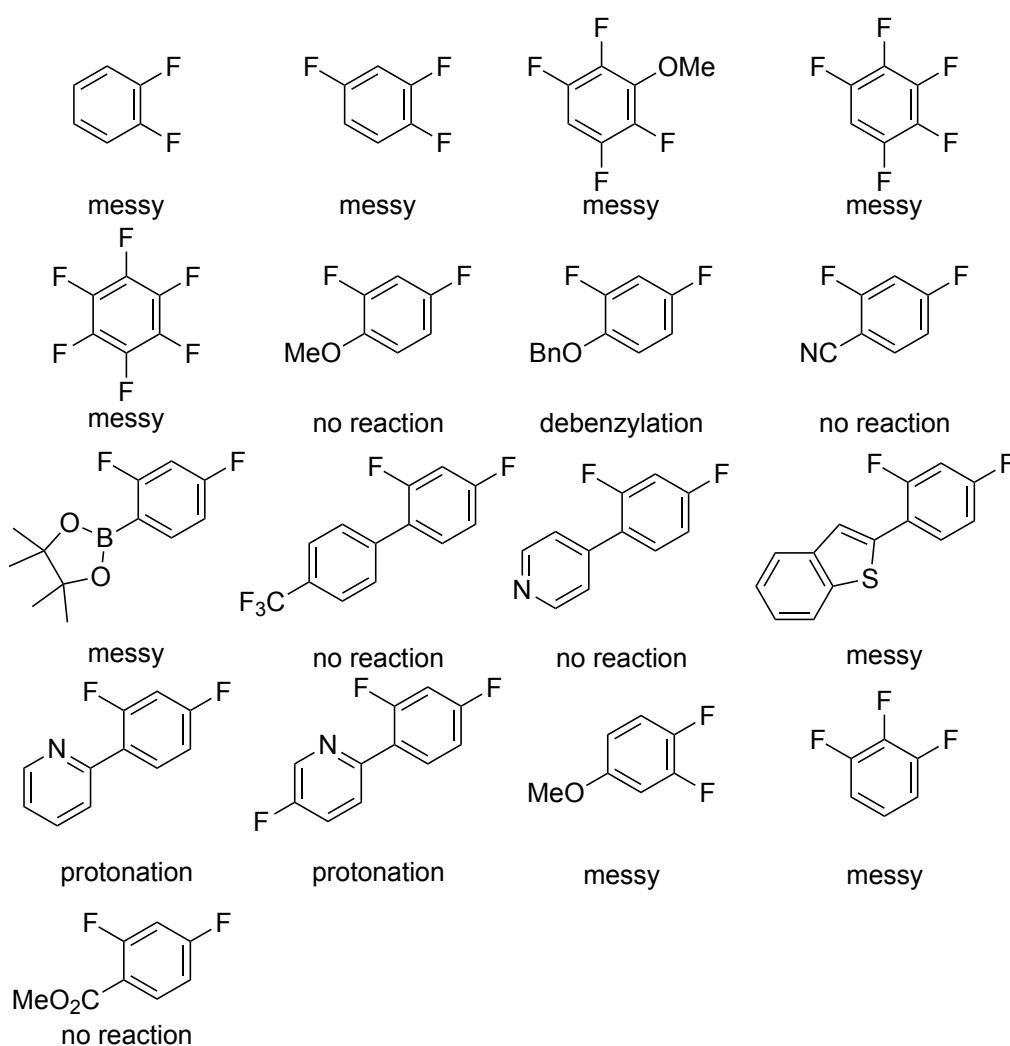
2,5-Difluorophenol (5.0 g, 38 mmol, 1.0 eq.), 2-bromopropane (6.6 g, 54 mmol, 1.4 eq.), and sodium hydroxide (2.2 g, 30 mmol, 3.0 eq.) were combined in DMF (13 mL) and heated at 70 °C. After 24 h, the reaction was cooled to room temperature. The mixture was extracted with diethyl ether, washed with water and brine, and dried over  $\text{MgSO}_4$ . Removal of solvent under reduced pressure and vacuum distillation over  $\text{CaH}_2$  provided 2,5-difluoro-1-*iso*-propoxybenzene (**2l**) as a colorless viscous liquid (6.0 g, 35 mmol, 92%, volatile).



**2,5-Difluoro-1-*iso*-propoxybenzene (2l):**  $R_f$  0.90 [*n*-hexane/EtOAc (95:5)].  $^1\text{H}$  NMR (400 MHz,  $\text{CDCl}_3$ ):  $\delta$  6.99 (ddd,  $J = 10.6, 8.9, 5.3$  Hz, 1H), 6.69 (ddd,  $J = 9.9, 6.7, 3.0$  Hz, 1H), 6.56 (ddt,  $J = 9.0, 7.8, 3.2$  Hz, 1H), 4.50 (hept,

$J = 6.0$  Hz, 1H), 1.36 (d,  $J = 6.0$  Hz, 6H).  $^{13}\text{C}\{^1\text{H}\}$  NMR (101 MHz,  $\text{CDCl}_3$ ):  $\delta$  158.8 (d,  $J = 241.5$  Hz), 150.0 (dd,  $J = 240.6, 3.5$  Hz), 146.7 (t,  $J = 11.4$  Hz), 116.4 (dd,  $J = 21.3, 10.3$  Hz), 106.8 (dd,  $J = 23.8, 7.0$  Hz), 104.7 (d,  $J = 27.0$  Hz), 72.5, 21.9.  $^{19}\text{F}$  NMR (376 MHz,  $\text{CDCl}_3$ ):  $\delta$  -117.71, -139.86. colorless liquid. HRMS (EI)  $m/z$ :  $[\text{M}]^+$  Calcd. for  $\text{C}_9\text{H}_{10}\text{F}_2\text{O}_1$  172.0694; Found, 172.0697.

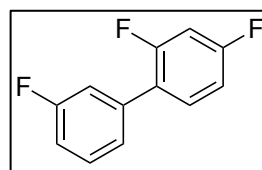
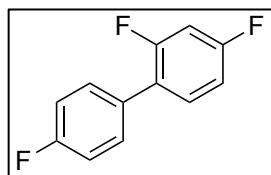
### Unsuccessful substrates in this study.



**Computational details.**

The geometry optimization was performed by the DFT method with the B3LYP functional in the gas phase, using 6-31G(d) basis sets.<sup>44</sup> Natural bond orbital (NBO) analysis<sup>45</sup> and electrostatic potential (ESP) mapping<sup>46</sup> were carried out using the same functional using the same basis sets. The natural populations were calculated by NBO6.<sup>47</sup> All DFT calculations were performed using Gaussian 16.<sup>48</sup>

## Cartesian coordinates for calculated structures.



<b>2q</b>			<b>2r</b>		
C 2.936434	-1.205316	-0.521937	C 3.126095	-0.744366	-0.216296
C 1.543106	-1.195863	-0.519153	C 1.748703	-0.906133	-0.274378
C 0.818922	-0.123304	0.029128	C 0.909841	0.143751	0.133841
C 1.540415	0.955522	0.570462	C 1.497786	1.338717	0.584494
C 2.933175	0.961220	0.573982	C 2.884562	1.472632	0.631649
C 3.611131	-0.122439	0.028038	C 3.720098	0.429051	0.231161
H 3.498640	-2.028301	-0.950779	H 1.343782	-1.836503	-0.657987
H 1.009156	-2.027502	-0.969600	H 0.868084	2.159640	0.905850
H 1.008438	1.796324	1.000321	H 3.321939	2.400833	0.988572
H 3.494923	1.788014	0.996132	C -0.563486	-0.044397	0.108382
C -0.665393	-0.161998	0.050126	C -1.147634	-1.268688	0.479418
C -1.360947	-1.352312	0.328236	C -1.450775	0.964713	-0.294486
C -1.457632	0.964131	-0.218450	C -2.524194	-1.479343	0.450956
C -2.752377	-1.421963	0.334665	H -0.499057	-2.069711	0.820325
H -0.788081	-2.243044	0.567079	C -2.828814	0.797559	-0.337881
C -2.846134	0.940311	-0.220437	C -3.344719	-0.435604	0.039538
C -3.474122	-0.266958	0.058108	H -2.962003	-2.425614	0.748829
H -3.275445	-2.344903	0.559405	H -3.474075	1.604176	-0.665021
H -3.414960	1.835560	-0.441843	F -0.964429	2.164473	-0.678819
F -0.861442	2.142356	-0.505102	F -4.678571	-0.616468	0.007641
F -4.820263	-0.310672	0.063843	F 3.913576	-1.764890	-0.619434
F 4.960356	-0.120832	0.028224	H 4.801373	0.511787	0.256555

**References and notes.**

- (1) (a) Dolbier, W. R. *J. Fluor. Chem.* **2005**, *126*, 157. (b) Müller, K.; Faeh, C.; Diederich, F. *Science* **2007**, *317*, 1881. (c) O'hagan, D. *Chem. Soc. Rev.* **2008**, *37*, 308. (d) Hiyama, T. *Organofluorine Compounds: Chemistry and Applications*; Springer: Berlin, 2000.
- (2) (a) Inoue, M.; Sumii, Y.; Shibata, N. *ACS Omega* **2020**, *5*, 10633. (b) Mei, H.; Remete, A. M.; Zou, Y.; Moriwaki, H.; Fustero, S.; Kiss, L.; Soloshonok, V. A.; Han, J. *Chinese Chem. Lett.* **2020**, *31*, 2401. (c) Han, J.; Remete, A. M.; Dobson, L. S.; Kiss, L.; Izawa, K.; Moriwaki, H.; Soloshonok, V. A.; O'Hagan, D. *J. Fluor. Chem.* **2020**, *239*, 109639. (d) Miller, M. A.; Sletten, E. M. *ChemBioChem* **2020**, *21*, 3451.
- (3) Ogawa, Y.; Tokunaga, E.; Kobayashi, O.; Hirai, K.; Shibata, N. *iScience* **2020**, *23*, 101467.
- (4) (a) Cardoso, V. F.; Correia, D. M.; Ribeiro, C.; Fernandes, M. M.; Lanceros-Méndez, S. *Polymers* **2018**, *10*, 161. (b) Zhang, C.; Yan, K.; Fu, C.; Peng, H.; Hawker, C. J.; Whittaker, A. K. *Chem. Rev.* **2022**, *122*, 167. (c) Hird, M. *Chem. Soc. Rev.* **2007**, *36*, 2070.
- (5) (a) Campbell, M. G.; Ritter, T. *Chem. Rev.* **2015**, *115*, 612. (b) Campbell, M. G.; Ritter, T. *Org. Process Res. Dev.* **2014**, *18*, 474. (c) Caron, S. *Org. Process Res. Dev.* **2020**, *24*, 470. (d) Okazoe, T. *Proc. Japan Acad. Ser. B Phys. Biol. Sci.* **2009**, *85*, 276. (e) Yerien, D. E.; Bonesi, S.; Postigo, A. *Org. Biomol. Chem.* **2016**, *14*, 8398. (f) Szpera, R.; Moseley, D. F. J.; Smith, L. B.; Sterling, A. J.; Gouverneur, V. The Fluorination of C–H Bonds: Developments and Perspectives. *Angew. Chemie - Int. Ed.* **2019**, *58*, 14824–14848. (g) Neumann, C. N.; Ritter, T. *Angew. Chem., Int. Ed.* **2015**, *54*, 3216.



- (6) Ma, X.; Kuang, Z.; Song, Q. *JACS Au* **2022**, *2*, 261.
- (7) (a) Balz, G.; Schiemann, G. *Ber. Dtsch. Chem. Ges. B* **1927**, *60*, 1186. (b) Cresswell, A. J.; Davies, S. G.; Roberts, P. M.; Thomson, J. E. *Chem. Rev.* **2015**, *115*, 566.
- (8) (a) Wang, W.; Yang, X.; Dai, R.; Yan, Z.; Wei, J.; Dou, X.; Qiu, X.; Zhang, H.; Wang, C.; Liu, Y.; Song, S.; Jiao, N. *J. Am. Chem. Soc.* **2022**, *144*, 13415. (b) Saikia, I.; Borah, A. J.; Phukan, P. *Chem. Rev.* **2016**, *116*, 6837. (c) Petrone, D. A.; Ye, J.; Lautens, M. *Chem. Rev.* **2016**, *116*, 8003. (d) Das, R.; Kapur, M. *Asian J. Org. Chem.* **2018**, *7*, 1524.
- (9) Seyferth, D. *Organometallics* **2009**, *28*, 1598.
- (10) (a) Krasovskiy, A.; Knochel, P. *Angew. Chem., Int. Ed.* **2004**, *43*, 3333. (b) Bruña, S.; Kennedy, A. R.; Fairley, M.; O'Hara, C. T. *Chem. Eur. J.* **2021**, *27*, 4134. (c) Desaintjean, A.; Haupt, T.; Bole, L. J.; Judge, N. R.; Hevia, E.; Knochel, P. *Angew. Chem., Int. Ed.* **2021**, *60*, 1513. (d) Ziegler, D. S.; Wei, B.; Knochel, P. *Chem. Eur. J.* **2019**, *25*, 2695. (e) Chow, W. K.; Yuen, O. Y.; Choy, P. Y.; So, C. M.; Lau, C. P.; Wong, W. T.; Kwong, F. Y. *RSC Adv.* **2013**, *3*, 12518.
- (11) (a) Snieckus, V. *Chem. Rev.* **1990**, *90*, 879. (b) Krasovskiy, A.; Krasovskaya, V.; Knochel, P. *Angew. Chem., Int. Ed.* **2006**, *45*, 2958. (c) Cheng, C.; Hartwig, J. F. *Chem. Rev.* **2015**, *115*, 8946. (d) Mkhaliid, I. A. I.; Barnard, J. H.; Marder, T. B.; Murphy, J. M.; Hartwig, J. F. *Chem. Rev.* **2010**, *110*, 890. (e) Batuecas, M.; Gorgas, N.; Crimmin, M. R. *Chem. Sci.* **2021**, *12*, 1993.
- (12) (a) Amii, H.; Uneyama, K. *Chem. Rev.* **2009**, *109*, 2119. (b) Henderson, A. S.; Medina, S.; Bower, J. F.; Galan, M. C. *Org. Lett.* **2015**, *17*, 4846. (c) Pummer, W. J.; Wall, L. A. *Science* **1958**, *127*, 643. (d) Ai, H. J.; Ma, X.; Song, Q.; Wu, X. F. *Sci. China Chem.* **2021**, *64*, 1630.

- (13) (a) Chen, W.; Bakewell, C.; Crimmin, M. R. *Synthesis* **2017**, *49*, 810. (b) Eisenstein, O.; Milani, J.; Perutz, R. N. *Chem. Rev.* **2017**, *117*, 8710. (c) Xu, W.; Zhang, Q.; Shao, Q.; Xia, C.; Wu, M. *Asian J. Org. Chem.* **2021**, *10*, 2454. (d) Kuehnel, M. F.; Lentz, D.; Braun, T. *Angew. Chem., Int. Ed.* **2013**, *52*, 3328. (e) Aizenberg, M.; Milstein, D. *Science* **1994**, *265*, 359. (f) Ishii, Y.; Chatani, N.; Yorimitsu, S.; Murai, S. *Chem. Lett.* **1998**, *27*, 157. (g) Clot, E.; Eisenstein, O.; Jasim, N.; MacGregor, S. A.; McGrady, J. E.; Perutz, R. N. *Acc. Chem. Res.* **2011**, *44*, 333. (h) Sun, A. D.; Love, J. A. *Dalton Trans.* **2010**, *39*, 10362.
- (14) Luo, Y.-R. *Comprehensive Handbook of Chemical Bond Energies*, 1st Ed.; CRC Press: Boca Raton, 2007.
- (15) (a) Barbour, A. K.; Thomas, P. *Ind. Eng. Chem.* **1966**, *58*, 48. (b) Coates, G.; Rekhroukh, F.; Crimmin, M. R. *Synlett* **2019**, *30*, 2233. (c) Fowler, R. D.; Burford, W. B., III; Hamilton, J. M., Jr.; Sweet, R. G.; Weber, C. E.; Kasper, J. S.; Litant, I. *Ind. Eng. Chem.* **1947**, *39*, 292.
- (16) (a) Yakobson, G. G.; Vlasov, V. M. *Synthesis* **1976**, 652. (b) Iguminov, S. M.; Zabolotskikh, A. V. U.S. Patent US 6,265,627 B1, July 24, 2001.
- (17) Guo, W. H.; Min, Q. Q.; Gu, J. W.; Zhang, X. *Angew. Chem., Int. Ed.* **2015**, *54*, 9075.
- (18) Bakewell, C.; White, A. J. P.; Crimmin, M. R. *J. Am. Chem. Soc.* **2016**, *138*, 12763.
- (19) Rekhroukh, F.; Chen, W.; Brown, R. K.; White, A. J. P.; Crimmin, M. R. *Chem. Sci.* **2020**, *11*, 7842.
- (20) (a) Tian, Y. M.; Guo, X. N.; Kuntze-Fechner, M. W.; Krummenacher, I.; Braunschweig, H.; Radius, U.; Steffen, A.; Marder, T. B. *J. Am. Chem. Soc.* **2018**, *140*, 17612. (b) Zhou, J.; Kuntze-Fechner, M. W.; Bertermann, R.; Paul, U. S. D.;

- Berthel, J. H. J.; Friedrich, A.; Du, Z.; Marder, T. B.; Radius, U. *J. Am. Chem. Soc.* **2016**, *138*, 5250.
- (21) Fujii, I.; Semba, K.; Li, Q. Z.; Sakaki, S.; Nakao, Y. *J. Am. Chem. Soc.* **2020**, *142*, 11647.
- (22) Seki, R.; Hara, N.; Saito, T.; Nakao, Y. *J. Am. Chem. Soc.* **2021**, *143*, 6388.
- (23) Rieke, R. D.; Bales, S. E. *J. Am. Chem. Soc.* **1974**, *96*, 1775.
- (24) Hansch, C.; Leo, A.; Taft, R. W. *Chem. Rev.* **1991**, *91*, 165.
- (25) Matsui, S.; Ando, T.; Miyazawa, K.; Takeuchi, H.; Hisatsune, Y.; Takeshita, F.; Nakagawa, E. JP. Patent WO1998012166A1, March 26, 1998.
- (26) Fujii, I.; Semba, K.; Nakao, Y. *Org. Lett.* **2022**, *24*, 3075.
- (27) Jin, M.; Adak, L.; Nakamura, M. *J. Am. Chem. Soc.* **2015**, *137*, 7128.
- (28) Chen, Z.; Gu, C.; Yuen, O. Y.; So, C. M. *Chem. Sci.* **2022**, *13*, 4762.
- (29) Paridala, K.; Lu, S.-M.; Wang, M.-M.; Li, C. *Chem. Commun.* **2018**, *54*, 11574.
- (30) Anderson, K. W.; Ikawa, T.; Tundel, R. E.; Buchwald, S. L. *J. Am. Chem. Soc.* **2006**, *128*, 10694.
- (31) Grainger, R.; Cornella, J.; Blakemore, D. C.; Larrosa, I.; Campanera, J. M. *Chem. Eur. J.* **2014**, *20*, 16680.
- (32) Khurana, J. M.; Chauhan, S.; Bansal, G. *Monatsh. Chem.* **2004**, *135*, 83.
- (33) Sawama, Y.; Morita, K.; Asai, S.; Kozawa, M.; Tadokoro, S.; Nakajima, J.; Monguchi, Y.; Sajiki, H. *Adv. Synth. Catal.* **2015**, *357*, 1205.
- (34) Tang, L.; Guo, X.; Li, Y.; Zhang, S.; Zha, Z.; Wang, Z. *Chem. Commun.* **2013**, *49*, 5213.
- (35) Mao, Y.; Liu, Y.; Hu, Y.; Wang, L.; Zhang, S.; Wang, W. *ACS Catal.* **2018**, *8*, 3016.
- (36) Lee, Y. H.; Morandi, B. *Nat. Chem.* **2018**, *10*, 1016.

- (37) Friest, J. A.; Maezato, Y.; Broussy, S.; Blum, P.; Berkowitz, D. B. *J. Am. Chem. Soc.* **2010**, *132*, 5930.
- (38) Nozawa-Kumada, K.; Osawa, S.; Sasaki, M.; Chataigner, I.; Shigeno, M.; Kondo, Y. *J. Org. Chem.* **2017**, *82*, 9487.
- (39) Raders, S. M.; Moore, J. N.; Parks, J. K.; Miller, A. D.; Leibing, T. M.; Kelley, S. P.; Rogers, R. D.; Shaughnessy, K. H. *J. Org. Chem.* **2013**, *78*, 4649.
- (40) Noël, T.; Kuhn, S.; Musacchio, A. J.; Jensen, K. F.; Buchwald, S. L. *Angew. Chem., Int. Ed.* **2011**, *50*, 5943.
- (41) Marciasini, L.; Richy, N.; Vaultier, M.; Pucheault, M. *Chem. Commun.* **2012**, *48*, 1553.
- (42) Heiss, C.; Leroux, F.; Schlosser, M. *Eur. J. Org. Chem.* **2005**, 5242.
- (43) Morgan, D. L.; Martinez-Castro, N.; Storey, R. F. *Macromolecules* **2010**, *43*, 8724.
- (44) (a) Lee, C.; Yang, W.; Parr, R. G. *Phys. Rev. B* **1988**, *37*, 785. (b) Becke, A. D. *J. Phys. Chem.* **1993**, *98*, 5648.
- (45) Weinhold, F. *J. Comput. Chem.* **2012**, *33*, 2363.
- (46) Wheeler, S. E.; Houk, K. N. *J. Chem. Theory Comput.* **2009**, *5*, 2301.
- (47) Glendening, E. D.; Landis, C. R.; Weinhold, F. *J. Comput. Chem.* **2013**, *34*, 1429.
- (48) M. J. Frisch, G. W. Trucks, H. B. Schlegel, G. E. Scuseria, M. A. Robb, J. R. Cheeseman, G. Scalmani, V. Barone, G. A. Petersson, H. Nakatsuji, X. Li, M. Caricato, A. V. Marenich, J. Bloino, B. G. Janesko, R. Gomperts, B. Mennucci, H. P. Hratchian, J. V. Ortiz, A. F. Izmaylov, J. L. Sonnenberg, D. Williams-Young, F. Ding, F. Lipparini, F. Egidi, J. Goings, B. Peng, A. Petrone, T. Henderson, D. Ranasinghe, V. G. Zakrzewski, J. Gao, N. Rega, G. Zheng, W. Liang, M. Hada, M. Ehara, K. Toyota, R. Fukuda, J. Hasegawa, M. Ishida, T. Nakajima, Y. Honda, O.

Kitao, H. Nakai, T. Vreven, K. Throssell, J. A. Montgomery, Jr., J. E. Peralta, F. Ogliaro, M. J. Bearpark, J. J. Heyd, E. N. Brothers, K. N. Kudin, V. N. Staroverov, T. A. Keith, R. Kobayashi, J. Normand, K. Raghavachari, A. P. Rendell, J. C. Burant, S. S. Iyengar, J. Tomasi, M. Cossi, J. M. Millam, M. Klene, C. Adamo, R. Cammi, J. W. Ochterski, R. L. Martin, K. Morokuma, O. Farkas, J. B. Foresman, and D. J. Fox, Gaussian 16, revision B.01; Gaussian, Inc.: Wallingford, CT, 2016.

## Chapter 5

### Magnesium of Alkyl Fluorides

#### Catalyzed by Rhodium–Aluminum Bimetallic Complexes

Since the pioneering work by Grignard in 1900, organomagnesium reagents, so-called Grignard reagents, have been considered as indispensable reactive reagents for building various organic molecules. Conventionally, alkyl Grignard reagents are prepared from the corresponding alkyl iodides, bromides, or chlorides with Mg, whereas the reaction of alkyl fluorides are usually not viable due to the high stability of the C–F bonds. Herein, the author describes that the Al–Rh bimetallic complexes catalyze the magnesiumation of C(*sp*<sup>3</sup>)–F bonds of alkyl fluorides using Mg powder as an easy-to-handle reducing agent. The magnesiumation of secondary and tertiary alkyl fluorides has also been achieved under the same conditions.

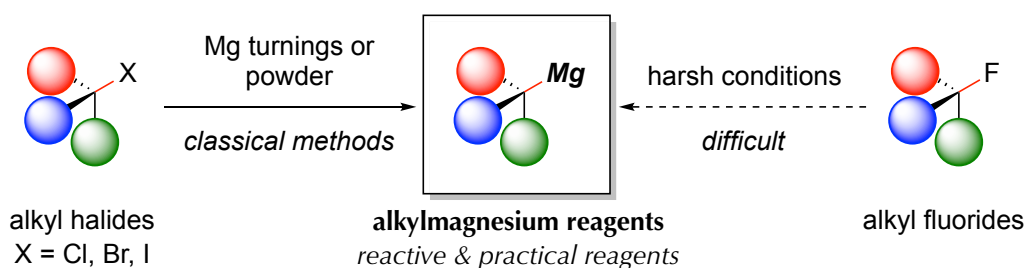
## Introduction

Since the seminal discovery of organomagnesium reagents (Grignard reagents) by Grignard, the reagents have been indispensable in organic synthesis due to their high reactivity toward various electrophiles to construct a wide variety of organic molecules.<sup>1</sup> Alkylmagnesium reagents are conventionally prepared from alkyl halides ( $R-X$ ;  $X = Cl, Br, \text{ or } I$ ) and Mg turnings or powder (Scheme 5-1, A). Knochel and co-workers have pioneered the halogen/magnesium exchange reaction of the alkyl halides with *i*-PrMgCl•LiCl (turbo Grignard reagent) as another reliable and practical method to prepare the Grignard reagents, enabling the preparation of alkylmagnesiums bearing functional groups.<sup>2</sup>

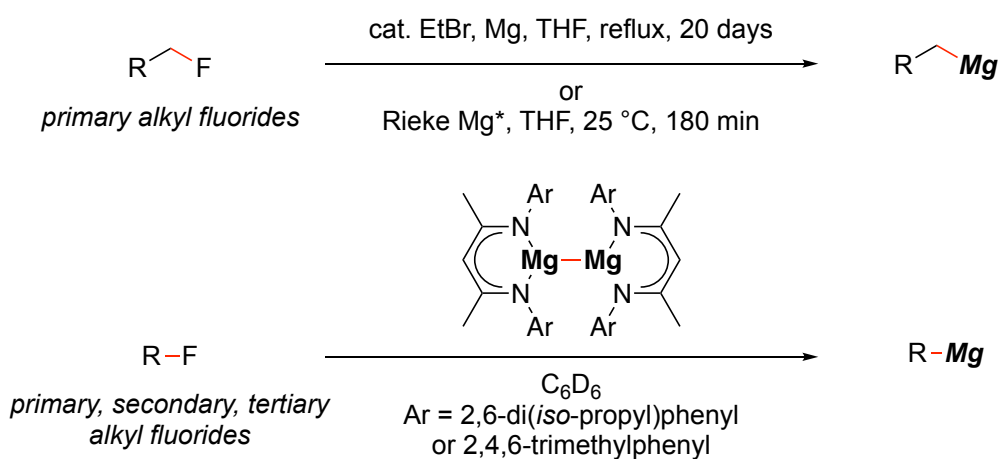
On the other hand, preparation of alkylmagnesium reagents from alkyl fluorides has been difficult due to the high bond-dissociation energy of C–F bonds (BDE of  $CH_3-X$ ;  $X = F$ : 115 kcal/mol vs.  $X = Br$ : 72 kcal/mol,  $X = H$ : 105 kcal/mol).<sup>3</sup> In order to magnesiate a C–F bond of alkyl fluorides, harsh reaction conditions (high temperature and prolonged time)<sup>4</sup> or pyrophoric highly dispersed magnesium reagents are required (Scheme 5-1, B). For example, the magnesiation of 1-fluorooctane proceeds reportedly in moderate efficiency even with a large excess amount of Rieke Mg in THF.<sup>5</sup> These protocols allow the magnesiation of primary alkyl fluorides, whereas that of secondary and tertiary ones are elusive. Recently, Crimmin and co-workers have demonstrated the magnesiation of primary, secondary, and tertiary alkyl fluorides using their own dimeric  $Mg(I)-Mg(I)$  complex, which is prepared by using stoichiometric amounts of alkaline metals.<sup>6</sup> There have been no reports of general methods for the magnesiation of these alkyl fluorides with a readily available and easy-to-handle Mg agent.

**Scheme 5-1.** Conventional methods for preparation of alkyl Grignard reagents and magnesiation of alkyl fluorides.

### A. Alkylmagnesium Reagents



### B. Magnesiation of Alkyl Fluorides

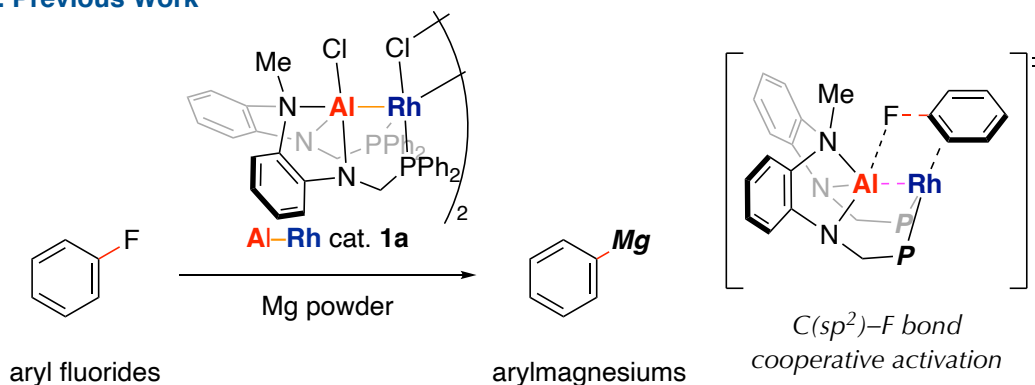


Recently, the author has developed the magnesiation of aryl fluorides catalyzed by Al–Rh bimetallic complex **1a**, which activates the Ar–F bonds by the polarized Al–Rh bond effectively in a cooperative manner (Scheme 5-2, A).<sup>7</sup> Theoretical calculations and stoichiometric experiments have revealed that the cooperative Ar–F bond activation requires a small activation barrier of 3.7 kcal/mol. Accordingly, the author has anticipated that the Al–Rh bimetallic complexes could also be effective for the catalytic magnesiation of alkyl fluorides through C(*sp*<sup>3</sup>)–F bond activation in a similar cooperative manner (Scheme 5-2, B).

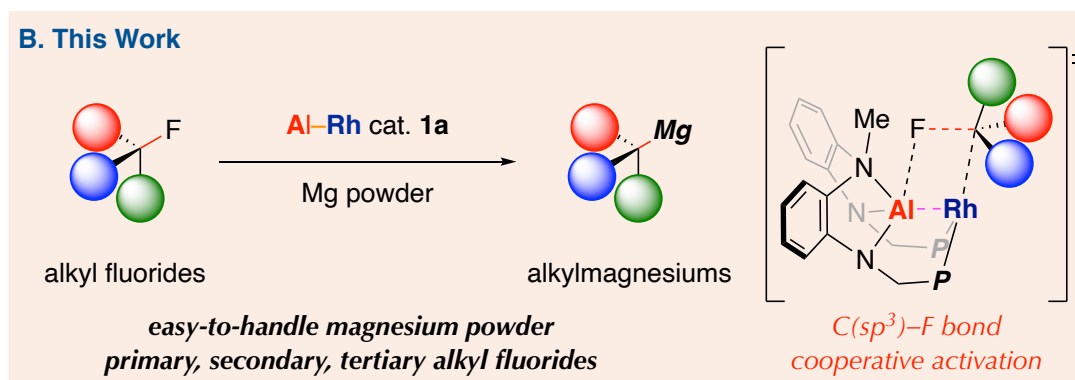


Scheme 5-2. Previous work and this work.

## A. Previous Work



## B. This Work

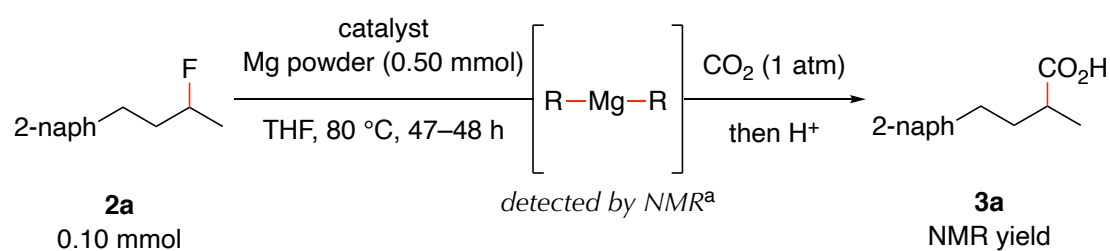


## Results and discussion

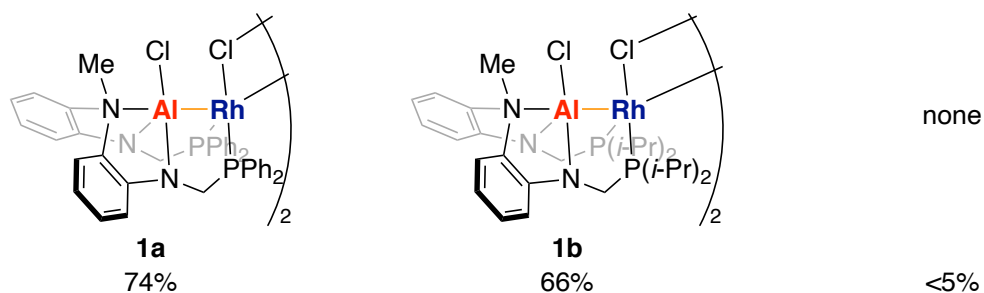
The catalytic  $C(sp^3)-F$  bond magnesiation of 2-(3-fluorobutyl)naphthalene (**2a**, 0.10 mmol, 1.0 eq.) with Mg powder (0.50 mmol, 5.0 eq.) was conducted in the presence of several different bimetallic Rh catalysts **1** in THF at 80 °C for 47–48 h (Scheme 5-3, above). 2-Methyl-4-(naphthalen-2-yl)butanoic acid (**3a**) was obtained in 74% NMR yield with **1a** (5.0 mol% of Rh) as a catalyst after quenching the reaction mixture with CO<sub>2</sub> (1 atm) followed by an acidic work-up with 3 M HCl aq. Al–Rh complex **1b**, bearing isopropyl groups on the phosphorus instead of phenyl, also produced **3a** in 66% NMR yield. The reaction was completely suppressed in the absence of the Al–Rh complexes **1**. Combinations of [RhCl(nbd)]<sub>2</sub> (5.0 mol% of Rh)/ligand (10 mol% of L) and Et<sub>2</sub>AlCl (20 mol%) did not convert 3-fluoro-1-phenylbutane (**2b**), while Rh/PPh<sub>3</sub> catalyst alone in the

absence of  $\text{Et}_2\text{AlCl}$  interestingly gave **3a** in moderate yield (Scheme 5-3, below). Accordingly, Al–Rh complexes **1** was found to be the most effective for the catalytic magnesiumation of alkyl fluorides to give the corresponding dialkylmagnesium species, possibly through the Schlenk equilibrium,<sup>8</sup> based on NMR analyses of the reaction mixture before quenching with electrophiles.

**Scheme 5-3.** Optimization and control experiments.

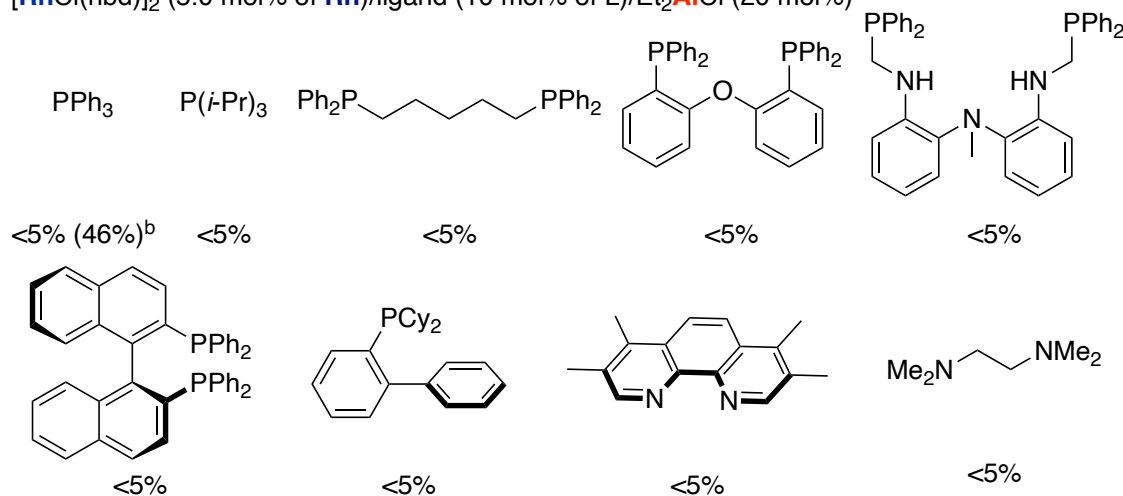


**Al–Rh complexes** (5.0 mol% of Rh)



**In-situ-generated catalysts<sup>a</sup>**

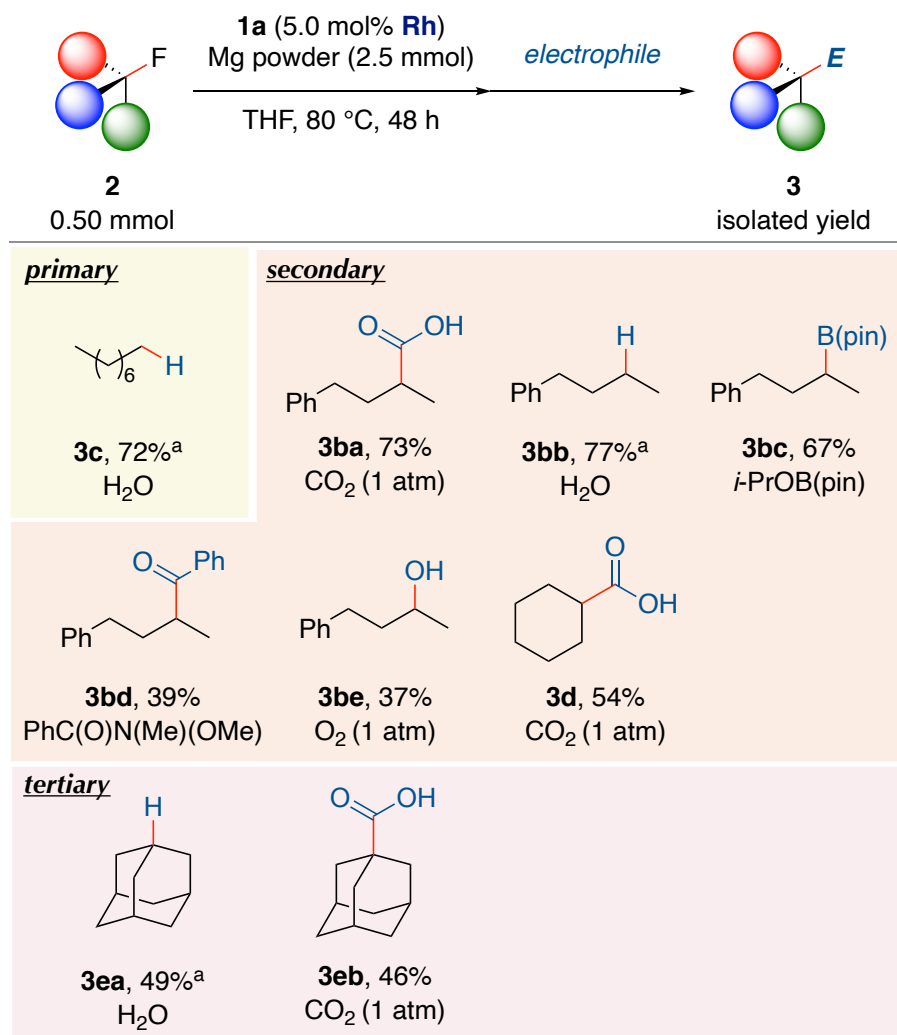
$[\text{RhCl}(\text{nbd})_2]$  (5.0 mol% of Rh)/ligand (10 mol% of L)/ $\text{Et}_2\text{AlCl}$  (20 mol%)



<sup>a</sup> The reactions were carried out with 3-fluoro-1-phenylbutane (**2b**) instead of **2a**. <sup>b</sup> Without  $\text{Et}_2\text{AlCl}$ .

Various fluoroalkanes were examined for the magnesiation on a 0.50 mmol-scale under the **1a**-catalyzed conditions (Scheme 5-4). The reaction using primary alkyl fluoride, *n*-octyl fluoride (**2c**), afforded *n*-octane (**3c**) in 72% GC yield after quenching the reaction with H<sub>2</sub>O. Secondary alkyl fluoride **2b** could be magnesiated and reacted with a variety of electrophiles, such as H<sub>2</sub>O, CO<sub>2</sub>, electrophilic borane reagent, benzaldehyde, the Weinreb amide,<sup>9</sup> and O<sub>2</sub> to obtain the corresponding products **3ba–3bg** in good to moderate yield. Fluorocyclohexane (**2d**) was also reacted, and even tertiary alkyl fluoride **2e** gave adamantane (**3ea**) and 1-adamantyl carboxylic acid (**3eb**) products through the magnesiation reaction.

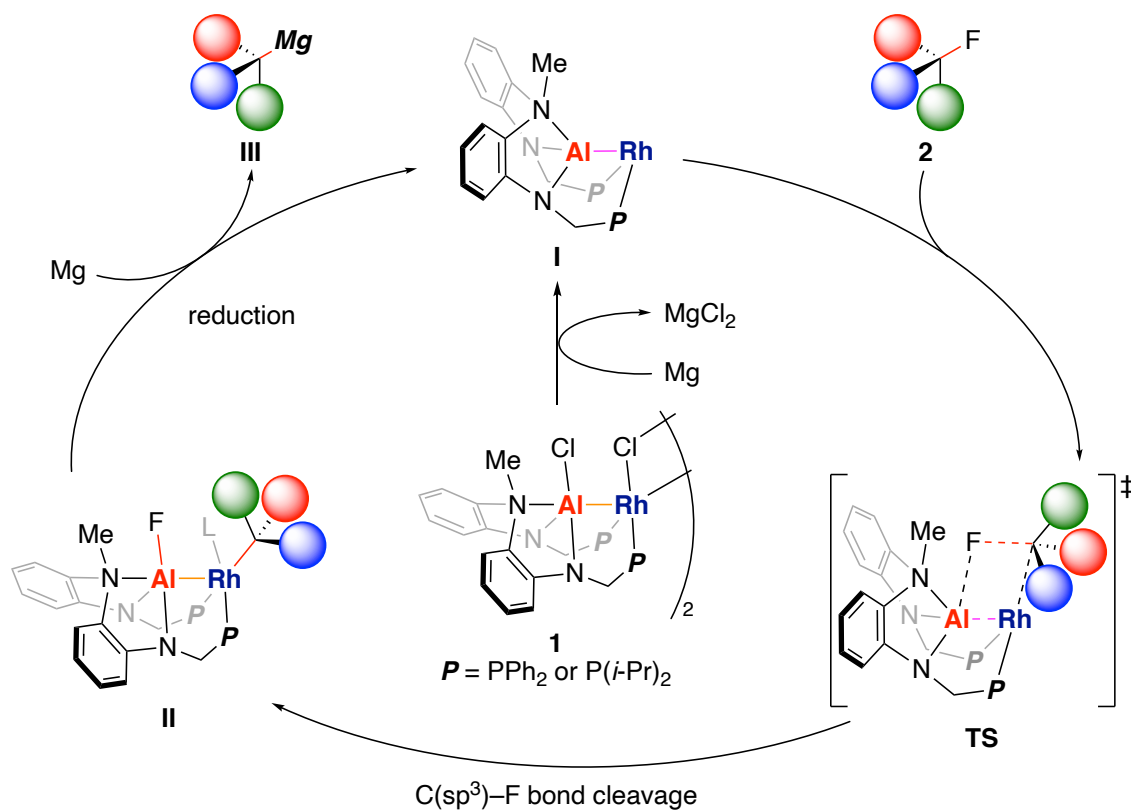
Scheme 5-4. Substrate scope.



<sup>a</sup> The yield was estimated by GC analysis (internal standard: C<sub>13</sub>H<sub>28</sub>).

A plausible catalytic cycle of the magnesiation of alkyl fluorides is shown in Scheme 5-5. Initially, catalyst precursor **1** is reduced by Mg powder to generate reactive X-type Al–Rh complex **I**, which cleaves the C(*sp*<sup>3</sup>)–F bond of alkyl fluoride **2** across the polarized Al–Rh bond in the cooperative activation manner **TS** to give bimetallic oxidative addition product **II**. Finally, Mg powder reduces **II** to produce the corresponding alkylmagnesium species **III** and regenerate the catalytically active species **I**.

Scheme 5-5. Plausible mechanism.



### Conclusion

In conclusion, the author has developed a catalytic magnesiation of alkyl fluorides using Mg powder. It is worth noting that the protocol can be applicable to a range of alkyl fluorides including secondary and tertiary ones.

## Experimental section

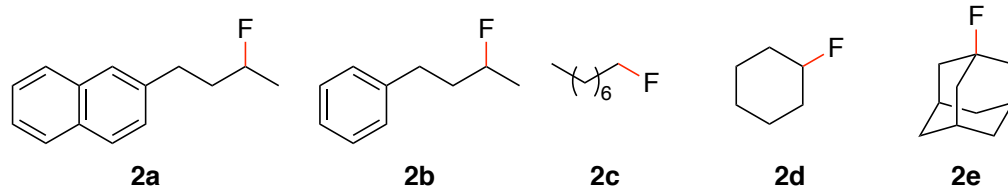
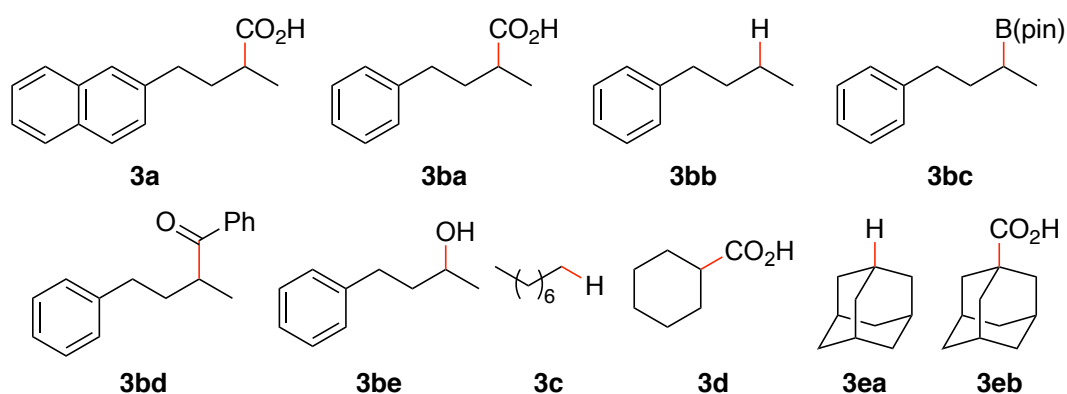
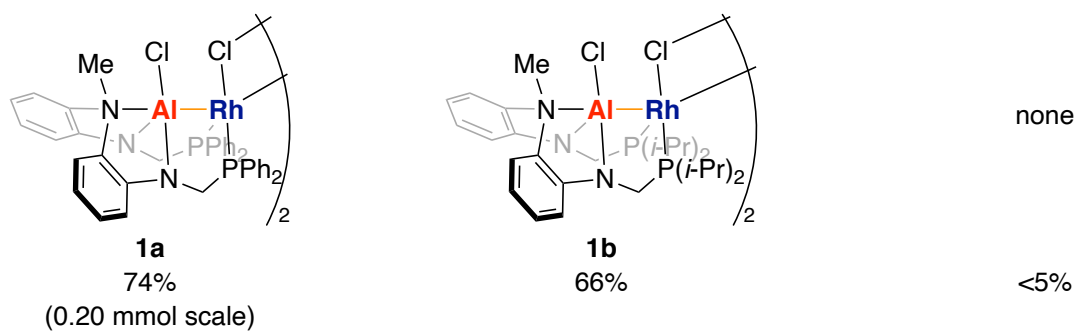
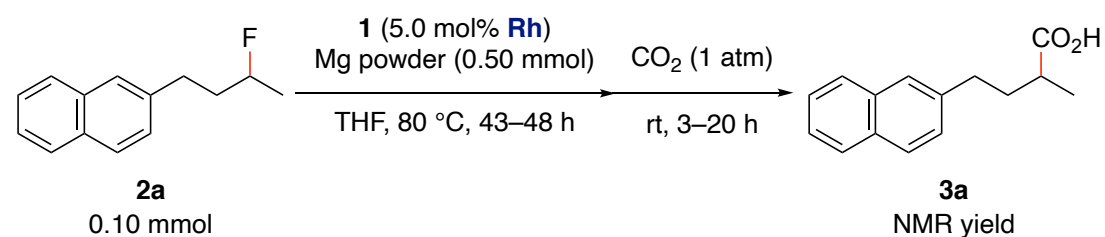
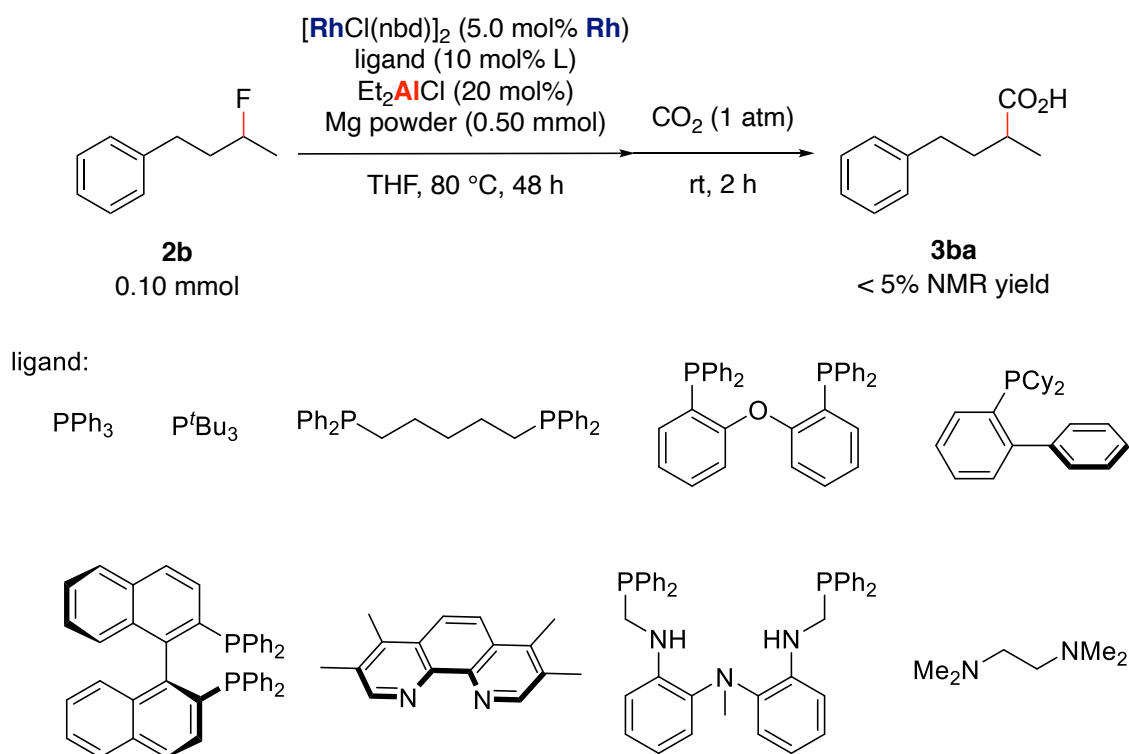
substratesproducts

Figure S5-1. A list of substrates and products in this study.

## General procedure for optimization and control experiments (Scheme 5-3).

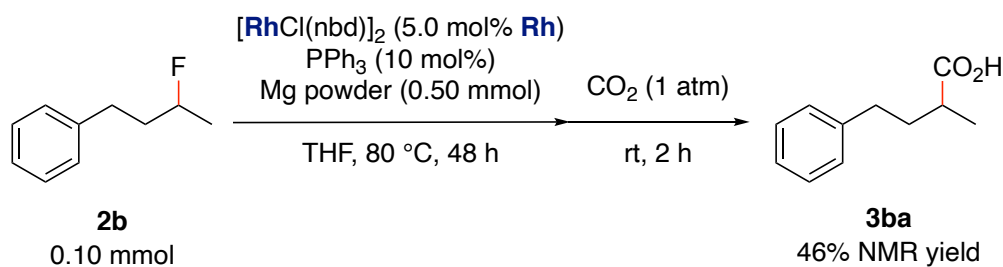


In a glove box, a 4 mL vial with a stirring bar was charged with magnesium powder (12 mg, 0.50 mmol, 5.0 eq.) and 2-(3-fluorobutyl)naphthalene (**2a**, 20 mg, 0.10 mmol, 1.0 eq.). A THF (300  $\mu$ L) suspension of **1** (13  $\mu$ mol, 5.0 mol% of Rh) were added to the vial. After stirring for 43–48 h at 80  $^{\circ}$ C, the reaction mixture was stirred under atmospheric pressure of CO<sub>2</sub> at room temperature for 3–20 h. To the mixture, 3 M HCl aq. (1.5 mL) was added. The mixture was extracted with EtOAc (2.0 mL) x 3. All the volatiles were removed in vacuo. The yield of **3a** was determined by <sup>1</sup>H NMR spectroscopy with 1,3,5-trimethoxybenzene as an internal standard.<sup>10</sup>



In a glove box, a 4 mL vial with a stirring bar was charged with indicated ligand (10 mol% of L). A THF (300  $\mu$ L) solution of  $[\text{RhCl}(\text{nbd})_2]$  (1.2 mg, 2.5  $\mu$ mol, 5.0 mol% of Rh) were added to the vial. The mixture was stirred at room temperature for 30 min.

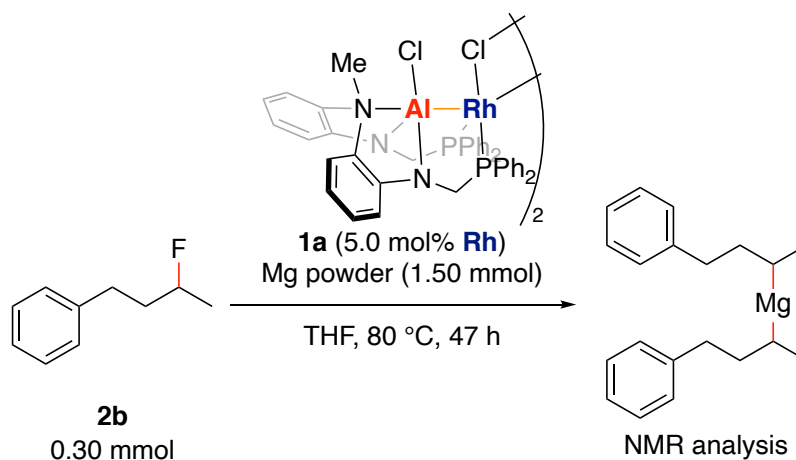
To the reaction mixture, 2-fluoro-4-phenylbutane (**2b**, 15 mg, 0.10 mmol, 1.0 eq.), magnesium powder (12 mg, 0.50 mmol, 5.0 eq.), Et<sub>2</sub>AlCl (23 μL, 20 μmol, 20 mol%; 0.87 M hexane solution) were added in this order. After stirring for 48 h at 80 °C, the reaction mixture was stirred under atmospheric pressure of CO<sub>2</sub> at room temperature for 2 h. To the mixture, 3 M HCl aq. (1.5 mL) was added. The mixture was extracted with EtOAc (2.0 mL) x 3. All the volatiles were removed in vacuo. The yield of **3ba** was determined by <sup>1</sup>H NMR spectroscopy with 1,3,5-trimethoxybenzene as an internal standard.



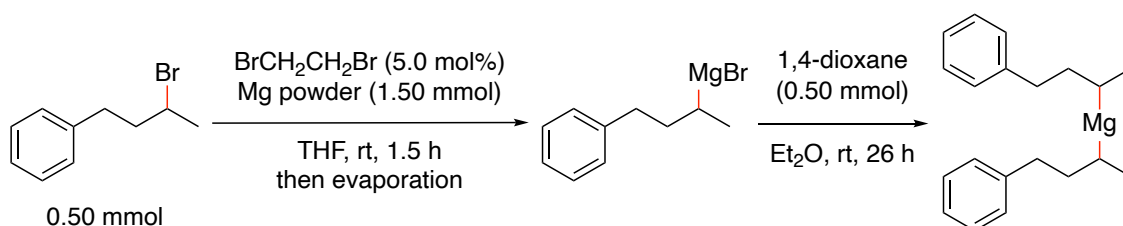
In a glove box, a 4 mL vial with a stirring bar was charged with PPh<sub>3</sub> (2.6 mg, 10 μmol, 10 mol%). A THF (300 μL) solution of [RhCl(nbd)<sub>2</sub>] (1.2 mg, 2.5 μmol, 5.0 mol% of Rh) were added to the vial. The mixture was stirred at room temperature for 30 min. To the reaction mixture, **2b** (15 mg, 0.10 mmol, 1.0 eq.) and magnesium powder (12 mg, 0.50 mmol, 5.0 eq.) were added in this order. After stirring for 48 h at 80 °C, the reaction mixture was stirred under atmospheric pressure of CO<sub>2</sub> at room temperature for 2 h. To the mixture, 3 M HCl aq. (1.5 mL) was added. The mixture was extracted with EtOAc (2.0 mL) x 3. All the volatiles were removed in vacuo. The yield of **3ba** was determined by <sup>1</sup>H NMR spectroscopy with 1,3,5-trimethoxybenzene as an internal standard.



### Identification of organomagnesium species.



In a glove box, a 4 mL vial with a stirring bar was charged with magnesium powder (37 mg, 1.50 mmol, 5.0 eq.) and **2b** (46 mg, 0.30 mmol, 1.0 eq.). A THF (900  $\mu\text{L}$ ) suspension of **1a** (12 mg, 7.5  $\mu\text{mol}$ , 5.0 mol% of Rh) were added to the vial. The mixture was stirred at 80 °C for 47 h and then, all the volatiles were removed in vacuo. The residue was diluted by  $\text{C}_6\text{D}_6$  and filtered through a Pasteur pipette filter, which was filled with a glass fiber filter (GB-100R ADVANTEC®).



The corresponding dialkylmagnesium compound was prepared by the following procedure based on the literature.<sup>11</sup> In a glove box, a 4 mL vial with a stirring bar was charged with magnesium powder (37 mg, 1.50 mmol, 3.0 eq.), 1,2-dibromoethane (4.7 mg, 25  $\mu\text{mol}$ , 5.0 mol%), and THF (500  $\mu\text{L}$ ). After stirring for 15 min at room temperature,

2-bromo-4-phenylbutane (107 mg, 0.50 mmol, 1.0 eq.) was added. The reaction mixture was stirred at room temperature for 1.5 h, and then, filtered through a Pasteur pipette filter, which was filled with a glass fiber filter (GB-100R ADVANTEC®). The obtained filtrate was put into another 4 mL vial with a stirring bar, 1,2-dioxane (44 mg, 0.50 mmol, 1.0 eq.) and Et<sub>2</sub>O (1.0 mL). The reaction mixture was stirred at room temperature for 26 h. All the volatiles were removed in vacuo. The residue was diluted by C<sub>6</sub>D<sub>6</sub> and filtered through the Pasteur pipette filter same as above.

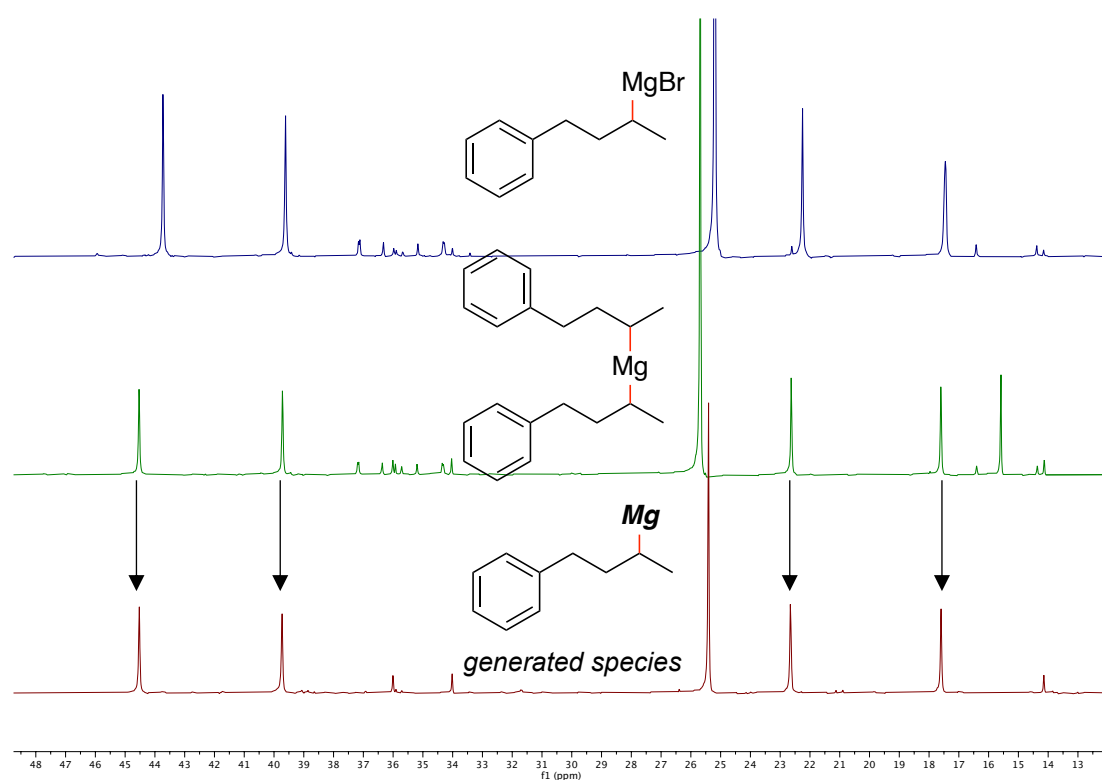
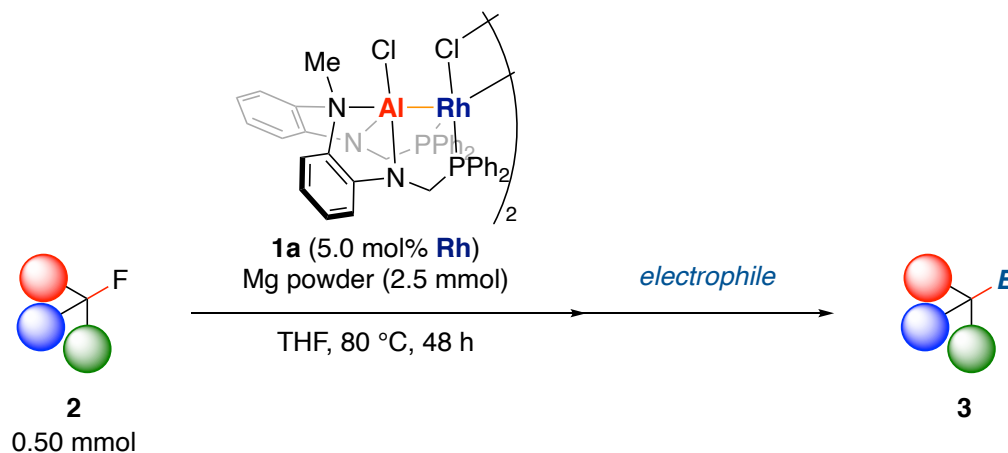
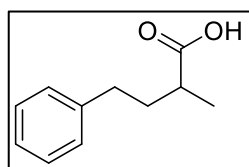


**Figure S5-2.** <sup>13</sup>C NMR spectra of the generated alkylmagnesium and the corresponding independently prepared alkylmagnesium bromide and di(alkyl)magnesium.

## General procedure for Scheme 5-4.

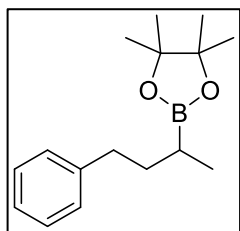


In a glove box, a 4 mL vial with a stirring bar was charged with magnesium powder (61 mg, 2.50 mmol, 5.0 eq.) and alkyl fluoride **2** (0.50 mmol, 1.0 eq.). A THF (1.5 mL) suspension of **1a** (20 mg, 13  $\mu$ mol, 5.0 mol% of Rh) were added to the vial. The mixture was stirred at 80 °C for 48 h and then, reacted with an indicated electrophile.



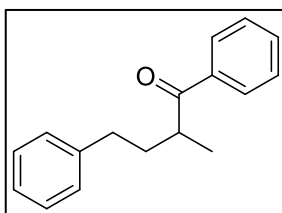
**2-Methyl-4-phenylbutanoic acid (3ba):** The reaction of 2-fluoro-4-phenylbutane (**2b**, 76 mg, 0.50 mmol, 1.0 eq.) was followed by being stirred under atmospheric pressure of CO<sub>2</sub> at room temperature for 2 h. To the mixture, 3 M HCl aq. (1.5 mL) was added. The mixture was extracted with EtOAc (2.0 mL) x 3. All the volatiles were removed in vacuo. After MPLC purification [*n*-hexane/EtOAc (70:30) containing AcOH (10 vol%)], the title compound (65 mg, 0.37 mmol, 73%) was obtained as a colorless oil. *R*<sub>f</sub> 0.44 [*n*-hexane/EtOAc (70:30) containing AcOH (10 vol%)]. <sup>1</sup>H NMR (400 MHz, CDCl<sub>3</sub>):  $\delta$  7.33–7.27 (m, 2H), 7.23–7.14 (m, 3H), 2.68 (t, *J* = 8.0 Hz, 2H), 2.52 (h, *J* = 6.9 Hz, 1H), 2.14–1.99 (m, 1H), 1.76 (ddt, *J* = 13.9, 8.4, 6.8 Hz, 1H), 1.24 (d, *J* = 6.9 Hz, 3H). <sup>13</sup>C{<sup>1</sup>H} NMR (101 MHz,

CDCl<sub>3</sub>):  $\delta$  183.0, 141.6, 128.6, 128.5, 126.1, 38.9, 35.3, 33.5, 17.1. All resonances of <sup>1</sup>H and <sup>13</sup>C NMR spectra were consistent with the reported values.<sup>12</sup>



**4,4,5,5-Tetramethyl-2-(1-methyl-3-phenylpropyl)-1,3,2-dioxaborolane (3bc):** The reaction of **2b** (76 mg, 0.50 mmol, 1.0 eq.) was followed by addition of 2-isopropoxy-4,4,5,5-tetramethyl-1,3,2-dioxaborolane (186 mg, 1.0 mmol, 2.0 eq.). After being stirred

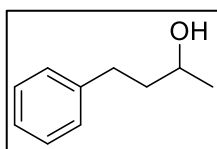
at room temperature for 17 h, purification of the mixture by MPLC [*n*-hexane/EtOAc (95:5)] gave the title compound (87 mg, 0.33 mmol, 67%) was obtained as a colorless oil. *R<sub>f</sub>* 0.44 [*n*-hexane/EtOAc (95:5)]. <sup>1</sup>H NMR (400 MHz, CDCl<sub>3</sub>):  $\delta$  7.31–7.25 (m, 2H), 7.22–7.15 (m, 3H), 2.64 (ddd, *J* = 8.6, 6.5, 1.6 Hz, 2H), 1.81 (ddt, *J* = 14.0, 8.8, 7.1 Hz, 1H), 1.73–1.51 (m, 1H), 1.27 (s, 12H), 1.17–1.05 (m, 1H), 1.04 (d, *J* = 6.8 Hz, 3H). <sup>13</sup>C{<sup>1</sup>H} NMR (101 MHz, CDCl<sub>3</sub>):  $\delta$  143.2, 128.6, 128.3, 125.6, 83.0, 35.4, 24.92, 24.86, 16.9 (br), 15.5. All resonances of <sup>1</sup>H and <sup>13</sup>C NMR spectra were consistent with the reported values.<sup>13</sup>



**2-Methyl-1,4-diphenyl-1-one (3bd):** After the reaction of **2b** (76 mg, 0.50 mmol, 1.0 eq.), the resulting mixture were filtered through a Pasteur pipette filter, which was filled with a glass fiber filter (GB-100R ADVANTEC®). After filtration, *N*-methoxy-*N*-

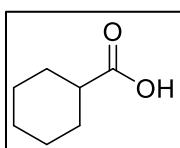
methylbenzamide (165 mg, 1.0 mmol, 2.0 eq.) was added to the filtrate. After being stirred at room temperature for 3 h, 3 M HCl aq. (1.5 mL) was added. The reaction mixture was extracted with EtOAc (2.0 mL) x 3. All the volatiles were removed in vacuo. After MPLC purification [*n*-hexane/EtOAc (95:5 to 80:20)], the title compound (46 mg, 0.19

mmol, 39%) was obtained as a pale yellow oil.  $R_f$  0.22 [*n*-hexane/EtOAc (95:5)].  $^1\text{H}$  NMR (400 MHz,  $\text{CDCl}_3$ ):  $\delta$  7.86 (dd,  $J = 8.1, 1.5$  Hz, 2H), 7.55 (tt,  $J = 7.0, 1.4$  Hz, 1H), 7.44 (t,  $J = 7.6$  Hz, 2H), 7.32–7.23 (m, 2H), 7.23–7.11 (m, 3H), 3.47 (h,  $J = 6.8$  Hz, 1H), 2.65 (td,  $J = 7.6, 1.9$  Hz, 2H), 2.22–2.13 (m, 1H), 1.75 (ddt,  $J = 13.7, 8.6, 6.7$  Hz, 1H), 1.24 (d,  $J = 6.9$  Hz, 3H).  $^{13}\text{C}\{^1\text{H}\}$  NMR (101 MHz,  $\text{CDCl}_3$ ):  $\delta$  204.3, 141.9, 136.7, 133.0, 128.8, 128.6, 128.5, 128.4, 126.1, 39.9, 35.3, 33.6, 17.4. All resonances of  $^1\text{H}$  and  $^{13}\text{C}$  NMR spectra were consistent with the reported values.<sup>14</sup>



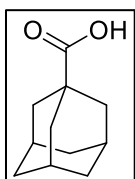
**4-Phenylbutane-2-ol (3be):** This compound was prepared by the following procedure based on the literature.<sup>15</sup> After the reaction of **2b** (76 mg, 0.50 mmol, 1.0 eq.), the resulting mixture was filtered through

a Pasteur pipette filter, which was filled with a glass fiber filter (GB-100R ADVANTEC®). The filtrate was stirred under atmospheric pressure of  $\text{O}_2$  at 10 °C for 16 h. The reaction mixture was quenched by 3 M HCl aq. (1.5 mL) and extracted with  $\text{Et}_2\text{O}$  (2.0 mL) x 3. All the volatiles were removed in vacuo. After MPLC purification [*n*-hexane/EtOAc (70:30)], the title compound (28 mg, 0.19 mmol, 37%) was obtained as a colorless oil.  $R_f$  0.30 [*n*-hexane/EtOAc (70:30)].  $^1\text{H}$  NMR (400 MHz,  $\text{CDCl}_3$ ):  $\delta$  7.29 (dd,  $J = 8.1, 6.8$  Hz, 2H), 7.24–7.15 (m, 3H), 3.84 (dq,  $J = 12.4, 6.2$  Hz, 1H), 2.86–2.59 (m, 2H), 1.78 (m, 2H), 1.24 (d,  $J = 6.3$  Hz, 3H).  $^{13}\text{C}\{^1\text{H}\}$  NMR (101 MHz,  $\text{CDCl}_3$ ):  $\delta$  142.2, 128.5 (overlapped), 126.0, 67.6, 41.0, 32.3, 23.8. All resonances of  $^1\text{H}$  and  $^{13}\text{C}$  NMR spectra were consistent with the reported values.<sup>16</sup>



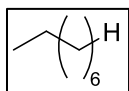
**Cyclohexanoic acid (3d):** The reaction of fluorocyclohexane (**2d**, 51 mg, 0.50 mmol, 1.0 eq.) was followed by being stirred under atmospheric

pressure of CO<sub>2</sub> at room temperature for 2 h. To the mixture, 3 M HCl aq. (1.5 mL) was added. The mixture was extracted with EtOAc (2.0 mL) x 3. All the volatiles were removed in vacuo, and the residue was extracted with sat. NaHCO<sub>3</sub> aq. (8.0 mL) x 5. The combined aqueous layers were acidified by 3 M HCl aq. The acidified aqueous layer was extracted with EtOAc (80 mL) x 3 and dried over anhydrous Na<sub>2</sub>SO<sub>4</sub>. After filtration, all the volatiles were removed in vacuo. The title compound (35 mg, 0.27 mmol, 54%) was obtained as a yellow oil. R<sub>f</sub> 0.38 [*n*-hexane/EtOAc (70:30) containing AcOH (10 vol%)]. <sup>1</sup>H NMR (400 MHz, CDCl<sub>3</sub>): δ 2.33 (tt, *J* = 11.3, 3.6 Hz, 1H), 1.93 (dt, *J* = 14.7, 3.7 Hz, 2H), 1.85–1.71 (m, 2H), 1.64 (dq, *J* = 11.0, 3.8 Hz, 1H), 1.45 (qd, *J* = 11.7, 3.4 Hz, 2H), 1.34–1.20 (m, 3H). <sup>13</sup>C{<sup>1</sup>H} NMR (101 MHz, CDCl<sub>3</sub>): δ 182.6, 43.0, 28.9, 25.8, 25.5. All resonances of <sup>1</sup>H and <sup>13</sup>C NMR spectra were consistent with the reported values.<sup>17</sup>



**1-Adamantylcarboxylic acid (3eb):** The reaction of 1-fluoroadamantane (**2e**, 77 mg, 0.50 mmol, 1.0 eq.) was followed by being stirred under atmospheric pressure of CO<sub>2</sub> at room temperature for 2 h. To the mixture, 3 M HCl aq. (1.5 mL) was added. The mixture was extracted with EtOAc (2.0 mL) x 3. All the volatiles were removed in vacuo, and the residue was extracted with sat. NaHCO<sub>3</sub> aq. (8.0 mL) x 5. The combined aqueous layers were separated and acidified by 3 M HCl aq. The acidified aqueous layer was extracted with EtOAc (80 mL) x 3 and dried over anhydrous Na<sub>2</sub>SO<sub>4</sub>. After filtration, all the volatiles were removed in vacuo. The title compound (42 mg, 0.23 mmol, 46%) was obtained as a yellow oil. R<sub>f</sub> 0.47 [*n*-hexane/EtOAc (70:30) containing AcOH (10 vol%)]. <sup>1</sup>H NMR (400 MHz, CDCl<sub>3</sub>): δ 2.03 (m, 3H), 1.91 (d, *J* = 2.9 Hz, 6H), 1.79–1.66 (m, 6H). <sup>13</sup>C{<sup>1</sup>H} NMR (101 MHz, CDCl<sub>3</sub>):

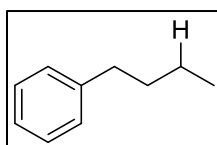
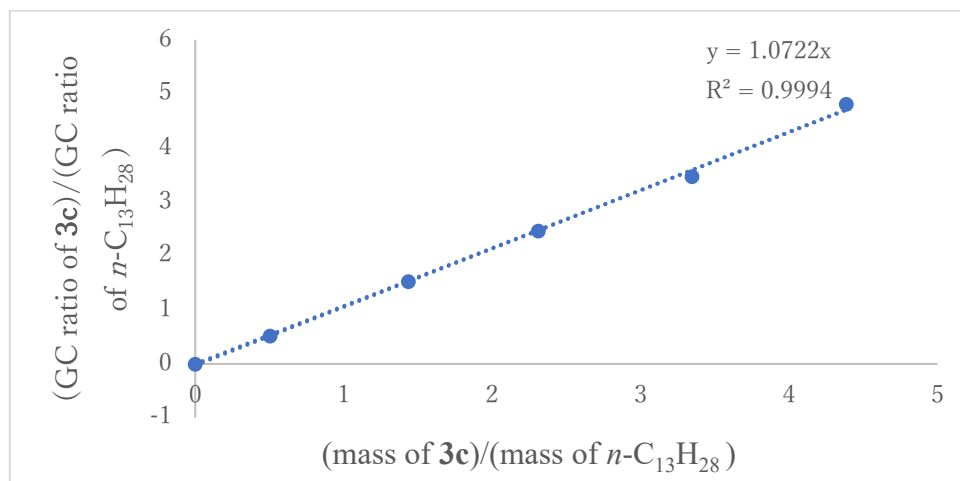
$\delta$  183.7, 40.6, 38.7, 36.5, 27.9. All resonances of  $^1\text{H}$  and  $^{13}\text{C}$  NMR spectra were consistent with the reported values.<sup>18</sup>



***n*-Octane (3c):** After the reaction of *n*-octyl fluoride (**2c**, 66 mg, 0.50 mmol, 1.0 eq.), the reaction mixture was quenched by  $\text{H}_2\text{O}$ . The yield of **3c** was estimated in 72% yield by GC with *n*- $\text{C}_{13}\text{H}_{28}$  as an internal standard (Table S5-1).

**Table S5-1.** Data for the GC calibration curve obtained using an authentic sample of *n*-octane (**3c**).

mass (mg)		x =	mass	of	GC area	y =	GC area of <b>3c</b> /GC
<b>3c</b>	<i>n</i> - $\text{C}_{13}\text{H}_{28}$		<b>3c</b> /mass	of	<b>3c</b>	<i>n</i> - $\text{C}_{13}\text{H}_{28}$	area of <i>n</i> - $\text{C}_{13}\text{H}_{28}$
			<i>n</i> - $\text{C}_{13}\text{H}_{28}$				
12.0	23.8		0.504202		370098	711968	0.51982
34.7	24.2		1.43388		771606	505839	1.52540
55.9	24.2		2.30992		1411943	571833	2.46915
81.0	24.2		3.34711		1752334	505233	3.46837
103.1	23.5		4.38723		2157202	448826	4.80632

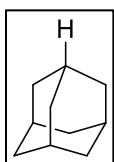
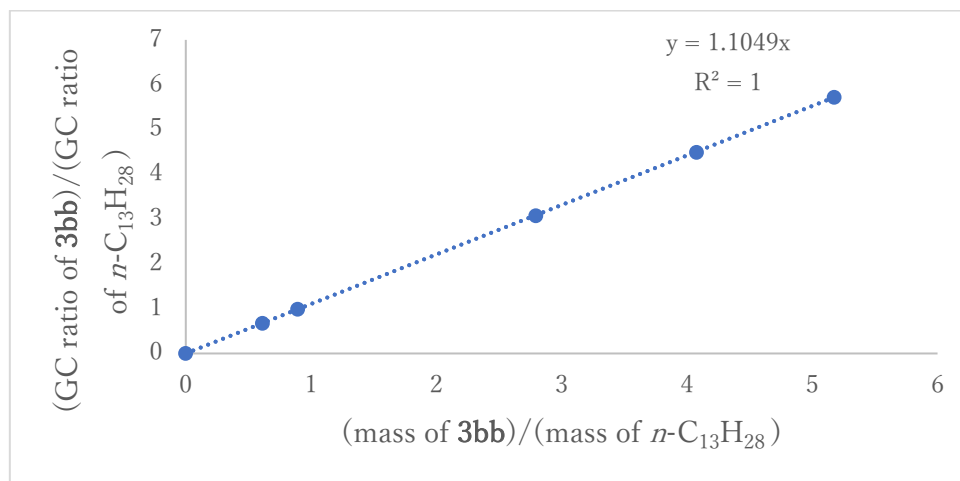


***n*-Butylbenzene (3bb):** After the reaction of 2-fluoro-4-phenylbutane (76 mg, 0.50 mmol, 1.0 eq.), the reaction mixture was quenched by H<sub>2</sub>O. The yield of **3bb** was estimated in 77% yield by GC with *n*-C<sub>13</sub>H<sub>28</sub> as an internal standard (Table S5-2).

**Table S5-2.** Data for the GC calibration curve obtained using an authentic sample of *n*-butylbenzene (**3bb**).

mass (mg)	x =	mass	of	GC area	y =	GC area of <b>3bb</b> /GC
<b>3bb</b>	<i>n</i> -C <sub>13</sub> H <sub>28</sub>	<b>3bb</b> /mass	of	<b>3bb</b>	<i>n</i> -C <sub>13</sub> H <sub>28</sub>	area of <i>n</i> -C <sub>13</sub> H <sub>28</sub>
		<i>n</i> -C <sub>13</sub> H <sub>28</sub>				
14.7	24.0	0.61250		296209	434821	0.68122
21.7	24.3	0.89300		385633	390788	0.98681
66.7	23.9	2.79080		1081056	350337	3.08576
97.0	23.8	4.07563		1811189	403057	4.49363
123.2	23.8	5.17647		2272092	396861	5.72516

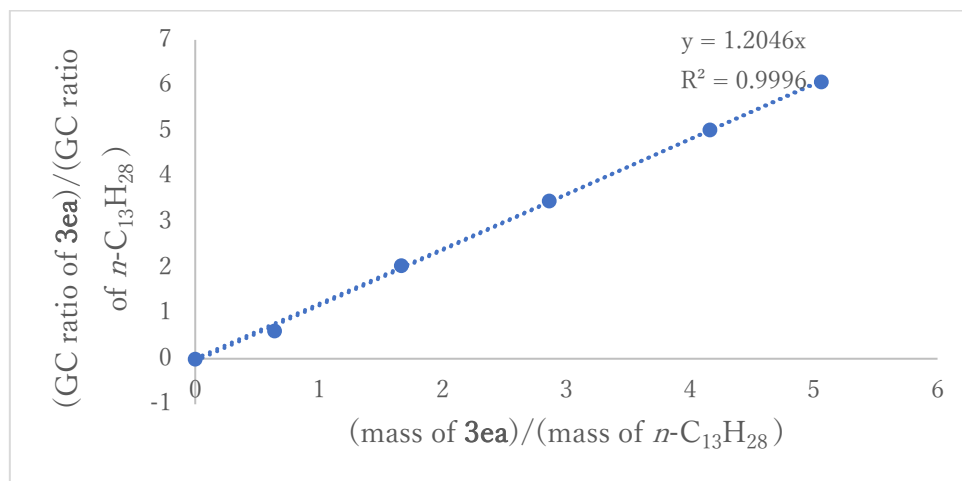




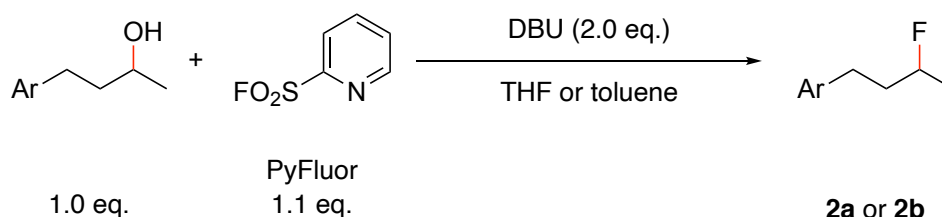
**Adamantane (3ea):** After the reaction of 1-fluoroadamantane (**2d**, 77 mg, 0.50 mmol, 1.0 eq.), the reaction mixture was quenched by H<sub>2</sub>O. The yield of **3ea** was estimated in 49% yield by GC with *n*-C<sub>13</sub>H<sub>28</sub> as an internal standard (Table S5-3).

**Table S5-3.** Data for the GC calibration curve obtained using an authentic sample of adamantane (**3ea**).

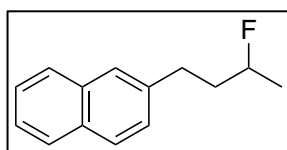
mass (mg)	x	mass of <b>3ea</b> /mass	GC area	y =	GC area of <b>3ea</b> /GC
<b>3ea</b>	<i>n</i> -C <sub>13</sub> H <sub>28</sub>	= of <i>n</i> -C <sub>13</sub> H <sub>28</sub>	<b>3ea</b>	<i>n</i> -C <sub>13</sub> H <sub>28</sub>	area of <i>n</i> -C <sub>13</sub> H <sub>28</sub>
15.3	23.8	0.64286	213410	349824	0.61005
40.2	24.1	1.66805	458312	224238	2.04386
68.4	23.9	2.86192	812481	234719	3.46151
97.4	23.4	4.16239	1575602	313119	5.03196
117.9	23.3	5.06009	1770227	291052	6.08217



**General procedure for preparation of alkyl fluorides.**

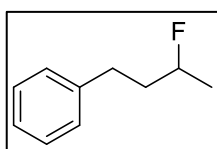


Alkyl fluorides were prepared by the following procedure based on the literature.<sup>19</sup> A round-bottom flask with a stirring bar was charged with corresponding alcohol (1.0 eq.), PyFluor (1.1 eq.), and solvent. DBU (2.0 eq.) was added to the reaction mixture. After stirring at room temperature for 48–65 h under ambient atmosphere, the crude material was purified by MPLC.



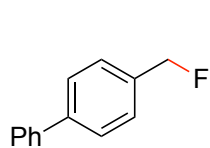
**2-(3-Fluorobutyl)naphthalene (2a):** To a solution of 4-(naphthalen-2-yl)butan-2-ol (541 mg, 2.7 mmol, 1.0 eq.) and PyFluor (483 mg, 3.0 mmol, 1.1 eq.) in toluene (3.0 mL), DBU (822 mg, 5.4 mmol, 2.0 eq.) were slowly added at 0 °C. The reaction mixture was stirred for 48 h at room temperature. After adding water (100 mL), the reaction mixture was extracted with EtOAc (60 mL) x 3. The combined organic layers were dried over anhydrous Na<sub>2</sub>SO<sub>4</sub> and filtered. After removal of solvent, the crude material was purified by MPLC [silica gel, *n*-hexane/EtOAc (100:0 to 90:10)] to give the title compound (322 mg, 1.6 mmol, 59%) as white powder. *R*<sub>f</sub> 0.16 [*n*-hexane]. <sup>1</sup>H NMR (400 MHz, CDCl<sub>3</sub>): δ 7.81 (d, *J* = 7.4 Hz, 1H), 7.78 (d, *J* = 8.5 Hz, 2H), 7.64 (br s, 1H), 7.44 (pd, *J* = 6.7, 1.5 Hz, 2H), 7.34 (dd, *J* = 8.3, 1.8 Hz, 1H), 4.82–4.58 (m, 1H), 2.97 (ddd, *J* = 14.7, 9.6, 5.4 Hz, 1H), 2.86 (ddd, *J* = 13.9, 9.2, 6.9 Hz, 1H), 2.17–2.00 (m, 1H), 2.00–1.81 (m, 1H), 1.37 (dd, *J* = 23.8, 6.0 Hz, 3H). <sup>13</sup>C{<sup>1</sup>H} NMR (101 MHz, CDCl<sub>3</sub>): δ 139.1, 133.8, 132.2, 128.2, 127.8, 127.6,

127.4, 126.7, 126.1, 125.4, 90.2 (d,  $J = 164.8$  Hz), 38.7 (d,  $J = 21.1$  Hz), 31.7 (d,  $J = 4.7$  Hz), 21.2 (d,  $J = 22.3$  Hz).  $^{19}\text{F}$  NMR (376 MHz,  $\text{CDCl}_3$ ):  $\delta$  -174.06 (dq,  $J = 43.3, 22.9$  Hz). All resonances of  $^1\text{H}$ ,  $^{13}\text{C}$  and  $^{19}\text{F}$  NMR spectra were consistent with the reported values.<sup>20</sup>

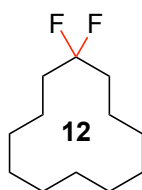


**2-Fluoro-4-phenylbutane (2b):** To a solution of 4-phenylbutane-2-ol (5.1 g, 34 mmol, 1.0 eq.) and PyFluor (6.0 g, 37 mmol, 1.1 eq.) in THF (40 mL), DBU (10 g, 67 mmol) were slowly added at room temperature.

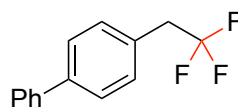
The reaction mixture was stirred for 65 h at room temperature. After adding water (50 mL), the reaction mixture was extracted with *n*-hexane (100 mL) x 2. The combined organic layers were dried over anhydrous  $\text{Na}_2\text{SO}_4$  and filtered with filter paper. After removal of the solvents, the crude material was purified by MPLC [silica gel, *n*-hexane] followed by distillation to give the title compound (1.7 g, 11 mmol, 33%) as a colorless oil.  $R_f$  0.35 [*n*-hexane].  $^1\text{H}$  NMR (400 MHz,  $\text{CDCl}_3$ ):  $\delta$  7.32–7.27 (m, 2H), 7.22–7.19 (m, 3H), 4.73 (dq,  $J = 8.3, 6.1, 3.9$  Hz, 1H), 2.81 (ddd,  $J = 13.7, 9.9, 5.3$  Hz, 1H), 2.69 (ddd,  $J = 13.8, 9.5, 6.9$  Hz, 1H), 2.08–1.91 (m, 1H), 1.91–1.74 (m, 1H), 1.35 (dd,  $J = 23.9, 6.3$  Hz, 3H).  $^{13}\text{C}\{^1\text{H}\}$  NMR (101 MHz,  $\text{CDCl}_3$ ):  $\delta$  141.6, 128.6 (overlapped), 126.1, 90.2 (d,  $J = 165.0$  Hz), 38.8 (d,  $J = 20.6$  Hz), 31.5 (d,  $J = 4.3$  Hz), 21.2 (d,  $J = 23.0$  Hz).  $^{19}\text{F}$  NMR (376 MHz,  $\text{CDCl}_3$ ):  $\delta$  -174.77 (tq,  $J = 43.8, 20.7$  Hz). All resonances of  $^1\text{H}$ ,  $^{13}\text{C}$  and  $^{19}\text{F}$  NMR spectra were consistent with the reported values.<sup>19</sup>

**Unsuccessful Substrate**

protonation  
&  
homocoupling



no reaction



no reaction

## References and notes

- (1) (a) Grignard, V. *Compt. rend. Hebd. Séances Acad. Sci.* **1900**, *130*, 1322. (b) Seyferth, D. *Organometallics* **2009**, *28*, 1598.
- (2) (a) Krasovskiy, K.; Knochel, P. *Angew. Chem. Int. Ed.* **2004**, *43*, 3333. (b) Li-Yuan Bao, R.; Zhao, R.; Shi, L. *Chem. Commun.* **2015**, *51*, 6884. (c) Ziegler, D. S.; Wei, B.; Knochel, P. *Chem. Eur. J.* **2019**, *25*, 2695.
- (3) (a) Pietrasiak, E.; Lee, E. *Chem. Commun.* **2022**, *58*, 2799. (b) Blanksby, S. J.; Ellison, G. B. *Acc. Chem. Res.* **2003**, *36*, 255. (c) O'Hagan, D. *Chem. Soc. Rev.* **2008**, *37*, 308.
- (4) (a) Swarts, F. *Bull. Soc. Chim. Belgique* **1921**, *30*, 302. (b) Pattison, F. L. M.; Howell, W. C. *J. Org. Chem.* **1956**, *21*, 879. (c) Ashby, E. C.; Yu, S. H.; Beach, R. G. *J. Am. Chem. Soc.* **1970**, *92*, 433. (d) Bernstein, J.; Roth, J. S.; Miller, W. T. *J. Am. Chem. Soc.* **1948**, *70*, 2310. (e) Ashby, E. C.; Yu, S. H. *J. Org. Chem.* **1971**, *36*, 2123.
- (5) (a) Rieke, R. D.; Hudnall, P. M. *J. Am. Chem. Soc.* **1972**, *94*, 7178. (b) Rieke, R. D.; Bales, S. E. *J. Am. Chem. Soc.* **1974**, *96*, 1775.
- (6) Coates, G.; Ward, B. J.; Bakewell, C.; White, A. J. P.; Crimmin, M. R. *Chem. Eur. J.* **2018**, *24*, 16282.
- (7) Fujii, I.; Semba, K.; Li, Q.-Z.; Sakaki, S.; Nakao, Y. *J. Am. Chem. Soc.* **2020**, *142*, 11647.
- (8) Schlenk, W.; Schlenk, W., Jr. *Ber. Dtsch. Chem. Ges.* **1929**, *62*, 920
- (9) Basha, A.; Lipton, J. L.; Weinreb, S. M. *Tetrahedron Lett.* **1977**, *18*, 4171.
- (10) Zhang, X.; Gao, Y.; Laishram, R. D.; Li, K.; Yang, Y.; Zhan, Y.; Luo, Y.; Fan, B. *Org. Biomol. Chem.* **2019**, *17*, 2174.

- (11) Tang, H.; Richey, H. G. *J. Organometallics*. **2001**, *20*, 1569.
- (12) Zhu, Y.; Wen, X.; Song, S.; Jiao, N. *ACS Catal.* **2016**, *6*, 6465.
- (13) Wu, J.; He, L.; Noble, A.; Aggarwal V. K. *J. Am. Chem. Soc.* **2018**, *140*, 10700.
- (14) Zhang, L.; Si, X.; Yang, Y.; Witzel, S.; Sekine, K.; Rudolph, M.; Rominger, F.; Hashmi, S. K. *ACS Catal.* **2019**, *9*, 6118.
- (15) Sultanov, R. M.; Ismagilov, R. R.; Popod'ko, N. R.; Tulyabaev, A. R.; Dzhemilev, U. M. *J. Organomet. Chem.* **2013**, *724*, 51.
- (16) Zhao, Q.; Curran, D. P.; Malacria, M.; Fensterbank, L.; Goddard, J. P.; Lacôte, E. *Chem. Eur. J.* **2011**, *17*, 9911.
- (17) Schmidt, A. K. C.; Stark, C. B. W. *Org. Lett.* **2011**, *13*, 4164.
- (18) Pfennig, V. S.; Vilella, R. C.; Nikodemus, J.; Bolm, C. *Angew. Chem. Int. Ed.* **2022**, *61*, e202116514.
- (19) Nielsen, M. K.; Ugaz, C. R.; Li, W.; Doyle, A. G. *J. Am. Chem. Soc.* **2015**, *137*, 9571.
- (20) Song, P.; Zhu, S. *ACS Catal.* **2020**, *10*, 13165.

## List of Publications

All the present Thesis have been published in the following journals.

The following parts of the accepted materials were modified:

- (a) A word 'we' is replaced to 'the author'.
- (b) Words 'see supporting information' and similar expressions are deleted and corresponding materials (text, figures, and/or schemes) are moved from supporting information of accepted works to the main text of the Thesis or the Experimental section.
- (c) Subtitles are inserted to the section heads.
- (d) Parts of the introduction, results and discussion, and conclusion are modified according to the context of the Thesis.
- (e) Words listed in Abbreviations are replaced to the corresponding abbreviations.

### Chapter 2

- (2) Reprinted with permission from Fujii, I.; Semba, K.; Li, Q. Z.; Sakaki, S.; Nakao, Y. Magnesium of Aryl Fluorides Catalyzed by a Rhodium–Aluminum Complex. *J. Am. Chem. Soc.* **2020**, *142*, 11647–11652. Copyright 2020 American Chemical Society. To access the final edited and published work, see [<https://pubs.acs.org/doi/10.1021/jacs.0c04905>].

### Chapter 3

- (3) Reprinted with permission from Fujii, I.; Semba, K.; Nakao, Y. The Kumada–Tamao–Corriu Coupling Reaction Catalyzed by Rhodium–Aluminum Bimetallic Complexes. *Org. Lett.* **2022**, *24*, 3075–3079. Copyright 2022 American Chemical Society. To access the final edited and published work, see [<https://pubs.acs.org/doi/10.1021/acs.orglett.2c01060>].

### Chapter 4

- (4) Fujii, I.; Semba, K.; Nakao, Y. Site-Selective Magnesium of Multi-Fluorinated Arenes Catalyzed by Rhodium–Aluminum Bimetallic Complexes. *to be*



*submitted.*

## **Chapter 5**

- (5) Fujii, I.; Semba, K.; Nakao, Y. Magnesiumation of Alkyl Fluorides Catalyzed by Rhodium–Aluminum Bimetallic Complexes. *to be submitted.*

The following publication is not included in this Thesis.

- (6) Semba, K.; Fujii, I.; Nakao, Y. A PAIP Pincer Ligand Bearing a 2-Diphenylphosphinophenoxy Backbone. *Inorganics* **2019**, *7*, 140.

## Acknowledgments

The study presented in this Thesis has been carried out under the direction of Professor Yoshiaki Nakao at Kyoto University. The author would like to express his sincerest gratitude to Professor Nakao for his constant support, guidance, encouragement, and enthusiasm throughout this work.

The author also wishes to express his gratitude to Professor Seiji Matsubara and Professor Michinori Suginome for their helpful discussions and suggestions. He is also deeply thankful to Professor Shigeyoshi Sakaki for his help for this study by theoretical calculations, helpful discussions, and thoughtful suggestions. He is deeply indebted to Professor Kazuhiko Semba, Professor Ayumi Osawa, Professor Yusuke Kuroda, Professor Takuya Kurahashi, and Professor Keisuke Asano for their practical guidance, continuous advice, helpful discussions, and suggestions. He would like to thank Professor Takuya Koizumi in Kobe City College of Technology for his enthusiastic coaching.

The author is thankful to Dr. Karin Nishimura for mass spectrometry measurements and Ms. Fumie Sakata for elemental analyses. He is much grateful to Professor Tetsuaki Fujihara and Dr. Hiroyasu Sato for their valuable support in X-ray diffraction analysis.

The author would like to thank Ms. Haruka Kido, Mr. Ryota Higo, and Mr. Joseph Parr for their kind assistance. He also wishes to express his appreciation to the collaboration with Dr. Qiao-Zhi Li in Sakaki group at Kyoto University.

The author is grateful to Mr. Akito Ohgi, Mr. Naoki Ohta, Dr. Shogo Okumura, Dr. Ryohei Kameyama, Mr. Yasuhiro Ohtagaki, Dr. Naofumi Hara, Dr. Myuto Kashihara, Mr. Yuto Shimazaki, Ms. Nao Uemura, Mr. Tomohiro Akahori, Mr. Kaito Dosaka, Mr. Hiroshi Shiraishi, Mr. Fumiya Shimoura, Mr. Konosuke Yamamoto, Mr. Koki Aso, Mr. Shunta Notsu, Mr. Yoshiki Kobayashi, Ms. Momoe Ishimura, Mr. Masaki Ohata, Mr. Rin Seki, Mr. Koji Takeuchi, Mr. Naoki Matsushita, Mr. Kohei Kosaka, Ms. Riko Shimada, Mr. Kotaro Nagase, Mr. Keitaro Yamaguchi, Ms. Zuyi Xue, Mr. Yoichi Tokunaga, Mr. Kaoru Fukuda, Mr. Shuji Murakami, Mr. Yoshitaka Yamada, Mr. Jiayin Sun, Mr. Hayato Asano, Mr. Teppei Tada, Mr. Shuto Tomiyama, Ms. Maanashaa Balasubramanian, Mr. Kouki Fujita, Dr. Michele Formica, Dr. Wu Ge, Mr. Fritz Paulus, Dr. Solange Da Silva Pinto, Mr. Marius Lutz, and Mr. Marc Jaspers in Nakao group at

Kyoto University for their active and helpful discussions, and warm friendship. He is also greatly thankful to the secretary of Nakao group, Ms. Kaori Yamasaki for her kind support.

The author is thankful deeply to Professor Tristan Lambert for giving him a chance to join the exciting and stimulating research group at Cornell University from April 2022 to June 2022. The author is also grateful to all Lambert group members for their kind assistance during his stay in Ithaca

The author is grateful for the financial support of Research Fellowships of the Japan Society for the Promotion of Science (JSPS) for Young Scientists, the G-7 Scholarship Foundation, and the Iwadare Scholarship Foundation.

Finally, the author would like to express his sincere acknowledgment to his family, Noboru, Megumi, Minako, Hiroki, Mamiko, Kazuki, Yuto, and Yuma, for their constant assistance and encouragement.

Ikuya Fujii  
Department of Material Chemistry  
Graduate School of Engineering  
Kyoto University